JPRS L/9937

25 August 1981

Translation

CHEMICAL LASERS

By

V.K. Ablekov, Y.N. Denisov and V.V. Proshkin

FBIS FOREIGN BROADCAST INFORMATION SERVICE

FOR OFFICIAL USE ONLY

APPROVED FOR RELEASE: 2007/02/09: CIA-RDP82-00850R000400040049-0

NOTE

JPRS publications contain information primarily from foreign newspapers, periodicals and books, but also from news agency transmissions and broadcasts. Materials from foreign-language sources are translated; those from English-language sources are transcribed or reprinted, with the original phrasing and other characteristics retained.

Headlines, editorial reports, and material enclosed in brackets [] are supplied by JPRS. Processing indicators such as [Text] or [Excerpt] in the first line of each item, or following the last line of a brief, indicate how the original information was processed. Where no processing indicator is given, the information was summarized or extracted.

Unfamiliar names rendered phonetically or transliterated are enclosed in parentheses. Words or names preceded by a question mark and enclosed in parentheses were not clear in the original but have been supplied as appropriate in context. Other unattributed parenthetical notes within the body of an item originate with the source. Times within items are as given by source.

The contents of this publication in no way represent the policies, views or attitudes of the U.S. Government.

APPROVED FOR RELEASE: 2007/02/09: CIA-RDP82-00850R000400040049-0

JPRS L/9937

25 August 1981

CHEMICAL LASERS

Moscow KHIMICHESKIYE LAZERY in Russian 1980 (signed to press 5 Sep 80) pp 1-224

[Book "Chemical Lasers", by Valeriy Konstantinovich Ablekov, Yuriy Nikiforovich Denisov and Viktor Vasil'yevich Proshkin, Atomizdat, 2,850 copies, 224 pages, UDC 621.375.826]

CONTENTS

UDC 621.375.826

CHEMICAL LASERS

Moscow KHIMICHESKIYE LAZERY in Russian 1980 (signed to press 5 Sep 80) pp 1-224

[Book "Chemical Lasers", by Valeriy Konstantinovich Ablekov, Yuriy Nikiforovich Denisov and Viktor Vasil'yevich Proshkin, Atomizdat, 2850 copies, 224 pages]

[Text] The book presents the principles of gas-phase reactions typical of chemical lasers, gives fundamentals of the quantum mechanical description of molecular systems, and outlines processes of formation of excited particles in the course of nonequilibrium chemical reactions. An examination is made of the kinetics of processes in chemical lasers classified according to their hydrogasdynamic characteristics into devices with a stationary medium, with subsonic and supersonic flow, and with detonation processes in the medium. Designs and working principles of present-day chemical lasers are described.

For engineers and scientists working in laser research and development. May be of use to undergraduate and graduate students majoring in physics and in engineering physics.

Tables 7, figures 100, references 475.

INTRODUCTION

Lasers, or *optical quantum generators* as they are called in the Soviet literature, are more and more widely used each year in industrial technology, medicine, communications, geodesy and other areas of science and engineering. Quantum-mechanical engineering is used in holography, in locating remote objects and the measurement of great distances in astronomy, in research on transmitting television images by light beam and so on. Results have been promising in the use of quantum generators for solving the problem of nuclear fusion [Ref. 1].

The expansion of areas of use of quantum generators is accompanied by improvement of the systems that have been produced and by development of quantum generators based on new active media, and on new physical and chemical principles. Industry has now mastered production of solid-state, gas-discharge, semiconductor and dye lasers.

The development of generators and amplifiers of stimulated emission in the visible and infrared bands of electromagnetic waveforms [Ref. 2-7] is the outcome of fundamental research by N. G. Basov, A. M. Prokhorov, and by Townes et al., who achieved coherent radiation [Ref. 8, 9] in the microwave band on the basis of the phenomenon of amplification of electromagnetic waves [Ref. 10, 11].

In addition to pumping of quantum generators by optical or electrical energy, other methods have been developed as well. The most promising among these have been thermal and chemical pumping techniques. In the former method, heat energy is converted to coherent stimulated radiation, while the transformed energy in the latter case is that released during exothermal reactions with the formation of atoms and molecules in excited states [Ref. 12-15].

The *chemical laser* is a device in which population inversion and lasing are achieved either directly as a result of a chemical reaction, or after the reaction in the exchange of energy between components of the medium, at least one of which is a product of this reaction.

The branch of science on chemical lasers includes divisions of quantum mechanics, physics, chemical kinetics, optics, hydrodynamics, gas dynamics and plasma dynamics. With respect to the particulars of chemical energy transformations of reagents A, B, C, D, G, we can represent the major processes in chemical lasers graphically in the following diagram [Ref. 16]:

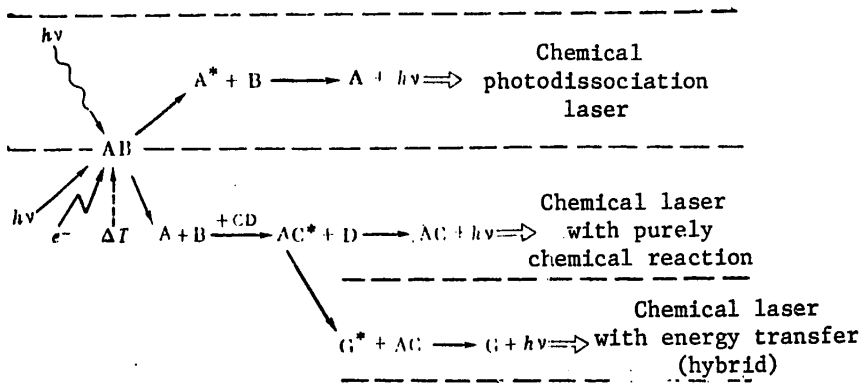

Most chemical reactions take place comparatively slowly, and therefore they are not suitable for population inversion. Before they have time to accumulate, the excited particles (indicated by an asterisk) make a transition to the ground state, and quantum-mechanical emission is not stimulated. Therefore, chemical lasers can operate only on fast reactions: photodissociation or other chemical reactions initiated by the action of light (hν), combustion, explosion (ΔT), electric discharge (e^-) or chemical reaction between atoms or molecules, e. g. in colliding beams of atoms or molecules of various substances.

In principle, the chemical method of population inversion permits creation of quantum generators with high efficiency and output power. Especially large power can be obtained from quantum generators with explosive chemical reaction.

Chemical energy is directly converted to optical emission in quantum generators with chemical pumping. We should add to the advantages of chemical lasers over other known quantum generators the fact that they have a wide spectrum of lasing wavelengths from 2 μm [Ref. 17, 18] to 100 μm [Ref. 19]. The development of chemical laser research extends the range into the ultraviolet and millimeter regions of the spectrum.

The spectra of coherent emission of chemical lasers coincide with the region of vibrational frequencies of many molecules, and this enables the use of chemical lasers for directed selective stimulation of chemical reactions by the action of radiation on selected vibrational degrees of freedom [Ref. 20].

Chemical lasers can be used to study the distribution and transfer of energy in chemical reactions and to get information on the nature of excited particles with respect to wavelength. Methods have been developed for measuring the cross sections of relaxational and other chemical-kinetic processes, based on using the radiation of chemical lasers and the peculiarities of their spectral-temporal characteristics.

Chemical lasers utilize exothermal processes during which excited inverse-population products are produced. Therefore the features of chemical lasers enumerated above include the fact that the energy required for excitation is produced by the chemical reaction proper rather than by an external source as in solid-state and gas quantum generators. However, further developments of the field of chemical lasers in science and engineering have shown that they should cover a wider class of quantum mechanical systems, including with external sources of energy (such as γ-quanta, electrons and the like) that are used as initiators of a chemical reaction since these reactions may be photolytic and radiolytic. Excimer lasers can also be included in the clase of chemical lasers with consideration of the kinetics of conversions of substances during a reaction. Inversion can also be obtained in plasma chemical reactions under the influence of nuclear fission products in fuel elements --evels [Ref. 21].

Ref. 22 presents still another qualitatively new possibility of pumping quantum generators. It is proposed that quantum generators utilize phototransitions that arise upon collision of two molecules that are capable of exothermal conversion. Such phototransitions correspond to the change of chemical bonds in molecules, i. e. they are identical to elementary chemical acts. Optical stimulation of a phototransition leads to photostimulation of the chemical process itself.

Ref. 23 also includes with chemical lasers detonation quantum generators in which the active medium is provided by detonation products.

In this book, chapters 1 and 2 are devoted to exposition of the principles of gas-phase chemical reactions typical of chemical lasers under various conditions, the fundamentals of the quantum-mechanical description of molecular systems, some processes of formation of excited particles in the course of nonequilibrium chemical reactions. These chapters explain the concepts and processes utilized in subsequent presentation of the material. Chapter 3 gives the kinetics of processes in chemical lasers.

The subsequent presentation develops the classification of quantum generators as given in Ref. 23, 24 in accordance with hydrogasdynamic characteristics that characterize both the construction of chemical laser systems and their operating principles. Therefore chapter 4 singles out chemical lasers with a stationary working medium (gas-static lasers). Chemical lasers with subsonic circulation of the medium are considered in chapter 5, while chapter 6 examines lasers with diffusion of components in a supersonic flow. Chapter 7 is devoted to chemical detonation lasers.

The considerable number of papers that have now been published on chemical lasers, and the limited scope of this book have precluded a more exhaustive presentation. The reader can fill in this gap by acquainting himself with the monographs of Ref. 16 and 25, the surveys of Ref. 23, 24, 26-42 and the specific articles of Ref. 43. Ref. 44 presents an analysis of different areas in the field of chemical lasers and the history of their development.

This book uses the SI system of units. The principal units of this system and their derivatives (N, W, J, Hz, V, F, Ω and so on), including prefixes to designate multiple and fractional values have been introduced by CEMA Standard 1052-78 and will be familiar to the reader, with the exception of the recently introduced pressure unit Pa [pascal]. Therefore we will give here the conversion of this unit to the previously widely used nonstandard units of physical and technical atmospheres, and millimeters of mercury: 1 Pa = $9.8692 \cdot 10^{-6}$ atm (physical) = $10.1972 \cdot 10^{-6}$ at (technical) = $7.5006 \cdot 10^{-3}$ mm Hg.

For approximate calculations it is convenient to use the relations 1 MPa ≈ 10 atm (at), 1 kPa ≈ 7.5 mm Hg.

REFERENCES

1. Basov, N. G., Krokhin, O. N., "Conditions of Plasma Heating by Laser Emission", ZHURNAL EKSPERIMENTAL'NOY I TEORETICHESKOY FIZIKI, Vol 46, 1964, p 171;

   Pashinin, P. P., Prokhorov, A. M., "Production of a Dense High-Temperature Plasma With Laser Heating of a Special Gas Target", Preprint No 160, Lebedev Physics Institute [FIAN], Moscow, 1970; ZHURNAL EKSPERIMENTAL'NOY I TEORETICHESKOY FIZIKI, Vol 60, 1971, p 1630;

   Velikhov, Ye. P., Filyukov, A. A., "New Approach to Using Lasers for Controlled Fusion" in: "Problemy lazernogo termoyadernogo sinteza" [Problems of Laser-Driven Nuclear Fusion], Moscow, 1976, pp 3-14.

2. "Molecular Amplifier and Oscillator on Submillimeter Waves", ZHURNAL EKSPERIMENTAL'NOY I TEORETICHESKOY FIZIKI, Vol 34, No 6, 1958, p 1658.

3. Basov, N. G., Krokhin, O. N., Popov, Yu. M., "Generation, Amplification and Display of Infrared and Optical Radiation Using Quantum Systems", USPEKHI FIZICHESKIKH NAUK, Vol 72, No 2, 1960, pp 161-209;

   Basov, N. G., Vul, B. M., Popov, Yu. M., "Quantum-Mechanical Semiconductor Generators and Amplifiers of Electromagnetic Waveforms", ZHURNAL EKSPERIMENTAL'NOY I TEORETICHESKOY FIZIKI, Vol 37, No 2, 1959, pp 587-588.

4. Shawlow, A. L., Townes, C. H., "Infrared and Optical Masers", PHYS. REV., Vol 112, No 6, 1958, pp 1940-1949.

5. Maiman, T. H., "Stimulated Optical Radiation in Ruby", NATURE, Vol 187, No 4736, 1960, pp 493-494.

6. Ablekov, V. K., Pesin, M. S., Fabelinskiy, I. L., "Realization of a Medium With Negative Absorption Coefficient", ZHURNAL EKSPERIMENTAL'NOY I TEORETICHESKOY FIZIKI, Vol 39, No 3, 1960, pp 892-893.

7. Javan, A., Bennett, W. R., Harriott, D. R., Jr., "Population Inversion and Continuous Optical Maser Oscillation in a Gas Discharge Containing an He-Ne Mixture", PHYS. REV. LETT., Vol 6, No 3, 1961, pp 106-110.

8. Basov, N. G., Prokhorov, A. M., "Using Molecular Beams for Radiospectroscopic Investigation of Rotational Spectra of Molecules", ZHURNAL EKSPERIMENTAL'NOY I TEORETICHESKOY FIZIKI, Vol 27, No 4, 1954, pp 431-438; "Molecular Oscillator and Amplifier", USPEKHI FIZICHESKIKH NAUK, Vol 57, No 3, 1955, pp 481-501.

9. Gordon, J. P., Zeiger, H. J., Townes, C. H., "Molecular Microwave Oscillator and New Hyperfine Structure in the Microwave Spectrum of NH_3", PHYS. REV., Vol 95, No 1, 1954, pp 282-284.

10. Fabrikant, V. A., "Radiation Mechanism of a Gas Discharge", TRUDY VSESOYUZNOGO ORDENA LENINA ELEKTROTEKHNICHESKOGO INSTITUTA IMENI V. I. LENINA, No 41, 1940, p 236.

11. Fabrikant, V. A., Vudynskiy, M. M., Butayeva, F. A., "A Method of Amplifying Electromagnetic Emissions", USSR Patent No 123209 (filing No 5767491, 18 Jun 51), BYULLETEN' IZOBRETENIY No 20, 1959, p 29; "Phenomenon of Amplification of Electromagnetic Waves", Certificate of Discovery No 12, 18 Jun 51, BYULLETEN' IZOBRETENIY No 8, 1962.

12. Polanyi, J. C., "Proposal for an Infrared Maser Dependent on Vibrational Excitation", J. CHEM. PHYS., Vol 34, No 1, 1961, pp 347-348.

13. Orayevskiy, A. N., "Arisal of Sub-Zero Temperatures in Chemical Reactions", ZHURNAL EKSPERIMENTAL'NOY I TEORETICHESKOY FIZIKI, Vol 45, No 2, 1963, p 177.

14. Tal'roze, V. L., "The Problem of Generation of Coherent Induced Radiation in Chemical Reactions", KINETIKA I KATALIZ, Vol 5, No 1, 1964, pp 11-27.

15. Kasper, J. V. V., Pimentel, G. C., "HCl Chemical Laser", PHYS. REV. LETT., Vol 14, No 10, 1965, pp 352-354.

16. Kompa, K. L., "Chemical Lasers", Berlin, Springer Verlag, 1973.

17. Suchard, S. N., Pimental, G. C., "Dueterium Fluoride Overtone Chemical Laser", APPL. PHYS. LETT., Vol 18, 1971, pp 530-531.

18. Sadie, F. G., Büger, P. A., Malan, O. G., "Continuous-Wave Overtone Bands in a CS_2-O_2 Chemical Laser", J. APPL. PHYS., Vol 43, 1972, pp 2906-2907.

19. Skribanowitz, N., Herman, I. P., Osgoot, R. M., Jr., et al., "Anisotropic Ultrahigh Gain Emission Observed in Rotational Translations in Optically Pumped HF Gas", APPL. PHYS. LETT., Vol 20, 1972, pp 428-432.

20. Tal'roze, V. L., Barashev, P. P., "Chemical Action of Laser Emission", ZHURNAL VSESOYUZNOGO KHIMICHESKOGO OBSHCHESTVA IMENI D. I. MENDELEYEVA, Vol 8, No 1, 1973, p 5.

21. Gudzenko, L. I., Yakovlenko, S. I., "Plazmennyye lazery" [Plasma Lasers], Moscow, Atomizdat, 1978.

22. Pekar, S. I., "High-Pressure Chemical Lasers and Light-Stimulated Chemical Reactions", DOKLADY AKADEMII NAUK SSSR, Vol 187, No 3, 1969, pp 555-557.

23. Warren, W. R., Jr., "Chemical Lasers", ASTRON. AND AERON. Vol 13, No 4, 1975.

24. Christiansen, W. H., Russel, D. A., Hertzberg, A., "Flow Lasers", ANNUAL REV. FLUID MECH., Vol 7, 1975, pp 115-139.

25. Bashkin, A. S. et al., "Chemical Lasers" in: "Itogi nauki i tekhniki. Radiotekhnika" [Advances in Science and Technology. Radio Engineering], Vol 8, Moscow, VINITI, 1975, p 382.

26. Orayevskiy, A. N., "Chemical Lasers", KHIMIYA VYSOKIKH ENERGIY, Vol 8, No 1, 1974, pp 3-20.

27. Solimeno, S., "Chemical Lasers", PHYS. BULL., Nov 74, pp 517-520.

28. Dzhidhoyev, M. S., Platonenko, V. T., Khokhlov, R. V., "Chemical Lasers", USPEKHI FIZICHESKIKH NAUK, Vol 100, No 4, 1970, pp 641-679.

29. Heavens, O. S., "Some Recent Developments in Gas Lasers", CONTEMP. PHYS., Vol 17, No 6, 1976, pp 529-552.

30. Cool, T. A., "The Transfer Chemical Lasers: a Review of Recent Research", IEEE J. OF QUANTUM ELECTRONICS, Vol QE-1, No 1, 1973, pp 72-83.

31. Karnyushin, V. N., Soloukhin, R. I., "Using Gasdynamic Flows in Laser Technology", FIZIKA GORENIYA I VZRYVA, No 2, 1972, pp 163-202.

32. Jones, C. R., Broida, H. P., "Chemical Lasers in the Visible", LASER FOCUS, Vol 10, No 3, 1974, pp 37-47.

33. Basov, N. G. et al., "Dynamics of Chemical Lasers (Survey)", KVANTOVAYA ELEKTRONIKA, No 2, 1971, pp 3-24.

34. Chester, A. N., "Chemical Lasers: A Survey of Current Research", PROC. IEEE, Vol 61, No 4, 1973, pp 414-422;

Chester, A. N., Hess, L. D., "Study of the HF Chemical Laser by Pulse-Delay Measurements", IEEE J. OF QUANTUM ELECTRONICS, Vol QE-8, No 1, 1972, pp 3-13.

35. Gross, R. W. F., Bott, J. F., ed., "Handbook of Chemical Lasers", a Wiley Interscience Publication, New York, 1976.

36. Ewing, J. J., "New Laser Sources" in: "Chemical and Biochemical Applications of Lasers", Vol II, edited by C. B. Moore, N. Y.-San Francisco-London, Academic Press, 1977, pp 241-278.

37. Soloukhin, R. I., "State of the Art and Outlook for Gasdynamic Combustion Lasers" in: "Goreniye i vzryv" [Combustion and Explosion], Moscow, Nauka, 1977, pp 30-49.

38. Orayevskiy, A. N., "Chemical Lasers" in: "Spravochnik po lazeram" [Laser Handbook], edited by A. M. Prokhorov, Vol 1, Moscow, Sovetskoye radio, 1978, pp 158-183.

39. "Chemical and Molecular Lasers", J. OPT. SOC. AMER., 1978, Vol 68, No 5, pp 651-656.

40. Yeletskiy, A. V., "Excimer Lasers", USPEKHI FIZICHESKIKH NAUK, Vol 125, No 2, 1978, pp 279-314.

41. "UV and Excimer Lasers. I", J. OPT. SOC. AMER., Vol 68, No 5, 1978, pp 702-706; II, Ibid., pp 711-718.

42. Knyazev, I. N., Letokhov, V. S., "Gas Lasers in the UV and XUV Regions of the Spectrum" in: "Spravochnik po lazeram", edited by A. M. Prokhorov, Vol 1, Moscow, Sovetskoye radio, 1978, pp 197-220.

43. Bashkin, A. S., Kupriyanov, N. L., Orayevskiy, A. N., "Chain-Reaction Chemical Lasers in the Optical Band", KVANTOVAYA ELEKTRONIKA, Vol 5, No 12, 1978, pp 2611-1619; "Use of Excited Atoms in Optical-Band Chemical Lasers with Thermal Initiation", Ibid., pp 2567-2576.

44, Dunskaya, I. M., "Lazery i khimiya" [Lasers and Chemistry], Moscow, Nauka, 1978, 164 pages.

CHAPTER 1: PRINCIPLES OF KINETICS OF GAS-PHASE CHEMICAL REACTIONS

§1.1. Law of Effective Masses

In chemical lasers, processes take place chiefly in the gas phase, and to get an idea of the chemical reactions in these lasers it is necessary to know the rates and proportions of reactions of the initial gases, and the composition of intermediate and final products. Therefore we will consider the principles that govern chemical reactions in gaseous media.

Reaction Rate. Rate Constant. Consider a gas made up in the general case of chemical components A_i ($i = 1, 2, \ldots, n$), i. e. of N_1 molecules of component A_1, N_2 molecules of component A_2, N_3 molecules of component A_3 and so on. Then a chemical reaction that converts initial components $A_1, A_2, \ldots, A_i$ into reaction products $A_1', A_2', \ldots, A_i'$ can be recorded by the stoichiometric equation

$$\sum_{i=1}^{N} r_i A_i \rightarrow \sum_{i=1}^{N} r_i' A_i', \qquad (1.1)$$

where r_i and r_i' are the *stoichiometric coefficients* of the reaction for the i-th substance that is in the state of an initial reagent and a reaction product respectively.

For a system with fixed volume V and fixed composition, the relation between changes of concentration of any two substances i and j taking part in the reaction is expressed on the basis of relation (1.1) as

$$\bar{w}_i/(r_i' - r_i) = \bar{w}_j/(r_j' - r_j). \tag{1.2}$$

Here $\bar{w} = V^{-1}\Delta N/\Delta t$ mole/(cm^3·s) is the change in mole concentration $c = N/V$ of the substance in time Δt, i. e. the average rate of the chemical reaction.

The chemical reaction rate w in the general case is a function of the concentrations of the reacting substances, pressure and temperature [Ref. 1]. The dependence of the reaction rate on concentrations of the reagents c_i is defined by the law of effective masses: *the reaction rate is proportional to the product of concentrations of the reacting substances.* Thus for a reaction of general form (1.1)

$$w = kc_1^{r_1} c_2^{r_2} \ldots = k \prod_{i=1}^{N} c_i^{r_i}, \tag{1.3}$$

where k is the *rate constant* or *specific reaction rate.* The value of k usually increases rapidly with rising temperature.

Simple Reaction. Order of a Reaction. Molecularity. According to the derivation of the *law of effective masses* from the kinetic theory of gases, the number of simultaneous collisions when r_1 molecules of substance A_1 (of concentration c_1) interact with r_2 molecules of substance A_2 (of concentration c_2) and so on, is proportional to the product $c_1^{r_1}c_2^{r_2}\ldots$ Or vice versa: the rate of single-stage reactions that involve the simultaneous interaction of $r_1 + r_2 + \ldots = r$ molecules must be expressed by the law of effective masses [Ref. 2]. Reactions that meet this condition are called *simple reactions.*

By definition

$$dc_i/dt = w_i, \qquad i = 1, \ldots, N, \tag{1.4}$$

and in the elementary stage of the reaction

$$w_i = (r_i' - r_i)\, w. \tag{1.5}$$

With consideration of relations (1.3) and (1.5), we get for the i-th and j-th substances instead of equation (1.4)

$$dc_i/dt = [(r_i' - r_i)\, k] \prod_{j=1}^{N} c_j^{r_j}, \tag{1.6}$$

where $(r_i' - r_i)k$ is constant for isothermal systems. Usually measurements of the quantity dc_i/dt in isothermal systems lead to

$$dc_i/dt \sim \prod_{j=1}^{N} c_j^{n_j}, \tag{1.7}$$

where exponents n_j are constants. In such cases, the number n_i is called the *order of the reaction* with respect to the i-th substance, and $n \equiv \sum_{i=1}^{N} n_i$ is called the *resultant order*, or simply the order of the reaction.

We can see from formulas (1.6) and (1.7) that if the reaction is simple, $n_i = r_i$. Then the quantity n_i is the molecularity of the reaction with respect to substance i, and n is the total molecularity of the reaction. Thus the *molecularity* of a reaction is determined by the number of molecules participating in the process: at r = 1, the reaction is of the first order, or monomolecular; when r = 2, the reaction is of the second order and so on.

A relation of form (1.7) often holds even when equation (1.6) is invalid, i. e. when the reaction consists of several stages. In such cases the relation between the order of a reaction and molecularities becomes complicated, and n_i may take on non-integer values [Ref. 3].

§1.2. Mechanisms of Simple Reactions

First-Order Reaction. When the rate of change in concentration is proportional to concentration, it is said that a first-order reaction is taking place. Such a reaction is the simplest chemical process. According to the law of effective masses (1.3), the reaction rate of a first-order reaction for reagent A_1 (i=1) is

$$w = -dc_1/dt = kc_1, \tag{1.8}$$

where

$$k\,[c^{-1}] > 0.$$

After integration of equation (1.8), we get at concentration c_1^0 known at the initial instant t = 0:

$$c_1 = c_1^0 \exp(-kt) = c_1^0 \exp(-t/\tau). \tag{1.9}$$

From (1.9) we get an expression for the reaction rate constant

$$k = (1/t) \ln (c_1^0/c_1). \tag{1.10}$$

At $t = \tau$, the concentration of reagent A_1 decreases by a factor of e. The quantity $\tau_e = 1/k$ is called the *characteristic reaction time*. We can also judge the rate of the chemical reaction from the *half-life* or *half-period* of the reaction $\tau_{1/2}$-- the time during which the initial concentration c_1^0 decreases to one-half: $\tau_{1/2} = \ln 2/k$. The simplest type of reaction that conforms to equation (1.8) is the monomolecular reaction of dissociation of a substance

$$AB \rightarrow A + B. \tag{1.11}$$

[Note: Hereafter in addition to the purely numerical designations of reagents A_i and reaction products A_i', we will also use letter combinations: A, B, C, ..., AB, BC, ...]

It is assumed that molecule AB is stable and will not spontaneously dissociate into reaction products. What then is the mechanism of the monomolecular process?

It is assumed that not all molecules are subject to dissociation, but rather only the especially activated molecules that have internal energy exceeding the *activation energy* E_a. Such molecules are called *active*. According to Ref. 4, many monomolecular reactions occur in two stages

$$AB + M \underset{k_2}{\overset{k_1}{\rightleftarrows}} AB^* + M; \tag{1.12}$$

$$AB^* \xrightarrow{k_3} AB^{\neq} \rightarrow A + B, \tag{1.13}$$

The first of which is activation (k_1) and deactivation (k_2) of the molecules, while the second is dissociation (k_3). In (1.12), (1.13), M denotes an arbitrary molecule, the asterisk after AB means that the molecule is in the excited (in this case unstable) state, and the rate constants k_1, k_2, k_3 for elementary stages of the reaction are indicated above and below the arrows.

On the second stage (1.13), monomolecular transformation takes place due to intramolecular redistribution of energy. Since such transformation requires that the energy of the active particle be concentrated on certain degrees of freedom, we introduce the concept of the *activated molecule* $AB^{\neq}$ that is the instantaneous state of the molecule through which the reaction is terminated.

First-order reactions and the second-order reactions described below play an essential part in chemical kinetics since most elementary stages are monomolecular or bimolecular reactions.

Reactions of Second and Higher Orders. When molecules A_1 and A_2 form molecules of type A' in reaction (1.1), and when the reaction rate in this case is proportional to the concentrations of both initial substances, it is said that a second-order reaction is taking place.

The kinetics of a second-order chemical reaction for reagents A_1, A_2 is described by the equation

$$-\frac{dc_1}{dt} = -\frac{dc_2}{dt} = kc_1c_2, \tag{1.14}$$

where k has the dimensionality of $cm^3/(mole \cdot s)$.

After integration of equation (1.14) like (1.9), (1.10), we get under known initial conditions $c_1 = c_1^0$ and $c_2 = c_2^0$:

$$\frac{c_1}{c_2} = \frac{c_1^0}{c_2^0} \exp\left[-(c_2^0 - c_1^0)kt\right]. \tag{1.15}$$

whence the expression for the reaction rate constant will be

$$k = \frac{1}{t}\frac{1}{c_2^0 - c_1^0}\ln\frac{c_2 c_1^0}{c_2^0 c_1}. \tag{1.16}$$

Examples of second-order reactions are bimolecular reactions of dissociation of hydrogen iodide $2HI \rightarrow H_2 + I_2$, and thermal dissociation of chlorine oxide $2\ Cl_2O \rightarrow 2Cl_2 + O_2$.

Consider the n-th order reaction

$$A + B + C + \ldots \rightarrow \text{reaction products.}$$

If $c_1^0 = c_2^0 = \ldots = c^0$, the reaction rate will be

$$-dc/dt = kc^n. \tag{1.17}$$

Integrating (1.17), we get an expression for the reaction rate constant

$$k = \frac{1}{t(n-1)}\left(\frac{1}{c^{(n-1)}} - \frac{1}{(c^0)^{(n-1)}}\right), \tag{1.18}$$

with dimensionality of $(cm^3/mole)^{(n-1)} \cdot s^{-1}$.

For $c = c^0/2$, $t = \tau_{1/2}$,

$$k = \frac{(2^{(n-1)} - 1)}{\tau_{1/2}(n-1)}\frac{1}{(c^0)^{(n-1)}} \tag{1.19}$$

and

$$\tau_{1/2} = \frac{(2^{(n-1)} - 1)}{k(n-1)}\frac{1}{(c^0)^{(n-1)}}. \tag{1.20}$$

Thus, for the general case of an n-th order reaction

$$\tau_{1/2} \sim (c^0)^{-(n-1)}, \tag{1.21}$$

i. e. the way that the half-period of the reaction depends on the initial concentration characterizes the actual order of the reaction. It is taken as unlikely that chemical reactions with molecularity of more than three will play a role in chemical processes, since reactions with higher molecularity take place extremely slowly.

§1.3. Chemical Equilibrium

Equilibrium Conditions and Equilibrium Constant. Since chemical reactions go in both directions, equation (1.1) should be rewritten as

$$\sum_{i=1}^{N} r_i A_i \underset{k_b}{\overset{k_f}{\rightleftarrows}} \sum_{i=1}^{N} r_i' A_i', \tag{1.22}$$

i. e., side by side with *forward reaction* (1.1) is its *reverse reaction.*

If the equilibrium concentrations are denoted by c_{ie} and c_{je}, then the condition of equilibrium of the forward and reverse reactions will be

$$k_f \prod_{i=1}^{N} c_{ie}^{r_i} = k_b \prod_{j=1}^{N} c_{je}^{r_j'}. \tag{1.23}$$

Whence we get the *equilibrium constant*

$$K_c = \frac{k_f}{k_b} = \prod_{j=1}^{N} c_{je}^{r_j'} \Big/ \prod_{i=1}^{N} c_{ie}^{r_i}. \tag{1.24}$$

Tables and handbooks usually give values of the equilibrium constant K_p expressed in terms of the partial pressures p_i, p_j of the substances participating in the reaction

$$K_p = \prod_{j=1}^{N} p_j^{r_j'} \Big/ \prod_{i=1}^{N} p_i^{r_i}. \tag{1.25}$$

Arrhenius Law. Ref. 5 gives the temperature dependence of the equilibrium constant K measured at constant volume or pressure as a function of the heat of reaction Q:

$$d \ln K/dT = -Q/RT^2. \tag{1.26}$$

where R is the gas constant.

For the temperature dependence of the rate constant k, Arrhenius [Ref. 6] proposed the analogous equation

$$d \ln k/dT = E_a/RT^2,$$

where E_a is the difference of energies of the active and inactive molecules of the initial substances, i. e. the *activation energy*. If E_a is constant, then

$$\ln k = \text{const} - E_a/RT,$$

or, setting $\ln A = \text{const}$, we get

(1.27)

where A is the *frequency factor* or *preexponential factor.*

In the Arrhenius law (1.27) quantity A may be weakly dependent on temperature T. In this event the approximate formula

$$A = BT^{\alpha} \tag{1.28}$$

is used for all reactions within the limits of experimental error, with consideration of the fact that B = const, α = const and $0 \leqslant \alpha \lesssim 1$.

Research results of Ref. 7 give the concept of the order of preexponential factor A from investigation of reactions of dissociation and isomerization of substances.

In general in accordance with the method of the transitional state [Ref. 8-10] the preexponential factor A is represented as the product of the *gas-kinetic number of collisions* Z_0 multiplied by the so-called *steric factor* P that characterizes the effectiveness of a single collision of molecules with respect to the course of the chemical reaction or directionality of interaction leading to the formation of a chemical bond.

Sometimes the reaction proceeds with considerable deviations of the preexponential factor A from the usual values of 10^{12}-10^{15} s^{-1}. For especially large values of A it is assumed [Ref. 11] that the monomolecular reaction law is only apparent, and in reality the reaction takes place by a chain mechanism.

Arrhenius law (1.27) may be theoretically substantiated by using assumptions of the kinetic theory of gases (see for example Ref. 12).

Activation Energy. Only a small number of all colliding molecules enter into reaction, and only those whose total kinetic energy upon collision exceeds some critical value E_a. These molecules are lower in number the more this energy exceeds the average energy of the system ($(3/2)k^0T$ for monatomic gases, $(5/2)k^0T$ for diatomic gases; k^0 is Boltzmann's constant). Usually E_a for the reaction is several tens of thousands of joules per mole, whereas the average energy at a temperature of 1000°C is only a few thousand. This means that on the maxwellian curve of velocity distribution of the molecules the reaction is characterized only by the branch in the region of velocities that exceed some critical velocity.

For example for $E_a \approx 84$ kJ/mole the percentage of molecules that are capable of entering into reaction is only 0.0045% at 1000°C, and increases to 0.67% at 2000°C.

Concepts of the molecular structure of matter imply that a homogeneous reaction in an ideal gas takes place upon collisions of two or three molecules. The collision and the subsequent reaction are described by the Schrödinger equation in which the independent variables are the coordinates of all electrons and nuclei of the interacting molecules. For a collisional process that is slow enough that the solution of the unsteady Schrödinger equation is not different from that of the steady-state Schrödinger equation, and the kinetic energy of each nucleus is small compared with that of the electrons, we can assume that the nuclei move over trajectories on the *potential energy surface*.

The height of the energy barrier of a reaction on the potential energy surface is equal to the activation energy E_a necessary for rearrangement of intramolecular

bonds. This definition can be illustrated by an examination of the change of energy states in the bimolecular chemical reaction $A + BC \rightarrow AB + C$ in coordinates of potential energy E_p versus the reaction coordinate (Fig. 1.1), for example the instantaneous reaction time t.

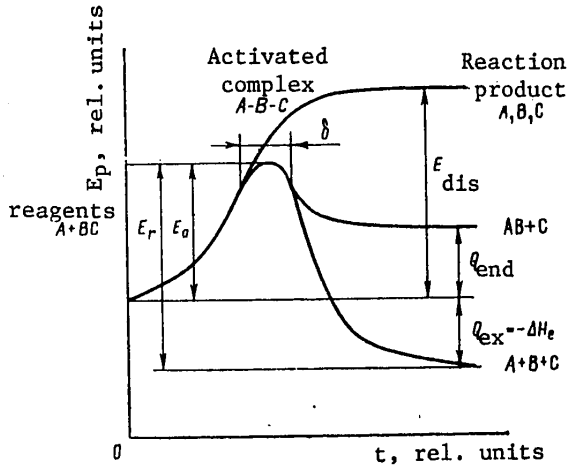

Fig. 1.1. Change of potential energy of system in the process of collision of A with BC

If the energy of atom A is quite high, the bonds between atoms A, B and C will be totally broken--dissociation of molecule BC will occur (upper curve on Fig. 1.1). If a chemical reaction takes place between A and BC, the potential energy reaches a maximum (middle curve on Fig. 1.1), the interatomic bonds are not completely broken, and the system is in unstable equilibrium--the activated state of A-B-C. Then depending on the type of reaction the process will follow either the middle or lower curve. In the former case the reaction is endothermic, and in the latter case it is exothermic.

The activation energies are different for forward and reverse reactions. From Fig. 1.1. we see that the endothermic reaction that is the reverse of the exothermic reaction has activation energy $E_r = E_a + Q_{ex}$, where Q_{ex} is the *reaction energy release.*

§1.4. Complex Reactions

Sequential Reactions. The simplest kinetic equations of first, second and third orders for chemical reactions describe only an extremely small number of the processes that take place. However, most chemical reactions take place in separate monomolecular or bimolecular stages with formation of intermediate products.

Many complex reactions have two or more stages that follow each other:

$$A \xrightarrow{k_1} B \xrightarrow{k_2} C \text{ and so on}$$

or

$$A + B \xrightarrow{k_1} C + D \xrightarrow{k_2} M + N.$$

Such reactions are called *reactions with sequential stages*. In these reactions, the substance that is formed in the first stage is capable of continued chemical reaction, and further chemical transformation is realized in subsequent stages of the reaction. Such substances are called *intermediate substances*.

It follows from Ref. 13 that each stage has its own potential energy surface that is independent of the others. Reaction systems, in passing through the highest energy barrier, do not necessarily have to go through all intermediate states. Therefore the rate of a reaction with sequential stages is determined by the rate of transition of the activated complex through the highest energy barrier.

Parallel Reactions. The simplest type of *parallel reaction* is one in which the initial substance is transformed by two or more independent paths resulting in either identical or different reaction products:

$$\mathrm{A} \underset{k_2}{\overset{k_1}{\rightarrow}} \begin{matrix} \mathrm{M} \\ \mathrm{N} \end{matrix}.$$

Let us write out the kinetic equations for such reactions, assuming that each of them is monomolecular:

$$dc_M/dt = k_1 c_A, \quad dc_N/dt = k_2 c_A. \tag{1.29}$$

After dividing one equation by the other and integrating, we get

$$c_M/c_N = k_1/k_2, \tag{1.30}$$

i. e. the yields of products of parallel reactions are to each other as the rate constants of these reactions.

Let us determine the rate constant of such an ultimate reaction:

$$-dc_A/dt = dc_M/dt + dc_N/dt = (k_1 + k_2)\, c_A = kc_A. \tag{1.31}$$

Consequently, the rate constant of the ultimate reaction in the case of two or more parallel stages is equal to the sum of the rate constants of these stages $k = \Sigma k_i$.

Conjugate Reactions. Chemical Induction. A peculiarity of some parallel reactions that are quite widespread in chemistry is the fact that one of these reactions (A + B) can proceed only when the other parallel reaction (A + C) is taking place simultaneously in the system. These reactions are called *conjugate*; this phenomenon in chemistry has been termed *chemical induction*. The inducing reaction (A + B) is called *primary*, and the conjugate reaction (A + C) that it induces is called *secondary*. Substance A that takes part in both reactions is called the *actor*, substance B whose interaction with the actor induces the secondary reaction, is called the *inductor*, and substance C is called the *acceptor*.

Such a process is characterized by the *induction factor*--the ratio of the fraction of the actor that takes part in transformation of the acceptor, to the fraction of the actor that takes part in transformation of the inductor.

As an example of conjugate reactions, Ref. 2 gives simultaneous oxidation of carbon monoxide and hydrogen. In the absence of impurities, the reaction $2CO + O_2 = 2CO_2$ does not occur up to quite high temperatures, but when hydrogen is present in the mixture the reaction takes place readily [Ref. 14, 15]. In these reactions, hydrogen is the inductor, CO is the acceptor and O_2 is the actor that takes part in reactions with both H_2 and CO. The induction factor is the ratio of the amounts of CO_2 and H_2O that are formed.

The effect of chemical induction is based on the formation of intermediate substances in the course of the primary reaction that produce direct transfer of the inductive effect of the primary reaction to the secondary reaction [Ref. 16].

Based on this reasoning, conjugate reactions are described by a set of two elementary processes $A + B = X + \ldots, + X + C = M + \ldots$ (A is the actor, B is the inductor, C is the acceptor, X is the intermediate substance, M is the reaction product), for which the following equations are valid:

$$\left.\begin{aligned} -dc_A/dt = -dc_B/dt &= k_1 c_A c_B; \\ dc_X/dt &= k_1 c_A c_B - k_2 c_C c_X; \\ -dc_C/dt = dc_M/dt &= k_2 c_C c_X. \end{aligned}\right\} \qquad (1.32)$$

When $c_A^0 = c_B^0 = c_C^0 = c^0$:

$$-dc_A/dt = k_1 c_A^2;\ dc_X/dt = k_1 c_A^2 - k_2 (c_A + c_X) c_X.\} \qquad (1.33)$$

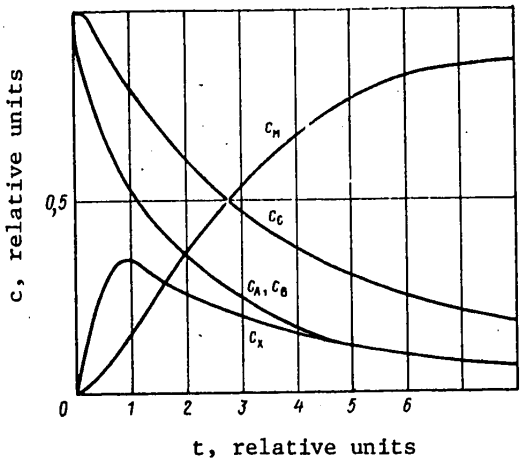

Fig. 1.2. Kinetic curves for conjugate reactions

From the solution of these differential equations (Fig. 1.2) we can see that the acceptor C is expended more slowly than the actor A and the inductor B, and the

curve for expenditure of C is S-shaped, i. e. it can be seen that substance C is brought into the reaction only via intermediate substance X, which is low in concentration at the initial instant. The limiting case of conjugate reactions can be taken as homogeneous catalytic reactions since here as well an active intermediate substance is formed upon primary interaction of the actor with the catalyst inductor. In the case of acceleration of the reaction this inductor is a *positive catalyst*, while in the case of retardation it is a *negative catalyst* or *inhibitor*. The reactions frequently fall into time-separated macroscopic stages, the inhibitor influencing only the first of these--the inducing stage [Ref. 17]. There are reactions [Ref. 18, 19] during which direct accumulation of catalyst takes place that is a product of the reaction itself. This leads to self-acceleration of the reaction--*autocatalysis*. The kinetic equations of autocatalysis in most cases do not describe the actual reaction mechanism. For example it is shown in Ref. 20, 21 that it is the rate of branched-chain reactions with a complex mechanism that corresponds to the kinetics of autocatalysis.

§1.5. Chain Reactions

Kinetics of Chain Reactions. Sometimes a series of sequential reactions has a rate that exceeds the rate of the forward reaction according to equation (1.1). This occurs in cases where the active particles or *centers* A are replaced in the course of one or more stages of the reaction $1 \to 3$, as shown in the diagram of Fig. 1.3. An active particle A arises simultaneously with a molecule of reaction

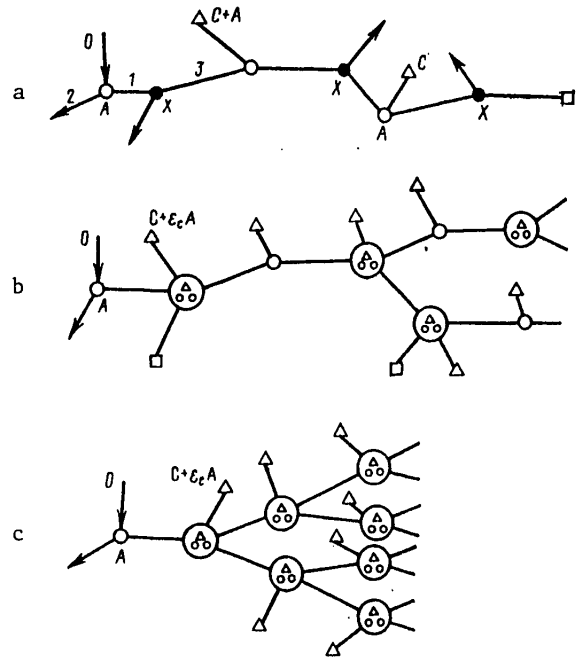

Fig. 1.3. Diagram of simple, $\varepsilon_c > 1$ (a), branched $2 > \varepsilon_c > 1$ (b) and continuously branched, $\varepsilon_c = 2$ (c) chain reactions: ○--active centers A; △--reaction products C; □--reaction byproducts; ●--intermediate substance

product C. The rate of such a reaction in the steady-state case (see Fig. 1.3a) can be expressed by the equation

$$w = w_0 P_1 P_3 + w P_1 P_3, \tag{1.34}$$

where w_0 is the rate of thermal activation of a molecule, and P_i is the probability of each of i = 1, 2, 3, 4 elementary processes.

Introducing chain length l_C, we find from (1.34)

$$w = \frac{w_0}{[(1/P_1 P_3) - 1]} = w_0 l_c, \tag{1.35}$$

$$l_c = \frac{1}{[(1/P_1 P_3) - 1]} = \frac{P_1 P_3}{(1 - P_1 P_3)}. \tag{1.36}$$

It has been experimentally demonstrated that the principal active centers of such *chain reactions* are chemically unsaturated fragments of molecules--*free atoms and molecules*. The chains realized by these fragments are called *radical chains*.

Simple Chain Reactions. The reactions described by expressions (1.34)-(1.36) are called *simple chain reactions*. In these reactions, in each link of the chain there is no more than one newly formed center for each disappearing active center.

In the kinetics of chain reactions [Ref. 21], the probability of a reaction following path 1 is called the *chain continuation probability* $P_1 = \alpha_C$ with steady-state reaction rate

$$w = \frac{dc_C}{dt} = \frac{w_0 \alpha_c}{1 - \varepsilon \alpha_c} = w_0 l_c, \tag{1.37}$$

where

$$l_c = \alpha_c/(1 - \varepsilon\alpha_c). \tag{1.38}$$

For simple chain reactions $\varepsilon = 1$ and the chain length l_C is the average number of links per active center, i. e. the *average chain length*. The chain continuation probability for s links is

$$P_s = \alpha_c^s (1 - \alpha_c). \tag{1.39}$$

where $1 - \alpha_C = \beta_C$ is the chain breaking probability.

The time development of a reaction is described by the following expression for reaction rate

$$w = \nu_1^{\alpha_c} c_A = \frac{w_0 \alpha_c}{1 - \varepsilon \alpha_c} \left[1 - \exp\left(-\frac{t}{\tau}\right)\right] = w_0 l_c \left[1 - \exp\left(-\frac{t}{\tau}\right)\right], \tag{1.40}$$

where ν^{α_C} is the frequency of particle interaction events, τ is the lifetime of an active center.

For a chain reaction with chain breaking $\alpha_c < 1$. In this case the probability of chain breaking β_c is proportional to chain length l_c:

$$\beta_c \sim l_c^{-1}. \tag{1.41}$$

Active particles with a mean free path shorter than the dimensions of the vessel are brought to the walls by diffusion flux

$$q_D = -D dc_A/dx, \tag{1.42}$$

where D is the coefficient of diffusion, dc_A/dx is the concentration gradient of active centers along the normal to the wall of the vessel.

If we now consider the process along this normal and introduce the concept of the "normalized film" with thickness Δ [Ref. 22], then (1.42) implies

$$q_D = (D/\Delta)(c_A - c'_A), \tag{1.43}$$

where c'_A is the concentration of active centers close to the surface.

In the steady-state case, setting q_D equal to the flux due to the reaction of chain breaking on the wall surface, we get

$$(D/\Delta)(c_A - c'_A) = kc'_A, \tag{1.44}$$

whence

$$c'_A = \frac{D/\Delta}{k+(D/\Delta)} c_A, \tag{1.45}$$

and the reaction rate is

$$w = kc'_A = \frac{kD/\Delta}{k+(D/\Delta)} c_A. \tag{1.46}$$

Designating the effective rate constant by k*, we have

$$k^* = \frac{kD/\Delta}{k+(D/\Delta)} \quad \text{or} \quad \frac{1}{k^*} = \frac{1}{k} + \frac{1}{D/\Delta}, \tag{1.47}$$

where k^{-1} and $(D/\Delta)^{-1}$ are the *diffusional* and *kinetic resistances* respectively.

We can see from formulas (1.46) and (1.47) that when $k \gg D/\Delta$ $k^* = D/\Delta$ and the reaction rate is determined by diffusion. In such an event the reaction is said to take place in the *diffusion region* with $c'_A \ll c_A$. At $k \ll D/\Delta$ we have $k^* = k$ and the ultimate reaction rate is determined by the rate of the chemical process itself, i. e. the reaction takes place in the *kinetic region* with concentration c'_A nearly equal to c_A.

Reactions With Branched Chains. Chain reactions in which an average of more than one active center is produced for every disappearing center in the course of the reaction are called *branched*. The probability of branching at each link of the chain is [Ref. 21]

$$\delta_c = \varepsilon_c - 1. \tag{1.48}$$

When $\delta_C > 0$, branchings arise from time to time on individual sections of the chain, and the additional active centers give rise to secondary branched chains (see Fig. 1.3b). When $\delta_C = 1$ ($\varepsilon_C = 2$), branching takes place on every link of the chain (see Fig. 1.3c). Chains that arise in this way are called *continuously branched*.

Let us calculate the length of a branched chain l'_C, i. e. the number of elementary reactions caused by the appearance of a single primary active center. The effective chain breaking probability will be equal to the difference $\beta_C - \delta_C$. Consequently with consideration of (1.41):

$$l'_c = 1/(\beta_c - \delta_c) = l_c/(1 - l_c\delta_c); \tag{1.49}$$

$$w = c_X^0 l'_c = c_X^0 l_c/(1 - l_c\delta_c). \tag{1.50}$$

Since β_C and δ_C are functions of temperature and pressure, under certain conditions it may happen that $\beta_C - \delta_C \cong 0$, and then the length of the chain $l'_C \to \infty$. This means that if at least one branching takes place on the length of a simple chain, i. e. $l_C\delta_C = 1$, an explosive process arises.

Limiting Phenomena. At a certain vapor pressure of phosphorus in a mixture with oxygen, the region of ignition is bounded by two limiting oxygen pressures $(p_{O_2})_1$ and $(p_{O_2})_2$. Outside this region, phosphorus vapor does not ignite. Quantitative investigations of this process together with a study of ignition of a stoichiometric mixture of hydrogen with oxygen [Ref. 26-28] have yielded fundamental results for the theoretical description of the effect by N. N. Semenov [Ref. 21, 29].

The existence of such limiting pressures--lower and upper limits of ignition of substances--can be explained by peculiarities of kinetics and the mechanism of the branched chain reaction. In a simple chain reaction ($\varepsilon_C\alpha_C < 1$) the rate of a comparatively slow steady-state reaction is $w = w_0\alpha_C/(1 - \varepsilon_C\alpha_C)$. In the case of a branched chain reaction ($\varepsilon_C\alpha_C \geqslant 1$), the reaction rate (1.40) is

$$w = w_0 \frac{\alpha_c}{\varepsilon_c \alpha_c - 1} (\exp \varphi t - 1), \tag{1.51}$$

where

$$\varphi = -\frac{1}{\tau} = (\nu_1^{\alpha_c} + \nu_2^{\alpha_c})(\varepsilon_c \alpha_c - 1). \tag{1.52}$$

For $\phi t \gg 1$ from (1.51) and (1.52) with consideration of the fact that $\alpha_c = P_1 = \nu_1^{\alpha_c}/(\nu_1^{\alpha_c} + \nu_2^{\alpha_c})$, we get *Semenov's law*:

$$w = \frac{w_0 \nu_1^{\alpha_c}}{\varphi} \exp \varphi t. \tag{1.53}$$

When $\varepsilon_c \alpha_c > 1$ the reaction becomes rapid and self-accelerating, terminating in an explosion. Transition from the steady to the unsteady state is determined by the condition

$$\varepsilon_c \alpha_c = 1. \tag{1.54}$$

From this, considering (1.48) and the relation for the chain continuation probability $\alpha_c = \nu_1^{\alpha_c}/(\nu_1^{\alpha_c} + \nu_2^{\alpha_c})$, we get

$$\delta_c \nu_1^{\alpha_c} = \nu_2^{\alpha_c}. \tag{1.55}$$

The pressure dependences of $\nu_1^{\alpha_c}$ and $\nu_2^{\alpha_c}$ can be written as

$$\nu_1^{\alpha_c} = ap \text{ and } \nu_2^{\alpha_c} = bp^2 + b', \tag{1.56}$$

where $\nu_2^{\alpha_c}$ is expressed as the sum of terms, of which the first characterizes the volumetric breaking of chains by the triple collision mechanism, while the second term characterizes breaking of chains on the walls in the kinetic region of the reaction.

Expressions (1.55) and (1.56) imply

$$p^2 - \delta ap/b + b'/b = 0, \tag{1.57}$$

with a solution that gives the pressures on the lower (p_1) and upper (p_2) limits of ignition:

$$p_1 = \delta a/2b - \sqrt{\delta^2 a^2/4b^2 - b'/b}, \tag{1.58}$$

$$p_2 = \delta a/2b + \sqrt{\delta^2 a^2/4b^2 - b'/b}. \tag{1.59}$$

The graph of the temperature dependence of p_1 and p_2 (Fig. 1.4) is conventionally called the "ignition peninsula" and $p = p_M$ is called the "cape of the ignition peninsula."

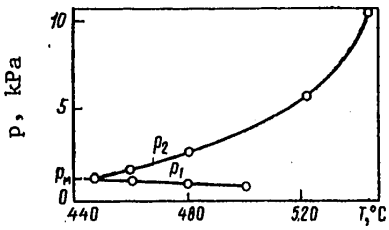

Fig. 1.4. Ignition peninsula of a mixture of $2H_2/O_2$

§1.6. Elementary Processes of Excitation of Systems in Chemical Reactions

Principles of Quantum-Mechanical Description of Molecular Systems. Quantum mechanics describes the relation between the structure of atoms and molecules and their spectra, gives a representation of the energy distribution in a molecular system, its excitation, relaxation and chemical reactivity. Transition of the system from one state to another is accompanied by absorption or radiation of energy:

$$h\nu = E_2 - E_1, \tag{1.60}$$

where h is Planck's constant, $\nu = c/\lambda$ is the frequency of a quantum, λ is wavelength, c is the speed of light. Or, replacing ν with the wave number $\omega = \nu/c$ [cm^{-1}], we get

$$\omega = (E_2 - E_1)/ch. \tag{1.61}$$

When the molecular system absorbs light quanta, the energy of the system changes depending on the energy of the absorbed quanta: rotational motion of the molecule (R) when the energy of the absorbed quanta is 0.125-1.25 kJ/mole; vibration of nuclei (V) at 1.25-50 kJ/mole; electron motion (E) at energies of the order of tens and hundreds of kJ/mole.

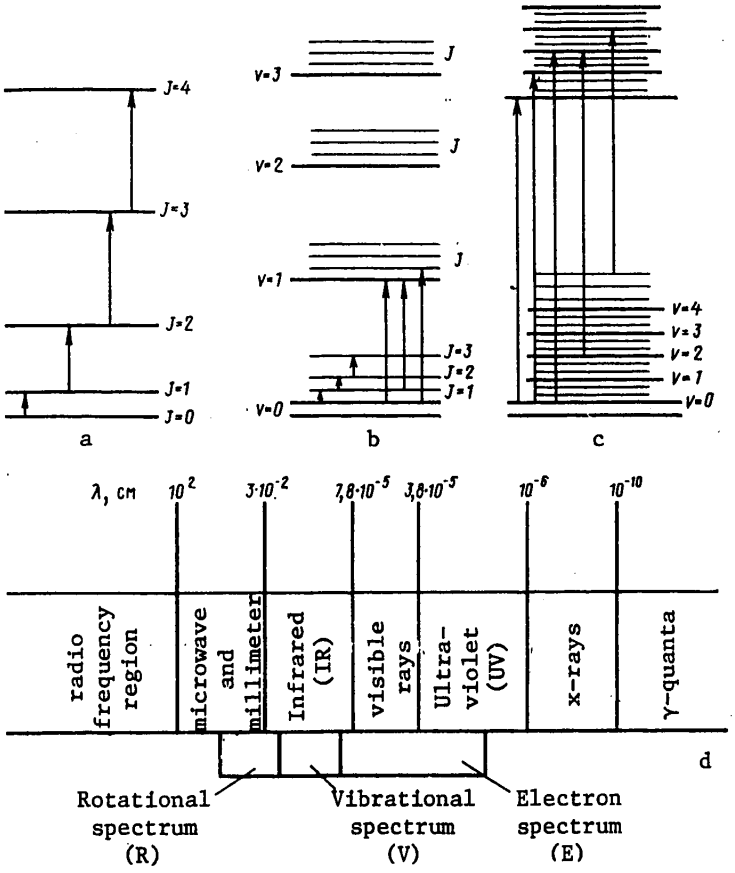

Fig. 1.5. Diagrams of energy levels and transitions R (a), V-R (b), E-V-R (c) of spectra, and their corresponding regions of electromagnetic radiation (d)

Corresponding to such changes of energy are the schemes of energy levels and transitions shown in Fig. 1.5a-c, and also regions of the spectrum of electromagnetic radiation (Fig. 1.5d). Here the far infrared, microwave and millimeter regions correspond to rotation R-spectra (a), the IR-region corresponds to vibrational-rotational spectra V-R (b), and the visible and ultraviolet correspond to electron (E) or electronic-vibrational-rotational (E-V-R) spectra (c).

A molecule can be represented as a harmonic oscillator with energy

$$E_v = hc\omega_e (v + 1/2), \tag{1.62}$$

where v = 0, 1, 2, 3... is the *vibrational quantum number* that defines the level of vibrational energy, ω_e corresponds to the ground state v = 0 with energy $E_0 = \frac{1}{2}hc\omega_e$, that exists even at the zero of temperature. For the harmonic oscillator the difference of energies of adjacent states is

$$E_{v+1} - E_v = hc\omega_e. \tag{1.63}$$

From (1.61) we have

$$E_{v+1} - E_v = hc\omega, \tag{1.64}$$

i. e. $\omega = \omega_e$.

However, the model of a real molecule is an anharmonic oscillator, and ω must differ from ω_e, but this difference is small at low values of the vibrational quantum number v.

Because of anharmonicity, the V-levels of energy with increasing v gradually get closer together, and (1.62) is replaced by the two-term formula

$$E_v = hc\omega_e (v + 1/2) - hc\omega_e x_e (v + 1/2)^2 \tag{1.65}$$

with constant $x_e \ll 1$ characterizing anharmonicity. In this case, transitions with $\Delta v > 1$ become possible--*overtones*. Upon a further increase in v, the energy of the molecule reaches the value E_{max}, and when $E_{max} - E_0 = D_0$ the molecule dissociates.

The R-structure of the vibrational band is determined by the change in rotational energy $E_J = BJ(J+1)$ in the V-transition:

$$E'_J - E''_J = B'J'(J' + 1) - B''J''(J'' + 1), \tag{1.66}$$

where J = 0, 1, 2, ... is the *rotational quantum number*, B *is the rotational constant.*

For dipole radiation $\Delta J = J' - J'' = 0, \pm 1$ respectively we get the three branches of the spectrum $\mathcal{Q}$, $\mathcal{R}$, $\mathcal{P}$. But since transitions $\Delta J = 0$ are forbidden in the ground electronic state for most diatomic molecules, only the positive $\mathcal{R}$- and negative $\mathcal{P}$-branches are observed.

The E-energy or E-V-R-energy of molecules depends in a complicated way on their structure, and the electronic energy states of molecules are classified by symmetry types. For example the electronic states or terms of diatomic and axially symmetric linear polyatomic molecules are classified according to:

a) quantum numbers Λ characterizing the absolute value of the projection of the complete orbital moment $\vec{L}$ on the axis of the molecule (in units of $h/2\pi$). The quantum number Λ can take on values of $\Lambda = 0, 1, 2, 3, \ldots, L$ denoted by Σ, Π, Δ, Φ respectively.

b) multiplicity $2S+1$, where S is the quantum number of the resultant spin of all electrons in the molecule. Multiplicity is placed to the upper left in the symbol of state, e. g. $^3\Sigma$;

c) total orbital moment $\vec{L}+\vec{S}$ characterized by a figure at the lower right for terms different from Σ, e. g. $^3\Pi_2$;

d) the property of symmetry of the electronic eigenfunction of the molecule symbolized by the sign "+" or "-" for state Σ to the upper right. In any plane that passes through the line connecting the nuclei, the electronic eigenfunction either remains unchanged (Σ^+) or changes sign (Σ^-);

e) evenness (g) or oddness (u) of the state for molecules in which the nuclei have the same charge, e. g. $^1\Sigma_g^+$, $^1\Sigma_u^+$.

In the potential energy surface system the electronic state with the minimum that lies lowest is called the ground state and is denoted by the symbol X placed before the symbol of state ($X^1\Sigma_g^+$), and the letters A, B, C,... are used for the characteristics of a sequence of excited electron states. For light molecules, a sequence of excited states that differ in multiplicity from the ground state is symbolized by the letters a, b, c,..., while states that are the same in multiplicity are denoted by A, B, C,... The state with the greatest possible value of S and the greatest possible value of L (at the given S) has the lowest energy for a given electron configuration (*Hund's rule*).

Since the energies of electrons, vibrations of nuclei and rotations of molecules are quantized, the total energy is also quantized

$$E = E_{el} + E_{vib} + E_{rot}. \tag{1.67}$$

The quantity $|E_i|/hc$ for each i-th level is called a *term*. The corresponding term can be represented in the form of a sum of three terms:

$$T = E_i/hc = T_{el} + G(v) + F(J), \tag{1.68}$$

where T_{el}, $G(v)$, $F(J)$ are the electronic, vibrational and rotational terms respectively.

At E-transitions in molecules, as can be seen from the diagram of Fig. 1.5d, a quantum of light is emitted in the UV and visible regions of the spectrum, or more rarely in the near-IR region. Superposition of V- and R-transitions on electron transitions produces a fine structure of the electron spectrum (see Fig. 1.5c).

The system of V-R levels (see Fig. 1.5b) can be obtained by solving the Schrödinger equation for a molecule in the nonrigid rotator approximation--the anharmonic vibrator. In doing this, the value of the potential energy is substituted in the Schrödinger equation in the form of some function of the internuclear distance r. In Ref. 30, the convenient empirical equation

$$E_{\text{п}}(r) = D_0\{1 - \exp[-a(r - r_e)]\}^2 \tag{1.69}$$

is proposed as the potential energy curve for diatomic molecules, where D_0 is the energy of dissociation, r_e is equilibrium distance, a is a constant for the molecule. Also used is the form of the Lennard-Jones potential close to the real form:

$$E_{\text{п}}(r) = 4\varepsilon[(\sigma/r)^{12} - (\sigma/r)^{6}], \tag{1.70}$$

where ε is the force constant, and σ is the average diameter of the colliding spheres.

Energy Distribution of Products of Chemical Reactions. The energy released in elementary chemical processes is distributed over different energy levels or degrees of freedom of the ultimate reaction products [Ref. 13, 31-33]. The nature of this distribution determines for example the nonequilibrium luminescence in the course of the reaction in the visible or UV regions of cool flames of hydrocarbons and CS_2 [Ref. 14, 34, 35]. In combustion reactions, nonequilibrium luminescence is observed in the IR region of the spectrum [Ref. 36] corresponding to V-transitions.

Reactions can be divided into two types: those that take place within the limits of a single potential energy surface, and are usually accompanied by V-excitation--*adiabatic reactions* [Ref. 77]--and those that include more than one potential energy surface and are frequently accompanied by E-excitation--*nonadiabatic reactions*.

The concept of a reaction in the form of a curve or potential energy surface is particularly useful in cases where the relation between E- and V-motions is weak. If we know the potential energy, we can get the electronic energy of the system for arbitrary fixed positions of nuclei. The potential energy surface is either calculated or determined from experimental data [Ref. 38]. In doing this, two problems are solved: finding the surface, and using it to describe the experimental results.

However, one need not know the complete structure of the surfaces to interpret experimental data. The energy distribution of reaction products can be determined even by such qualitative characteristics of the surfaces as the radius of action of forces, the relative slope of parts of the potential energy surface that correspond to the initial reagents and products, and energy parameters [Ref. 39]. Let us consider the energy distribution of products [Ref. 40-44] based on the example of a substitution reaction of the type

$$A + BC \rightleftarrows AB + C \tag{1.71}$$

that is typical of chemical lasers.

This reaction can be divided into three stages: first--approach of atom A to complex BC; second--an intermediate stage where the B-C bond is stretched out in the course of the continuing approach; third--separation of reaction products AB and C. Let E_1, E_2, E_3 be the energies released in these three stages of the process. The relation between E_1, E_2, E_3 is considerably dependent on the type of potential energy $E_{\text{п}}(r_{AB}, r_{BC})$. The major portion of E_1 is released as vibrational energy, E_3--in the form of kinetic energy, and the percentage of E_2 converted to the E_{vib} of the molecules is higher, the heavier the atom A as compared with B and C [Ref. 41]. For example, in the case of the interaction $H + Cl_2$, most of the energy is

released on the second and third stages [Ref. 40, 41]. Of interest for chemical lasers are reactions with high ratios of E_{vib}/E_{kin}. Large values of E_{vib}/E_{kin} can be attained in reactions in which a hydrogen atom is replaced by a heavier atom such as deuterium or a metal, and also in the reactions $F+H_2$, $Cl+HI$ and so on.

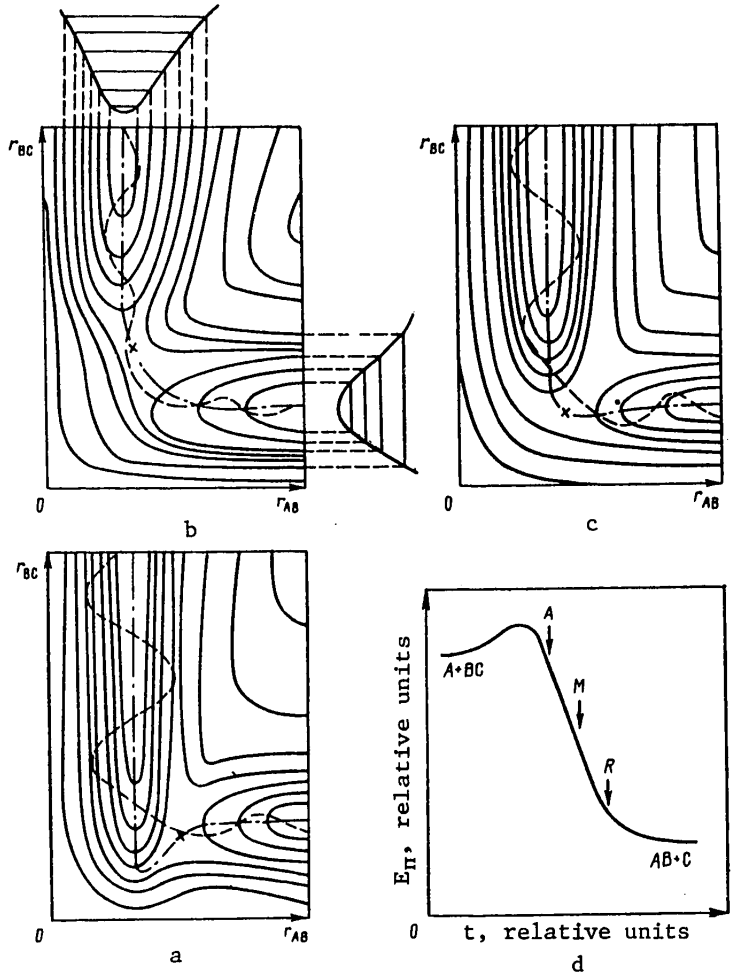

Fig. 1.6. The potential energy surfaces of a system of atoms in phases of attraction (a), repulsion (b), and mixed energy release (c), and a graph of the reaction

The potential energy surfaces of a system of atoms are shown in Fig. 1.6 in phases of attraction (a), repulsion (b) and mixed energy release (c). The solid curves show lines of constant energy, the dot-and-dash curves indicate the coordinate of the reaction (the potential energy increases to both sides of this line), and the broken curves show the possible trajectory of motion of the system during the

reaction (1.71). If the energy of the system is slightly greater than the activation energy of the reaction, these trajectories pass close to the saddle point on the potential energy surface indicated by the cross.

If the form of the function $E_{\Pi}(r_{AB}, r_{BC})$ corresponds to Fig. 1.6a, then the most probable trajectories are those with energy release on the stage of approach of A and BC since after the system has passed the potential barrier, r_{AB} decreases, and r_{BC} changes but little, i. e. here we have energy release in the attraction phase.

For the reaction corresponding to Fig. 1.6b, after the system has passed the potential barrier there is little change in r_{AB}, while r_{BC} increases, i. e. energy release takes place on the stage of dispersal, or in other words on the repulsion phase.

In the intermediate case of Fig. 1.6c, we have mixed energy release in region M of the graph of the reaction in Fig. 6.1d, where the phases of attraction and repulsion are indicated by the letters A and R respectively. With energy release in region M, the nature of the most probable trajectories depends to a great extent on the ratio between masses of particles.

Adiabatic and Nonadiabatic Interactions, Energy Resonance. If two or more colliding particles have relative velocities that are small compared with the orbital velocities of electrons, then the electrons will have time for rearrangement in accordance with the instantaneous positions of the nuclei, and as a result their energy will depend only on the relative positions of the nuclei of the atoms. This simplification is known as the *Born-Oppenheimer approximation*. It is applicable not only to slow molecular collisions, but also to rotational and vibrational motions of nuclei in a single molecule. According to this approximation, the nuclei have certain potentials relative to one another, the approximate form of which for two different initial E-states is shown by the solid curves AB and A'B' in Fig. 1.7 [Ref. 45]. Such a slow collision without E-transitions is called adiabatic (B-A). Obviously, adiabatic collisions between two atoms will be elastic, i. e. the atoms will fly apart, if the energy is not expended on a third particle or on radiation. Adiabatic collisions of polyatomic molecules may be accompanied by rotational or vibrational excitation or a chemical reaction. On the other hand,

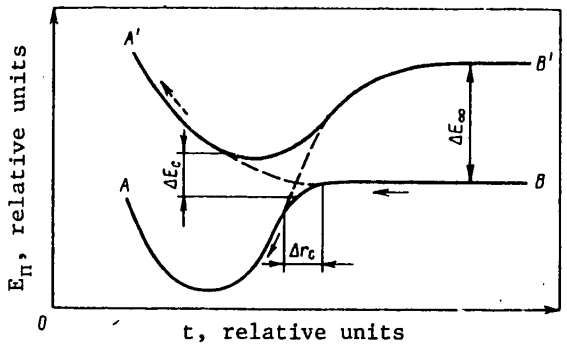

Fig. 1.7. Potential curves of collision of nuclei: B-A--adiabatic process; B-A'--nonadiabatic process

in collisions that are fast enough the electrons will not have time to rearrange, and the nuclei will follow the broken curve B-A'--a nonadiabatic collision. If the relative velocity u is still high upon separation of the nuclei, then the nuclei following this curve will again enter state B, and the collision will again be elastic.

To achieve the E-transition from B to B', the nuclei in converging must move along the solid curve, and in diverging--along the broken curve, or vice versa. Consequently, the excitation cross section has a maximum at certain intermediate velocities where the probabilities of following the solid or broken curves are equal. Quantum-mechanical analysis shows that this occurs if the time in the crossing region $\Delta r_c/u$ is approximately equal to the characteristic time of energy exchange $h/(2\pi\Delta E_e)$ (see Fig. 1.7). Under such conditions, the cross section may be nearly equal to the gas-kinetic value.

The potential curves may come together at very low ΔE_∞, i. e. when there is energy resonance between the initial and final states. However, in the thermal energy range the existence of resonance is neither a necessary nor a sufficient condition for a large excitation cross section. Potential curves that are far apart at great internuclear distances may get much closer together when these distances decrease. The reverse situation may also be realized. This is confirmed by careful measurements in exothermic reactions and "quenching" reactions [Ref. 46-48].

In the process of electronic excitation, a molecule makes a transition from the ground electron state to an excited state. The *Franck-Condon* principle answers the question of just what is the vibrational state to which the molecule will make its transition, and whether it will remain intact or be dissociated. According to this principle, the change in state of the electron shell of a molecule takes place so much more rapidly than vibrations of the atomic nuclei that there is not time for a change in either the velocity of motion nor the position of the nuclei in an E-transition [Ref. 49]. For many important transitions the relative probabilities of vibrational levels, called Franck-Condon factors, have been calculated [see for example Ref. 50].

In nonadiabatic transitions a transitional complex A-B-C may form, which may also radiate. Such a mechanism is more preferential for converting the energy of the chemical bond to the energy of radiation since it does not involve competing processes of energy dissipation. From the potential energy surface (see Fig. 1.6) it is also clear that the lower potential curves of AB and C may have a dispersive nature, and this means that complex A-B-C does not have a lower level in the usual sense of the word, and exists only in the excited state.

Such complexes made up of elements from groups I and VII of the periodic table were observed in Ref. 51. An investigation was made of chemiluminescence spectra arising in a circulating system of Na and halides X. The spectra of Na + F (0.6-0.81 μm), and Na + Cl_2 (0.42-0.55 μm) have a vibrational structure. It was concluded that the band carrier is the NaX_2 molecule formed in the reaction in the electronically excited state.

§1.7. Chemical Reactions in a Closed Space and in a Stream

Exothermic Reactions in a Closed Space. Heat of Reaction. In contrast to the rarely observed isothermic chain explosion [Ref. 52], the cause of thermal explosion

of a gas mixture in a closed volume V is a rise in temperature when the rate of heat release q^+ exceeds the rate of heat removal q^-. A general representation of such a process is given in the quantitative theory of Ref. 53 with consideration of temperature leveling within the volume.

The conditions of the explosion are characterized by the balance of q^+ and q^-

$$Qw(T_2) = \alpha_Q (S/V)(T_2 - T_0) \tag{1.72}$$

and by equality of temperature derivatives at point T_2

$$Q(dw/dT) = \alpha_Q (S/V), \tag{1.73}$$

where T_2 is the temperature of the combustion zone corresponding to explosion, α_Q is the heat transfer coefficient, S is the area of the wall surface.

For the fast processes that take place in chemical lasers it is of interest to examine the adiabatic conditions of occurrence of an incipient reaction in a closed volume [Ref. 2]. Under such conditions, all the heat released by the reaction goes to raising the temperature of the mixture, i. e.

$$c_V dT = -Qdc, \tag{1.74}$$

where c_V is the specific heat of the mixture for constant volume.

Introducing T_{max}, the temperature of complete combustion, we can get

$$dT/dt = k_0 (c_V/Q)^{n-1} (T_{max} - T)^n \exp(-E/RT). \tag{1.75}$$

The solution of this equation shows that for a certain time interval--the *ignition induction period*--the gas temperature rises slowly, and then the reaction takes place with rapid consumption of the reagent and a rapid rise in temperature.

The heat released in the closed system is equal to the *heat of reaction* $-Q \equiv -\int dQ$. We know from thermodynamics that $dQ = dH_e - V\,dp$, whence for isobaric processes $Q = \int dH_e \equiv \Delta H_e$ --the enthalpy increment of the system during the reaction. For any reaction in ideal gases, the heat released can be calculated by the formula

$$-\Delta H_e = -\sum_{i=1}^{N} (r_i' - r_i)\,\Delta H_{f,i}, \tag{1.76}$$

where $\Delta H_{j,i}$ are the tabular values of the heats of formation of molecules i.

Exothermic Reactions in a Stream. For a reacting mixture of ideal gases of density ρ moving at mass velocity $\vec{u}$, the following equations are satisfied [Ref. 3]:

the equation of continuity

$$\partial\rho/\partial t + \nabla(\rho\mathbf{u}) = 0; \tag{1.77}$$

the equation of conservation of momentum with consideration of the external force $\vec{f}_i$ acting on a unit mass of component fraction Y_i, and stress tensor P

$$\partial \mathbf{u}/\partial t + \mathbf{u}\nabla\mathbf{u} = -\nabla P/\rho + \sum_{i=1}^{N} Y_i \mathbf{f}_i; \tag{1.78}$$

the equation of conservation of energy including specific internal energy u_e and with consideration of the diffusion rate $\vec{u}_i^D$ of the i-th component

$$\rho \partial u_e/\partial t + \rho (\mathbf{u}\nabla) u_e = -(\nabla \mathbf{q}) - P:(\nabla \mathbf{u}) + \rho \sum_{i=1}^{N} Y_i (\mathbf{f}_i \mathbf{u}_i^D) \tag{1.79}$$

[the colon (:) denotes a double convoluted tensor];

the equation of continuity of chemical components

$$\partial Y_i/dt + (\mathbf{u}\nabla) Y_i = w_i/\rho - (1/\rho)(\nabla \rho Y_i \mathbf{u}_i^D). \tag{1.80}$$

The stress tensor P is defined by the formula

$$P = [p + (2\eta/3 - \eta')(\nabla \mathbf{u})] U - \eta [(\nabla \mathbf{u}) + (\nabla \mathbf{u})^{\tau}], \tag{1.81}$$

where η and η' are the coefficients of shear and volumetric viscosity respectively; U is a unit tensor, τ denotes transposition of the tensor.

The heat flux density vector $\vec{q}$ in equation (1.79), disregarding radiative heat transfer, is determined by the formula

$$\mathbf{q} = -\lambda_Q \nabla T + \rho \sum_{i=1}^{N} (h_e)_i Y_i \mathbf{u}_i^D + RT \sum_{i=1}^{N} \sum_{j=1}^{N} \left(\frac{X_j D_{T,i}}{\mu_i D_{ij}} \right) (\mathbf{u}_i^D - \mathbf{u}_j^D), \tag{1.82}$$

where λ_Q is the coefficient of heat conduction, $(h_e)_i$ and μ_i are the specific enthalpy and molar mass respectively of the i-th component, X_j is the mole fraction of the j-th component, D_{ij} is the coefficient of binary diffusion of components.

The quantity $\vec{u}_i^D$ in equations (1.79) and (1.80) for i = 1, 2,..., N components is defined by the formula

$$\nabla X_i = \sum_{j=1}^{N} \left(\frac{X_i X_j}{D_{ij}} \right) (\mathbf{u}_j^D - \mathbf{u}_i^D) + (Y_i - X_i) \left(\frac{\nabla p}{p} \right) +$$
$$+ \left(\frac{\rho}{p} \right) \sum_{j=1}^{N} Y_i Y_j (\mathbf{f}_i - \mathbf{f}_j) + \sum_{j=1}^{N} \left[\left(\frac{X_i X_j}{\rho D_{ij}} \right) \left(\frac{D_{T,j}}{Y_j} - \frac{D_{T,i}}{Y_i} \right) \right] \left(\frac{\nabla T}{T} \right). \tag{1.83}$$

External forces $\vec{f}_i$ are taken as given, w_i in equation (1.80) in accordance with the law of chemical kinetics (1.3) with consideration of (1.27) and (1.38) is defined by the expression

$$w_i = \mu_i \sum_{k=1}^{M} (r'_{i,k} - r_{i,k}) B_k T^{\alpha_k} \exp(-E_k/RT) \prod_{j=1}^{N} (X_j p/RT)^{r_{i,k}} \tag{1.84}$$

(M is the total number of chemical reactions).

The quantities Y_i, ρ, T and $\vec{u}$ can be the variables defined in equations (1.77)-(1.80). Then the other variables can be expressed through them by the equation of state of an ideal gas

$$p = \rho RT \sum_{i=1}^{N} \frac{Y_i}{\mu_i}, \tag{1.85}$$

the expression for the specific internal energy of the gas mixture

$$u_e = \sum_{i=1}^{N} (h_e)_i Y_i - p/\rho, \tag{1.86}$$

the caloric equation of state, including the specific heat of formation $(h_j)_i$ of component i at temperature T_0

$$(h_e)_i = (h_f)_i + \int_{T_0}^{T} c_{p,i}\, dT \tag{1.87}$$

($c_{p,i}$) is the specific heat of component i at constant pressure) and the relation

$$X_i = Y_i \left(\mu_i \sum_{j=1}^{N} \frac{Y_j}{\mu_j} \right)^{-1}. \tag{1.88}$$

In the case of a homogeneous inviscid steady-state flow without mass forces, equations (1.77)-(1.83) are vastly simplified.

From (1.77) we get

$$\rho u = \text{const.} \tag{1.89}$$

Equation (1.78) is converted to

$$\rho u du/dx + dp/dx = 0, \tag{1.90}$$

in which the integral $\rho u^2 + p = \text{const}$. Equation (1.79) gives

$$\rho u (h_e + u^2/2) + q = \text{const} \tag{1.91}$$

and from (1.80) we have

$$\frac{d}{dx} [\rho Y_i (u + u_i^D)] = w_i. \tag{1.92}$$

If we disregard conductive heat transfer and take $q = 0$, then for steady-state flow of an inviscid medium equations (1.90)-(1.92) respectively take the form

$$\frac{u du}{dx} = -\frac{1}{\rho} \frac{dp}{dx}; \tag{1.93}$$

$$\frac{d}{dx} \left(h_e + \frac{u^2}{2} \right) = 0; \tag{1.94}$$

$$u dY_i/dx = w_i/\rho. \tag{1.95}$$

For a channel of variable cross section S(x) the equation of continuity takes the form

$$d(\rho u S)/dx = 0. \tag{1.96}$$

The equation of state (1.85) and equations (1.86), (1.87) together with expression $h_e = u_e + p/\rho$ relate the thermodynamic parameters h_e and p to the quantities ρ, T, $\vec{u}$, Y_i ($i = 1, 2, \ldots, N$). Then equations (1.93)-(1.96) are a system of $N+3$ ordinary differential equations of first order for the $N+3$ unknowns Y_i, T, ρ and u. If we assign all the parameters of the flow and the area S in some cross section as a function of x, we can get the flow characteristics at any other point of the channel by integrating equations (1.93)-(1.96) with consideration of relations (1.84)-(1.88).

More exact calculation should account for the boundary layer on the wall of the channel, the ratio of the thickness of displacement of the inviscid flow to the thickness of loss of momentum, and the local coefficient of friction on the wall with flow of a relaxing gas [Ref. 54]. In this case we can use as an approximation the dimensionless numbers obtained for laminar or turbulent flow around a flat plate [Ref. 55].

Photochemical Reactions. As pointed out in §1.2, it is only the activated molecule that undergo chemical transformation. If molecules are activated by redistribution of energy during collisions in thermal processes such as those described above, the necessary activation energy of a molecule in photochemical processes is provided by absorption of radiation from an external source with intensity I_ν.

In this case the *Stark-Einstein law of photochemical equivalence* is satisfied: in a photosensitive system subjected to the action of radiation with frequency ν, there is one activated molecule for every absorbed quantum of energy $h\nu$.

Thus the kinetics of photochemical reactions is dependent on the laws of absorption of light by the substance, and is associated with the *quantum yield of the reaction* ϕ defined as the ratio of the number of reacting molecules to the number of quanta absorbed by the molecules. When one absorbed quantum causes conversion of a single molecule, $\phi = 1$. In reality, due to deactivation $\phi < 1$, and vice versa, in the case of photoinitiation of secondary exothermic chain reactions $\phi \gg 1$. In the case of stimulated emission with photolytic or some other kind of initiation of a chemical reaction, the *quantum yield of stimulated emission* ϕ_{se} is defined as the ratio of the number of quanta of the medium participating in stimulated emission in a unit volume of the medium to the concentration n_a of active centers produced by the initiation:

$$se = \frac{\varepsilon_{se}/h\nu_{se}}{n_a} \qquad (1.97)$$

(ε_{se} and ν_{se} are respectively the specific energy and frequency of the stimulated emission).

Kinetic effects are characteristic of many reactions with pulsed photoinitiation: depending on initial conditions (initiation energy, temperature, concentration of reagents, total pressure of the mixture), an explosive state is realized with almost total chemical conversion, or a state with fairly weak conversion of the reagents.

There is a threshold of transition from one state to the other. A quantitative description of such threshold phenomena and of the kinetics of the photoinitiated reaction $F_2 + D_2(H_2)$ inhibited by O_2 is given in Ref. 56, 67 using concepts of the theory of thermal acceleration of the reaction that are the basis of the theory of thermal explosion [Ref. 21].

The regime of the photoinitiated chain reaction is considered in Ref. 57 in the adiabatic approximation in the absence of gradients of temperature and concentrations of active particles. It is assumed that the reaction goes through a single active center, and the nucleation of active centers is realized by volumetrically uniform photoinitiation. The solution of equations for the concentration of active particles and reaction heat balance implies that the kinetic nature of the curves changes sharply with a slight change in heating near its critical value. The branched reaction is typified by a sharp rise in the curves, associated with a sharply expressed reaction induction period.

The existence of the critical condition is due to competition between processes of thermal acceleration of the reaction and the deceleration due to annihilation of active centers. Such a course of pulse-photoinitiated chemical reaction under conditions of progressive self-acceleration due to the accumulation of heat or active cneters in the system is a photothermal explosion [Ref. 57].

Nonequilibrium Effects in Chemical Reactions. Chemical Reactions in an Electric Discharge. Real chemical reactions take place under appreciably nonequilibrium conditions, i. e. with deviation from the Maxwell-Boltzman distribution function of particles with respect to velocities and internal states. Such a deviation stems naturally from the fact that molecules with energies higher than E_a are reactive, and consequently the distribution function is continuously depleted in the high-energy region due to disappearance of reacting molecules.

The solution of equations that describe the behavior of the distribution function in nonequilibrium chemical processes and that comprise a system of nonlinear integral equations presents mathematical difficulties, and therefore recourse is taken to various simplifications of the problem in analyzing relaxation processes. For example the system is broken down into subsystems: equilibrium, "frozen" and relaxing.

In some cases we restrict ourselves to examining the distribution function for the number of particles n with respect to energies $n_A(E)\,dE$, i. e. the probability in a system with a surplus of molecules B of detecting relaxing molecules A in states with energies close to E in an interval dE. Then the rate of change in population is

$$\frac{dn_A(E)}{dt} = -c_B \int P(E, E')\, n_A(E)\, dE' + c_B \int P(E', E)\, n_A(E')\, dE', \tag{1.98}$$

where P(E, E') is the probability of a transition in a unit of time at unit concentrations of A and B for a molecule of A from energy level E to levels in the energy range E', E' + dE' at unit concentration of molecules of B. These probabilities satisfy the relation

$$\frac{P(E, E')}{P(E', E)} = \frac{\rho(E')}{\rho(E)} \exp\left[-\frac{E' - E}{k_0 T}\right], \tag{1.99}$$

which includes the density $\rho(E)$ of energy levels of the relaxing degrees of freedom of molecules of A.

In cases where reaction and relaxation overlap, the kinetic equations expressed in terms of concentrations are in general invalid, although even in this case the problem

can be reduced to macroscopic equations that describe the behavior of both the concentrations and other parameters of the nonequilibrium distribution function such as the temperatures corresponding to different types of degrees of freedom [Ref. 58-63].

Indeed it is the chemical reactions with sharply nonequilibrium parameters of the reaction products that are responsible for processes in chemical lasers. For example if the distribution of the products with respect to energy levels both during the reaction and after its completion is nonequilibrium, or if during the chemical reaction the rate of formation of products in upper energy states exceeds the rate of formation of products on lower levels, we have *population inversion* of energy levels. The same thing can be accomplished in redistribution of energy with respect to different degrees of freedom of a molecular system.

Excitation of reaction products to electronic, rotational and vibrational nonequilibrium states is possible in reactions of the following types:

photodissociation

$$ABC + h\nu \rightarrow AB^* + C; \tag{1.100}$$

exothermic exchange

$$A + BC \rightarrow AB^* + C,\ A + BC \rightarrow AB + C^*; \tag{1.101}$$

dissociative energy transfer

$$AB + M^* \rightarrow A^* + B + M; \tag{1.102}$$

the recombination process that is inverse to dissociation

$$A + B + M \rightarrow AB^* + M,\ A + B + M \rightarrow AB + M^*. \tag{1.103}$$

The next chapter deals with the excitation of products in a number of such nonequilibrium chemical reactions.

In the present section we will briefly take up appreciably nonequilibrium processes in chemical reactions that occur in an electric discharge plasma.

The electromagnetic gas dynamics of plasma flow in external electric and magnetic fields is considered for example in Ref. 64. The quantitative picture of distribution of these fields in the discharge region can be found by numerical methods such as those in Ref. 65, 66. An even more difficult problem is accounting for the chemical reaction in an appreciably nonequilibrium electric-discharge plasma.

In discharges, and especially in pulse discharges, the energy distribution of electrons is nonequilibrium, whereas the energy of translational motion of heavy particles conforms to quasiequilibrium distribution.

The approximate method of numerical calculation of the kinetic characteristics of nonequilibrium reactions in electric discharges without consideration of hydrodynamic processes (e. g. see Ref. 67) includes simultaneous consideration of:

equations of chemical kinetics

$$\frac{\partial n_i}{\partial t} = \sum_j k_{ij} n_j + \sum_{j,k} k_{ijk} n_j n_k \tag{1.104}$$

(n_j are the concentrations of components participating in the reaction: electrons, ions, neutral and excited particles; k_{ij}, k_{ijk} are rate constants of ionization, recombination, dissociation and other processes);

Maxwell's equations

$$\left.\begin{aligned} \text{curl } \mathbf{H} &= \frac{\partial \mathbf{D}}{\partial t} + \mathbf{j}; \\ \text{div } \mathbf{D} &= \rho_e; \\ \text{curl } \mathbf{E} &= -\frac{\partial \mathbf{B}}{\partial t}; \\ \text{div } \mathbf{B} &= 0; \\ \mathbf{D} &= \varepsilon' \mathbf{E}, \end{aligned}\right\} \tag{1.105}$$

where $\vec{E}$ and $\vec{D}$ are respectively the intensity and induction of the electric field; $\vec{H}$ and $\vec{B}$ are the intensity and induction of the magnetic field, $\vec{j}$ and ρ_e are the current and charge densities of the external sources.

In this system of equations the properties of the fluid are expressed in terms of the complex permittivity that depends on the specific conductivity of the plasma and the electromagnetic field frequency.

From (1.105) with satisfaction of the inequalities [Ref. 68]

$$\left|\frac{\partial \varepsilon'}{\partial t}\frac{\partial \mathbf{E}}{\partial t}\right| \ll \left|\varepsilon' \frac{\partial^2 \mathbf{E}}{\partial t^2}\right|; \quad \left|\frac{\partial^2 \varepsilon'}{\partial t^2}\mathbf{E}\right| \ll \left|\varepsilon \frac{\partial^2 \mathbf{E}}{\partial t^2}\right| \tag{1.106}$$

we get a steady-state wave equation that together with (1.104) forms a nonlinear system. In this system the reaction rate constants k_{ij}, k_{ijk} depend on electric field strength $\vec{E}(\vec{r})$, and the complex permittivity ε' depends on the time-variable electron concentration n_e obtained from the solution of equation (1.104), and on the effective frequency of sollisions of these electrons with heavy particles, which depends in turn on $\vec{E}(\vec{r})$ and on n_e.

Nonstationary equation (1.104) and the steady-state wave equation with boundary conditions determined in the course of numerical solution by a method of iterations were integrated in Ref. 68 for reactions in an appreciably nonequilibrium nitrogen plasma produced in a pulsed microwave discharge.

As an example of examination of a chemical reaction in an electric discharge we can also cite the analysis in Ref. 69, 70 of the reaction of dissociation of carbon dioxide in a low-pressure discharge.

REFERENCES

1. Emanuel', N. M., KNORRE, D. G., "Kurs khimicheskoy kinetiki" [Course in Chemical Kinetics], Moscow, Vysshaya shkola, 1962.

2. Kondrat'yev, V. N., Nikitin, Ye. Ye., "Kinetika i mekhanizm gazofaznykh reaktsiy" [Kinetics and Mechanism of Gas-Phase Reactions], Moscow, Nauka, 1974, 558 pages.

3. Williams, F. A., "Teoriya goreniya" [Theory of combustion]: translated from English by S. S. Novikov and Yu. S. Ryazantsev, Moscow, Nauka, 1971, 615 pages.

4. Lindemann, F. A., "Discussion on 'The Radiation Theory of Chemical Action'", TRANS. FARADAY SOC., Vol 17, 1922, pp 598-606.

5. Van't Hoff, J. H., "Ocherki po khimicheskoy dinamike" [Essays on Chemical Dynamics], Leningrad, Ob"yedineniye nauchno-tekhnicheskikh izdatel'stv [ONTI], 1936, 178 pages.

6. Arrhenius, S., "Über die reaktionsgeschwindigkeit bei der Inversion von Rohrzucker durch Säuern", Z. PHYS. CHEM., Vol 4, 1889, pp 226-248.

7. Vedeneyev, V. I., Kibalko, A. A., "Konstanty skorosti gazofaznykh monomolekulyarnykh reaktsiy" [Rate Constants of Gas-Phase Monomolecular Reactions], Moscow, Nauka, 1972, 164 pages.

8. Eyring, H., "Activated Complex in Chemical Reactions", J. CHEM. PHYS., Vol 3, 1935, pp 107-115.

9. Wigner, E. P., "The Transition-State Method", TRANS. FARADAY SOC., Vol 34, 1938, pp 29-41.

10. Pelzer, H., Wigner, E., "Velocity Coefficient of Interchange Reactions", Z. PHYS. CHEM., Vol 15, 1932, pp 445-471.

11. Semenov, N. N., "Mechanism of Chain Dissociation of Paraffin Halide Derivatives", USPEKHI KHIMII, Vol 21, 1952, pp 641-713.

12. Khitrin, L. N., "Fizika goreniya i vzryva" [Physics of Combustion and Explosion], Moscow, Izdatel'stvo Moskovskogo gosudarstvennogo universiteta [MGU], 1957, 442 pages.

13. Glasston, S., Leydler, K., Eyring, H., "Teoriya absolyutnykh skorostey reaktsiy" [Theory of Absolute Reaction Rates]: translated from English, edited by A. A. Balandin, N. D. Sokolov, Moscow, Izdatel'stvo inostrannoy literatury, 1948, 583 pages.

14. Kondrat'yev, V. N., "Kinetika khimicheskikh gazovykh reaktsiy" [Kinetics of Chemical Gas Reactions], Moscow, Izdatel'stvo Akademii nauk SSSR, 1958, 668 pages.

15. Kondrat'yeva, Ye. I., Kondrat'yev, V. N., "Active Centers in the Reaction of Combustion of Carbon Monoxide", ZHURNAL FIZICHESKOY KHIMII, Vol 21, 1947, pp 769-776.

16. Ostwald, W., "Über Oxydationen mittels freien Sauerstoffs", Z. PHYS. CHEM., Vol 34, 1900, pp 248-252.

17. Emanuel', N. M., "Kinetics of the Slow Reaction of Hydrogen Sulfide Oxidation", ZHURNAL FIZICHESKOY KHIMII, Vol 14, 1940, pp 863-876.

18. Ostwald, W., "Studien zur chemischen Dynamik", Z. PRACT. CHEM., Vol 28, 1883, pp 449-495.

19. Ostwald, W., "Lehrbuch der allgemeinen Chemie", Vol 2, Leipzig, 1887.

20. Semenov, N. N., "Types of Kinetic Curves of Chain Reactions", DOKLADY AKADEMII NAUK SSSR, Vol 43, 1944, pp 360-366.

21. Semenof, N. N., "Tsepnyye reaktsii" [Chain Reactions], Leningrad, GKhTI, 1934, 555 pages.

22. Frank-Kamenetskiy, D. A., "Diffuziya i teploperedacha v khimicheskoy kinetike" [Diffusion and Heat Transfer in Chemical Kinetics], 2-nd edition, Moscow-Leningrad, Nauka, 1967, 491 pages.

23. Khariton, Yu. B., Walta, Z. F., "Oxydation von Phosphordämpfen bei niedrigen Drucken", Z. PHYS., Vol 39, 1926, pp 547-556.

24. Semenov, N. N., "Die Oxydation des Phosphordampfes bei niedrigen Drucken", Z. PHYS., Vol 46, 1972, pp 109-131.

25. Kovalskii, A. A., "Kindling of Phosphorus Vapor in Oxygen", Z. PHYS. CHEM., Vol 4, 1929, pp 288-298.

26. Zagulin, A. V. et al., "Limits of Ignition of Mixtures of $2H_2 + O_2$ and $2CO + O_2$", ZHURNAL FIZICHESKOY KHIMII, Vol Vol 1, 1930, pp 263-280; Entzündungsgrenze des Gemisches $2H_2 + O_2$ und $2CO + O_2$", Z. PHYS. CHEM., Vol 6, 1930, pp 307-329.

27. Zagulin, A. V., "Explosion Temperatures of Gaseous Mixtures at Different Pressures", Z. PHYS. CHEM., Vol 1, 1928, pp 275-291.

28. Thompson, H. W., Hinshelwood, C. N., "The Mechanism of the Homogeneous Combination of Hydrogen and Oxygen", PROC. ROY. SOC., Vol A 122, 1929, p 610.

29. Semenov, N. N., "O nekotorykh problemakh khimicheskoy kinetiki i reaktsionnoy sposobnosti" [Some Problems of Chemical Kinetics and Reactivity], Moscow, Izdatel'stvo Akademii nauk SSSR, 1958, 686 pages.

30. Morse, P. M., "Diatomic Molecules According to the Wave Mechanics. II. Vibrational Levels", PHYS. REV., Vol 34, 1929, pp 57-64.

31. Dzhidzhoyev, M. S., Platonenko, V. T., Khokhlov, R. V., "Chemical Lasers", USPEKHI FIZICHESKIKH NAUK, Vol 100, No 4, 1970, pp 641-679.

32. Kondrat'yev, V. N., Nikitin, Ye. Ye., Reznikov, A. I. et al., "Termicheskiye bimolekulyarnyye reaktsii v gazakh" [Thermal Bimolecular Reactions in Gases], Moscow, Nauka, 1976, 191 pages.

33. Carrington, T., Gravin, D., "Formation of Excited Particles in Chemical Reactions" in: "Vozbuzhdennyye chastitsy v khimicheskoy kinetike" [Excited Particles in Chemical Kinetics]: translated from English, edited by A. A. Borisov, Moscow, Mir, 1973, pp 123-213.

34. Kondrat'yev, V. N., "Emission of a Low-Temperature Hydrogen Sulfide Flame", ZHURNAL FIZICHESKOY KHIMII, Vol Vol 14, 1940, pp 281-286.

35. Geydon, A. G., Wolfhard, H. G., "Plamya, yego struktura, izlucheniye i temperatura" [The Flame, its Structure, Radiation and Temperature]: translated from English by N. S. Chernetskiy, edited by S. A. Gol'denberg, Moscow, Metallurgizdat, 1959, 333 pages.

36. Geydon, A. G., "Spektroskopiya plamen" [Flame Spectroscopy]: translated from English by I. V. Veyts and L. V. Gurvich, edited by Academician V. N. Kondrat'yev, Moscow, Izdatel'stvo inostrannoy literatury, 1959.

37. London, F., "Probleme der modernen Physik", Berlin, Sommerfeld Festschrift, 1928, p 104; "Quantenmechanische Deutung des Vorgangs der Aktivierung", Z. ELEKTROCHEM., Vol 35, 1929, pp 552-555.

38. Bunker, D. L., Blais, N. C., "Monte Carlo Calculations. V. Three-Dimensional Study of a General Bimolecular Interaction Potential", J. CHEM. PHYS., Vol 41, 1964, pp 2377-2386.

39. Polanyi, J. C., "Dynamics of Chemical Reactions", DISCUSS. FARADAY SOC., Vol 44, 1967, pp 293-307.

40. Airey, J. R. et al., "Absolute Efficiency of Conversion of Heat of the Reaction H+Cl Into Vibration", J. CHEM. PHYS., Vol 41, 1964, pp 3255-3256.

41. Kuntz, P. J., Nemeth, E. M., Polanyi, J. C. et al., "Energy Distribution Among Products of Exothermic Reactions. II. Repulsive Mixed and Attractive Energy Release", J. CHEM. PHYS., Vol 44, 1965, pp 1168-1184.

42. Anlauf, K. J. et al., "Vibrational Population Inversion and Stimulated Emission From the Continuous Mixing of Chemical Reagents", PHYS. LETT., Vol 24A, 1967, pp 208-210.

43. Rankin, C. C., Light, J. C., "Quantum Solution of Collinear Reactive Systems: $H+Cl_2 \rightarrow HCl+Cl^*$", J. CHEM. PHYS., Vol 51, 1969, pp 1701-1719.

44. Russell, D., Light, J. C., "Classical Calculations of Linear Reactive Systems: $H+Cl_2 \rightarrow HCl+Cl^*$", J. CHEM. PHYS., Vol 51, 1969, pp 1720-1723.

45. Gilmore, F. R., Bauer, E., McGowan, J. W., "A Review of Atomic and Molecular Excitation Mechanisms in Nonequilibrium Gases to 20,000 K", J. QUANT. SPECTROSC. AND RADIAT. TRANSFER, Vol 9, No 2, 1969, pp 157-183.

46. Herschbach, D. R., "Molecular Beams", edited by J. Ross, Chapter 9, N.Y., Interscience Pub., 1966.

47. Karl, G., Kruus, P., Polanyi, J. C., "Infrared-Emission Studies of Electronic-to-Vibrational Energy Transfer. II. Hg* + CO", J. CHEM. PHYS., Vol 46, 1967, pp 224-243.

48. Karl, G. et al., "Infrared-Emission Studies of Electronic-to-Vibrational Energy Transfer. III. Hg* + CO", J. CHEM. PHYS., Vol 46, 1967, pp 244-253.

49. Vol'kenshteyn, M. V., "Stroyeniye i fizicheskiye svoystva molekul" [Structure and Physical Properties of Molecules", Moscow-Leningrad, Izdatel'stvo Akademii nauk SSSR, 1955, 638 pages.

50. Nicholls, R. W., "Transition Probabilities of Aeronomically Important Spectra", ANN. GEOPHYS., Vol 20, 1964, pp 144-181.

51. Ham, David O., Chang, H. W., ""Chemoluminescence Spectra of the New Molecules NaF_2 and $NaCl_2$ and Their Implications for Reaction Dynamics", CHEM. PHYS. LETT., Vol 24, 1974, pp 579-583.

52. Kovalskii, A. A., "Die Verbrennungskinetik von Wasserstoff", PHYS. Z. SOW., Vol 4, 1933, pp 723-734.

53. Semenov, N. N., "Zur Theorie des Verbrennungsprozesses", Z. PHYS., Vol 48, 1928, pp 571-582.

54. Losev, C. A., "Gazodinamicheskiye lazery" [Gasdynamic Lasers], Moscow, Nauka, 1977.

55. Avduyevskiy, V. S., Danilov, Yu. I., Koshkin, V. K. et al., "Osnovy teploperedachi v aviatsionnoy i raketnoy tekhnike" [Principles of Heat Exchange in Aerospace Technology], Moscow, Oborongiz, 1960;

Lapin, Yu. V., "Turbulentnyy pogranichenyy sloy v sverkhzvukovykh potokakh gaza" [Turbulent Boundary Layer in Supersonic Gas Flows], Moscow, Nauka, 1970.

56. Vasil'yev, G. K., Vizhin, V. V. et al., "Flash Photolysis of Mixtures of $F_2 + D_2 + O_2 + He$", KHIMIYA VYSOKIKH ENERGIY, Vol 9, No 2, 1975, pp 154-159;

Vasil'yev, G. K., Makarov, Ye. F., Chernyshev, Yu. A., "Measurement of Chain Continuation and Breaking Rate Constants in the Reaction $F_2 + H_2(D_2)$ Inhibited by O_2", KINETIKA I KATALIZ, Vol 16, No 2, 1975, pp 320-324.

57. Vasil'yev, G. K., Makarov, Ye. F., Chernyshev, Yu. A., "Regimes of Chain Reactions With Pulsed Photoinitiation", FIZIKA GORENIYA I VZRYVA, Vol 12, No 6, 1976, pp 896-906.

58. Nikitin, Ye. Ye., "Teoriya elementarnykh atomno-molekulyarnykh protsessov v gazakh" [Theory of Elementary Atomic-Molecular Processes in Gases", Moscow KHIMIYA, 1970, 455 pages.

59. Generalov, N. A. et al., "Simultaneous Analysis of Processes of Vibrational Relaxation and Thermal Dissociation of Diatomic Molecules", TEORETICHESKAYA I EKSPERIMENTAL'NAYA KHIMIYA, Vol 4, 1968, pp 311-315.

60. Kuznetsov, N. M., "Kinetics of Dissociation of Polyatomic Molecules in the Case of Nonuniform Distribution of Vibrational Energy", DOKLADY AKADEMII NAUK SSSR, Vol 202, 1972, pp 1367-1370; "Kinetics of Dissociation of Molecules in a Molecular Gas", TEORETICHESKAYA I EKSPERIMENTAL'NAYA KHIMIYA, Vol 7, 1971, pp 22-33.

61. Kuksenko, B. V., Losev, S. A., "Kinetics of Excited Oscillations, and Dissociation of Diatomic Molecules at Atomic-Molecular Collisions in a High-Temperature Gas", TEORETICHESKAYA I EKSPERIMENTAL'NAYA KHIMIYA, Vol 5, 1969, pp 475-483.

62. Osipov, A. I., "Relaxational Processes in Gases: I. Nonequilibrium Energy Distribtuion With Respect to Translational Degrees of Freedom", FIZIKA GORENIYA I VZRYVA, Vol 4, 1966, pp 42-61.

63. Polak, L. S., Khatchoian, A. V., "Rate Coefficient (Constant) of Nonequilibrium Chemical Reactions", TRANS. FARADAY SOC., Vol 67, 1971, pp 1980-1994.

64. Pai Shih-I, "Magnitnaya gazodinamika i dinamika plazmy" [Magnetogasdynamics and Plasma Dynamics]: translated from English by V. P. Korobeynikov and P. I. Chushkin, edited by A. G. Kulikovskiy, Moscow, Mir, 1964, 301 pages.

65. Coleman, R. L., Hudson, H. A., Garcia, B., "Potential and Current Distribution in MHD Plasma Arcs", RAKETNAYA TEKHNIKA I KOSMONAVTIKA, Vol 5, No 12, 1967, pp 144-148.

66. Denisov, Yu. N., Kirelenko, N. I., Kirilkin, V. S. et al., "Potential and Current Distribution in MHD Channel With External Azimuthal Magnetic Field", MAGNITNAYA GIDRODINAMIKA, No 3, 1975, pp 75-79.

67. Polak, L. S., "Plasmochemical Kinetics" in: "Ocherki fiziki i khimii nizkotemperaturnoy plazmy" [Notes on the Physics and Chemistry of Low-Temperature Plasma], Moscow, Nauka, 1971, pp 302-380.

68. Vurzel', F. B., Lysov, G. V., Polak, L. S. et al., "Kinetics of Nonequilibrium Chemical Reactions in a Pulsed Microwave Discharge. I. Method of Computer Calculation of Kinetic Characteristics of Nonequilibrium Chemical Reactions in a Pulsed Microwave Discharge", KHIMIYA VYSOKIKH ENERGIY, Vol 5, 1971, pp 105-111.

69. Corvin, K. K., Corrigan S. J. R., "Dissociation of Carbon Dioxide in the Positive Column of a Glow Discharge", J. CHEM. PHYS., Vol 50, 1969, p 2570.

70. Ivanov, Yu. A., Polak, L. S., Slovetskiy, D. I., "Kinetics of Dissociation of Carbon Dioxide in a Glow Discharge", KHIMIYA VYSOKIKH ENERGIY, Vol 5, 1971, pp 382-387.

CHAPTER 2: FORMATION OF EXCITED PARTICLES IN THE PROCESS OF A NONEQUILIBRIUM CHEMICAL REACTION

§2.1. The Recombination Mechanism of Excitation

Excitation of Electronic States of Atoms and Molecules. Theoretical analysis of quantum state distributions that arise as a result of chemical interaction is fairly complicated as a rule, even when simple models are used, and such analysis enables prediction of energy distributions only in simple cases [Ref. 1, 2].

Population kinetics is appreciably influenced by processes of energy exchange between reagents and reaction products, including intermediate products. Six different kinds of energy can be distinguished in reactions of excitation and energy exchange: T--translational; T_e--translational for the electron; R--rotational; V-vibrational; E--electronic; X--chemical, and accordingly 36 different methods of energy transfer: T-R, T-V, V-R, ... [Ref. 3]. The principal experimental results on energy distribution in chemical reaction products have been obtained by flash photolysis, investigation of luminescence in discharge tubes and crossed molecular beams [Ref. 2, 4-8].

From general theoretical considerations we can expect that during a chemical reaction, electronic population inversion on which chemical lasers must operate in the visible range occurs only rarely since E-transitions require large excitation energies. Besides, the interrelation between reagents and reaction products is limited by symmetry exclusions [Ref. 9]. However, the last decade has witnessed an increase in the number of reports on observation of inverse population of electronic states of chemical reaction products, and on E-transition chemical lasers (see for example Ref. 10-20).

Electronic excitation upon radiative recombination of atoms. At a thermal velocity of particles of the order of $v_T = 10^5$ cm/s and particle size of the order of $d = 10^{-8}$ cm, the duration of collisions is $\tau \sim d/v_T = 10^{-13}$ s. The radiative lifetime of the excited particle formed in the collision is about 10^{-7} s, and therefore the probability of radiative recombination is of the order of 10^{-6}. This probability gets even lower with a reduction in the moment of radiative transition as a result of increasing intermolecular distance, which is typical of recombining atoms in the ground or metastable state. As a consequence, radiative recombination in direct collisions of two reacting molecules is improbable, but its probability increases appreciably when a third particle participates. For example, radiative recombination of oxygen atoms is caused by the reactions [Ref. 13]:

$$\left.\begin{aligned} O + O + M &\rightarrow O_2(b^1\Sigma_g^+) + M, \\ O + O + M &\rightarrow O_2(A^3\Sigma_u^+) + M. \end{aligned}\right\} \qquad (2.1)$$

Both excited states of O_2 correlate with atoms in the ground state (Fig. 2.1), and are stabilized upon collision with a third particle or on the surface of metallic nickel [Ref. 14]. In the case of radiative recombination of atoms, for example behind a shock wave ($T = 2500$-3800 K, $\lambda = 230$-451.1 nm), the O_2 molecules that are formed make a transition from the initially repulsive potential energy curve to state $B^3\Sigma_u^-$, and then make a transition with radiation to the ground state [Ref. 15].

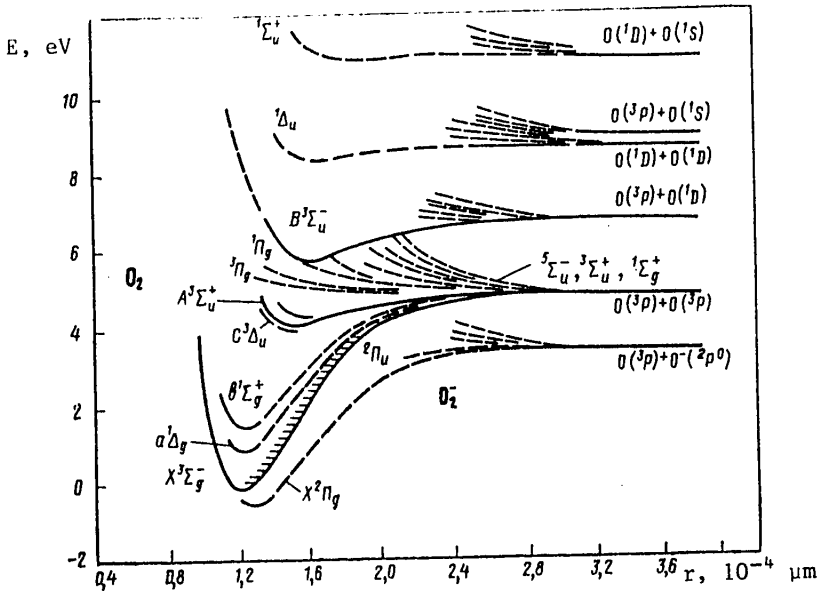

Fig. 2.1. Diagram of potential energy of O_2

In the reaction

$$N + NO \rightarrow N_2 + O \tag{2.2}$$

The intensity of afterglow emission drops off rapidly at $\lambda < 191.5$ nm, which is due to the energy of dissociation of NO (6.49 eV) [Ref. 16].

There are many data on recombination of nitrogen atoms. The principal radiation from a mixture with N_2 content of the order of one percent is due to the B state, and the remainder of the radiation is caused by states b_1 and a [Ref. 17].

Transfer of electronic recombination excitation to third particles. The possible mechanisms of electronic excitation of atom C upon recombination of atoms A and B are:

$$A + B + C \rightarrow AB + C^e; \tag{2.3}$$
$$A + C + C \rightarrow AC + C^e; \tag{2.3a}$$
$$A + B + M \rightarrow AB + M^*; \tag{2.3b}$$
$$M^* + C \rightarrow M + C^e, \tag{2.3c}$$

where M is the third particle.

Taking equation (2.3) as a collision of particle C with complex A-B, we can conclude that reaction (2.3b) is more preferntial from the standpoint of excitation rate if M* has a longer lifetime than complex A-B. Besides, in this reaction the

excited particles C^e may have a wider energy spectrum than those formed in reaction (2.3) if M* is vibrationally excited and relaxes in multistep collisions. These reactions can be interpreted either as reactions in a triple collision, or as reactions in which double collisions form intermediate complexes that then interact with a third body.

Atoms of alkali metals that have low-lying electronic states are excited with expenditure of only a part of the heat of reaction. The following reaction has been suggested [Ref. 18] to explain the radiation of flames with additives of salts of alkali metals to the initial medium in the presence of hydrogen:

$$H + H + Na \rightarrow H_2 + Na^e\,(^2p). \tag{2.4}$$

Calculations of potential energy surfaces for linear arrangement of the atoms H+H+Na [Ref. 19] show that the products of the reaction H+H+Na (2s) are H_2 + Na in the ground state or the excited ^{2}p-state. As a consequence, reaction (2.4) may take place adiabatically. Chemiluminescence of some metals occurs in recombination reactions H+H or H+OH [Ref. 20]. For example, atoms of thallium are excited mainly in reaction H+H, while lead atoms are excited mainly in reaction H+OH.

Oxygen may be excited as a result of the reactions [Ref. 21]

$$O + O + O \rightarrow O_2 + O\,(^1s); \tag{2.5}$$

$$O + N + N \rightarrow N_2 + O\,(^1s). \tag{2.5a}$$

The following reactions have been suggested for superequilibrium radiation of OH [Ref. 22]:

$$H + OH + OH \rightarrow H_2O + OH\,(^2\Sigma^+) \tag{2.6}$$

and

$$H + O_2 + H_2 \rightarrow H_2O + OH\,(^2\Sigma^+). \tag{2.6a}$$

The principal long-lived particles in active nitrogen are N, $N_2(A_3\Sigma_u^+)$, N_2^V and $N_2(^5\Sigma_g^+)$. It is the energy of these particles that leads to excitation of such additives as C_2N_2, ClCN, $CHCl_3$, C_2H_2, C_3O_2, $Ni(CO)_4$, $(C_2H_5)_2Zn$, I_2, PbI_2, SF_6 and $SeCl_4$.

Radiation of CN takes place both due to vibrational and rotational excitation, and due to electronic excitation of CN and subsequent transitions: $B^2\Sigma^+ \rightarrow X^2\Sigma^+$ for the violet band, and $A^2\Pi \rightarrow X^2\Sigma^+$ for the red band [Ref. 23].

Excitation of electronic states upon recombination of an atom with a diatomic molecule. Among the reactions of radiative recombination of an atom with a diatomic molecule, the most widely studied is

$$O + NO \rightarrow NO_2^e. \tag{2.7}$$

As in many other recombination reactions, the temperature coefficient of the rate of this reaction $k(T+10K)/k(T)$ is negative, and the rate constant of the reaction at $T = 270$ K accompanied by radiation in the vicinity of $\lambda = 0.4$–1.4 μm is equal to $3.9 \cdot 10^7$ $cm^3/(mole \cdot s)$, i. e. radiation results in about one collision out of 10^6 [Ref. 24]:

$$NO\,(X^2\Pi) + O\,(^3p) + M \rightarrow NO_2^*\,(C) + M; \tag{2.8}$$

$$NO_2^*\,(C) \rightarrow NO_2^*\,(B)\ \text{(nonradiative transition)}; \tag{2.9}$$

$$NO_2^*\,(B) \rightarrow NO_2\,(A) + h\nu. \tag{2.10}$$

Here A is the ground state, B and C are excited intersecting states.

Less well studied is the process of radiative recombination in the reaction

$$O + CO \rightarrow CO_2^*. \tag{2.11}$$

The emission spectrum of CO_2 in flames and arcs consists of diffuse bands superimposed on a continuous spectrum. In atomic flames at low pressure and room temperature, the spectrum is only discrete in the range of wavelengths of 0.3–0.6 μm. It is significant here that the ground state of CO_2 correlates with the ground state of CO and with the excited atom $O(^1D)$ [Ref. 25]. In contrast to the reaction N + NO, correlation with ground states $CO(^1\Sigma^+) + O(^3p)$ is forbidden by the rule of conservation of spin momentum. Consequently, the ground state cannot be immediately realized as a result of reaction $CO + O(^3p)$, and high-intensity radiation occurs.

According to the results of Ref. 26, the chemiluminescent reaction

$$O + SO = SO_2^* \tag{2.12}$$

has second order with respect to pressure, and the temperature dependence of the rate constant of the reaction can be represented as

$$k = 1{,}5 \cdot 10^8 \left(\frac{T}{298}\right)^{-1}\ cm^3/(mole \cdot s) \tag{2.12a}$$

The radiation spectrum is bounded by the value $\lambda_{min} = 224$ nm, and does not reach the value $\lambda = 218.3$ nm determined by the heat of reaction.

A typical chemiluminescent reaction [Ref. 27] resulting from triple collisions is

$$H + NO + M \rightarrow HNO^v + M,\ v \geq 0. \tag{2.13}$$

The following mechanism of transitions leads to chemiluminescence:

$$H\,(^2s) + NO\,(X^2\Pi) + M \rightarrow HNO^e\ (X^1A^1, {}^3A'', {}^1A', {}^3A') + M; \tag{2.13a}$$

$$HNO\,(^3A'') \rightarrow HNO\,(^1A'')\ \text{(nonradiative transition)}; \tag{2.13b}$$

$$HNO\,(^1A'') \rightarrow HNO\,(X^1A^1) + h\nu. \tag{2.13c}$$

Excitation of Vibrational Degrees of Freedom Upon Recombination of Atoms and Molecules. Recombination reactions due to triple collisions may lead to vibrational

excitation of reaction products that are in the ground electronic state. The reaction rate depends on the partial pressure of the third particles since a newly produced particle necessarily decays if upon collisions with a third particle its energy does not fall to excitation energy below the dissociation energy. Vibrational-vibrational V-V relaxation on reaction products appreciably accelerates the process of energy redistribution.

Molecules such as methylene H_2C participate effectively in recombination reactions with formation of vibrationally excited molecules. Vibrationally excited products of reaction are formed when atoms of H attach to olefins. For propene, this reaction can be written as [Ref. 28]

$$H + C_3H_6 \rightleftarrows C_3H_7^{v} \begin{matrix} \overset{M}{\nearrow} C_3H_7 \\ \searrow CH_3 + C_2H_4 \end{matrix}. \qquad (2.14)$$

The vibrationally excited intermediate product $C_3H_7^{v}$ may dissociate into H and C_3H_6, or into CH_3 and C_2H_4, and may also be stabilized in collisions with an intermediate particle.

Of interest from the standpoint of chemiexcitation is a reaction in which the excited product that is formed takes part in processes that differ from deactivation or decay into the initial products. Among such reactions is the formation of polyatomic molecules that have a weaker bond than the one that arises in recombination, for example

$$CH_3 + CH_2F \rightarrow C_2H_5F^{v} \qquad (2.15)$$

with liberation of excess energy of -380 J/mole [Ref. 5].

Rotational Excitation. Excitation of rotational degrees of freedom is restricted not only by the conservation of energy, as is the case in excitation of vibrational and electronic states, but also by conservation of total angular momentum. The total angular momentum of the transitional complex consists of the orbital angular momentum of the two reagents, which is associated with their translational motion relative to the common center of mass, and the internal rotational momenta of the reagents. Upon dissociation of the complex, the total momentum is divided into orbital and rotational components, the ratio between these components being associated with the characteristics of the potential energy surface. In second-order radiative recombination reactions the angular momentum consists of the total angular momentum of the reagents, including the rotational and orbital components.

In collisions with participation of a third particle, the excess energy or excess angular momentum of the reaction products is transferred to the third neutral particle, and in this event excess rotational excitation is improbable. When intermediate complexes are formed in the reaction

$$A + BC \rightarrow (A - B - C)^* \rightarrow AB + C$$

the rotational angular momentum of product AB may considerably surpass the total momentum of the complex since particle C carries off a large orbital angular momentum

approximately equal in magnitude and opposite in direction to the momentum of particle AB. The maximum momentum is approximately equal to the orbital angular momentum of the departing particle C and is determined by the product of the momentum and impact parameter of separation, which is equal to the radius of action of forces between C and AB. For example in the case of photodissociation of H_2O [Ref. 29], the initial complex H_2O^e has a small angular momentum $3h/2\pi$, while the angular momentum of the dissociation product OH^e is greater than $20h/2\pi$.

§2.2. Nonequilibrium Excitation of Particles in Volumetric Reactions

Excitation of Electronic Transitions. Exchange reactions of the type

$$A+BC\rightarrow\begin{cases}AB^e+C\\AB+C^e\end{cases}$$

in pure form are nearly never realized, and may be considered as elementary stages of a complex chemical reaction with formation of intermediate product A-B-C, which requires that the energy of bond AB be much greater than that of BC. The probability of excitation increases when there is a lower-lying electronic state AB in the case where formation of AB in the ground state is forbidden by the rule of spin conservation. Considered quite probable is the reaction

$$H+HI\rightarrow H_2+I\,(^2P_{1/2}). \tag{2.16}$$

In this reaction, only a few percent of the iodine atoms are formed in the excited state [Ref. 30].

An example of an exchange reaction with participation of more than three atoms is

$$Br+ClO_2\rightarrow BrCl^e+O_2, \tag{2.17}$$

although in reality it is more complicated than mere exchange of the Cl atom.

In the reaction

$$O_3+NO\rightarrow O_2+NO_2^e\ (-217.7\ \text{kJ/mole}), \tag{2.18}$$

approximately 10% of the collisions lead to formation of NO_2 ($^2B_1$), only a few of the lower V-levels of this state being populated [Ref. 31]. The reaction

$$O_3+SO\rightarrow O_2+SO_2 \tag{2.19}$$

has considerably higher exothermicity (-446.3 kJ/mole). The rate constants of formation of the three possible E-states [Ref. 32] [in $cm^3/(mole\cdot s)$] are:

$$\left.\begin{aligned}k(\tilde{X}\,^1A_1)&=1{,}5\cdot10^{12}\exp(-2100/RT);\\k(\tilde{A}\,^1B_1)&=10^{11}\exp(-4200/RT);\\k(\tilde{a}\,^3B_1)&=3\cdot10^{10}\exp(-3900/RT).\end{aligned}\right\} \tag{2.20}$$

Vibrational Excitation in Exchange Reactions. Flash photolysis of O_3, NO_2, ClO_2 produces vibrationally excited oxygen molecules. Since the process takes place

analogously for all three substances, we may limit ourselves to examining the formation of excited oxygen in photolysis of O_3. We have the following significant reactions that take place with the formation of atomic oxygen [Ref. 2]:

$$\left.\begin{array}{l} O_3+h\nu\to O(^3P)+O_2; \\ O_3+h\nu\to O(^1D)+O_2(^1D); \\ O(^3P)+O_3\to O_2^v+O_2 \ \ (-389.4\ \text{kJ/mole}) \\ O(^1D)+O_3\to O_2^v+O_2 \ \ (-745.2\ \text{kJ/mole}) \\ \ldots\ldots\ldots\ldots\ldots\ldots\ldots \end{array}\right\} \qquad (2.21)$$

Excited oxygen molecules in state $X^3\Sigma_g^-$ are observed up to levels $v\leqslant 29$. A maximum in the distribution of excited molecules occurs on $v=12$, 13 and 14, and the populations of other levels decrease monotonically. Atoms of $O(^3P)$ play an appreciable part in the formation of vibrationally excited oxygen molecules. This applies to thermal dissociation of ozone in shock waves and flash photolysis of NO_2. As a result of the reactions considered above, the formation of the oxygen molecule takes place on high V-levels and is not accompanied by chemiluminescence since vibrational-rotational V-R transitions are forbidden for homonuclear molecules.

Of greatest interest among reactions with halide derivatives are

$$\begin{array}{c} H+Cl-Cl\to HCl^v+Cl \ \ (-188.4\ \text{kJ/mole}), \\ Cl+H-I\to HCl+I \ (-310\ \text{kJ/mole}), \end{array} \qquad (2.22)$$

in which population inversion takes place at low pressures. In the case of Cl+H-I the inversion is considerable, and quantum-mechanical stimulated emission is observed. More than half the heat of reaction is converted to vibrational excitation. The remainder goes to rotational energy, and as a consequence the energy of translational motion of the products is comparable to the energy of the initial reaction products.

The distributions of populations of vibrationally excited oxygen molecules and hydrogen chloride molecules are basically similar. The distribution maximum falls to levels that correspond to half the reaction energy. The distribution with respect to V-levels of both molecules is quite close to the initial distribution due to the reaction. This distribution may be distorted due to the high rate of R-relaxation in collisions.

Vibrational-translational V-T relaxation takes place at a rate that is considerably lower than rotational-translational R-T relaxation, and it differs appreciably for HCl and O_2, since for O_2 the gas-kinetic number of collisions is $Z_0=8\cdot10^5$, while for HCl $Z_0=(0.5\text{-}1.5)\cdot10^3$. Radiative transitions are forbidden for oxygen, and the radiative lifetime for HCl lies in a range of 10^{-2}-10^{-4} s. Thus it can be expected that the original distribution at high pressures is retained much longer for O_2 than for HCl. However, as a result of V-V energy exchange this distribution may be considerably changed. For example in experiments with HCl and OH (reaction $H+O_3\to OH^V+O_2$) at $p=13.33$ Pa nearly Maxwell-Boltzmann distribution was observed with respect to V-levels, but the vibrational temperature was much higher than the translational, and amounted to several thousand degrees. This shows that by

the time of the observation there had been effective energy exchange as a result of R- and V-V-relaxation, but V-T relaxation had not been completed.

Widely known reactions that lead to effective chemiexcitation are reactions of atoms of sodium and potassium with halides, nitrogen oxides and alkyl halides. These reactions are fast, and the activation energy as a rule is less than 21 kJ/mole. Radiation of the sodium doublet is predominant since the lifetime of $NaCl^V$ is fairly long, electronic-vibrational E-V exchange of energy is effective, and the radiative lifetime is only 10^{-8} s.

These patterns are typical of systems that contain atoms with low-lying states to which transitions are energetically allowed.

The equation of an exchange reaction that takes place with formation of a four-center complex can be written

$$A - B + C - D \rightarrow A - C + B - D. \tag{2.23}$$

An example of known reactions of this type in which the formation of vibrationally excited particles has been established is [Ref. 2]

$$CN + O_2 \rightarrow CO + NO^v.$$

Rotational Excitation in Exchange Reactions. In the reaction

$$K + HBr \rightarrow KBr + H, \tag{2.24}$$

according to conservation law we should expect excitation of rotational energy of the reaction product. Actually, the initial rotational moment of the K atom should be large due to the relatively large mass of K and the appreciable cross section of the reaction ($0.34 \cdot 10^{-14}$ cm^2), whereas the moment of HBr is small due to the small moment of inertia of this molecule. In the reaction products, KBr has a relatively large moment of inertia, and therefore, according to conservation laws, we can expect that most of the total momentum wil go to rotation of KBr.

For strongly nonequilibrium rotational excitation, as in the reaction

$$Cl + HI \rightarrow HCl\ (v = 2) + I \tag{2.25}$$

nearly all the difference between the heat of reaction and the energy necessary for excitation of level v = 2 goes to rotational excitation.

Strongly nonequilibrium rotational distributions are usually observed in chemiluminescent reactions that lead to formation of electronically excited molecules in ordinary atomic flames in a discharge. In these cases R-relaxation is impeded by the short lifetime of E-states.

REFERENCES

1. Nikitin, Ye. Ye., "Nonequilibrium Chemical Reactions" in: "Problemy kinetiki elementarnykh khimicheskikh reaktsiy" [Problems of Kinetics of Elementary Chemical Reactions], Moscow, Nauka, 1973, pp 5-50.

2. Harrington, G., Gravin, D., "Formation of Excited Particles in Chemical Reactions" in: "Vozbuzhdennyye chastitsy v khimicheskoy kinetike" [Excited Particles in Chemical Kinetics]: translated from English, edited by A. A. Borisov, Moscow, Mir, 1973, pp 123-213.

3. Gilmore, F. R., Bauer, E., McCowan, J. W., "A Review of Atomic and Molecular Excitation Mechanisms in Nonequilibrium Gases up to 20,000 K", J. QUANT. SPECTR. AND RAD. TRANSFER, Vol 9, No 2, 1969, pp 157-183.

4. Rabinovich, B. S., Flauers, M. S., "Chemical Activation" in "Khimicheskaya Kinetika i tsepnyye reaktsii" [Chemical Kinetics and Chain Reactions]: edited by V. N. Kondrat'yev, Moscow, Nauka, 1966, pp 61-144.

5. Kondrat'yev, V. N., "Kinetika khimicheskikh gazovykh reaktsiy" [Kinetics of Chemical Gas Reactions], Moscow, Nauka, 1974, 558 pages.

6. "Fizicheskaya khimiya bystrykh reaktsiy" [Physical Chemistry of Fast Reactions]: translated from English by Ye. V. Mozzhukhin and Yu. P. Petrov, edited by I. S. Zaslonko, Moscow, Mir, 1976, 394 pages.

7. Kondrat'yev, V. N., "Konstanty skorostey gazofaznykh reaktsiy" [Rate Constants of Gas-Phase Reactions], Moscow, Nauka, 1970.

8. McCowan, J. W., ed., "Advances in Chemical Physics, Vol 28. The Excited State in Chemical Physics", N. Y.-London, Interscience Publ., 1976.

9. Thrush, B. A., "Gas Reactions Yielding Electronically Excited Spectra", ANN. REV. PHYS. CHEM., Vol 19, 1968, pp 371-388.

10. Zuyev, V. S., Kormer, S. B., Mikheyev, L. D. et al., "Arisal of Inversion on the Transition $^1\Sigma_g^+ \rightarrow {}^3\Sigma_g^-$ of Molecular Sulfur Upon Photodissociation of COS", PIS'MA V ZHURNAL EKSPERIMENTAL'NOY I TEORETICHESKOY FIZIKI, Vol 16, No 4, 1972, pp 222-224.

11. Jones, C. R., Broida, H. P., "Chemical Lasers in the Visible", LASER FOCUS, Vol 10, No 3, 1974, pp 37-47.

12. "Electronic Transition Lasers", Cambridge, Massachusetts-London, MIT Press, 1976.

13. Young, R. A., Sharpless, J. L., "Chemiluminescent Reactions Involving Atomic Oxygen and Nitrogen", J. CHEM. PHYS., Vol 39, No 4, 1963, pp 1071-1102.

14. Gilmore, F. R., "Potential Energy Curves for N_2, NO, O_2 and Corresponding Ions", J. QUANT. SPECTR. AND RAD. TRANSFER, Vol 5, No 2, 1969, pp 369-390.

15. Mayers, B. F., Bartle, E. R., "Shock-Tube Study of the Radioactive Combination of Oxygen Atoms by Inverse Predissociation", J. CHEM. PHYS., Vol 48, No 9, 1968, pp 3935-3934.

16. Tanaka, Y., "Emission Bands of NO in the Vacuum Ultraviolet Region Excited in the NO Afterglow", J. CHEM. PHYS., Vol 22, No 12, 1954, pp 2045-2048.

17. Gross, R. W. F, Cohen, H., "Temperature Dependence of Chemiluminescent Reactions. II. Nitric Oxide Afterglow", J. CHEM. PHYS., Vol 48, No 6, 1968, pp 2582-2588.

18. Sugden, T. M., "Excited Species in Flames", ANN. REV. PHYS. CHEM., Vol 13, 1963, pp 369-390.

19. Magee, J. L., Ri, T., "The Mechanism of Reaction Involving Excited Electronic States", J. CHEM. PHYS., Vol 9, No 8, 1944, pp 638-644

20. Padley, P. J., Sugden, T. M., "Chemiluminescence and Radical Recombination in Hydrogen Flames" in: Symp. Combustion 7th Lond., Butterworth, Publ. for the Combustion Institute, 1959, pp 235-244.

21. Kaplan, J. et al., "Atomic Reactions in the Upper Atmosphere", CANAD. J. CHEM., Vol 38, No 10, 1960, pp 1688-1692.

22. Geydon, A. G., "Spektroskopiya plamen" [Flame Spectroscopy]: translated from English by M. V. Veyts and L. V. Gurvich, edited by Academician V. N. Kondrat'yev, Moscow, Izdatel'stvo inostrannoy literatury, 1959, 382 pages.

23. Kiess, N. H., Broida, H. P., "Emission Spectra From Mixtures of Atomic Nitrogen and Organic Substances" in: Symp. Combustion 7th Lond., Butterworth, Publ. for the Combustion Institute, 1959, pp 207-214.

24. Fontijn, A., Meyer, C. B., Schiff, H. J., "Absolute Quantum Yield Measurements of the NO-O Reaction and its Use as Standard for Chemiluminescent Reactions", J. CHEM. PHYS., Vol 40, No 1, 1964, pp 64-70.

25. Laidler, K. J., "The Chemical Kinetics of Excited States", Clarendon, Oxford University Press, 1955, p 180.

26. Fletcher, S. R., Levitt, B. P., "O + SO Recombination Emission at 3500 K", TRANS. FARADAY SOC., Vol 65, No 558, part 6, 1969, pp 1544-1549.

27. Clune, M. A. A., Thrush, B. A., "Mechanism of Chemiluminescent Reaction Involving Nitric Oxide--the H + NO Reaction", DISCUSS. FARADAY SOC., No 33, 1962, pp 139-148.

28. Thrush, B. A., "The Reaction of Hydrogen Atoms", PROGR. REACTION KINETICS, Vol 3, 1965, pp 65-95.

29. Carrington, T., "Angular Momentum Distribution and Emission Spectrum of $OH(^2\Sigma^+)$ in the Photodissociation of H_2O", J. CHEM. PHYS., Vol 41, No 7, 1964, pp 2012-2018.

30. Cadman, P., Polanyi, J. C., "Production of Electronically Excited Atoms. II. $H + HI \rightarrow H_2 + I^*(P_{\frac{1}{2}})$", J. PHYS. CHEM., Vol 72, No 11, 1968, pp 3715-3724.

31. Clough, P. N., Thrush, B. A., "Mechanism of Chemiluminescent Reaction Between Nitric Oxide and Ozone", TRANS. FARADAY SOC., Vol 63, No 532, part 4, 1967, pp 915-925.

32. Halstead, C. J., Thrush, B. A., "The Kinetics of Elementary Reactions Involving the Oxide of Sulfur. III. The Chemiluminescent Reaction Between Sulfur Monoxide and Ozone", PROC. ROY. SOC. (Lond.), Vol A295, No 1443, 1966, pp 380-398

CHAPTER 3: BASIC EQUATIONS OF PROCESSES IN CHEMICAL LASERS

§3.1. General Conditions of Lasing Onset

The main purpose of investigations of processes in chemical lasers is to study different chemical reactions in which atoms or molecules may be formed with energy level distribution such that at least one optical transition satisfies conditions that lead to synchronization of the individual emitters both in the case of inverse population of levels, and in the case of phase correlation of the emitters. Setting up nonequilibrium excitation of atoms with respect to internal degrees of freedom is a necessary but insufficient condition for stimulation of coherent emission during a chemical reaction. It is also necessary to have a reserve of inversion that would compensate for losses in the resonant system. These losses determine the limiting value of the difference in the concentration of populations. In lasers whose operation is determined by phase correlation of the radiating particles there is a threshold of absolute concentration of these particles.

For lasers based on using the inversion effect, the critical density of inversion of populations of energy levels is determined by the probability of a given induced optical transition, the relative width of the emission line ($\Delta\nu/\nu$), and also by the properties of the excited modes in the resonator. If the radiation line width is determined by Doppler broadening, which is usually the case at pressures of the order of a few millimeters of mercury, the kinetics of atoms and molecules in the quantum-mechanical process of stimulated emission will show little difference. At high pressures in photostimulated chemical reactions the ratio $\Delta\nu/\nu$ is a significant factor in both the process of chemical reaction and the conditions of stimulation of coherent radiation.

Calculations of radiation probabilities are based on the Born-Oppenheimer approximation that enables proper evaluation of the E-transition probability. The total probability of the E-transition for an allowed molecular transition has the same order as for atoms ($\sim 10^7$ s^{-1}). However, when the interaction of V- and R-levels is considered, the probability of an individual allowed E-transition is several orders less than the total probability of all transitions from the level. This circumstance increases the threshold values of the critical density of inversion and absolute values of concentrations of radiating centers.

The critical density of population inversion of levels is determined both by the oscillatory properties of the resonator and by nonoptical transitions that lead either to further excitation or to relaxation processes that restore the system to the equilibrium state. Chemical processes of excitation usually lead to an increase in population over a fairly wide region of V- and R-levels. Thanks to the small distance between R-levels, they are easily excited or relax on thermal molecules that have energy of ~0.1 eV. These relaxational processes are an important factor in the kinetics of the process of energy redistribution among molecules, which takes place in only a few collisions in weakly bound molecules like I_2, and in up to $\sim 10^7$ collisions in strongly bound molecules like N_2.

Relaxational processes within the limits of each degree of freedom determine the corresponding temperature whose behavior is responsible for a given energy transition. As a rule, the temperature settles rapidly within a single degree of freedom, and then energy E is exchanged between degrees of freedom. For example, if

a system is in the inverse state with respect to V-levels, rapid R-relaxation may raise the population of the upper energy level of stimulated emission due to adjacent R-levels, and accordingly may reduce the population of the lower energy level of stimulated emission due to rapid transitions to adjacent R-levels in collisions.

Besides, the different times of relaxation of V- and R-levels enable inversion of the individual V-R levels even when both the vibrational and rotational distributions are characterized by normal law with temperatures T_V and T_R.

According to §1.6, the energy of the V-R level of a molecule in the harmonic oscillator approximation can be represented as

$$E(V, J) = E(V) + B(J+1)J, \tag{3.1}$$

where $V(v_1, v_2, \ldots, v_n)$ is the spectrum of vibrational quantum numbers.

For complete (vibrational) inversion, we have the relation

$$n(V_1) - [g(V_1)\, n(V_2)/g(V_2)] > 0. \tag{3.2}$$

Writing out the equilibrium distribution of V-levels

$$\left.\begin{aligned} n(V) &= [g(V)/z_{\text{vib}}] \exp\left[-\sum_l (v_l h\nu_l/k^0 T_l)\right], \\ z_{\text{vib}} &= \prod_l [1 - \exp(-h\nu_l/k^0 T_l)]^{-g_l}, \end{aligned}\right\} \tag{3.3}$$

where the v_l are numbers from the set $V(v_1, v_2, \ldots, v_n)$, ν_l, g_l, T_l are the frequency, degree of degeneracy and temperature of the l-th mode of vibrations, g(V) is the statistical weight of V, we get the condition of existence of inversion between levels $V_1(\ldots, v_{l+1}, \ldots, v_l, \ldots)$ and $V_2(\ldots, v_l, \ldots, v_{l+1}, \ldots)$

$$T_l/T_i > \nu_l/\nu_i > 1. \tag{3.4}$$

Satisfaction of this condition necessitates comparatively small values of T_i/T_l since the ratio ν_i/ν_l is small in cases of practical importance.

In the case of partial inversion with Boltzmann distribution of rotational levels

$$n(V_1, J) - \frac{g(V_1, J)\, n(V_2, J+1)}{g(V_2, J+1)} > 0 \tag{3.5}$$

and for inversion between v + 1, J and v, J + 1 we must have

$$\frac{n(v+1)}{n(v)} \exp\left[-\frac{E(v+1, J)}{k^0 T} + \frac{E(v, J+1)}{k^0 T}\right] > 1 \tag{3.6}$$

or

$$\frac{T_{\text{vib}}}{T} > h\nu/[2(J+1)B_v + (B_v - B_{v+1})J(J+1)] > 1. \tag{3.7}$$

The latter condition enables us to estimate the maximum population inversion

$$\Delta n_{\max} = \frac{2(J_m+1)}{z_{\text{rot}}} n(v+1)\exp\left[-\frac{BJ_m(J_m+1)}{k^0 T}\right] \times$$
$$\times\left\{1-\exp\left[\frac{h\nu}{k^0 T_{\text{vib}}}-\frac{2B(J_m+1)+(B_v-B_{v+1})J_m(J_m+1)}{k^0 T}\right]\right\}, \quad (3.8)$$

where

$$J_m \approx J_0 + \frac{1}{2J_m+3}\frac{k^0 T}{B}\frac{2J_0+1}{2J_m+1},$$
$$J_0 \approx \frac{B}{(B_v-B_{v+1})}\left[\left(1+\frac{h\nu(B_v-B_{v+1})}{B^2}\frac{T}{T_{\text{vib}}}\right)^{1/2}-1\right]-1.$$

The exchange exothermic reaction

$$A+BC \rightarrow \begin{cases} AB^*+C \\ AB+C^* \end{cases}$$

under conditions of an optical wave field may take the following short path with emission of light

$$A + BC \rightarrow (A-B-C)^* \rightarrow AB + C + h\nu,$$

where (A-B-C)* is a complex that contains a chemical energy bond.

Chemical lasers based on reactions of this type are capable of converting chemical energy to luminous energy with high efficiency by the shortest path since in a number of these reactions the (A-B-C)* complex, as pointed out in §1.6, does not have the usual lower state, i. e. it is always inversely populated. The concentration of the complexes increases with increasing pressure up to levels where triple collisions begin to play a significant part.

As the concentration of radiating particles increases, they can no longer be treated as isolated emitters. In this case, as a result of collective interaction spontaneous emission becomes coherent with a considerable increase in intensity [Ref. 1]. It can be shown that for some conditions the rate of a chemical reaction due to synchronization of emitters becomes comparable to the rate of the chemical reaction due to induced transitions. In both cases, the reaction rate is proportional to the square of the concentration of initial reagents, and this means that both mechanisms may compete with one another, depending on the absolute values of the radiating transitions and the volume of phase correlation.

For the threshold of concentrations of radiating particles (N_{th}) in the case of phase correlation we have the estimate [Ref. 1]

$$VN_{th}/4 > 1. \quad (3.9)$$

where $V \cong \lambda^3$ and λ^2/L respectively depending on the method of carrying out the chemical reaction. Here λ is the radiated wavelength, L is the length of the resonator.

§3.2. Equations of Motion of a Chemically Reacting Gas With Consideration of Nonequilibrium Effects and Emission

Equations for describing a multicomponent interacting mixture of gases in the presence of radiation are rather complicated for solving practical problems. With

consideration of (1.77)-(1.80) we give here a simplified system of equations based on using the phenomenological approach to problems of energy exchange and diffusion of components.

The equation of continuity in Euler variables (ρ, $\vec{u}$) remains valid in the presence of chemical reactions and radiation, and has the usual form

$$d\rho/dt + \rho \operatorname{div}(\mathbf{u}) = 0. \tag{3.10}$$

In the presence of chemical interaction and diffusion this equation for component i can be written as

$$\partial\rho_i/\partial t + \operatorname{div}(\rho_i\mathbf{u}) = w_i - \operatorname{div}\mathbf{D}_i, \tag{3.11}$$

where $\mathbf{D}_i = \rho_i(\mathbf{u}_i - \mathbf{u})$ is the diffusion flow of mass; w_i is the change in mass of the i-th component due to chemical reaction (or ionization).

The equation of momentum disregarding radiation pressure in accordance with (1.78):

$$\rho d\mathbf{u}/dt + \nabla P = 0. \tag{3.12}$$

The equation of energy takes the form

$$\rho dh_e/dt = \operatorname{div}(P\mathbf{u}) - \operatorname{div}\mathbf{q}. \tag{3.13}$$

The conservation equations for the i-th component can be written out, taking as the component a particle that is in a definite chemical and quantum state. It is convenient to convert to concentrations of particles in a unit of volume, n.

As an example, for a molecule of type m that is in vibrational state v, we can write in place of (3.11) the equation

$$dn_v^m/dt = K_v^m. \tag{3.14}$$

Here K_v^m is the change in number of particles of type m on vibrational level v as a result of chemical reactions, collisions with other particles, or radiation.

The equation for the density of quanta q_ν takes the form

$$dq/dt = -\alpha I_\nu + w_\nu, \tag{3.15}$$

where I_ν is the intensity of resonant emission with frequency ν, w_ν is the pumping rate, α is the coefficient of absorption (or amplification) of light.

§3.3. Principal Characteristics of Chemical Lasers

The major characteristics of chemical lasers and the fundamental quantitative criteria of lasing onset may be found on the basis of the mathematical models of Ref. 2-5.

Let us consider the kinetics of chemical pumping and stimulated emission of chemical lasers on the basis of the simplest two-level model that includes chemical pumping of two working levels with population n_1, n_2, relaxation, and stimulated emission.

The equation of balance for the density of photons in the resonator in this case is written as

$$dq_\nu/dt = A_{1,2}n_1 + B_{1,2}n_1q_\nu - B_{2,1}n_2q_\nu - q_\nu/\tau_\phi. \tag{3.16}$$

Here $A_{1,2}$ is the coefficient of spontaneous radiation; $B_{1,2}$ and $B_{2,1}$ are the coefficients of induced radiation for transitions 1-2 and 2-1 respectively, n_1, n_2 are the number of particles on levels 1 and 2 respectively, τ_ϕ is the lifetime of a photon in the resonator.

Considering that $A_{1,2} = B_{1,2}\ 8\pi\nu^3/c^3$, $B_{1,2}q_{\nu,1} = q_{\nu,2}B_{2,1}$ and introducing $\sigma = \sigma_{1,2} = B_{1,2}\,q_\nu/\Delta\nu c$, $\Delta n = n_2 - nn_1$, where $\sigma_{1,2}$ is the cross section of the stimulated transition, we get

$$dq_\nu/dt = A_{1,2}n_1 + \sigma c\Delta n q_\nu - q_\nu/\tau_\phi. \tag{3.17}$$

Analogously for n_1 and n_2 we have

$$dn_1/dt = P_1w + n_2/\tau_p + \sigma c q_\nu \Delta n, \tag{3.18}$$
$$dn_2/dt = P_2w - n_2/\tau_p - \sigma c q_\nu \Delta n, \tag{3.19}$$

where τ_p is the time of relaxation of the level, P_1, P_2 are the probabilities of formation of populations n_1, n_2.

The limiting energy of radiation, defined as

$$E_{max} = \int_0^\infty (h\nu q_\nu/\tau_p)\,dt,$$

will be

$$E_{max} = (1/2)\,h\nu\,(P_2 - P_1)\int_0^\infty w(t)\,dt. \tag{3.20}$$

The limiting (maximum) efficiency is the ratio of the maximum energy of coherent radiation to the reaction energy, and is called the *chemical efficiency* η_X, which is independent of the reaction rate [Ref. 2-5]:

$$\eta_{max} = \eta_x = \frac{1}{2}\,\frac{h\nu\,(P_2 - P_1)}{|-\Delta H_e|}. \tag{3.21}$$

Lasing arises at the initial instant if the rate of the chemical reaction satisfies the condition

$$w > w_{th} = 1/\tau_p\ \sigma c\tau_\phi = \Delta/\tau_p, \tag{3.22}$$

where $\Delta = (\sigma c\tau_\phi)^{-1}$ is the threshold density of inversion.

During steady-state chemical pumping, a time arrives when lasing stops due to relaxation on reaction products. This is the critical time of lasing cutoff

$$t_{cr} = (P_2 - P_1)\tau_p. \tag{3.23}$$

When inversion is created in molecules by energy transfer with probability P from other molecules excited by the chemical reaction, the system of equations is supplemented by the equation for the density of excited particles a* that arise as a result of the chemical reaction

$$\frac{dn^*}{dt} = w - (P_{p,1} + P_3) n^* \quad (P_{p,i} = \frac{1}{\tau_{p,i}},\ i = 1, 2). \tag{3.24}$$

Considering the creation of inversion due to energy transfer from excited particles, we have for n_2

$$dn_2/dt = P_3 n^* - P_{p,2} n_2 - \sigma c q_v (n_2 - n_1). \tag{3.25}$$

Also valid is equation (3.17) without the first term.

Lasing ensues under the condition

$$w > w_{th} = P_{p,2} (n_1^p + \Delta) (P_{p,1} + P_3)/P_3, \tag{3.26}$$

where n_1^p is the equilibrium population of the lower working level.

Let us consider amplification of radiation under conditions of an unsteady three-dimensional medium [Ref. 4]. In the case of partial inversion with unsteady chemical pumping of vibrational levels of a diatomic molecule, the gain on the R-V transition $(v+1, J-1) \to (v, J)$ for the $\mathcal{P}$-branch with equilibrium distribution of rotational levels is written as

$$\alpha_v = \alpha_{v,J}^{v+1,J-1} = \sigma_{v,J}^{v+1,J-1} \left(n_{v+1} - n_v \exp\left(-\frac{2\theta_r J}{T} \right) \right). \tag{3.27}$$

Here θ_r is the characteristic rotational temperature, $\sigma_{v,J}^{v+1,J-1}$ is the cross section of induced transitions.

In the harmonic approximation

$$\sigma_{v,J}^{v+1,J-1} = (v+1)\, \sigma_{0,J}^{1,J-1}, \tag{3.28}$$

$$\sigma_{0,J}^{1,J-1} = \frac{c^2}{8\pi (\nu_{0,J}^{1,J-1})^2} A_{0,J}^{1,J-1} (2J-1) \frac{\theta_r}{T} g(0) \exp\left(-\frac{\theta_r}{T} J(J-1) \right), \tag{3.28a}$$

where $\nu_{0,J}^{1,J-1}$ is the frequency of the transition, g(0) is the form factor, $A_{0,J}^{1,J-1}$ is the Einstein coefficient. From (3.27) and (3.28), (3.28a) we get

$$\alpha = \sum_v \alpha_v = \sigma [q_v - \varepsilon_J N], \tag{3.29}$$

where $\varepsilon_J = (\exp(2\theta_r J/T) - 1)^{-1}$; $N = \Sigma n_v$;

$$\sigma = \sigma_{0,J}^{1,J-1} (1 - \exp(-2\theta_r J/T)); \quad q_v = \sum_v v n_v.$$

Using expression (3.15) as the equation of the medium, we get

$$\frac{dq_v}{dt} = -\alpha I_v + \sum_{i=1}^{p} \beta_i w_i(x, t), \tag{3.30}$$

where β_i and $w_i(x,t)$ are respectively the average number of excitation quanta and the rate of excitation due to the i-th channel of the chemical reaction. For example, for pumping in the process of a chain chemical reaction

$$A+B_2 \xrightarrow{P_{1v}k_1} AB(v)+B,\quad B+A_2 \xrightarrow{P_{2v}k_2} AB(v)+A$$

with probabilities of formation of reaction products on the v-th vibrational level P_{1v} and P_{2v} at p = 2 we have

$$\beta_1=\sum_v vP_{1v};\quad \beta_2=\sum_v vP_{2v};\quad w_1=k_1[A][B_2];\quad w_2=k_2[B][A_2].$$

Using (3.29) and (3.30), we get the equation of the medium:

$$\partial\alpha/\partial t = -\sigma\alpha I_\nu + K(x,\ t), \tag{3.31}$$

where $K(x,t)=\sigma\left[w(x,t)-\frac{\partial}{\partial t}(e_J N)\right]$.

In the case of complete inversion for molecules in which the upper and lower laser levels belong to different modes (ν_3, ν_1), the expression for the gain on transition $00^\circ1 \to 10^\circ0$ can be taken as

$$\begin{gathered}\alpha=\sigma(q_{v,3}-q_{v,1});\\ \sigma=f\sigma_{10^\circ0}^{00^\circ1};\ f=(1+q_{v,1}/N)^{-2}(1+q_{v,2}/N)^{-2}(1+q_{v,3}/N)^{-2}.\end{gathered} \tag{3.32}$$

Here $q_{\nu,i}$ is the density of vibrational quanta of the i-th mode.

§3.4. Kinetics of Chemical Pumping and Lasing in the Pulsed Mode

Since high pumping powers and low energy losses can be achieved in pulsed operation without difficulty, lasing in this mode is realized in many more active media and on a considerably greater number of transitions over a wider spectral range than in cw operation [Ref. 6].

Reactions with branched chains are the fastest. This includes reactions such as oxidation of H_2, PH_3, SiH_4, CS_2, CO, P, dissociation of NCl_3, some reactions of molecular fluorine with H_2, CH_3, I, HI and several others. Taking survey Ref. 7 as our guide, let us present the patterns of occurrence of branched chain reactions with inverse excitation of products based on the well studied reaction of hydrogen oxidation [Ref. 8], for example when hydrogen reacts with fluorine.

It is shown in Ref. 9-11 that this is a branched chain reaction with energetic branching in accordance with the scheme

inception of chains $F_2 \to F+F$;	(3.33a)
continuation of chains $F+H_2 \to HF\ (v\leqslant 3)+H$;	(3.33b)
continuation of chains $H+F_2 \to HF\ (v\leqslant 6)+F$;	(3.33c)
branching of chains $HF\ (v\geqslant 4)+F_2 \to HF\ (v'\leqslant 4)+F+F$;	(3.33d)
annihilation of chains $H+O_2+M \to HO_2+M$, $HO_2 \to$ wall;	(3.33e)
annihilation of chains $H \to$ wall, $F \to$ wall;	(3.33f)
V-V relaxation and deactivation of vibrations of HF.	(3.33g)

In the low-temperature region, collisions are rare, continuation and branching of chains takes place at low rates, whereas the probability of annihilation of active centers H, F, HF ($v \geqslant 4$) on the walls is high. Thus at low pressures the mixture is stable and does not self-ignite. The mixture is also stable in the high-pressure region since there is an appreciable increase in the probability of annihilation of active atoms of hydrogen in triple collisions (3.33e). Self-ignition of the mixture takes place with progressive development and predominance of processes (3.33b), (3.33c) and (3.33d) in some intermediate pressure region that is a function of the temperature of the mixture.

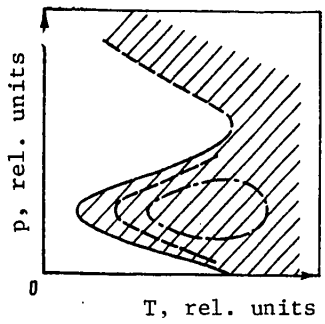

Fig. 3.1. Lasing limits for branched chain reactions

Such behavior of a chemical reaction in coordinates T, p is described by graphing the region of the ignition peninsula (Fig. 3.1) typical of the branched chain reactions described in §1.5. The boundaries of this peninsula (solid line) are the lower and upper ignition limits, or to say it another way, the first and second limits of ignition. For reactions $HO_2 + F_2 \rightarrow HF + O_2 + F$ there is even a third limit of ignition (shown by the broken line in Fig. 3.1).

Let us set up equations for the concentrations of particles n_H, n_F, $n_{HF(v)}$:

$$dn_H/dt = -(k_3 n_{F_2} + k_5 n_{O_2} n_M + k_6) n_H + k_2 n_{H_2} n_F; \tag{3.34}$$

$$dn_F/dt = k_3 n_{F_2} n_H - (k_2 n_{H_2} + k_7) n_F + n_{F_2} \sum_{v \geqslant 4} k_{4,v} n_{HF(v)} + w(t); \tag{3.35}$$

$$dn_{HF(v)}/dt = k_3 k_v n_{F_2} n_H - k_{4,v} n_{F_2} n_{HF(v)} + \Omega(t), \tag{3.36}$$

where $\Omega(t)$ is a term that describes relaxation and annihilation on the walls; k_2, k_3, $k_{4,v}$, k_5 are the rate constants of the corresponding processes ($k_{4,v>4} = 0$); $w(t)$ is the rate of the reaction of chain initiation (3.33a); k_6, k_7 are certain averaged constants that take consideration of the size, configuration and material of the walls of the reaction space in the case of linearity of equations (3.34)-(3.36).

Let us consider the initial period of the reaction, assuming that $w(t)$ is a deltoid function. In this case, the solution of linear system (3.34)-(3.36) will be the sum of exponential terms

$$n_{HF} = n_0 \exp(st),$$

where s is the largest of the determinants of system (3.34)-(3.36) [Ref. 2, 12].

The ignition peninsula is defined by the condition $s \geqslant 0$. The initial stage of the reaction is typified by an exponential rise in the concentration of reaction products and the reaction rate.

The distribution of n_v for exponential growth of concentration without V-V relaxation is constant at large st, and is determined by the expression $\bar{n} = s\bar{k}/(s + \tilde{b})$. Corresponding to the assigned quantities $\tilde{b}$ and k_v is a minimum value s_{min} at which inversion still exists in the system of vibrational levels. Let $k \approx 0$, $k_{v+1} \approx 0$, $\tilde{b}$ be assigned in the form of a harmonic approximation. Then for large st we have

$$n_1 n_0 \approx s\tau_p (1 - \exp(-h\nu/kT))^{-1} \approx s\tau_p. \qquad (3.37)$$

This implies that the condition of existence of inversion in the given case will be $s\tau_p > 1$. The region of satisfaction of condition $s\tau_p > 1$ is located inside the ignition peninsula (dot-and-dash line on Fig. 3.1) or is absent entirely.

The initial mixture has temperature and pressure far from the ignition region. External factors typical of the given chemical lasers design such as the fast action of an exothermic discharge, photolysis, transfer the mixture to the ignition region, and when the energy of this action is sufficient, into the inversion region [Ref. 13].

From (3.34)-(3.36) we can make a qualitative estimate of the influence that V-V relaxations have on the course of the reaction. If processes (3.33e) take place very rapidly, relaxation will cause population of level $v = 4$ due to transitions from the third level. In this case the reaction rate may increase somewhat. On the other hand if processes (3.33e) are slow, relaxation leads to establishment of Boltzmann distribution n_v, and the reaction rate decreases.

Accounting for V-V relaxation within the framework of the linearized problem for the case of radical chains was included in Ref. 8, 13 for a two-level model with estimates of the possible efficiency of a laser based on a branched chain reaction.

§3.5. Principal Equations of the cw Chemical Laser

Theoretical analysis of the characteristics of the cw chemical lasers presents considerable difficulties due to the necessity of simultaneously accounting for the influence of diffusion, chemical reactions and radiation [Ref. 14].

In theoretical models the nonequilibrium nature of energy distribution can be taken into consideration by considering the gas as a mixture of several components in analogy with gas reactions, each long-lived V-level of the active molecule being taken as an individual gas component. It is assumed that the formation of active molecules in mixing and combustion of the fuel and oxidant is determined by diffusion, while combustion takes place along the flame front [Ref. 15]. Collisional deactivation of each vibrational level of the active molecule by resonant V-V and V-T energy transfer is taken into consideration by expansion in a series with respect to powers of the ratio of the axial distance to the characteristic deactivation length.

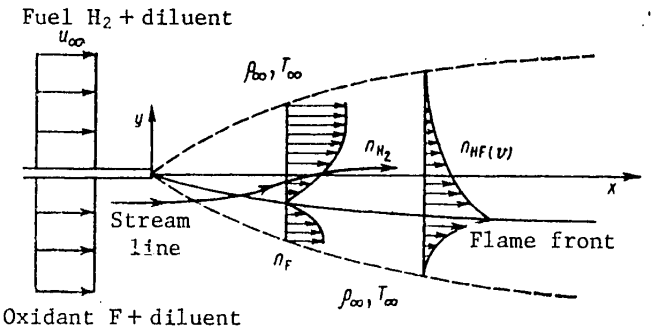

Fig. 3.2. Flow diagram in diffusional chemical laser

The flow scheme is shown in Fig. 3.2. Two homogeneous semi-infinite parallel gas flows (one consisting of oxidant and diluent, the other of fuel and diluent) begin mixing and burning at point x = y = 0. Here x is the coordinate in the direction of flow, y is the coordinate in the direction perpendicular to x, the positive direction of y corresponding to the fuel-filled region.

Such a configuration is an idealization of the flow in the channel of the chemical laser, and is analogous to flow in a boundary layer with velocity components u along the x-axis and v along the y-axis.

System of equations (3.10)-(3.14) with consideration of boundary layer theory implies [Ref. 14]:

$$\frac{\partial}{\partial x}(\rho u)+\frac{\partial}{\partial y}(\rho v)=0; \tag{3.38}$$

$$\rho\left(u\frac{\partial u}{\partial x}+v\frac{\partial u}{\partial y}\right)=\frac{\partial}{\partial y}\left(\eta\frac{\partial u}{\partial y}\right); \tag{3.39}$$

$$\rho\left(u\frac{\partial h_0}{\partial x}+v\frac{\partial h_0}{\partial y}\right)=\frac{\partial}{\partial y}\left[\frac{\eta}{\mathrm{Pr}}\left(\frac{\partial h_0}{\partial y}+(\mathrm{Pr}-1)\,u\frac{\partial u}{\partial y}\right)\right]-\sum_{v,J}\sum\alpha_{v,J}I_{v,J}; \tag{3.40}$$

$$\rho\left(u\frac{\partial Y_i}{\partial x}+v\frac{\partial Y_i}{\partial y}\right)=\frac{\partial}{\partial y}\left(\rho D_{ij}\frac{\partial Y_i}{\partial y}\right)+w_i+\frac{\mu_{\mathrm{HF}}}{hN_A}\delta_{i,v}\sum_J\left(\frac{\alpha_{v,J}I_{v,J}}{\nu_{v,J}}-\frac{\alpha^{v,J}I^{v,J}}{\nu^{v,J}}\right); \tag{3.41}$$

$$\frac{\partial I_{v,J}}{\partial y}=\alpha_{v,J}I_{v,J}, \tag{3.42}$$

where $\mathrm{Pr}=\eta c_p/\lambda_Q$; η is the coefficient of viscosity; $c_p=\Sigma c_{p,i}Y_i$;

$$p=\rho RT\Sigma(Y_i/\mu_i);\quad h_0=h_e+1/2u^2;$$

$$h_e=\sum_i Y_i\left(\int_0^T c_{p,i}\,dT+h_{f,i}\right).$$

Superscript v, J denotes transitions of the branch from level v, J to level v - 1, J + 1, while the subscript denotes transitions from level v + 1, J - 1 to level v, J.

The last term in the second member of equation (3.40) is the energy loss per unit of volume due to stimulated radiation and absorption. It is equal to zero for all $i \neq v$. Term w_i characterizes the arisal of the i-th component as a result of the chemical reaction. The optical gain $\alpha_{v,J}$ corresponds to its value in the center of the line, and is defined by the formula

$$\alpha_{v,J}=A\,(Y_{v+1}-\varkappa Y_v), \tag{3.43}$$

where

$$A=\frac{8\pi^{5/2}N_A}{3(2k\mu_{\mathrm{HF}})^{1/2}}\,\frac{|H_v^{v+1}|^2JF_{v,J}\rho}{R_J(v+1,\,J-1)\,T^{1/2}}\exp[-E(v+1,\,J-1)/k^0T];$$

$$R_J(v,\,J)=\sum_{J=0}^{\infty}(2J+1)\exp[-E(v,\,J)/k^0T];$$

$$\varkappa=\frac{R_J(v+1,\,J-1)}{R_J(v,\,J)}\exp\{-[E(v,J)-E(v+1,\,J-1)]/k^0T\}.$$

Here Y_V is the mass fraction of excited molecules, N_A is Avogadro's number, R_J is internal energy for rotational degrees of freedom. The term $|H_v^{v+1}|^2$ accounts for the contribution of vibrational degrees of freedom to the electrical dipole moment, and $F_{V,J}$ is the parameter of interaction of vibrational and rotational degrees of freedom.

To describe the process of amplification of radiation in a premixed moving gas stream in cw operation we have the system of equations [Ref. 4]:

$$\partial I_\nu/\partial x = \alpha I_\nu;\ v\partial\alpha/\partial y = -\sigma\alpha I_\nu + K(x, y), \tag{3.44}$$

where v is the velocity of gas flow along the y-axis.

Cross section y = 0 is the left-hand limit of the reference signal propagating along the x-axis. The boundary condition is written as

$$I_\nu(0, y) = I_{\nu,0} = \begin{cases} 0, & 0 \leqslant y \leqslant y_0, \\ I_{\nu,0}(y), & y > y_0; \end{cases} \tag{3.45}$$

$$\alpha(x, y_0) = \tilde{\alpha}(x, 0) + \frac{1}{v}\int_0^{y_0} K(x, y')\,dy'. \tag{3.45a}$$

In variables $\zeta = x$, $\theta = y/c$ the system of equations and boundary conditions will be

$$\left.\begin{aligned} &\partial I_\nu/\partial\zeta = \alpha I_\nu; \\ &\partial\alpha/\partial\vartheta = -\sigma\alpha I_\nu + K(\zeta, \vartheta); \\ &\zeta = 0;\ I_\nu = I_{\nu,0}(\vartheta) = \begin{cases} 0, & 0 < \vartheta < \vartheta_0 = y_0/u; \\ I_{\nu,0}(\vartheta), & \vartheta > \vartheta_0; \end{cases} \\ &\vartheta = \vartheta_0;\quad \alpha = \tilde{\alpha}(\zeta) = \alpha(\zeta, 0) + \int_0^{\vartheta_0} K(\zeta, \vartheta')\,d\vartheta'. \end{aligned}\right\} \tag{3.46}$$

The solution of this problem is

$$I_\nu(\zeta, \vartheta) = I_{\nu,0}\frac{1}{z}\exp\left[\int_{\vartheta_0}^{\vartheta}\left(\sigma I_{\nu,0} + \int_0^{\zeta} K\,d\zeta'\right)d\vartheta'\right]; \tag{3.47}$$

$$\left.\begin{aligned} &\alpha(\zeta, \vartheta) = \int_{\vartheta_0}^{\vartheta} K\,d\vartheta' - \frac{1}{z}\left\{\int_{\vartheta_0}^{\vartheta}\sigma I_{\nu,0}\times\right. \\ &\left.\times\exp\left[\int_{\vartheta_0}^{\vartheta'}\left(\sigma I_{\nu,0} + \int_0^{\zeta} K\,d\zeta'\right)d\vartheta''\right]\left(\int_{\vartheta_0}^{\vartheta'} K\,d\vartheta''\right)d\vartheta' - \tilde{\alpha}\exp\left(-\int_0^{\zeta}\tilde{\alpha}\,d\zeta'\right)\right\}; \\ &z = \int_{\vartheta_0}^{\vartheta}\sigma I_{\nu,0}\exp\left[\int_{\vartheta_0}^{\vartheta'}\left(\sigma I_{\nu,0} + \int_0^{\zeta} K\,d\zeta'\right)d\vartheta''\right]d\vartheta' + \exp\left(-\int_0^{\zeta}\tilde{\alpha}\,d\zeta'\right). \end{aligned}\right\} \tag{3.48}$$

In the case of a homogeneous reference signal ($I_{\nu,0} = \text{const}$), and pumping that depends only on the coordinate θ, relations (3.47), (3.48) are considerably simplified. Upon amplification of a narrow signal

$$I_{\nu,0} = \begin{cases} I_{\nu,0} = \text{const}, & \vartheta_0 < \vartheta < \vartheta_1, \\ 0, & \vartheta > \vartheta_1. \end{cases} \tag{3.49}$$

For the condition

$$\vartheta_1 - \vartheta_0 \ll \frac{2K(\vartheta_0)}{(\partial K/\partial\vartheta)|_{\vartheta=\vartheta_0}} = \tilde{\vartheta}$$

we can assume in the absence of radiation $K \approx \text{const}$, and then

$$\frac{I_\nu}{I_{\nu,0}} = \left[\frac{1}{\bar{G}_c} + \left(\frac{1}{\bar{G}} - \frac{1}{\bar{G}_c}\right)\exp\left(-\frac{\vartheta-\vartheta_0}{\vartheta_y}\right)\right]^{-1}, \tag{3.50}$$

$$\alpha = \alpha_c \frac{\vartheta-\vartheta_0}{\vartheta_y} + \frac{\tilde{\alpha} - \alpha_c \dfrac{\bar{G}}{\bar{G}_c}\left[1 + \exp\left(\dfrac{\vartheta-\vartheta_0}{\vartheta_y}\right)\left(\dfrac{\vartheta-\vartheta_0}{\vartheta_y} - 1\right)\right]}{1 + \dfrac{\bar{G}}{\bar{G}_c}\left(\exp\left(\dfrac{\vartheta-\vartheta_0}{\vartheta_y}\right) - 1\right)}, \tag{3.51}$$

where

$$\left.\begin{aligned} &\bar{G} = \exp(\tilde{\zeta\alpha});\ \bar{G}_c = 1 + K\zeta/(\sigma I_{\nu,0});\ \tilde{\alpha} = \alpha(0) + K\vartheta_0; \\ &\alpha_c = K/(\sigma I_{\nu,0} + K\zeta);\ \vartheta_y = (\sigma I_{\nu,0} + K\zeta)^{-1}. \end{aligned}\right\} \tag{3.52}$$

The solution implies that "spiking" of the pulse of output radiation takes place with an increase in the length of the amplifier.

Using (1.104), we give here the general form for the equation of vibrational relaxation:

$$\frac{dn_{m,i}}{dt} = \sum_{s,p,q,j} k^{ij}_{s\to m;\ p\to q} n_{s,i} n_{p,j} - \Sigma k^{ij}_{m\to s;\ q\to p} n_{m,i} n_{q,j}, \tag{3.53}$$

where $n_{m,i}$ is the concentration of molecules of type i on level m, $k^{ij}_{s\to m;\ p\to q}$ is the rate constant of transition of molecule i from level s to level m, and molecule j from level p to level q. For a polyatomic molecule, each of the subscripts s, m, p, q is described by a set of vibrational quantum numbers (v_1, v_2,..., v_n).

Direct solution of system of equations (3.53) is practically impossible without simplifying assumptions. Most important of these are the following: the influence of electronic excitation is negligible; translational and rotational degrees of freedom are in equilibrium; only transitions between nearest levels are considered; the simplest model of a harmonic oscillator is used.

Naturally the solutions found with the use of these simplifications are not universal and have their own region of application. For example, in particular, use of the harmonic oscillator model is valid at fairly small deviations from the equilibrium state and for lower vibrational levels.

§3.6. Laser Kinetics Under Conditions of Cooperative Spontaneous Emission

Coherence in Spontaneous Emssion. Usually spontaneous radiation is considered on the assumption that all gas molecules are independent. In this case the intensity of radiation is equal to the sum of the intensities of radiation of the individual molecules, and the width and shape of the emission line of the gas are determined by the properties of an isolated molecule. This is true only when the distance between individual molecules is much greater than the radiated wavelength.

However, when working in the high-pressure region at distances comparable with the radiation wavelength, there are many radiating particles, and they emit as a unified quantum-mechanical system with intensity of spontaneous radiation proportional to the square of the number of these particles [Ref. 1]. It should be emphasized that the collective properties of the system of particles have a direct influence only on spontaneous and non-radiative processes in the system. The atoms of the system behave as if they were independent with respect to stimulated transitions. This is due to the fact that collective effects in absorption or stimulated emission mutually compensate each other, whereas there is no such compensation for spontaneous and nonradiative processes.

Collective interaction of radiating particles leads to a considerable change in the characteristics of chemical lasers that operate at high pressures of the mixture. The condition of onset of coherent radiation of the entire volume of emitting particles in the case of such synchronization will be the absolute concentration of emitters (chemical complexes, excited products of chemical reactions and the like), rather than the difference in concentration of populated levels. Superradiation is described in Ref. 1 for a system with dimension less than the radiation wavelength. It is assumed for the sake of simplicity that the gas molecules have only two nondegenerate energy levels E_2 and E_1 ($E_2 > E_1$). Radiation of the molecules is treated in the dipole approximation. The hamiltonian of the system of molecules without consideration of the radiation field is written as

$$H = H_0 + E \sum_{j=1}^{n} R_{j3}, \tag{3.54}$$

where $E = h\nu_e = E_2 - E_1$, H_0 and R_{j3} characterize respectively the energy of translational motion of molecules upon intermolecular interaction, and the internal energy of the j-th molecule with eigenvalues $\pm\frac{1}{2}E$.

The eigenfunctions take the form

$$\psi_{gm} = U_g(\bar{r}_k)[R_k], \tag{3.55}$$

where the $\bar{r}_k$ are coordinates of the center of mass.

If the number of molecules that are in the upper and lower states sre denoted by n_2 and n_1 respectively, then

$$m = (n_2 - n_1)/2. \tag{3.56}$$

Obviously $n = n_2 + n_1$ is the total number of molecules. The total gas energy is

$$E_{gm} = E_g + E_m, \tag{3.57}$$

where E_g is the energy of translational motion and interaction of the molecules.

Energy E_{gm} has degenerate multiplicities

$$\frac{n!}{n_+!\,n_-!} = \frac{n!}{(n/2+m)!\,(n/2-m)!}. \tag{3.58}$$

We introduce the quantum number r, the so-called cooperation number of the gas, which satisfies the following inequality:

$$|m| \leqslant r \leqslant n/2. \tag{3.59}$$

As a result, for the intensity of spontaneous radiation of the gas in state (r,m) we get the expression

$$I = (r+m)(r-m+1)\,I_0, \tag{3.60}$$

where I_0 is the intensity of spontaneous radiation of an isolated molecule.

Thus, special bound states of the gas are possible where the intensity of spontaneous radiation is proportional to the square of the number of molecules. Such for example is the state $r=n/2$, $m=0$. The intensity of radiation of gas that is in such a state is

$$I = (n/2)(n/2+1)\,I_0 \cong n^2 I_0/4. \tag{3.61}$$

Gas states are possible that radiate no energy at all, such as $r=m=0$.

It should be noted that in all transitions of the system that are accompanied by radiation, the quantum cooperation number r does not change.

In the general case where the state of the gas is a superposition of states with different r and m, or for a mixture with different states r and m, the intensity is

$$I = I_0 \sum_{r,n} P_{r,m}(r+m)(r-m+1), \tag{3.62}$$

where $P_{r,m}$ is the probability that the system at the instant of radiation is in state (r,m).

In the state of thermal equilibrium, where

$$n_2/n_1 = \exp(-E/k^0 T), \tag{3.63}$$

the average value

$$m = (n_2-n_1)/2 = [n \operatorname{th}(E/k^0 T)]/2 \cong -nE/(4k^0 T). \tag{3.64}$$

Here the line denotes averaging over the set with Boltzmann distribution. The average value of r coincides with $|\bar{m}|$

If r coincides in accuracy with (-m) the intensity of radiation is zero. On the other hand if r differs by unity from (-m), then

While the intensity of spontaneous radiation depends on the state of the gas (r,m), the intensity of the total radiation or absorption in the presence of an external field is always proportional to the number of active molecules.

If the dimensions of the system are comparable to or much greater than the wavelength, but the distances between the individual molecules are much less than a wavelength or comparable with it, coherent emission is possible, but the gas can emit coherently only in one direction.

A classical system of harmonic oscillators distributed in a large region may be so phased relative to one another that coherent radiation is obtained in one definite direction.

Influence of Collective Phenomena on a Radiative Chemical Reaction. Among chemical reactions from the standpoint of an appreciable increase in radiation intensity in the case of phase correlation of emitters for producing a laser, of particular interest are reactions whose rates depend on the presence of electromagnetic radiation. Such reactions include for example reactions of photorecombination, where a mechanism of an increase in the light-stimulated rate of the chemical reaction is possible [Ref. 16]. In realization of reactions of this kine, the phototransition is realized during the elementary act of the chemical reaction itself. In such a radiative reaction mechanism, the energy of the chemical bond is de-excited by the phototransition, whereas in ordinary chemical reactions the energy is transferred to a third molecule, or is carried off by the products of the chemical reaction. The photostimulated chemical reaction can be appreciably accelerated by bringing about conditions for realization of a mechanism of phase correlation of spontaneously emitting particles, where the time of de-excitation of excited particles is sharply reduced as a result of collective interaction of the particles via the common electromagnetic field [Ref. 17]. If the rate of formation of the energetically excited particles exceeds the rate of their deactivation as a result of superradiation, the process is an increasing one.

The inverse process contains a series of pulses with damping amplitude and increasing duration. In this connection, the cooperative phenomena in spontaneous radiation naturally lead to an appreciable increase of lasing power in individual pulses. In steady-state lasing, when the rate of the process is determined by the rate of formation of excited particles, the contribution of cooperative phenomena may in principle be of the same order of magnitude as other processes of deactivation and emission. Just the same, the necessity of bringing about conditions for manifestation of cooperative effects is offset by a number of obvious advantages of the reaction. For example, chemical lasers may utilize a wider range of reactions since the working molecules for getting coherent emission are not only reaction products with inverse population, but also simply excited particles. Besides, when the radiators are phase-correlated, the threshold of the required equilibrium density of excited reaction products (n^*_ϕ) will be less than the threshold of concentration of inversely populated particles n^*_{ind} for a mechanism of chemical rezction stimulated by induced phototransitions.

Actually, the rate of a chemical reaction in the case of phase correlation can be represented as

$$w_{\varphi} \approx w_{sp}(V/4)\, n^{*}_{\varphi}, \tag{3.66}$$

where $w_{sp} = Pn^{*}_{\varphi}$ is the rate of spontaneous radiation of n^{*}_{φ} regardless of the radiating particles, P is the probability of spontaneous radiation of excited reaction products, V is the phase correlation volume.

In the resonant process

$$w = w_{\varphi} = w_{ind} = k_1 n^2, \tag{3.67}$$

where k_1 is the rate constant of formation of excited reaction products, n is the concentration of initial reagents.

For w_{ind} we have [Ref. 16]

$$w_{ind} \approx 10^{-12} P (n^{*}_{ind})^2. \tag{3.68}$$

Whence

$$n^{*}_{\varphi}/n^{*}_{ind} = \sqrt{4b^2/pV k (T_0)}, \tag{3.69}$$

where $b = P\pi^2 \times c^3/\omega_m^2 \Delta\omega_m$, and ω_m, $\Delta\omega_m$ are the angular frequency and effective bandwidth of spontaneous radiation at the maximum of radiation intensity. Setting $P = 10^6\ s^{-1}$, $b = 10^{-6}\ cm^3/s$, $k(T_0) = 2 \cdot 10^{-15}\ cm^3/s$, $V = 1\ cm^3$, we get $n^*/n^{*}_{ind} \sim 0.05$.

Thus the use of a photostimulated chemical reaction in the state of phase correlation of reaction products that are in an excited (not necessarily inversely populated) state enables the use of a wider range of initial reagents. The reaction is realized by choosing the concentration of initial reagents and the temperature of the mixture (T_0) so as to satisfy the inequality for two components

$$\sqrt{(V/4)(k (T_0)/P)\, n_1 n_2} > 1. \tag{3.70}$$

§3.7. The Optical Cavity

The resonator cavity is one of the main components of any quantum generator, as it forms the radiation pattern. A cavity made up of two plane-parallel mirrors [Ref. 18] was the first to enable attainment of directional coherent radiation in the optical range. Cavities based on interferometers with spherical, parabolic and other surfaces have come into extensive use [Ref. 19]. Unstable resonators to some extent resolve the problem of more complete filling of the active medium with radiation [Ref. 20], but in these the ratio between aperture and cavity length does not permit development of a compact laser. Resonators of periodic modes have been developed thanks to the creation of a theory of cavity resonators with the use of concepts of the theory of linear systems. Different types of cavities and their theory are presented for example in Ref. 22, and their peculiarities in operation with chemical lasers are described in detail in Ref. 23. Let us consider as an example of a resonator of periodic modes a system with mirrors with surfaces determined by radii of curvature R_1, R_2. The space-frequency characteristic of such a system takes the form

$$H_0 (\xi) = [1 - H_1 (\xi)]^{-1}, \tag{3.71}$$

where ξ is a variable that describes excitation of the electromagnetic field in the cavity; $H_1(\xi)$ is the space-frequency characteristic that corresponds to one pass of electromagnetic excitation in the cavity, $H_1(\xi)$ can be expressed in terms of the space-frequency characteristics H_{11} and H_{12} corresponding to the first and second mirrors as

$$H_1(\xi) = H_{11}(\xi)\, H_{12}(\xi); \tag{3.72}$$

$$H_{11}(\xi, x) = \exp i\left[\frac{-\xi^2}{4(2\alpha-\beta_1)}\right]\exp(-i\beta_1 x^2); \tag{3.73}$$

$$H_{12}(\xi, x) = \exp i\left[\frac{-\xi^2}{4(2\alpha-\beta_2)}\right]\exp(-i\beta_2 x^2), \tag{3.74}$$

where $\alpha = k/2L$, $\beta_1 = k/2f_1$, $\beta_2 = k/2f_2$, f_1 and f_2 are the focal lengths of the first and second mirrors respectively, L is the distance between mirrors, $k = 2\pi/\lambda$ is the wave number.

The inverse Fourier transform obtained from (3.71)-(3.74) for the general space-frequency characteristic $H_1(\xi,x)$ as a linear system with feedback gives the pulse response of the system or the Green's function of the given problem:

$$h_0(x) = \frac{1}{2\pi}\int_{-\infty}^{\infty} H_0(\xi, x)\exp(i\xi x)\, d\xi, \tag{3.75}$$

which is expressed by the sum of the eigenfunctions--the modes of the optical cavity.

The residues of the integral function $H_0(\xi,x)\exp(i\xi x)$ give eigenfunctions of the form

$$\exp(i\xi_m x), \tag{3.76}$$

where the values of ξ_m are determined from the relation

$$\left|\left(\frac{1}{4(2\alpha-\beta_1)}+\frac{1}{4(2\alpha-\beta_2)}\right)\xi_m^2+(\beta_1+\beta_2)x^2\right| = 2\pi m,\ m=0,1,2,\ldots. \tag{3.77}$$

This implies

$$\xi_m = \sqrt{-\frac{4(\beta_1+\beta_2)(2\alpha-\beta_1)(2\alpha-\beta_2)}{4\alpha-(\beta_1+\beta_2)}x^2+2\pi m\frac{2(2\alpha-\beta_1)(2\alpha-\beta_2)}{4\alpha-(\beta_1+\beta_2)}}. \tag{3.78}$$

This formula gives the field distribution on the cavity mirror for any distances and radii of curvature of the mirrors, and is the most general formula. For cavities with identical mirrors $R_1 = R_2 = R$ and $m = 0$ we have

$$\xi_0 = i2\alpha x\sqrt{2\bar{l}-\bar{l}^2} = i\frac{2\pi}{\lambda L}\sqrt{2\bar{l}-\bar{l}^2}\,x,$$

(here $\bar{l} = \beta/\alpha = L/R$), whence

$$\psi_0(x) = \exp(i\xi_0 x) = \exp\left(-\frac{2\pi}{\lambda L}\sqrt{2\bar{l}-\bar{l}^2}\,x^2\right). \tag{3.79}$$

Due to linearity of the entire system and the operation of differentiation, the n-th derivative of function (3.79) is a solution and eigenfunction of the resonator equation. For Hermite polynomials $H_n(x)$ we have the relation

$$(-1)^n \frac{d^n}{dx^n} \exp(-x^2/2) = \exp(-x^2/2) H_n(x). \tag{3.80}$$

Differentiating (3.79) n times, we get an expression for the n-th eigenfunction

$$\psi_n(x) = H_n(\sqrt{2}x/r) \exp(-x^2/r^2) \tag{3.81}$$

(r is the radius of the mirror).

In the case of infinite plane-parallel mirrors the optical cavity can be considered as a spatially invariant system with general space-frequency characteristic

$$H_0(\xi) = [1 - \exp i(-L\xi^2/k)]^{-1}. \tag{3.82}$$

The pulse response of such a system has first-order poles at points

$$\xi_m = \pm \sqrt{2\pi m L/k} \tag{3.83}$$

and a second-order pole at point $\xi = 0$. The residue at point $\xi = 0$ is equal to zero. The residue at point $\xi = \xi_m$ is equal to $k(2L\xi_m)^{-1} \exp(i\xi_m x)$. Consequently the pulse response of the cavity takes the form of the sum

$$h_0(x) = \sum_m \frac{\cos \xi_m x}{L\xi_m/k}, \tag{3.84}$$

each term of which is an eigenfunction representing the periodic distribution of the field on the mirror, which depends on the length of the cavity. This reasoning implies

$$L_N = N x_0^2/\lambda \tag{3.85}$$

--the condition of optimum synchronization of harmonics of the periodic mode for a cavity with plane-parallel mirrors, one having a periodic structure such as alternating reflective and transparent bands of identical width $x_0/2$, or holes. For the general case with radii of curvature of the mirrors R_1 and R_2,

$$[\lambda L - \lambda L^2 (1/R_1 + 1/R_2)] = N x_0^2, \quad N = 1,2,... \tag{3.86}$$

Periodic modes guarantee complete filling of the working medium, and enable us to make resonators with the structurally necessary ratios of aperture and length. Experimental studies with a grating in the cavity [Ref. 24] have shown that when the length of the resonator differs from L_N (3.85), fields of alternating sign are excited, while at a length equal to L_N the fields are in phase with a greater contribution of energy in the central lobe of the radiation pattern.

REFERENCES

1. Dicke, R. N., "Coherence in Spontaneous Radiation Processes", PHYS. REV., Vol 93, No 1, 1954, pp 99-111; "Swept-Gain Superradiance Theory Draws Wide Acclain", ARMY RESEARCH, DEVELOPMENT AND ACQUISITION MAGAZINE, Vol 19, No 5, 1978, p 28.

2. Bashkin, A. S. et al., "Chemical Lasers" in: "Itogi nauki i tekhniki. Radiotekhnika" [Advances in Science and Engineering. Radio Engineering], Vol 8, Moscow, VINITI 1975, 382 pages.

3. Kompa, K. L., "Chemical Lasers", Berlin-Heidelberg-New York, Springer Verlag, 1973, p 92.

4. Pimenov, V. P., Shcheglov, V. A., "Amplification of Monochromatic Radiation Under Conditions of Unsteady and Spatially Inhomogeneous Excitation of a Gas Medium", KVANTOVAYA ELEKTRONIKA, Vol 3, No 5, 1976, pp 1041-1050.

5. Basov, N. G. et al., "Dynamics of Chemical Lasers", KVANTOVAYA ELEKTRONIKA, No 2, 1971, pp 3-24.

6. Petrash, G. G., "Pulsed Gas-Discharge Lasers", USPEKHI FIZICHESKIKH NAUK, Vol 105, No 4, 1971, pp 645-676.

7. Dzhidzhoyev, M. S., Platonenko, V. T., Khokhlov, R. V., "Chemical Lasers", USPEKHI FIZICHESKIKH NAUK, Vol 100, No 4, 1970, pp 642-679.

8. Orayevskiy, A. N., "Chemical Laser Based on Branched Reactions", ZHURNAL EKSPERIMENTAL'NOY I TEORETICHESKOY FIZIKI, Vol 55, No 4, 1968, pp 1423-1429;

Igoshin, V. I., Orayevskiy, A. N., "Kinetic Phenomena in Thermal Ignition With Inverse Excitation of Products", ZHURNAL EKSPERIMENTAL'NOY I TEORETICHESKOY FIZIKI, Vol 59, No 10, 1970, pp 1240-1250.

9. Semenov, N. N., Shilov, A. Ye., "The Role of Excited Particles in Branched Chain Reactions", KINETIKA I KATALIZ, Vol 6, No 1, 1965, pp 3-6.

10. Kapralova, G. A., Trofimova, T. M., Shilov, A. Ye., "Upper Limit of Ignition in Reaction of Fluorine With Oxygen", KINETIKA I KATALIZ, Vol 6, No 6, 1965, pp 977-983.

11. Kapralova, G. A., Trofimova, T. M., Rusin, L. Yu. et al., "Experimental Proofs of Branching in Chain Reactions of Molecular Fluorine", KINETIKA I KATALIZ, Vol 4, No 4, 1963, pp 653-654.

12. Basov, N. G., Kulakov, L. V., Markin, Ye. P. et al., "Emission Spectrum of Chemical Laser Based on a Mixture of $H_2 + F_2$", PIS'MA V ZHURNAL EKSPERIMENTAL'NOY I TEORETICHESKOY FIZIKI, Vol 9, No 11, 1969, pp 613-617.

13. Batovskiy, O. M. et al., "Chemical Laser Based on Chain Reaction of Fluorine With Hydrogen", PIS'MA V ZHURNAL EKSPERIMENTAL'NOY I TEORETICHESKOY FIZIKI, Vol 9, No 6, 1969, pp 341-343.

14. Holland, R., Mirels, H., "Flame-Sheet Analysis of CW Diffusion-Type Chemical Laser. I. v_n-Coupled Radiation", AIAA JOURNAL, Vol 10, No 4, 1972, pp 420-428;

King, W. S., Mirels, H., "Numerical Study of a Diffusion-Type Chemical Laser", AIAA JOURNAL, Vol 10, No 12, 1972, pp 1647-1654.

15. Williams, F. A., "Combustion Theory: the Fundamental Theory of Chemically Reacting Flow Systems", Massachusetts, Addison-Wesley Publishing Company, 1965, p 447.

16. Pekar, S. I., "High-Pressure Chemical Lasers, and Light-Stimulated Chemical Reactions", DOKLADY AKADEMII NAUK SSSR, Vol 246, No 4, 1979, p 899.

17. Prokhorov, A. M., "Submillimeter Amplifier and Maser", ZHURNAL EKSPERIMENTAL'NOY I TEORETICHESKOY FIZIKI, Vol 34, No 6, 1958, pp 1658-1659.

Schawlow, A. L., Townes, C. H., "Infrared and Optical Masers", PHYS. REV., Vol 112, No 6, 1958, pp 1940-1949.

19. Mikaelyan, A. L., Turkov, Yu. G., Savel'yev, V. G., "High-Coherence Ruby Laser With Diffraction Divergence", PIS'MA V ZHURNAL EKSPERIMENTAL'NOY I TEORETICHESKOY FIZIKI, Vol 6, No 6, 1967, pp 675-677.

20. Anan'yev, Yu. A., Sventsitskaya, N. A., Sherstobitov, V. Ye., "Properties of Unstable-Cavity Lasers", ZHURNAL EKSPERIMENTAL'NOY I TEORETICHESKOY FIZIKI, Vol 55, No 1(7), 1968, pp 130-140.

21. Ablekov, V. K., Belyayev, V. S., "Systems Approach to the Problem of the Optical Cavity", ZHURNAL PRIKLADNOY SPEKTROSKOPII, Vol 23, No 6, 1975, pp 1110-1112; "Optical Resonator as a Linear System" in: "Issledovaniye sistem" [Systems Research], No 2, Vladivostok, Izd. DVNTs AN SSSR, 1973, pp 32-54;

Ablekov, V. K., Frolov, A. V., "Opticheskaya i optoelektronnaya obrabotka informatsii" [Optical and Optoelectronic Data Processing], Moscow, Mashinostroyeniye, 1976;

Ablekov, V. K., Belyayev, V. S., Marchenko, V. M. et al., "Diffraction Properties of Periodic Modes of an Optical Cavity", DOKLADY AKADEMII NAUK SSSR, Vol 230, No 5, 1976, pp 1066-1068.

Ablekov, V. K., Belyayev, V. S., Vasil'yev, V. P. et al., "Periodic Methods of the Optical Cavity", ZHURNAL PRIKLADNOY SPEKTROSKOPII, Vol 28, No 1, 1978, pp 57-59.

Ablekov, V. K., Vinogradov, V. I., Marchenko, V. G. et al., "Field of Radiation of a Neodymium Glass Laser with Grating Reflector", OPTIKA I SPEKTROSKOPIYA, Vol 44, No 6, 1978, pp 1208-1210.

22. Maitland, A., Dann, M., "Vvedeniye v fiziku lazerov" [Introduction to Laser Physics]: translated from English by V. A. Batanov, edited by A. I. Anisimov, Moscow, Nauka, 1978, 407 pages;

Anan'yev, Yu. A., "Opticheskiye rezonatory i problema raskhodimosti lazernogo izlucheniya" [Optical Cavities and the Problem of Divergence of Laser Emission], Moscow, Nauka, 1979, 328 pages.

23. Chodzko, R. A., Chester, A. N., "Optical Aspects of Chemical Lasers" in: "Handbook of Chemical Lasers", N. Y., a Wiley-Interscience Publication, 1976, pp 95-201.

24. Ablekov, V. K., Marchenko, V. G., "Angle Spectrum of Laser Radiation With Grid in the Cavity, and Distribution of the Field of Periodic Modes on the Grid", ZHURNAL PRIKLADNOY SPEKTROSKOPII, Vol 29, No 4, 1978, pp 607-613.

CHAPTER 4: GAS-STATIC CHEMICAL LASERS

§4.1. Photochemical Gas-Static Lasers

Chemical lasers with stationary working fluid in a fixed volume, or in other words gas-static chemical lasers are the simplest in design. Their principal elements include systems for preliminary preparation of the working medium, initiation of the chemical reaction, selection and extraction of the stimulated emission. With respect to working principle, such chemical lasers are pulsed--the coherent radiation of energy is produced in a short time span: $h\nu = f(t)$. The mixture of initial gases is prepared in the working volume (reactor), or else is introduced into the reactor from a separate vessel. Thereafter, an external source initiates the chemical reaction practically simultaneously throughout the working volume. Part of the energy of the excited reaction products is coupled out through windows in the reactor in the form of radiation that is generated in the system for selection and extraction of this energy--the resonator. The depleted gas mixture is then expelled from the reactor, and the system is returned to the initial state by refilling the reactor with fresh working mixture.

Photodissociative Gas-Static Chemical Lasers. Working Principle and Major Characteristics. The iodine chemical laser with working process diagrammed in Fig. 4.1 belongs to this class. The photodissociative iodine gas-static chemical laser is

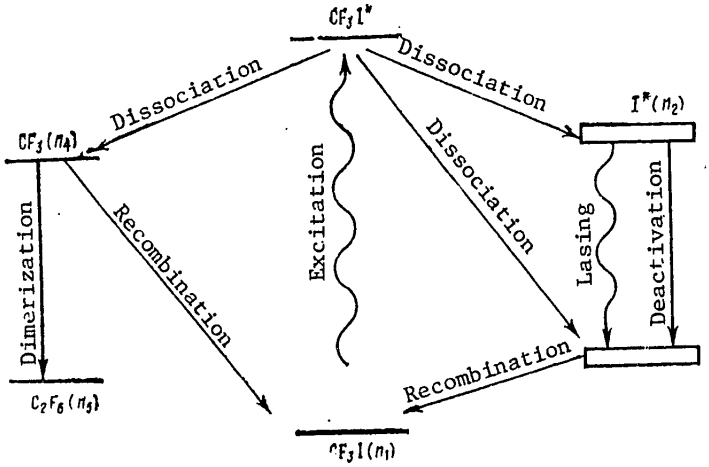

Fig. 4.1. Diagram of processes in iodine photochemical laser

optically pumped on a wavelength of 0.28 μm [Ref. 1]. The following reactions deserve attention in the pumping pulse stage before the onset of pyrolysis:

1) $I^* + CF_3 \xrightarrow{k_1} CF_3I$;
2) $I^* + CF_3 \xrightarrow{k_2} I + CF_3$;
3) $I + CF_3 \xrightarrow{k_3} CF_3I$;
4) $2I + CF_3I \xrightarrow{k_4} I_2 + CF_3I$;
5) $2CF_3 \xrightarrow{k_5} C_2F_6$;
6) $I^* + I_2 \xrightarrow{k_6} I + I_2$;

$$
\left.\begin{array}{ll}
7)\ I_2 + CF_3 \xrightarrow{k_7} CF_3I + I; & 10)\ CF_3 + CF_3I \xrightarrow{k_{10}} C_2F_6 + I^*; \\
8)\ I_2 + h\nu \xrightarrow{k_8} 2I; & 11)\ CF_3 + CF_3I \xrightarrow{k_{11}} C_2F_6 + I; \\
9)\ \widetilde{CF}_3 + CF_3I \xrightarrow{k_9} C_2F_6 + I^*; & 12)\ \widetilde{CF}_3 + CF_3I \xrightarrow{k_{12}} CF_3 + CF_3I.
\end{array}\right| \quad (4.1)
$$

Here I* is an iodine atom in state $5^2P_{1/2}$, $\widetilde{CF}_3$ is a "hot" radical. The transition $^2P_{1/2} \rightarrow {}^2P_{3/2}$ ($\lambda = 1.315$ μm) ensures generation of stimulated emission right up to the kilowatt range, with duration of several microseconds. Photodissociative iodine gas-static chemical lasers have been made with energy of several tens of joules [Ref. 2] and lasing duration of several nanoseconds [Ref. 3] with efficiency of about 0.5%. In Ref. 4 the energy of stimulated emission was brought up to 1000 J at efficiency equal to 1.4%. The efficiency of photodissociative gas-static chemical lasers is increased by expanding the absorption spectrum of working substances, and also by using a variety of chemical reactions corresponding to photolysis [Ref. 5, 6]. The working substances used in the photodissociative iodine gas-static chemical laser contain the C-I bond in molecules of type RI, where $R = CF_3$, C_2F_5, C_3F_7 and the like. The use of other promising working substances for such a chemical laser is limited by the requirement for rather high vapor pressure of these substances, which is necessary for getting high concentrations of excited molecules in the gas phase, and consequently high values of ε_V--the specific energy output per unit volume of the working chamber.

Excitation of chemical lasers in the process of photodissociation was studied in Ref. 7. An investigation was made of the processes of photodissociation of a number of compounds that contain the bond of the iodine atom with elements of group V: P, As, Sb, N. It has been experimentally shown that about 6.5% of the stored energy can be released as radiation. The cross section for stimulated emission is regulated by adding a buffer gas to the working medium. A typical diagram of an experimental photodissociative iodine gas-static chemical laser is shown in Fig. 4.2 [Ref. 5].

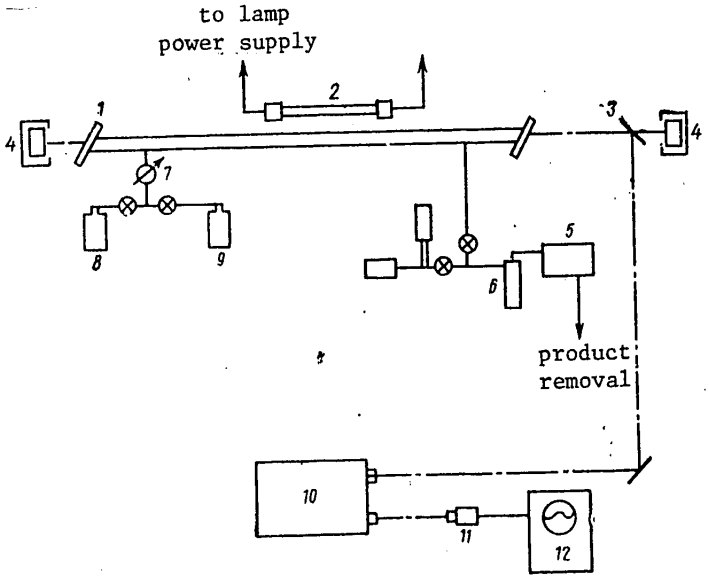

Fig. 4.2. Diagram of a photodissociative iodine gas-static chemical laser: 1--Brewster window; 2--flashlamp; 3--beam splitter; 4--mirror; 5--vacuum pump; 6--cold trap; 7--manometer; 8--tank with inert gas; 9--tank with working gas; 10--spectrometer; 11--infrared detector; 12--oscilloscope

A working tube 1 m long with inside diameter of 10 mm is equipped with quartz Brewster windows. The cavity is formed by two spherical confocal mirrors with gold coating. Pumping is by a straight xenon flash tube with average pulse rise time of 20 μs and duration of 150 μs. The flashlamp and working tube are placed at the conjugate foci of a polished elliptical reflector.

The flashlamp was supplied by a capacitance of 18 μF charged to 15 kV by energy of up to 1760 J. The minimum energy supplied to the system was 225 J. Premature discharge was prevented by control of the discharge gap. Two triggering units with voltage of 30 kV simultaneously ionized the lamp, the discharge gap and triggered the oscilloscope scan.

Up to 4% of the energy of the stimulated beam was deflected by a quartz plate to a spectrometer and to a detector connected to the oscilloscope. This detector was a germanium diode or an InSb photoresistor. The system was evacuated by a two-stage vacuum pump. A cold trap removed the condensable products. The operation of such a chemical laser depends mainly on the pressure of the reagents and the energy of the flashlamp. Since only part of the reagent is dissociated during a single flash, repeated flash exposures enable more efficient use of the reagent. The duration of the stimulated pulse can be increased by adding inert gas.

However, the substances ordinarily used as the active medium (CF_3I or $n\text{-}C_3F_7I$) still have to be changed after each pumping pulse, since lasing power drops off considerably otherwise. Ref. 8 gives data of experimental studies on repeated use of the same medium $(CF_3)_2AsI$. The experiments were done on the facility shown in Fig. 4.3.

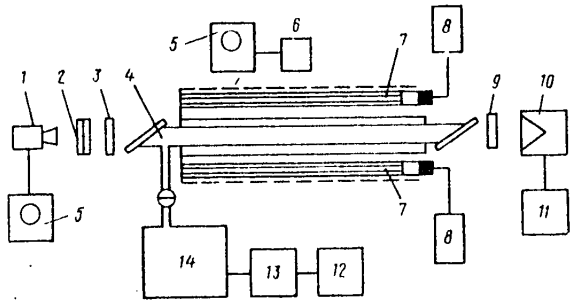

Fig. 4.3. Diagram of experimental facility: 1--photodiode; 2--scatterers and neutral filters; 3--mirror; 4--working chamber of the laser; 5--oscilloscope; 6--photomultiplier; 7--xenon flashlamps IFP-5000; 8--capacitor bank; 9--output mirror; 10--calorimeter; 11--microammeter; 12--roughing vacuum pump; 13--oil-vapor pump; 14--vacuum receiver

The cavity included two flat dielectric mirrors with distance of about 1 m between them. The transmission factor of one of the mirrors was 0.2%, and of the other was 0.6-50% for $\lambda = 1.315$ μm. The working chamber was made of a quartz tube with outside diameter of 10-20 mm, and had glass windows on the end faces placed at the Brewster angle ($\alpha_B \cong 57°$). Welded onto the illuminated part of the working chamber ($l_{ef} \cong 25$ cm) was a quartz jacket filled with distilled water. The pumping light source was two IFP-5000 lamps with supply from separate capacitor banks with capacitance of $C = 47$ μF at maximum voltage of 7 kV. Both lamps and the working

chamber were covered on the outside with polished aluminum foil as a reflector. To get a short pulse ($\tau_{1/2} \approx 3$ μs), a capacitance C = 5 μF with voltage of 25 kV was connected to the lamp through a vacuum discharger. The energy E of stimulated emission was measured by a KIM-1 calorimeter. The lasing pulse shape was registered by an FD9E11 photodiode and an S1-37 oscilloscope. Radiation of the pumping lamp was monitored by an FEU-18 photomultiplier with filter corresponding to the absorption band of the substance. The gas phase of compound $(CF_3)_2AsI$ has two absorption regions in the ultraviolet band: long-wave ($\sigma_{max} = 3.3 \cdot 10^{-18}$ cm^2 at $\lambda_{max} = 290$ nm), and short-wave ($\sigma_{max} = 10^{-17}$ cm^2 at $\lambda_{max} = 217$ nm). At the same time, in substances with the C-I bond (such as CF_3I, C_3F_7I), the maximum absorption cross section in the "quartz" ultraviolet is four or five times smaller than in the long-wave band of $(CF_3)_2AsI$.

The spectral composition of the pumping light source was limited by using a liquid filter consisting of a 0.003% solution of $NaNO_2$ in distilled water. This filter does not change its properties with time, does not pass radiation in the region of the short-wave band of $(CF_3)_2AsI$ and does not hold back the long-wave band of CF_3I and C_3F_7I.

An investigation of lasing in mixtures of $(CF_3)_2AsI/CF_3I$ and $(CF_3)_2AsI/CF_3F_7I$ shows that at low pressures p of the mixture the energy E of the stimulated emission is determined by the energy characteristics of the components of the mixture.

From the way that E depends on the number of flashes produced without changing the mixture at low pumping energy, we find that for $n\text{-}C_3F_7I$ the value of E decreases by a factor of about four after the first flash, while $(CF_3)_2AsI$ withstands more than 50 flashes without an appreciable reduction in E.

Investigation of processes of photodissociation of other substances such as cyanides has also been directed at use in gas-static chemical lasers [Ref. 9].

Other Photochemical Gas-Static Lasers. The first photochemical gas-static laser was realized on the basis of reacting chlorine with hydrogen [Ref. 10]. A flash-lamp causing partial dissociation of Cl_2 was used for rapid initiation of the reaction in the Cl_2/H_2 mixture. The mechanism of the photochemical chain reaction of $H_2 + Cl_2$, taking place with formation of vibrationally excited HCl, can be described as follows:

$$\left.\begin{aligned}
&1)\ Cl_2 + h\nu \xrightarrow{k_1} 2\,Cl \quad \text{(initiation)}\\
&2)\ Cl + H_2 \xrightarrow{k_2} HCl\,(v=0) + H \quad \text{(chain growth)}\\
&3)\ H + Cl_2 \xrightarrow{k_3''} HCl^*\,(v=n) + Cl\,;\\
&4)\ H + HCl^*\,(v=n) \xrightarrow{k_3''} H_2 + Cl \quad \text{(inhibition)}\\
&5)\ Cl + Cl + M \xrightarrow{k_4} Cl_2 + M \quad \text{(chain breaking)}
\end{aligned}\right\} \qquad (4.2)$$

A high concentration of chlorine atoms must be produced to maximize the number of parallel chain processes in (4.2). Consequently, to increase the energy E of stimulated emission it is necessary to increase the pressure of Cl_2, the energy and power of the light flash. To prevent the slow link of the chain 2) from limiting the overall rate of growth of the chain, the hydrogen must be kept at a high concentration.

Another way of increasing chain growth in reaction 2) is to raise the temperature of the mixture. These conclusions have been experimentally confirmed. For example, at room temperature lasing could not be attained on DCl molecules over a wide range of pressures of the reagents and energies of the light flash, whereas at elevated temperatures, lasing on DCl molceules presents no difficulties [Ref. 11]. Reducing the temperature of a medium with partial pressures of 2.4 kPa Cl_2 and 23.3 kPa D_2 from 510 to 450 K led to a five-fold reduction of lasing intensity.

The sequence of lasing onset on different V-R transitions within the limits of one band conforms to a pattern that is common to chemical lasers based on mixtures of either H_2/Cl_2 or D_2/Cl_2, namely: first radiation appears on the transition with low value of J, and then in sequence on transitions with higher values of J. This apparently due to the fact that the gas temperature is raised by the release of energy during the chemical reaction with subsequent change in the gain of the different V-R transitions. Besides, sequential lasing on transitions with different J is also possible at constant temperature if the radiation process changes the ratio of populations of different vibrational levels.

The necessity of increasing the temperature of the mixture and the concentration of hydrogen leads in the final analysis to limitation of chemical efficiency since there is an increase in the rate of relaxation of excited HCl molecules. More advantageous from the energy standpoint is the reaction described in §2.2

$$Cl + HI \rightarrow HCl^* (v \leqslant 4) + I (- 134 \text{ kJ/mole}), \qquad (4.3)$$

in which up to 70% of the energy of the chemical reaction is converted to vibrational energy of HCl molecules, and inversion may be formed between upper vibrational levels [Ref. 12]. In Ref. 13, a chemical laser based on such a reaction used circulation of the gas mixture through a tube (length 60 cm, inside diameter 14 mm) to reduce the influence of the spontaneous reaction that takes place in a Cl_2/HI mixture at a relatively high rate. Lasing was observed in the pressure region p = 0.8-5.33 kPa with emission spectrum on transitions $\mathcal{P}_{3-2}(4) - \mathcal{P}_{3-2}(5)$, $\mathcal{P}_{2-1}(5) - \mathcal{P}_{2-1}(7)$, $\mathcal{P}_{1-0}(9) - \mathcal{P}_{1-0}(13)$ (i. e. on transitions v = 3 → v = 2 of the $\mathcal{P}$-branch from J = 4 to J = 5 and so on).

It should be noted that the operation of chemical lasers on a Cl_2/HI mixture involves considerable difficulties, most serious among them being iodine condensation on the cold components of the system. This disadvantage is eliminated in chemical lasers based on a Cl_2/HBr mixture [Ref. 14] in which the reaction

$$Cl + HBr \rightarrow HCl^* + Br (- 65 \text{ kJ/mole})$$

takes place with radiation density W = 12 kW and E = 0.12 J, p = 0.87 kPa, energy of the initiating flash E_I = 1350 J. Limitation of the energy of stimulated emission is due to the high rate of relaxation as a result of collisions

$$HCl\ (v = 1) + HBr\ (v = 0) \rightarrow HCl\ (v = 0) + HBr\ (v = 1) \qquad (4.4)$$

At pressure of the working mixture $p \approx 1.33$ kPa, the time of relaxation is of the order of a few microseconds. Increasing p to several kPa with simultaneous increase in pumping power gives values of W up to 30 kW and $E \sim 0.2$-0.3 J.

Chemical lasers can be made that are based on bromine atoms formed in the photolytic reaction

$$I^* + Br_2 \rightarrow IBr + Br^*,$$

with lasing on electronic transition $4^2P_{1/2} \rightarrow 4^2P_{3/2}$ at $\lambda = 2.714$ μm [Ref. 15].

The high rate of reaction $F + H_2$, the great energy that is released, and the fact that a considerable part of this energy (about 65%) is converted to vibrational energy of the resultant molecules [Ref. 16, 17] make this reaction attractive for use in gas-static chemical lasers. At room temperature, the rate constant of reaction $F + H_2$ is equal to $2.5 \cdot 10^{-11}$ cm^3/s, which is much higher than the rate constant of the main pumping reaction in chemical lasers based on a mixture of H_2/Cl_2, which is equal to $1.7 \cdot 10^{-12}$ cm^3/s [Ref. 18].

Lasing was first achieved on HF molecules in photoinitiation of the mixture UF_6/H_2 [Ref. 19, 20]. In this case, the following reactions are possible:

$$\left.\begin{array}{l} 1)\ UF_6 + h\nu \rightarrow UF_5 + F; \\ 2)\ F + H_2 \rightarrow HF^* + H \quad (-134\ \text{kJ/mole}); \\ 3)\ H + UF_6 \rightarrow HF^* + UF_5 \quad (-192{,}6\ \text{kJ/mole}); \\ 4)\ UF_6 + UF_5 \rightarrow UF_4 + UF_6; \\ 5)\ H + UF_5 \rightarrow HF^* + UF_4. \end{array}\right\} \qquad (4.5)$$

Radiation of HF molecules takes place on transitions $\mathcal{P}_{2\text{-}1}(3) - \mathcal{P}_{2\text{-}1}(9)$. When H_2 is replaced by D_2, the DF molecules radiate on transitions $\mathcal{P}_{3\text{-}2}(4) - \mathcal{P}_{3\text{-}2}(9)$ and $\mathcal{P}_{2\text{-}1}(3) - \mathcal{P}_{2\text{-}1}(8)$.
Transitions between high vibrational levels of the HF molecule are typical of the reaction

$$H + F_2 \rightarrow HF^*\ (v \leqslant 9) + H \quad (-410\ \text{kJ/mole}), \qquad (4.6)$$

in which the energy release is sufficient for population of high vibrational levels. Other processes that determine formation of the radiation spectrum of photochemical lasers are:

population of vibrational levels

$$F + H_2 \rightarrow HF^*\ (v \leqslant 3) + H\ (-134\ \text{kJ/mole}); \qquad (4.7)$$

V-V and V-T exchange

$$\left.\begin{array}{l} HF(v) + HF(v) \rightarrow HF(v+1) + HF(v-1); \\ HF + M \rightarrow HF(v-1) + M; \\ (M = HF, H_2, F_2, H, F, He, O_2); \end{array}\right\} \qquad (4.8)$$

stimulated emission

$$HF(v) \rightarrow HF(v-1) + h\nu. \tag{4.9}$$

As a result of reaction (4.6), the level with $v = 5 (k_1:k_2:k_3:k_4:k_5:k_6 = 0.2:0.75:0.6:0.7:1.0:0.95)$ is populated at the maximum rate. Most intensely populated as a result of reaction (4.7) is the level with $v = 2 (k_1:k_2:k_3 = 0.29:1.0:0.47)$ [Ref. 16]. The behavior of populations of the levels of the HF molecule as a function of quantum number v as a result of reactions (4.6) and (4.7) takes the form of a smooth curve with two maxima, the chief one corresponding to level $v = 2$, and the other--to $v = 5$.

Experimental results unambiguously confirm the chain nature of this chemical reaction. Actually, the intensity of the radiation remains constant or increases after the cessation of pumping. The main influence on the formation of HF is from the reaction of vanishing of F atoms as a result of reaction with H_2, the damping constant being $\tau_F \leqslant 3$ μs, and the formation of H with $\tau_H \leqslant 8$ μs. The influence of other reactions such as recombination of atoms or thermal dissociation of F_2 and H_2 at $T < 1200$ K is several orders of magnitude weaker. Therefore the existence of lasing over a duration of a few tens of microseconds after termination of pumping in mixtures that are rich in hydrogen presupposes the presence of a chain mechanism of reaction. In this case we can readily explain the existence of lasing with a reduction in pumping power (or even total cessation), since the rate of a chain reaction may increase with time due to self-heating of the mixture through the release of chemical energy. When the possibility of a chain reaction has been eliminated, e. g. by replacing F_2 with MoF_6, lasing duration has not exceeded the duration of the pumping pulse.

In parametric analysis of a photochemical laser based on reaction $H_2 + F_2$ [Ref. 21], the following expression is obtained for specific energy output from a unit volume:

$$\varepsilon_V = h\nu \frac{\Omega}{\bar{k}_n} \left(1 - \frac{\bar{k}_N N}{\Omega}\right)^2. \tag{4.10}$$

where hν is the energy of a lasing quantum, $\bar{k}_n = 2k_n\psi\chi^{-2}$ and $\bar{k}_N = k_n\psi\chi^{-1}$ are the effective model constants of relaxation of vibrationally excited molecules of HF on molecules of HF and F_2 respectively; $\chi = (w_2 - w_1)/(2\Omega n)$; $\psi = (n_1^0 - n_2^0)/2n$; $\Omega = (1/n)dn/dt$; n_2, n_1 are the respective populations of the upper and lower lasing levels.

To find the effective model constants, a graph is plotted (Fig. 4.4) in coordinates $(\varepsilon_{V ex}\Omega_{th}^{-1})^{\frac{1}{2}}$ vs. $N\Omega_{th}^{-1}$, where subscripts "ex" and "th" denote the experimental and theoretical quantities respectively. It can be seen that the aggregate of the results is described by a linear relationship. From this we get $h\nu k_n^{-1} = 0.8 \cdot 10^{-8}$ J/(cm³·s), $\bar{k}_N = 1.5 \cdot 10^{-13}$ cm³/s and $\varepsilon_V = 0.8 \cdot 10^{-8} \Omega(1 - 1.5 \cdot 10^{-13} N/\Omega)$ J/cm³.

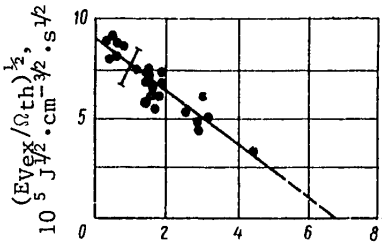

Fig. 4.4. Parametric dependence

Comparative analysis of the effectiveness of using different photolytic sources of fluorine atoms shows that the greatest gain on HF molecules is realized on a mixture of WF_6/H_2 [Ref. 22]. However, work with WF_6 is made difficult by the poor reproducibility of results and the complexity of getting pure WF_6.

The CO molecule is of interest as a working molecule of photochemical gas-static lasers. Many reactions that lead to the formation of CO have high exothermicity, enabling relatively easy excitation of CO to high vibrational levels ($v \leqslant 17$). This results in low rates of relaxation of the CO molecule in collision with unexcited particles.

The first photochemical gas-static CO laser was based on the reaction of oxidation of carbon disulfide [Ref. 23]. The working chamber was a quartz tube with KCl Brewster windows 7 mm in diameter placed in a resonator 1 m long. The $CS_2/O_2/He$ mixtures were pumped by a xenon lamp 50 cm long. Emission power increased with increasing He pressure, and at the optimum pressure $p = 20$ kPa He, the energy of excitation reached about 0.5 W.

Lasing was observed on 31 transitions of the $\mathcal{P}$-branch. Another 270 transitions have been detected on the $\mathcal{P}$- and $\mathcal{R}$-branches of the CO molecule [Ref. 24]. A common pattern is that lasing on transitions with low values of J shows up earlier than on transitions with high values of J.

Lasing with $\lambda = 4.7$-5.7 μm is observed over a wide range of mixture compositions, initiating energies (from 0.5 to 4 kJ) and pressures (from 0.066 to 13.3 kPa) [Ref. 25]. The pressure corresponding to maximum power increases approximately as $\sqrt{E_I}$, where E_I is the initiation energy, and the maximum power first increases very rapidly, and then in proportion to $E_I^{1.5-2}$.

The lasing process is unaffected by vibrational relaxation of CO molecules, and the characteristics of this process are determined only by chemical reactions [Ref. 26]. Most important of these are the following:

$$\left.\begin{aligned}
&0)\ CS_2 + h\nu\,(\lambda < 220\ \text{nm}) \rightarrow CS + S;\\
&1)\ S + O_2 \xrightarrow{k_1} SO + O \quad (-27{,}1\ \text{kJ/mole});\\
&2)\ O + CS_2 \xrightarrow{k_2} CS + O \quad (-96\ \text{kJ/mole});\\
&3)\ O + CS \xrightarrow{k_3} CO^* + S \quad (-313\ \text{kJ/mole});\\
&4)\ S + CS_2 \xrightarrow{k_4} CS_3 + M.
\end{aligned}\right\} \qquad (4.11)$$

According to data of Ref. 27, 28, $k_1 = 2 \cdot 10^{-12}$ cm^3/s, which is three orders of magnitude greater than the value assumed in Ref. 25 (at $T = 300$ K). In this case, not only reaction 4), but also any trimolecular reaction of disappearance of active particles (such as $SO + O + M \rightarrow SO_2 + M$) cannot be compared in rate to bimolecular reactions 1)-3) at low pressures of CS_2 ($p_{CS_2} \sim 0.1$ kPa) at which there is a drop in lasing energy and power. Therefore, in order to analyze the observed contradiction between the decisive role of trimolecular chain termination and the low calculated rate of such a reaction as compared with bimolecular reactions, special

experiments were done. The working tube of a chemical laser, made of optical quartz (with transmission to 200 nm), 50 cm long and 20 m in diameter, was closed on both sides with calcium fluoride (or barium fluoride) windows. The cavity was 120 cm long. Initiation was by two series-connected xenon lamps ($p_{Xe} = 0.266$ kPa). The lamps and the tube were placed inside a cylindrical reflector of aluminum foil. An investigation was made of the way that the energy E of stimulated emission depends on the partial pressure of CS_2 with dilution by gases He, Ar, Xe. The influence of dilution at high CS_2 pressures is evidence in favor of the hypothesis of trimolecular nature of the chemical process that limits energy and power of lasing.

The dependence of E and W on pressure of the components CO_2, N_2O, OCS is qualitatively the same as for dilution by inert gases. The effectiveness of CO_2 is close to that of helium ($k_{CO-CO_2} \approx 10^{-14}$ cm^3/s), and relaxation on N_2O is more effective ($k_{CO-N_2O} \approx 10^{-13}$ cm^3/s). The strongest resonant exchange with vibrational levels of CO ($4 \leqslant v \leqslant 13$) is shown by the OCS molecule ($k_{CO-OCS} \approx 10^{-12}$ cm^3/s).

Thus the above-mentioned contradiction persists, and to eliminate it, the scheme of the process must include new fast channels of active particle formation. For example the reaction $SO + CS \rightarrow OCS + S + 125$ kJ/mole has been suggested if its rate constant is of the order of or greater than 10^{-11} cm^3/s.

Photochemical Gas-Static Lasers With Pumping From Particles Excited During Chemical Reactions. The chemical efficiency of lasers is increased by using pumping of polyatomic working molecules such as CO_2 due to energy transfer from molecules of the HX type (where X = F, Cl, Br and so on) that are excited in the process of a chemical reaction. In this case, population inversion of the chemical reaction products is not obligatory for attaining lasing; it is sufficient that these products be in the excited state. Besides, the use of polyatomic molecules with pumping from chemical reaction products enables us to prolong the period of chemical pumping of the working molecules, and to realize selective pumping of individual levels, which is also conducive to an increase in efficiency.

In the first photochemical gas-static laser with energy transfer to molecules of CO_2 and N_2O, pumping was accomplished by excited molecules of DCl (HCl) and HI. The maximum value of E = 96 mJ on a wavelength of $\lambda = 10.6$ μm was attained in a mixture with partial pressures $p_{Cl_2} = 1.333$ kPa, $p_{HI} = 0.266$ kPa, $p_{CO_2} = 2$ kPa. On molecules of N_2O, E_{max} was only a third of the value obtained on molecules of CO_2. When CO_2 molecules are pumped by molecules of DF (HF) excited in the process of the reaction $F_2O + D_2$ (H_2), a peak power of about 10 kW can be attained, and about twice as much reaction energy can be extracted as is obtained on the DF molecules themselves [Ref. 30, 31]. In the range of low partial pressures of CO_2 a change toward an increase in this pressure leads to intensification of the process of energy transfer from DF to CO_2 and to linear dependence of energy on p_{CO_2}. At high CO_2 concentrations an increase in pressure leads to an increase in population of the lower level (00°0), and consequently to a reduction in the energy of stimulated emission.

The theoretical model of a photochemical laser based on energy transfer to CO_2 molecules from excited DF molecules includes the following elementary processes:

$$
\left.\begin{aligned}
&0)\ F_2 + h\nu \xrightarrow{k_0(t)} 2F;\\
&1)\ F + D_2 \xrightarrow{k_1} DF + D;\\
&2)\ D + F_2 \xrightarrow{k_2} DF + F;\\
&3)\ F + F + M \xrightarrow{k_3} F_2 + M;\\
&4)\ D + D + M \xrightarrow{k_4} D_2 + M;\\
&5)\ D + F + M \xrightarrow{k_5} DF + M;\\
&6)\ D + O_2 + M \xrightarrow{k_6} DO_2 + M;\\
&7)\ DF(v) + CO_2(v_1, v_2, v_3) \xrightarrow{k_7(v)} DF(v-1) + \\
&\quad + CO_2(v_1, v_2, v_3 + 1);\\
&8)\ \text{relaxation of asymmetric mode of } CO_2;\\
&9)\ \text{relaxation of deformation mode of } CO_2;\\
&10)\ DF(v) + M \xrightarrow{k_{10}^M} DF(v-1) + M;\\
&11)\ CO_2(00^0\,1) \xrightarrow{A} h\nu + CO_2(10^0\,0);\\
&12)\ CO_2(00^0\,1) + h\nu \xrightarrow{B} CO_2(10^0\,0) + 2h\nu.
\end{aligned}\right\} \qquad (4.12)
$$

Calculations based on such a model agree satisfactorily with the experimental data of Ref. 32, 33.

The pulse energy E_{max} obtained in the experiments is equal to 2.5 J. This corresponds to a value of $\varepsilon_V = 0.025$ J/cm^3 determined from the total volume of active medium equal to 100 cm^3, and $\eta_X = 2\%$. The introduction of He (up to $p_{He} \approx 8$ kPa) increases η_X by a factor of more than three (to 6.4%).

The characteristics of a chemical quantum amplifier on DF/CO_2 with higher parameters have been studied with initiation by a light pulse with duration shorter than the time of existence of inversion [Ref. 32, 34]. The working mixture of $D_2/F_2/CO_2/He$ was prepared by the method of dynamic mixing. Chemically compatible gases were mixed in the appropriate proportions at different total pressures in two identical stainless steel mixers, after which they were passed through a common pipeline into the working chamber. To slow down the dark reaction, oxygen was added to the mixture at a pressure corresponding to 6% of the fluorine pressure.

The use of a powerful light source with duration much shorter than the time of existence of inversion enabled attainment of $\varepsilon_{V_{max}} = 0.15$ J/cm at amospheric pressure on lines $\mathcal{P}(20)$ and $\mathcal{P}(22)$ for mixtures $D_2/F_2/CO_2/He = 1/1/4/5$, $\eta_X = 7\%$. The behavior of ε_V as a function of partial pressure of fluorine and the energy stored in the light source accumulator bank showed no tendency toward saturation under the experimental conditions.

In photochemical gas-static lasers based on energy transfer from molecules of DF to CO_2, one of the deficiencies that limit power increase and ε_V is the low rate

of energy transfer from DF to CO_2. In the TF/CO_2 system, energy transfer is nearly an order of magnitude faster than in the DF/CO_2 system. However, a comparison of processes on mixtures of T_2/F_2CO_2 and $D_2/F_2/CO_2$ has shown that the emission energy of the TF/CO_2 laser at all CO_2 pressures is lower than the energy of chemical lasers on DF/CO_2.

There is also a monotonic reduction of laser energy with increasing mixture storage time, which can be attributed to an increase in the rate of relaxation of CO_2 molecules on DF(TF) molecules that are formed in the mixture during preliminary storage. The increase in spontaneous initiation of chains due to the radioactivity of tritium does not permit an increase in its partial pressure above a few kPa, which limits the attainment of a large ε_V. Besides, an increase in the rate of chain initiation minimizes the time of preliminary storage of the working mixture.

The experiments of Ref. 35 yielded W = 200 kW, E = 5 J at a normal pressure of the mixture $D_2/F_2/CO_2/He$. The emission energy increases weakly with an increase in p from 1.33 kPa to 0.1 MPa. Pulse duration changed from 1.2 ms at p = 2 kPa to 100 μs at high pressure, which is caused by disruption of lasing due to thermal heating of the mixture. At optimum pressure, the gain $\alpha = 0.03$ cm^{-1}, $E \approx 5$ J. The value of η_x determined for the entire volume is equal to 3.2%, but is about 20% with consideration of only the radiating part of the volume.

The particulars of energy transfer $DF \rightarrow CO_2$ were analyzed in Ref. 36 on the basis of experimental studies of the output parameters of a photochemical laser on CO_2 mixtures of fluorides of chlorine with deuterium and fluorine with deuterium. It was shown that the $DF \rightarrow CO_2$ energy transfer was most efficient in a mixture of $F_2/D_2/CO_2$.

§4.2. Electric-Discharge Gas-Static Chemical Lasers

Most advantageous from the energy standpoint is initiation of the chemical reaction directly by an electric discharge. However, uniform excitation of the working volume by an electric discharge that is longitudinal with respect to the cavity axis can be accomplished only at pressures p of the mixture that are no higher than a few hundred Pa. At higher p, contraction of the discharge is observed that increases the time of propagation of the discharge throughout the volume, and this leads to cancellation of the inverse population of particles at foci of the chemical reaction. An arrangement of excitation by a transverse electric discharge raises the working pressure to several tens of kPa. However, even this arrangement has the disadvantage of complexity of uniform excitation of the entire working volume.

Fig. 4.5 shows two typical power supplies for initiating devices of a gas-static chemical laser with transverse electric discharge.

In the arrangement of the discharge circuit with needle electrodes 8, the capacitance of discharge capacitor C_D is from 0.005 to 0.05 μF, and it is discharged through working chamber 4 upon closure of spark discharger 2. In the supply circuit with flat electrodes 6, 7 and preliminary ionization of the discharge gap by an auxiliary discharge, the grounded electrode is an aluminum rod on which a copper wire is wound. The optimum distance between electrodes is 3.8 cm. Homogeneous discharge in the interelectrode gap is ensured by auxiliary discharge between

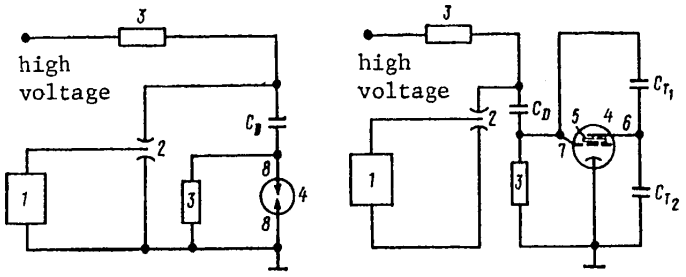

Fig. 4.5. Typical circuits of discharge devices for electrochemical lasers with needle electrodes (a) and with flat electrodes and preionization of the discharge gap by an auxiliary discharge (b): 1--damped pulse generator; 2--spark discharger; 3--resistors; 4--working chamber of the chemical laser; 5--insulator; 6--high-voltage electrode; 7--grid electrode; 8--needle electrodes

high-voltage electrode 6 and grid electrode 7. Usually the capacitance of discharge capacitor $C_D = 0.05$ μF, and the capacitors in the trigger circuit C_{T_1}, C_{T_2} have capacitances of the order of 0.005 μF.

Discharge homogeneity can also be ensured by preionization of the gas mixture with ultraviolet radiation or a beam of fast electrons. For strongly negative molecules of the fluorine type, the electroionization method of initiating a chemical reaction may be ineffective because of the high probability of disappearance of electrons as a result of sticking to molecules and reduction of electron mobility.

Radiation in hydrogen and deuterium halides under the effect of a pulsed electric discharge was studied in Ref. 37, 38. HF and DF are formed in chemical reaction of freons CF_4, $CBrF_3$, $CClF_3$, CCl_2F_2 with H_2. Other halides are formed when gaseous chlorine or bromine react with hydrogen or deuterium. Ten lines have been observed in HCl emission between 3.7 and 4.0 μm, and 24 lines of DCl between 5.2 and 5.6 μm. Transitions up to $v = 5$ have been observed for DCl and DBr. Electrodischarge initiation has been used for chemical reactions in hydrogen-oxygen and hydrogen-methane mixtures, during which radiation has been generated with $\lambda = 28.27$, 27.97 and 23.36 μm.

Lasing has also been realized on transitions of fluorine atoms radiating in the visible range [Ref. 39]. High gains have been realized on lines $\lambda = 0.7037$ and 0.7127 μm, as evidenced by the presence of superradiation with misalignment of mirrors. Lasing on these lines persisted even with strong scattering on the surface of the mirrors.

Helium is used as still another component of the working mixture in processes of this kind. Attempts to replace helium by other gases (Ar, N_2, O_2, H_2, CO_2) have been unsuccessful. This is due to the fact that the pumping mechanism is occasioned by excitation of F upon dissociative collisions between He and HF. On the other hand, other dissociative collisions such as Ar-HF do not lead to arisal of lasing since, despite the fact that metastable argon $Ar(^1S)$ has more than adequate energy for dissociation of HF, its energy is nonetheless insufficient for simultaneous

excitation of the electronic state of F. As a result of the process of formation of H upon dissociation of HF, which is nearly a resonant process (its cross section is $\sigma = 10^{-13}$-10^{-14} cm^2), and further deactivation, the lower levels are depleted. This process determines the lifetime of the excited F atom, which is equal to 10^{-7}-10^{-8} s at $p \sim 1$ Pa.

In Ref. 40, an analysis was made of an electrodischarge gas-static chemical laser based on a mixture of H_2/Br_2 with addition of SF_6. The reaction was initiated by a pulse discharge of a capacitor (0.03 μF, 25 kV) in a gas mixture introduced into the working chamber of the chemical laser, and after two pulses the gas was discharged and replaced with new mixture. The SF_6 was added to the H_2/Br_2 mixture with $p = 4$ kPa and the optimum ratio of molar concentrations $H_2/Br_2 = 29/1$. The overall energy of lasing on molecules of HBr (and HF) increases monotonically with increasing SF_6 pressure up to $p = 5.33$ kPa, and decreases at higher pressures. Selectively vibrationally excited HBr particles ($v = 3$, 4) are formed in the reaction

$$H + Br_2 \rightarrow HBr^* + Br \quad (-172 \text{ kJ/mole}). \tag{4.13}$$

The use of an inductive accumulator in the power supply of the electrodischarge HF chemical laser [Ref. 41] enables formation of a uniform longitudinal electric discharge in cells of considerable volume at SF_6/H_2 pressures of several kPa and gives intense pulses of stimulated emission with duration of ~0.1 μs. In this way a maximum value of $\varepsilon_V = 6.2$ mJ/cm was obtained from a volume of 290 cm at pressure of 9 kPa of a mixture of $SF_6/H_2 = 3/1$.

In the reaction $F + HI \rightarrow HF + I$, 270 kJ/mole of energy is released, whereas for excitation of the vibrational level of HF ($v = 6$) only 242 kJ/mole is required. In this connection, a comparison was made in Ref. 42 between the energy of stimulated emission and the energies produced in the reactions $H_2 + F_2$ and $F_2 + HI$ under similar experimental conditions on a facility with transverse pulse discharge. It was found that the energy of the stimulated emission is more than double when HI is used as the source of hydrogen atoms.

The following substances have been studied [Ref. 43] as sources of hydrogen atoms: CH_4, C_3H_8, SiH, GeH, AsH_2. As sources of fluorine atoms: SF_6, NF_3, N_2F_4, IF_7, OF_2, BrF_5, ClF_3, ClF_5, XeF_5. The mixtures were at room temperature, relative concentration c_F/c_H was varied from 0.5 to 5, and the pressure was varied over a range of 1.33-8 kPa. Some of these mixtures were stable, and others exploded spontaneously. Inhibitors had to be introduced in the latter systems.

In Ref. 44, an investigation was made of the mechanism of excitation of HBr molecules by initiation of a reaction in a mixture of H_2/Br_2 with transverse discharge in a working chamber 115 cm long and 4 cm in inside diameter. Voltage was applied to the electrodes from 20 capacitors with capacitance of 20 pF charged to 20 kV. It was found that for a mixture with $p_{H_2} = 13.3$ kPa and $p_{Br} = 4$ kPa the energy of stimulated emission increases sequentially on $\mathcal{P}$-transitions 1-0, 2-1 and 3-2. Upon a reduction of p_{Br_2} to 1.33 kPa (at the same p_{H_2}), this sequence is reversed.

The output characteristics of HF chemical lasers were examined in Ref. 45 over a wide range of pressure and composition of the working mixture. The mixture was stabilized by adding O_2 and He to F_2 with subsequent cooling to 84 K before mixing

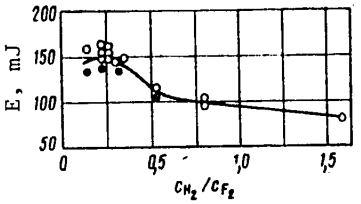

Fig. 4.6. Emission energy E as a function of molar ratio H_2/F_2 for mixture $F_2/H_2/O_2/He = 1/x/0.08/15$ at total pressure of 32 kPa: o--C = 250 pF, V = 35 kV; ●--C = 333 pF, V = 25 kV

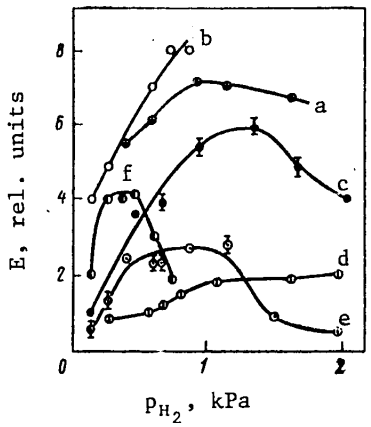

Fig. 4.7. Influence of hydrogen pressure on the total radiation energy when different substances are used: a--hydrogen; b--xylene; c--toluene; d--ligroin; e--acetone; f--methanol

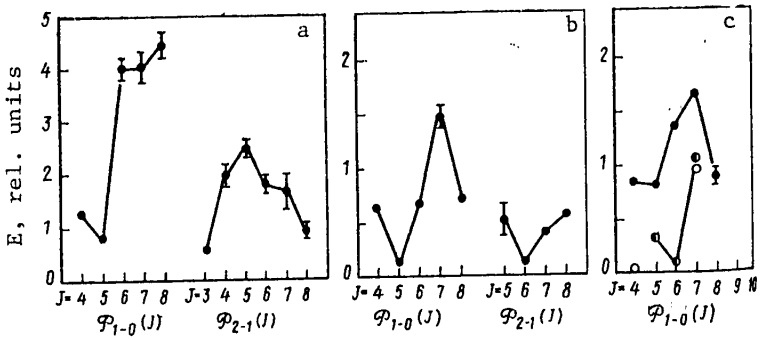

Fig. 4.8. Energy distribution of stimulated emission at p = 4.4 kPa on individual lines: a--SF_6/xylene = 30/3; b--SF_6/toluene = 30/3; c--●--SF_6/C_6H_6 = 30/3; ◐--SF_6/CH_3OH = 30/3; o--$SF_6/(CH_3)_2CO$ = 30/3

with H_2. E_{max} = 0.15 J was observed (Fig. 4.6) at a mixture pressure of 32 kPa and partial ratios of components $F_2/H_2/O_2/He = 1/0.23/0.08/12$. The *electrical efficiency* η_{el}, defined as the ratio ot the energy of the stimulated emission to the losses of electrical energy on initiation of the reaction, reached 140%.

The way that lasing is influenced by the compounds used as sources of hydrogen C_6H_6, $C_6H_5CH_3$, $C_6H_4(CH_3)_2$, CH_3OH, $(CH_3)_2CO$ when the reaction is initiated by a transverse electric discharge (21 kV, 30 pF) is characterized by the graphs of Fig. 4.7, 4.8 [Ref. 46].

§4.3. Gas-Static Chemical Lasers With Initiation of the Reaction by an Electron Beam

Considerable attention is currently being given to the method of initiation of gas-static chemical lasers by an electron beam. Initiation by electron beam has a number of advantages over other methods of initiating a reaction in chemical lasers: uniformity of pumping with respect to volume, high efficiency, capability of large energy input in a short time, dimensionally large volumes of active medium at fairly high working pressures. Besides there is the possibility of dissociation of the molecules that are suppliers of the initial active atoms, whose spectra lie in the far ultraviolet region inaccessible to operation with ordinary standard light sources.

In Ref. 47 an investigation was made of the characteristics of a gas-static chemical laser initiated by electron beam as a function of pressure and ratio of components IF_7 and H_2. A diagram of the experimental facility is shown in Fig. 4.9.

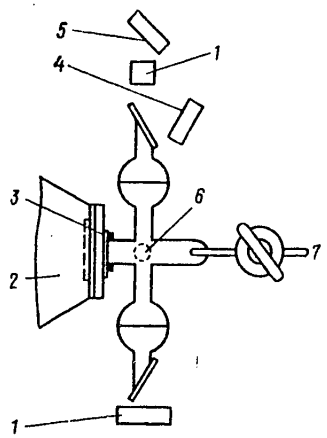

Fig. 4.9. Diagram of experimental facility with electron beam initiation of chemical reaction: 1--mirrors; 2--electron-beam tube; 3--aluminum foil; 4--detector; 5--thermopile; 6--active zone; 7--gas inlet and outlet

A monoenergetic pulsed electron beam with energy $E_e = 12$ J (500 keV) and duration $\tau_e = 3$ ns was injected by an electron-beam tube with diameter of 4.5 cm. The output radiation of the laser on $\lambda = 2.7$-3 μm was registered by a Ge-Au detector cooled to liquid nitrogen temperature. The energy E of the stimulated emission was measured by a ballistic thermopile.

The shape of the stimulated emission pulse depends on the change in pressure p of the mixture. The experiments were done with a glass chamber having inside diameter up to 2.5 cm, and with a chamber that was a sphere 4 cm in diameter in the central part. It was found that losses of energy of the electron beam dE_e/dx are small in both cases, and the energy absorbed by a mass unit of gas was constant for $p > 3.33$ kPa. The maximum energy E_{max} of the stimulated emission was reached at $p = 20$ kPa, and a ratio of mixture components $IF_7/H_2 = 6/1$, which differs strongly from the stoichiometric composition 2/7. This is evidence that less than 5% of the fluorine atoms contributed to lasing.

A diagram of a gas-static chemical laser based on a mixture of $SF_3/F_2/H_2$ (D_2) with pumping by an electron beam with maximum accelerating voltage of 50 kV and $E_e = 900$ J is shown in Fig. 4.10 [Ref. 48]. An electron beam from a cathode with dimensions of 3.8 x 20.3 cm passed through an aluminum foil 1 mm thick into a working chamber with variable dimensions of 3 x 4 x 20.3 and 10.2 x 10.2 x 40.6 cm. The D_2 was obtained by electrolysis of D_2O. The total lasing power is directly proportional to the pressure of H_2 and F_2, as implied by theory. It was found that power is not directly dependent on working volume. This is due mainly to the intensification of inhomogeneities in the working fluid as the volume increases. An electrical efficiency

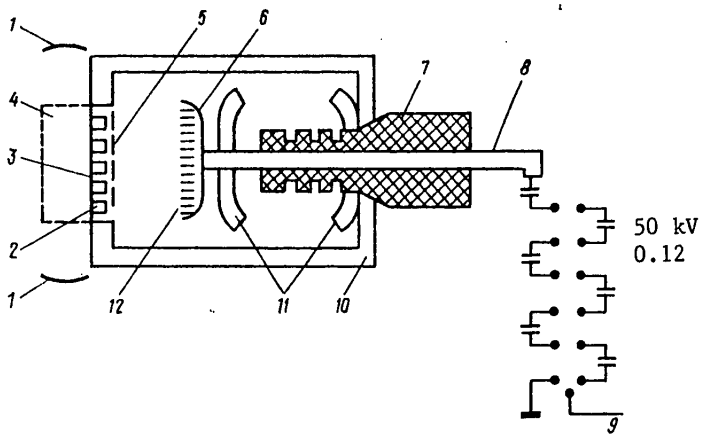

Fig. 4.10. Diagram of experimental setup of gas-static chemical laser on a mixture of $SF_3/F_2/H_2$ (D_2): 1--cavity; 2--foil holder; 3--foil; 4--lasing zone; 5--grounding grid; 6--cold cathode holder; 7--high-voltage insulator; 8--low-inductance lead-in; 9--flip-flop; 10--vacuum chamber; 11--corona discharge ring; 12--thermionic cathode

of $\eta_{el} = 6\%$ was obtained. The kinetic model of lasing was refined on the basis of the experimental data. Calculations by this model gave a specific energy output an order of magnitude higher than the experimental value, which can be attributed to parasitic waveforms in the vessel and low initial concentrations of F.

The effectiveness of electron-beam initiation of a gas-static chemical laser on a mixture of $H_2/F_2/He/O_2$ at a relatively low level of the current density j_e of the electron beam was studied in Ref. 49. To reduce the level of excitation, a mixture with elevated partial pressure of fluorine was used. To increase the overall pressure p to atmospheric level at relatively low partial pressure of H_2 and F_2, helium was used as ballast. To prevent the reaction from taking place during mixing, oxygen was added. Mixtures of H_2/He and $F_2/He/O_2$ passed through rapid-action valves into the mixer, from which the working mixture was slowly fed to the working volume. The initiating electron beam with $j_e = 20$ A/cm^2, accelerating voltage of 140 kV, $\tau_e = 200$ ns and cross section of 1 x 25 cm, was injected through an aluminized tantalum film 50.8 μm thick fastened on a structure of stainless steel.

The efficiency of conversion of electrical energy to electron-beam energy was 60%. A cavity 75 cm long with active volume of 100 cm was formed by a spherical copper mirror with a sapphire plate reflecting 10% of the light in the lasing region of $\lambda = 2.7$-3.1 μm. The energy E of stimulated emission at fixed concentrations of c_{H_2} and $c_{O_2} = 0.04c_{F_2}$ increased with increasing c_{F_2} until c_{F_2} was 2-4 times as high as c_{H_2}.

At $c_{F_2} = 30\%$ and $c_{H_2} = 8\%$ normalized to atmospheric pressure, $\varepsilon_{V_{max}} = 0.051$ J/cm^3, $\eta_{el} = 875\%$. The quantity η_x defined as the ratio of lasing energy to the chemical energy released in the active volume, assuming that all molecules of H_2 participate in the reaction, liberating 130 kcal per mole of H_2, was 0.75-2.8%. In chemical

lasers based on a mixture of H_2/F_2, the energy of the lasing pulse [Ref. 50] exceeds the value obtained in chemical lasers based on mixtures using SF_6 and C_2H_6 [Ref. 48].

For a mixture of H_2/F_2, $\varepsilon_V \approx 0.13$ J/cm^3, η_{el} and η_x are equal to 180 and 11.4% respectively. If we take $j_e \approx 80$ A/cm^2, these figures agree satisfactorily with calculations according to a simplified model of kinetic processes in chemical lasers based on a mixture of H_2/F_2 with electron-beam initiation of the reaction.

The lasing energy E in a mixture of $F_2/O_2/H_2 = 1/0.3/0.25$ increases nearly linearly with pressure p_{F_2}. Similarly, linear dependence is observed for the electron energy lost in the working mixture. With an increase in p_{SF_6}, the value of E and the electron beam energy lost in the gas increase nonmonotonically, the addition of SF_6 to a pressure of p = 13.3 kPa increasing the energy contributed by electrons to the gas by a factor of more than 1.8 over the value where SF_6 is absent.

For mixture $F_2/O_2/SF_6/H_2 = 3.6/1.4/1.0/1.0$ with electron-beam initiation ($E_e = 150$ J, $\tau_e = 30$ ns), the energy of stimulated emission attained in Ref. 51 was E = 67 J with duration of 100 ns, $\eta_{el} \approx 45\%$ and divergence of $5 \cdot 10^{-2}$ rad.

Initiation of the reaction by an electron beam of short duration under conditions of atmospheric pressure of the mixture $F_2/H_2/He/Ar = 6/3/54/37$ [Ref. 52] yields $\varepsilon_V = 0.042$ J/cm^3 at an energy contribution of 0.028 J/cm^3. In this case, η_x and η_{el} are equal to 6.3 and 150% respectively. A pulse energy of E = 2.52 J was obtained in a mixture of H_2 with 6% F_2 at an electric field strength of 11 kV/cm.

Increasing the pressure in the mixture to a few MPa enabled a considerable reduction in the volume of the chamber and an increase in the specific characteristics of the gas-static chemical laser [Ref. 50].

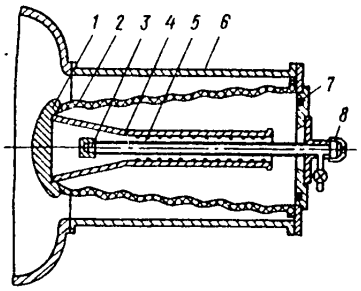

Fig. 4.11. Diagram of acceleration tube with coaxial diode: 1--electrode of acceleration tube; 2--insulator; 3--mirror; 4--cylindrical cathode; 5--working chamber of the chemical laser (anode); 6--housing of the acceleration tube; 7--Rogowski loop; 8--semitransparent mirror

A diagram of the experimental facility is shown in Fig. 4.11. The working chamber (anode) with length of 18.5 cm was part of a coaxial high-voltage field-emission diode placed inside the acceleration tube. To increase strength, it was made of separate sections 5 cm long that were destroyed at p = 11 MPa. The amplitude of a current pulse with duration of $4 \cdot 10^{-8}$ s was 5.7 kA, maximum electron energy was 2.9 MeV, $E_e = 420$ J. The cavity was formed by a flat opaque mirror with gold coating on a metallic surface and by a semitransparent mirror--interference mirrors with transmission of 20, 40% in band $\lambda = 2.5$-3.5 μm, and also plates of polished germanium and barium fluoride.

For mixture $SF_6/H_2 = 70/1$, $E_{max} = 0.79$ J is obtained at p = 0.27 MPa, $\varepsilon_V = 21$ mJ/cm^3.

The main barrier to increasing the characteristics of chemical lasers with initiation of the reaction in a mixture of SF_6/H_2 at $p \gtrsim 1$ MPa is apparently the collisional deactivation of active molecules of HF(v) by molecules of H_2 [Ref. 53]. The influence of collisional deactivation can be attenuated somewhat by reducing the duration of the initiating pulse [Ref. 50].

This, as well as an increase in the pressure of the $D_2/F_2/CO_2/He$ mixture to several hundred kPa and optimization of the composition of the mixture should appreciably increase the specific power output and quantum yield of stimulated emission in the chemical laser of Ref. 54 with electron-beam initiation of the reaction. In Ref. 55 on a mixture of $H_2/F_2/O_2/He = 30/75/6/250$, $\varepsilon_V = 91$ mJ/cm was attained at an efficiency with respect to invested energy $\eta_{el} = 936\%$, $\eta_x = 4.7\%$ and efficiency of utilization of the electron beam of 250%. Electron-beam initiation of the process in HCl chemical lasers (working mixture ClF/H_2) has also yielded high parameters for lasers of this type: $\varepsilon_V = 5$ mJ/cm , $W = 0.4$ MW.

The parameters of chemical lasers can also be increased by using a combined arrangement: master laser + amplifier [Ref. 56]. For example, a photochemical gas-static laser based on mixture $F_2/H_2/He/O_2$ can be used as the master laser, and the amplifier may be a tube with the same mixture components enclosed in a solenoid to confine and deflect the initiating electron beam. The use of such a combination system for high-energy chemical sources of coherent radiation can solve the problem of radiation strength of the reflectors of optical cavities and avoid the necessity of making large-scale optics, as well as reducing divergence of radiation.

§4.4. Excimer Gas-Static Chemical Lasers

One of the promising areas of research on new media for stimulated emission in the visible and ultraviolet regions of the spectrum is in the use of excimers--unstable molecules that are formed from radicals, one of which is in the excited state. These include such molecules as the halides XeF, XeCl, XeBr, KrF, XeO, KrO, ArO [Ref. 57]. The process of generation of emission in excimer chemical lasers based on halides of inert gases involves population of the upper working state during chemical reaction between the excited atoms of inert gases and molecules that include halide atoms. The molecules formed in the reaction, mainly in electronically excited state $^2\Sigma$, relax upon collision to lower vibrational levels, and then make a transition to the ground state of the molecule. Rapid decay of this molecule leads to inverse population.

Pumping in such chemical lasers is by: an intense electron beam, flashlamp, electric discharge, and also a number of combined arrangements. Chemical lasers based on excimers are compact, simple, can provide fairly high radiation power and efficiency of ~1-10% in the ultraviolet. For example, the peak power of chemical lasers based on KrF with emission wavelength $\lambda = 0.2484$ μm is $W = 1.9 \cdot 10^9$ W at a pulse energy of $E = 108$ J with $\eta \approx 3\%$. Cl_2, CH_2Cl_2, F_2, HBr, SF_6 and other molecules are used as sources of donor halide atoms.

To improve the homogeneity of energy release, the ultraviolet pumping source used in Ref. 58 was a special chamber filled with Ar at $p = 1.3$ MPa excited by a relativistic electron beam. Emission with energy of 1 J passed through a series of MgF_2 windows into another working chamber filled with an active medium of Ar (4.35 MPa) and N_2O (266.6 Pa. Within 0.25 μs after the pumping pulse, absorption of a probing radiation pulse was observed in the active medium with subsequent signal amplification for a time coinciding with the lifetime of the excited level. Lasing was on the $^1S_0$-$^1D_2$ transition of atomic oxygen. The form of the emission spectrum corresponded to the ArO* molecule in excited state $2^1\Sigma^+$, including the

excited state of the O atom and the ground state of Ar. The concentration of excited atoms O* is expressed by the formula

$$n(O^*) = n_0(O^*)\exp(-t/\tau') \tag{4.14}$$

with characteristic time of de-excitation of energy stored in the medium $\tau' = 10^{-3}$ s. The intensity of luminescence increases linearly with increasing p_{Ar}. Due to relaxation on N_2O, at $p_{N_2O} = 33$ Pa the lifetime of the excited state $\tau \sim 2.6$ μs, which is less than the calculated $\tau \sim 12$ μs, and remains at this level up to $p \sim 3$ MPa.

With electron-beam pumping, high efficiency and output energy are attained on excimers KrF and XeF [Ref. 59]. The radiation of these excimers is due to transition from the bound upper state to the separational or weakly bound ground state, which is formed from a combination of the atom of inert gas in state $^1S_0$ and a halide atom in states $^2P_{3/2}$ and $^2P_{1/2}$.

The energy of lasing on excimers KrF, XeF when the electron beam is injected perpendicular to the axis of the tube (transverse pumping) had a maximum with the addition of small amounts of Xe (4 kPa) or Kr (20 kPa) and halide donors (1.33 kPa) to the Ar. The beam energy was transferred to the Ar, and was then redistributed to the Kr or Xe as a result of collisions.

In the case of XeF chemical lasers the most important processes are the following [Ref. 60]:

$$\left.\begin{aligned}
&1)\ Ar + e \rightarrow Ar^* + Ar^+ + e;\\
&2)\ Ar^+ + 2\,Ar \rightarrow Ar_2^* + Ar;\\
&3)\ Ar_2 + e \rightarrow Ar^* + Ar;\\
&4)\ Ar^* + 2\,Ar \rightarrow Ar_2^* + Ar;\\
&5)\ Ar^* + NF_3 \rightarrow ArF^* + NF_2;\\
&6)\ Ar^* + Xe \rightarrow Ar + Xe^*;\\
&7)\ Xe^* + Xe + Ar \rightarrow Xe_2^* + Ar;\\
&8)\ Xe^* + NF_3 \rightarrow XeF^* + NF_2;\\
&9)\ XeF^* + NF_3(NF_2) \rightarrow Xe + F + NF_3(NF_2);\\
&10)\ XeF^* \rightarrow Xe + F + h\nu.
\end{aligned}\right\} \tag{4.15}$$

Here the energy of stimulated emission increases linearly with increasing pressure up to 0.3-0.4 MPa. The reduction in output power can be attributed to an increase in the rate of de-excitation, for example as a result of collision of the excited particles with argon, atomic fluorine, xenon, and also due to the formation of Xe_2^* as a result of the competing process [Ref. 61]

$$Xe^*(Kr^*) + Xe(Kr) + Ar \rightarrow Xe_2^*(Kr_2^*) + Ar.$$

At $\eta = 3\%$ we get maximum $W = 1.1 \cdot 10^8$ W and $E = 5.6$ J.

However, transverse pumping is inefficient since only a small part of the energy of the electron beam is transmitted to the gas. Other beam injection configurations

are used to increase the efficiency of energy input. For example in the case of axial beam injection the pulse energy increases to 200 J, and peak power rises to $5 \cdot 10^9$ W. This scheme of beam input to the working medium was the one used to get the appreciable lasing powers and energies on KrF and ArF reported in Ref. 57.

The *quantum efficiency* of a KrF chemical laser with electron-beam pumping when Ar is used as the buffer gas depends on the energy expended for excitation of Ar [E(Ar)], and is defined as $\phi \approx h\nu(KrF)/E(ar) \approx 24\%$, whereas the maximum attainable efficiency with consideration of reactions $Kr^* + F_2 \rightarrow KrF^* + F$, $Kr^+ + F^- + M \rightarrow KrF^* + M$ is equal to 8%. In electric-discharge chemical lasers the maximum efficiency is limited by the energy E* required to form metastable atoms of inert gas with minimum energy. In the case of a KrF electric-discharge chemical laser, the quantum efficiency is associated with the Kr, and is equal to $\phi = h\nu(KrF)/E^*(Kr) = 50\%$. The maximum attainable efficiency determined by the above-mentioned reactions is ~25% or less.

An electron beam has been used with success for pumping chemical lasers based on a mixture of Ar/I_2 [Ref. 62] on dimers of Xe_2^*, Kr_2^*, Ar_2^* [Ref. 63], on XeBr [Ref.64], XeO and KrO [Ref. 65].

When an electron beam is used for pumping, the attainment of high radiation power is limited by the strength of the thin foil layer used for beam injection that separates the vacuum chamber of the electron gun from the chamber of the chemical laser with high pressure of the working mixture, and also by the losses of beam energy in this layer. Heating of the foil also leads to limitation of the lasing pulse recurrence rate.

The method of pumping by electric discharge has none of these disadvantages, and in principle can be used to get high lasing power with a high recurrence rate with comparatively simple power supplies. A pulsed electric discharge is effective for pumping XeF chemical lasers since the lower electronic state in the XeF molecule is weakly bound, and the lifetime of the upper electronic state is comparatively long--50 ns.

In the range of relatively low pressures p = 27-53 kPa of a mixture of He/Xe/NF = 100/3/1, an investigation was made in Ref. 66 of the efficiency and intensity of lasing pumped by a pulsed electric discharge. Here the XeF* molecules are formed in the excited electronic state, and also in high vibrational states, and make the transition to lower vibrational levels as a result of collisions with the buffer gas (He, Ar). The research used an electric supply with discharge duration t_p of 10 ns and discharge space measuring 1 x 0.33 x 50 cm. The discharge voltage U_p ranged from 5 to 20 kV, and pressure p from 2.66 to 66.5 kPa. The pulse recurrence rate was several hundred Hz. Lasing was not observed up to p = 26.6 kPa. After this, lasing rose continuously with increasing p. Maximum lasing energy E was attained at p = 53.3 kPa. A further increase in p led to contraction of the discharge and a reduction in E. The output energy in a pulse E = 1 mJ at p = 46.6 kPa, and $\varepsilon_V = 0.07$ mJ/cm^3. In this case, $\eta_{el} = 0.2\%$, and with respect to the energy invested in the gas--1.2%. The emission lines were the same as for electron-beam pumping (351 and 353 nm). Besides, a weak line was observed at $\lambda = 349$ nm. $W_{max} \approx 25$ kW. Because of comparatively low pressure, the concentration of Xe_2^*

was low, and therefore the role of three-particle recombination (Xe^+, F, He) in the formation of XeF* was negligible.

Use of the simplified kinetic model leads to the following expression for concentration:

$$\left.\begin{aligned} n_{XeF^*} &= N\left\{\frac{T}{\tau}\left[1-\exp\left(-\frac{t}{T}\right)\right]+\left[\frac{T}{(T-\tau)}\right]\times\right. \\ &\left.\times\left[\exp\left(-\frac{t}{\tau}\right)-\exp\left(-\frac{t}{T}\right)\right]\right\}; \\ n_{Xe} &= N\left[1-\exp\left(-\frac{t}{\tau}\right)\right], \end{aligned}\right\} \qquad (4.16)$$

where $N = \langle\sigma v\rangle\, n_e n_{Xe}/k n_{NF_3}$; $\tau = (k n_{NF_3})^{-1}$; T is the lifetime of XeF*; σ is the excitation cross section.

For specific conditions: $He/Xe/NF_3 = 100/3/1$; $p = 46.6$ kPa; $U_p = 8$ kV; $j_e = 100$ A/cm^2; discharge duration $t = 10$ ns; $E_e = 4$ eV; at $k = 10^{-9}$ cm^3/s we get $\tau = 10$ ns $\approx t$, which is less than $T = 50$ ns. As a consequence $n_{Xe^*} \approx N = 10^{14}$ cm^{-3} $\ll n_{Xe} = 3.6\cdot10^{17}$ cm^{-3}. Then from (4.16) at $\tau/T \ll 1$, $t/\tau \sim 1$, $n^* \approx Nt/\tau = 10^{14}$ cm^{-3}, which corresponds to energy $E = h\nu n^* V \approx 10^{-3}$ J, and the gain is evaluated as $\alpha_0 = \sigma n^* \cong 10^{-2}$ cm^{-1}. This value agrees with experimental data.

An XeCl electric-discharge chemical laser has been made [Ref. 67] using CF_2Cl_2, C_2F_3Cl, CCl_4, BCl_3 as the donor with predominance of He in the mixture. Here the excited halide molecules are formed in the chemical reaction of excited atoms of the inert gas with the halide donors. When NF_3 is used as the donor, a fine structure of XeF chemical laser emission is observed with $\lambda = 353.54$, 353.05, 351.14, 350.97, 350.91 and 348.75 nm. For XeCl molecules, lasing was observed only at high pressures (>0.12 MPa). The maximum pulse energy for XeF obtained in Ref. 67 is equal to 2 mJ with corresponding values of 1 mJ for XeCl and 0.5 mJ for KrF. With operation on another composition of the mixture $He/Kr/NF_3 = 500/50/1$, which is optimum, and overall pressure of 93.3 kPa [Ref. 68], lasing was obtained on $\lambda = 248.5$ and 249.5 nm with $E = 0.8$ mJ, $\tau = 25$ ns, $W = 32$ kW, $\varepsilon_V = 0.08$ mJ/cm^3. Almost no reduction in power is observed at a pulse recurrence rate of $\leqslant$20 Hz.

Combined pumping arrangements offer extensive capabilities for making and studying excimer chemical lasers. For example, Ref. 69 shows the feasibility of pumping by a transverse discharge with preliminary photoionization of molecules of ArF, KrF and XeF by an auxiliary spark discharge. The spark discharge was fed from a separate source, enabling control of the preionization pulse delay and the delay of the main discharge over a range of 0.1-25 μs. The duration of the preionization light pulse was 400 ns, and the duration of the current pulse of the main discharge was 40 ns. The stored energy of the main discharge was about 10 J.

Discharge took place in a mixture of $He/F_2(NF_3)/Xe(Kr, Ar)$ prepared in a stainless steel fluorine-passivated mixing system. The working chamber of the chemical laser was pre-evacuated to $p = 13.3$ Pa, and then rinsed with helium and filled with mixture to $p = 0.2$ MPa.

Lasing on XeF molecules was observed on lines 351.1, 353.2 and 348.8 nm. An E_{max} of 65 mJ was attained in a mixture of $He/Xe/NF_3 = 100/1/0.3$ at $p = 0.2$ MPa. The cavity of the XeF chemical laser consisted of a totally reflecting mirror and a mirror with transparency of 70%. In the case where KrF was used, a maximum energy of 130 mJ was attained. For an output mirror with transparency of 50%, the emission spectrum showed a maximum in the vicinity of $\lambda = 248.4$ nm with width of about 0.3 nm. When a high-Q cavity was used, lasing was also observed on $\lambda = 248.1$ nm. Substituting NF_3 for F_2 reduced the pulse energy by a factor of two or three.

Maximum lasing energy of 60 mJ was attained in ArF chemical lasers on $\lambda = 193.3$ nm. The shape of the spectrum is about the same as with electron-beam pumping, but with a more precise structure.

The duration of the lasing pulses in all three of these types of chemical lasers was 20-25 ns, and the pulse shape was similar. Maximum emission power was 2-4 MW. It was found that the rate of reduction in lasing energy is very low compared with the rate of preionization due to dissociative sticking of electrons to the fluorine molecule, with a typical value of 10^9 s^{-1}. This means that the negative ions F^- act as an effective source of negative charges.

Excimer chemical lasers based on halides of inert gases are steadily being improved: lasing is being achieved at higher pressures, in the quasi-cw mode, in a closed-cycle system, with photodissociation of molecules, in a so-called double discharge, with stabilization of a beam of fast electrons and so on. Ref. 70 gives a systematic presentation of some characteristics of such chemical lasers with a bibliography.

REFERENCES

1. Solimento, S., "Chemical Lasers", PHYS. BULL., Nov 1974, pp 517-520.

2. Basov, N. G., Golubev, L. Ye., Zuyev, V. S. et al., "New Laser Emits Short Pulses With Energy of 50 J and Duration of 5 ms", KVANTOVAYA ELEKTRONIKA, No 6(18), p 116.

3. Brederlow, G., Fuss, W., Kompa, K. L. et al., "60-J 1-ns Iodine Laser", J. APPL. PHYS., Vol 46, No 2, 1975, pp 808-809.

4. Antonov, A. S., Belousova, I. M., Gerasimov, V. A. et al., "Flash Photodissociation Laser", PIS'MA V ZHURNAL EKSPERIMENTAL'NOY I TEORETICHESKOY FIZIKI, Vol 4, No 19, 1978, pp 1143-1145.

5. O'Brien, D. E., Bowen, J., "Parametric Studies of the Iodine Photodissociation Laser", J. APPL. PHYS., Vol 42, No 3, 1971, pp 1010-1015.

6. Kasper, J. V. V., Parker, J. H., Pimentel, G. C., "Iodine-Atom Laser Emission in Alkyl Iodide Photolysis", J. CHEM. PHYS., Vol 43, No 5, 1965, pp 1827-1828.

7. Andreyeva, T. L., Dudkin, V. A., Malyshev, V. I. et al., "Gas Laser Excited in Photodissociation Process", ZHURNAL EKSPERIMENTAL'NOY I TEORETICHESKOY FIZIKI, Vol 49, 1965, p 48.

8. Andreyeva, T. L. et al., "Investigations of Iodine Photodissociation Lasers Containing Bonds of Iodine Atoms with Elements of Group V. I. Experimental Studies on the $(CF_3)_2AsI$ Molecule", KVANTOVAYA ELEKTRONIKA, Vol 3, No 7(49), 1976, pp 1442-1456.

9. Knudtson, J. T., Berry, M. J., "Methyl Isocyanide Photodissociation Chemical-Laser Determination of Energy Partitioning Into the Cyanide Radical Photochemical Product", J. CHEM. PHYS., Vol 68, No 10, 1978, pp 4419-4430;

West, G. A., Berry, M. J., "ICN Photodissociation and Predissociation: CN* $(A^2\Pi_j)$ Fluorescence Excitation Spectrum and $CN^+(X^2\Sigma^+)$ Chemical Laser Emission", PHYS. REV. LETT., Vol 14, 1965, p 352;

IGOSHIN, V. I., ORAYEVSKIY, A. N., "Kinetics of Hydrogen-Chloride Chemical Laser", KHIMIYA VYSOKIKH ENERGIY, Vol 5, 1971, p 397.

11. Corneil, P. H., Pimental, G. C., "Hydrogen-Chlorine Explosion Laser. II. DCl", J. CHEM. PHYS., Vol 49, No 3, 1968, pp 1379-1386.

12. Polanyi, J. C., "Vibrational-Rotational Population Inversion", APPL. OPTICS, Suppl. 2, 1965, pp 109-127.

13. Airey, J. R., "A New Pulsed I-R Chemical Laser", IEEE J. QUANT. ELECTRON., Vol QE-3, No 5, 1967, p 208.

14. Airey, J. R., "Cl + HBr Pulsed Chemical Laser: a Theoretical and Experimental Study", J. CHEM. PHYS., Vol 52, No 1, 1970, pp 156-157.

15. Spencer, D. J., Wittig, C., "Atomic Bromine Chemical Laser", J. OPT. SOC. AMER., Vol 68, No 5, 1978, p 652.

16. Polanyi, J. C., Tardy, D. C., "Energy Distribution in the Exothermic Reaction $F + H_2$ and the Endothermic Reaction HF + H*", J. CHEM. PHYS., Vol 51, No 12, 1969, pp 5717-5719.

17. Jonathan, J. N., Melliar-Smith, C. M., Slater, D. H., "Initial Vibrational Energy Level Populations Resulting from the Reaction $H + F_2$ as Studied by Infrared Chemiluminescence", J. CHEM. PHYS., Vol 53, No 11, 1970, pp 4396-4397;

Polanyi, J. C., Woodal, K. B., "Energy Distribution Among Reaction Products. VI. $F + H_2$, D_2", J. CHEM. PHYS., Vol 57, No 4, 1972, pp 1574-1586.

18. Kondrat'yev, V. N., "Konstanty skorosti gazofaznykh reaktsiy" [Rate Constants of Gas-Phase Reactions], Moscow, Nauka, 1970, 351 pages.

19. Kompa, K. L., Pimentel, G. C., "Hydrofluoric Acid Chemical Laser", J. CHEM. PHYS., Vol 47, No 2, 1967, pp 857-858.

20. Kompa, K. L., Parker, J. H., Pimentel, G. C., "UF_6-H_2 Hydrogen Fluoride Chemical Laser: Operation and Chmistry", J. CHEM. PHYS., Vol 49, No 10, 1968, pp 4257-4264.

21. Agroskin, V. Ya. et al., "Parametric Channel of Pulsed H_2-F_2 Laser", KVANTOVAYA ELEKTRONIKA, Vol 3, No 9, 1976, pp 1932-1939.

22. Berry, M. J., "A Comparison of Photolytic Fluorine-Atom Sources for Chemical Laser Studies", CHEM. PHYS. LETT., Vol 15, No 2, 1972, pp 269-273.

23. Pollak, M. A., "Laser Stabilization in Chemically Formed CO", APPL. PHYS. LETT., Vol 8, No 9, 1966, pp 237-238.

24. Gregg, D. W., Thomas, S. J., "Analysis of the Cs_2-O_2 Chemical Laser Showing New Lines and Selective Emission", J. APPL. PHYS., Vol 39, No 9, 1968, pp 4399-4404.

25. Patel, C. K. N., "Vibrational-Rotational Laser Action in Carbon Monoxide", PHYS. REV., Vol 141, No 1, 1966, pp 71-83.

26. Gordon, Ye. B., Pavlenko, V. S., Moskvin, Yu. L. et al., "Kinetics of Pulsed Chemical CO Laser With Photodissociation Based on the Reaction of Oxidation of Carbon Disulfide", ZHURNAL EKSPERIMENTAL'NOY I TEORETICHESKOY FIZIKI, Vol 63, No 4, 1972, pp 1159-1172.

27. Davis, D. D., Klemm, R. B., Pilling, M., "A Flash-Photolysis-Resonance Fluorescence Kinetics Study of Ground-State Sulfur Atoms. I. Absolute Rate Parameters for Reaction of $S(^3P)$ With $O_2(^3\Sigma)$", INT. J. CHEM. KINETICS, Vol 4, No 4, 1972, pp 367-394.

28. Donovan, R. J., Little, D. J., "The Rate of the Reaction $S(^3P_j) + O_2$", CHEM. PHYS. LETT., Vol 13, No 5, 1972, pp 488-490.

29. Gordon, Ye. B. et al., "Nature of the Influence of Mixture Pressure on Stimulated Emission of a Carbon Monoxide Pulsed Chemical Laser", KVANTOVAYA ELEKTRONIKA, Vol 2, No 2, 1975, pp 327-331.

30. Gross, R. W. F. "Chemically Pumped CO_2 Laser", J. CHEM. PHYS., Vol 50, No 7, 1969, pp 1889-1890.

21. Gross, R. W. F., Cohen, N., Jacobs, T. A., "HF Chemical Laser Produced by Flash Photolysis of F_2O-H_2 Mixtures", J. CHEM. PHYS., Vol 48, No 8, 1968, pp 3821-3822.

32. Basov, N. G., Zavorotnyy, S. I., Markin, Ye. P. et al., "Pulsed Chemical Laser on Mixture of $D_2 + F_2 + CO_2 + He$", KVANTOVAYA ELEKTRONIKA, Vol 1, No 3, 1974, pp 560-564.

33. Kulakov, L. V., Nikitin, A. I., Orayevskiy, A. N., "Investigation of Characteristics of a Chemical Laser With Transfer of Vibrational Energy From Molecules of DF to Molecules of CO_2", KVANTOVAYA ELEKTRONIKA, Vol 3, No 8, 1976, pp 1677-1688.

34. Basov, N. G., Bashkin, A. S., Grigor'yev, P. G. et al., "Chemical Quantum DF-CO_2 Amplifier With High Specific Parameters", KVANTOVAYA ELEKTRONIKA, Vol 3, No 9, 1976, pp 2067-2069.

35. Pochler, T. O., Shandor, M., Walker, R. E., "High-Pressure Pulsed CO_2 Chemical Transfer Laser", APPL. PHYS. LETT., Vol 20, No 12, 1972, pp 487-499;

Pochler, T. O., Pirkle, J. C., Jr., Walker, R. E., "A High Pressure Pulsed CO_2 Chemical Transfer Laser", IEEE J. QUANT. ELECTRON., Vol QE-9, No 1, 1973, part 2, pp 83-93.

36. Chebotarev, N. F., Pshezhetskiy, S. Ya., "Particulars of DF-CO_2 Energy Transfer in Chemical Lasers Based on Fluorides of Chlorine", KVANTOVAYA ELEKTRONIKA, Vol 6, No 1, 1979, pp 231-235.

37. Deutsch, T. F., "Molecular Laser Action in Hydrogen and Deuterium Halides", APPL. PHYS. LETT., Vol 10, No 8, 1967, pp 234-236.

38. Deutsch, T. F., "New Infrared Laser Transitions in HCl, HBr, DCl and DBr", IEEE J. QUANT. ELECTRON., Vol QE-3, No 9, 1967, pp 419-421.

39. Kovacs, M. A., Ultee, C. J., "Visible Laser Action in Fluorine", APPL. PHYS. LETT., Vol 17, No 1, 1970, pp 39-40;

Jeffers, W. Q., Wiswall, C. E., "Laser Action in Atomic Fluorine Based on Collisional Dissociation of HF", APPL. PHYS. LETT., Vol 17, No 10, 1970, pp 444-447.

40. Oodate, H., Obara, M., Fujioka, T., "Enhanced HBr Chemical Laser Output With Addition of SF_6", APPL. PHYS. LETT., Vol 24, No 6, 1974, pp 272-274.

41. Zapol'skiy, A. F., Yushko, K. B., "Electric Discharge Laser on a Mixture of SF_6-H_2 With Pumping From an Inductive Accumulator", KVANTOVAYA ELEKTRONIKA, Vol 6, No 2, 1979, pp 408-411.

42. Mayer, S. W., Taylor, D., Kwok, M. A., "HF Chemical Lasing at Higher Vibrational Levels", APPL. PHYS. LETT., Vol 23, No 8, 1973, pp 434-436.

43. Parker, J. V., Stephens, R. R., "Pulsed HF Chemical Lasers With High Electrical Efficiency", APPL. PHYS. LETT., Vol 22, 1973, pp 450-452.

44. Inoue Gen., Tsuchiya Soji, "Mechanism of Transversely Excited Chemical HBr Laser", JAP. J. APPL. PHYS., Vol 13, No 9, 1974, pp 1421-1428.

45. Whitter, J. S., Kerber, R. L., "Performance of an HF Chain-Reaction Laser With High Initiation Efficiency", IEEE J. QUANT. ELECTRON., Vol QE-10, 1974, pp 844-847.

46. Obara, M. Fujioka, T., "Pulsed HF Chemical Laser From Reactions of Fluorine Atoms With Benzene, Toluene, Xylene, Methanol and Acetone", JAP. J. APPL. PHYS., Vol 14, No 8, 1975, pp 1183-1187.

47. Pan, V. L., Turner, C. E., Pettipiece, K. J., "The Characteristics of an Electron Beam-Initiated Pulsed Chemical Laser", CHEM. PHYS. LETT., Vol 10, No 5, 1971, pp 577-579.

48. Aprahamian, R., "Pulsed Electron Beam-Initiated Chemical Laser Operating on the H_2/F_2 Chain Reaction", APPL. PHYS. LETT., Vol 24, No 5, 1974, pp 239-242

49. Mangano, J. A. et al., "Efficient Electrical Initiation of an HF Chemical Laser", APPL. PHYS. LETT., Vol 27, No 5, 1975, pp 293-295.

50. Gerber, R. A. et al., "Multikilojoule HF Laser Using Intense Electron-Beam Initiation of H_2-F_2 Mixtures", APPL. PHYS. LETT., Vol 25, No 5, 1974, pp 281-283;

Gerber, R. A., Patterson, E. L., "Studies of High-Energy HF Laser Using an Electron Beam-Excited of [sic] High-Pressure F_2 and H_2", J. APPL. PHYS., Vol 47, No 8, 1976, pp 3524-3529.

51. Baranov, V. K., Demidenko, Yu. N., Zelenskiy, K. F. et al., "Chemical Laser Based on F_2-H_2 Mixture With Electronic Initiation", KVANTOVAYA ELEKTRONIKA, Vol 5, No 2, 1978, pp 415-417, 475.

52. Hofland, R. et al., "Atmospheric-Pressure H_2-F_2 Laser Initiated by Electron-Beam Irradiated Discharge", J. APPL. PHYS., Vol 47, No 10, 1976, pp 4543-4546.

53. Ponomarenko, A. G., Soloukhin, R. I., Khapov, Yu. I., "Energy Characteristics of Chemical HF Laser Initiated by Electron Beam" in: "Gazovyye lazery" [Gas Lasers], Novosibirsk, Nauka, 1977, pp 105-111.

54. Igoshin, V. I., Nikitin, V. Yu., Orayevskiy, A. I., "Feasibility of Increasing the Quantum Yield of Stimulated Emission and Specific Power Output of DF/CO_2 Chemical Laser", KRATKIYE SOOBSHCHENIYA PO FIZIKE, No 6, 1978, pp 20-25.

55. Bashkin, A. S., Konoshenko, A. F., Orayevskiy, A. N. et al., "Efficient HF Chemical Laser Using an Electron Beam With High Specific Power Output", KVANTOVAYA ELEKTRONIKA, Vol 5, No 7, 1978, pp 1608-1610;

Bashkin, A. S., Konoshenko, A. F., Orayevskiy, A. N. et al., "Investigation of Energy Parameters of ClF-H_2 Chemical Laser with Electron-Beam Initiation", KVANTOVAYA ELEKTRONIKA, Vol 5, No 12, 1978, pp 2657-2659.

56. Basov, N. G., Gashkin, A. S., Grigor'yev, P. G. et al., "Quantum Chemical DF-CO_2 Amplifier With High-Power Photoinitiation", Preprint, Lebedev Phys. Inst., Moscow, 1976, No 62, pp 1-12;

Tisone, G. C., Hoffman, J. M.,"Optical Energy Extraction From Electron Beam-Initiated H_2-F_2 Mixtures", J. APPL. PHYS., Vol 47, No 8, 1976, pp 3530-3532;

Basov, N. G., Bashkin, A. S., Golubev, L. Ye. et al., "Investigation of HF Master Laser-Amplifier System Based on Chain Hydrogen Fluoride Reaction", KVANTOVAYA ELEKTRONIKA, Vol 5, No 4, 1978, pp 910-913.

57. Velazco, J. E., Setser, D. W., "Bound-Free Emission Spectra of Diatomic Xenon Halides", J. CHEM. PHYS., Vol 62, No 5, 1975, pp 1990-1991;

Brau, C. A., Ewing, J. J., "Emission Spectra of XeBr, XeCl, XeF and KrF", J. CHEM. PHYS., Vol 63, No 11, 1975, pp 4640-4647;

Hoffman, J. M., Hays, A. K., Tisone, G. C., "High-Power UV Noble-Gas-Halide Lasers", APPL. PHYS. LETT., Vol 28, No 9, 1976, pp 538-539;

Basov, N. G., Brunin, A. N., Danilychev, V. A. et al., "High-Pressure KrF Laser in the Ultraviolet", KVANTOVAYA ELEKTRONIKA, Vol 4, No 7, 1977, pp 1595-1597;

Rokni, M. et al., "Rare Gas Fluoride Lasers", IEEE J. QUANT. ELECTRON., Vol QE-14, No 7, 1978, pp 464-481;

Shuntaro, W. et al., "Efficient Amplification of a Discharge-Pumped KrF Laser", APPL. PHYS. LETT., Vol 33, No 2, 1978, pp 141-143.

58. Hughes, W. M., Olson, N. T., Hunter, R., "Experiments on 558 nm Argon Oxide Laser System", APPL. PHYS. LETT., Vol 28, No 2, 1976, pp 81-83.

59. Tisone, G. C., Hays, A. K., Hoffman, J. M., "Studies of Rare-Gas/Halogen Molecular Lasers Excited by an Electron Beam" in: "Electron. Transit. Lasers", Cambridge, Massachusetts, London, MIT Press, 1976, pp 191-194.

60. Ault, E. R., Bradford, R. S. Jr., Bhaumik, M. L., "High-Power Xenon Fluoride Lasers", APPL. PHYS. LETT., Vol 27, No 7, 1975, pp 413-415.

61. Basov, N. G. et al., "Gazovyye lazery vyzokogo davleniya na elektronnykh perekhodakh molekul" [High-Pressure Gas Lasers on Electronic Transitions of Molecules], Preprint, Lebedev Phys. Inst., Moscow, 1977, No 23;

Brau, C. A., Ewing, J. J., "Spectroscopy, Kinetics and Performance of Rare Gas Monohalide Lasers" in: "Electron. Transit. Lasers", Cambridge, Massachusetts, London, MIT Press, 1976, pp 195-198.

62. Bradford, R. S. Jr., Ault, E. R., Bhaumik, M. L., "Three Efficient e-Beam Pumped High Power Lasers: XeF, Ar-I_2 and KrF", Ibid., pp 211-213.

63. Dzhonson, A. V., Zherardo, D. B., Pal'mer, R. Ye., "XUV Lasers Based on Noble Gas Dimers", KVANTOVAYA ELEKTRONIKA, Vol 3, No 4, 1976, pp 823-829.

64. Searles, S. K., Hart, G. A., "Stimulated Emission at 281.8 nm From XeBr", APPL. PHYS. LETT., No 4, 1975, pp 243-245.

65. Powell, H. T., Murray, J. R., Rhodes, C. K., "Laser Oscillator on the Green Bands of XeO and KrO", APPL. PHYS. LETT., Vol 27, 1974, pp 730-732.

66. Wang, C. P. et al., "Fast Discharge Initiated XeF Laser", APPL. PHYS. LETT., Vol 28, No 6, 1976, pp 326-328.

67. Kudryavtsev, Yu. A., Kuz'mina, I. P., "Excimer Ultraviolet Gas-Discharge XeF, XeCl and KrF Lasers", KVANTOVAYA ELEKTRONIKA, Vol 4, No 1, 1977, pp 220-222.

68. Sutton, D. G. et al., "Fast-Discharge-Initiated KrF Laser", APPL. PHYS. LETT., Vol 28, No 9, 1976, pp 522-523.

69. Burnham, R., Djeu, N., "Ultraviolet-Preionized Discharge-Pumped Lasers in XeF, KrF and ArF", APPL. PHYS. LETT., Vol 29, No 11, 1976, pp 707-709.

70. Knyazev, I. N., Letokhov, V. S., "Gas Lasers in the UV and XUV Regions of the Spectrum" in: "Spravochnik po lazeram" [Laser Handbook], Vol 1, edited by A. M. Prokhorov, Moscow, Sovetskoye radio, 1978, pp 197-220;

Danilychev, V. A., Kerimov, O. M., Kovsh, I. B., "High-Pressure Molecular Gas Lasers" in: "Itogi nauki i tekhniki. Radiotekhnika" [Advances in Science and Engineering. Radio Engineering], Vol 12, Moscow, VINITI, 1979, p 255.

Rhodes, Ch. K., ed., "Excimer Lasers", Berlin, Springer-Verlag, 1979.

CHAPTER 5: SUBSONIC CHEMICAL LASERS

§5.1. Chemical Lasers With Circulation of Premixed Components

The gas-static chemical lasers described in chapter 4 include units for replacing the depleted medium with fresh components. If the reagents and reaction products are continuously replaced at the necessary rate, a quasi-steady or steady level of stimulated emission can be achieved. Let us consider chemical lasers with subsonic circulation, and the peculiarities of their operation.

In order to realize quasi-cw lasing, particularly in HF chemical lasers, the active medium must be rapidly changed in the interval between pulses. Then the pulse develops in the medium that does not contain HF, which reduces the relaxation rate to an admissibly low level. With optimum selection of the parameters of chemical lasers (geometry and circulation rate) pulse recurrence rates up to 100 pps can be attained [Ref. 1]. Some papers [e. g. Ref. 2, 3] describe HF chemical lasers of this kind but with a lower pulse recurrence rate.

Some reactions give vibrationally excited HF, for example the reaction between atomic fluorine and molecular hydrogen. Atomic fluorine is fairly simply obtained from SF_6, which is a stable nontoxic gas. There are other possibilities as well: CF_4, freon, inorganic fluorine-containing compounds NF_3 and N_2F_4. However, SF_6 is preferable for reasons of safety in handling.

A mixture of gas SF_6 with H_2 is subjected to the action of a discharge that breaks down the SF_6 mainly into SF_4 and F, although free sulfur is also liberated. The fluorine then reacts with H_2:

$$\left.\begin{aligned} &SF_6 \rightarrow SF_4 + 2F, \\ &F + H_2 \rightarrow HF(v = 2, 1, 0) + H. \end{aligned}\right\} \qquad (5.1)$$

In this reaction, HF is initially formed in the state v = 2 [Ref. 4, 5] and therefore inversion takes place.

Other reactions, such as those with the participation of H atoms, are distinguished by very high activation energy, or require triple collisions, which makes them too slow for the given process. The reaction products are small amounts of SF_4 and HF mixed with large amounts of SF_6 and He added to increase the specific heat and maintain a stable discharge. Conventional laboratory pumps are completely capable of circulating the gases that take part in the reaction.

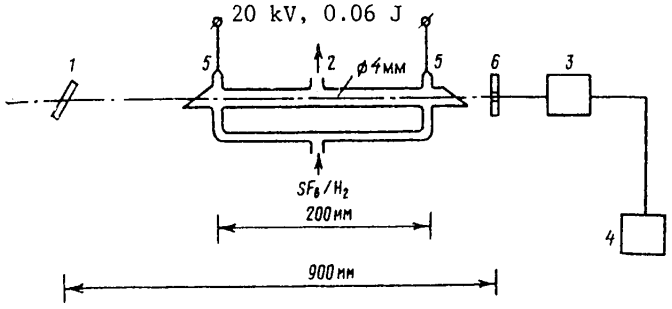

Fig. 5.1. Diagram of the simplest continuous-flow chemical laser: 1--diffraction grating; 2--evacuation; 3--receiver; 4--recording equipment; 5--electrodes; 6--mirror

The design of such a chemical laser is shown schematically in Fig. 5.1, where all connections are standard vacuum units, avoiding the necessity of using glass-to-metal seals. The dimensions indicated on Fig. 5.1 were found by optimization with respect to stability, recurrence rate, spectral range and output power. In particular, the small diameter of the discharge capillary gives good reproducibility of the discharge pulses. One of the mirrors of the cavity was replaced by a diffraction grating to realize single-frequency operation. The main experiments were done at a pulse energy of 0.06 J; increasing this energy to 0.2 J had no appreciable effect on the characteristics of the chemical laser. The rise time of a 0.75 A current pulse was about 0.1 μs.

The initial measurements were made on the multifrequency variant. The output radiation was recorded by a spectrometer that measured the average output power. The spectrum usually included lines $\mathcal{P}_{1-0}(2) - \mathcal{P}_{1-0}(17)$, $\mathcal{P}_{2-1}(2) - \mathcal{P}_{2-1}(9)$ and $\mathcal{P}_{3-2}(4) - \mathcal{P}_{3-2}(5)$ (this transition was not as pronounced as the two preceding ones). Spectral distribution did not change appreciably with variation of the composition and alignment of the cavity as long as the mixture used was $SF_6/H_2/He$. The average output power under such conditions was about 20 mW.

In the investigation of the chemical laser in the selective version, i. e. with the diffraction grating in place of the mirror, the total output power was lower. A reduction in output power was observed on transition 1-0, which is probably due to the absence of pumping from transition 2-1.

After a current pulse with delay of 0.15-2.0 μs, 21 transition lines were observed. Transition 0-1 has a delay of 0.4-0.5 μs. Good repeatibility of the output radiation pulses was observed. Their recurrence rate depends on the rate of renewal of

of the gas in the discharge. At a circulation rate of 0.021 cm^3/min, recurrence rates were 100 pps for transition 2-1 and 40 pps for transition 0-1.

In addition to HF in the described variant, it was found that chemical lasers can also operate on CO with the use of less toxic CS_2/O_2 mixture. In this case, modifications consisted in replacing the NaCl Brewster plates with sapphire, and the Irtran window with a mirror with radius of curvature of 10 m, gold coating, and a center hole of 1.5 mm. Besides, the oil in the pump was replaced with silicone oil that is resistant to oxidation. Because of the danger of detonation of CS_2/OD_2 mixture, the experiments were done at low pressure. A total power of 3.5 mW was attained, distributed among 65 lines of vibrational transitions from $v = 13 \rightarrow 12$ to $v = 5 \rightarrow 4$. The lasing pulses of 0.5 ms duration had a 0.1-0.2 ms delay relative to current, apparently as a result of slower reaction rates and relaxation of the CO system.

The possibilities of experimental realization of both pulsed and cw lasers on CO molecules produced in the excited state during various chemical reactions have been demonstrated in a considerable number of papers [Ref. 6-10].

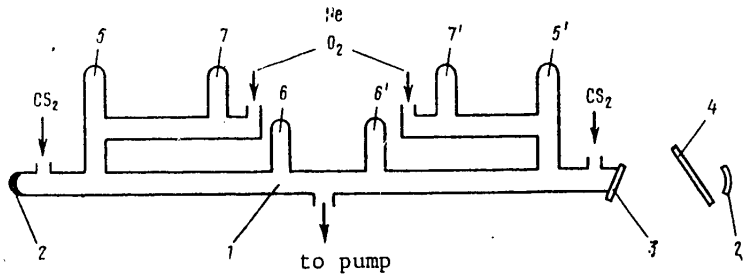

Fig. 5.2. Diagram of CO chemical laser with longitudinal circulation and longitudinal discharge: 1--working tube; 2--spherical mirrors of the cavity; 3--NaCl Brewster window; 4--NaCl plane-parallel plate; 5, 6, 7 (5', 6', 7')--electrodes

Ref. 13 describes a CO chemical laser with longitudinal circulation and longitudinal discharge. The construction of the laser is shown in Fig. 5.2. The gas was injected from the ends of tube 1 and evacuated at the center of this tube by a pump with capacity of 180 m^3/hr. The laser operated in modes with "internal" and "external" discharges. In the former case, a continuous discharge was struck between electrodes 5 and 6 and between symmetric electrodes 5' and 6'. The laser operated wither on a mixture of O_2 and CS_2 [see reaction (4.11)] or with additives of He or CO. Lasing occurred on R-V transitions from vibrational levels of CO having v from 13 to 7.

The experiments showed that adding He appreciably increases the power of this chemical laser--from 0.8 to 2.3 W. In addition to possible facilitation of O_2 dissociation and prevention of recombination of oxygen atoms, the addition of He leads to an increase in the rate of exchange of the mixture in the system. For example it was noted in Ref. 13 that upon addition of He, there was an increase in the pressure in the working tube and in the flowrate of the evacuating system. The CO additives had little effect. There was only a slight increase in power if this gas was added without helium.

In the case of external discharge, continuous discharge was realized in the tubes for delivery of O_2 and He. Here the O_2 and He were not excited by discharge between electrodes 5, 7 and 5', 7', and therefore there was a certain delay between the instant of formation of atomic oxygen and the instant of mixing with CS_2. The maximum power of the chemical laser in this case (0.35 W) was reached at flowrates of (in mole/s): O_2--1.34, He--36.8, CS_2--27.4, CO--0.9. The construction of such

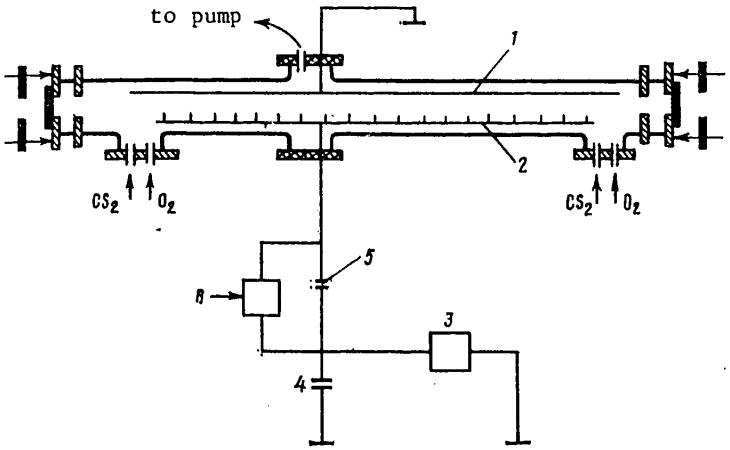

Fig. 5.3. Diagram of chemical laser with longitudinal circulation and transverse discharge: 1--cathode; 2--anode with resistor network; 3--power supply; 4--capacitor, 5--electric discharger; 6--flip-flop

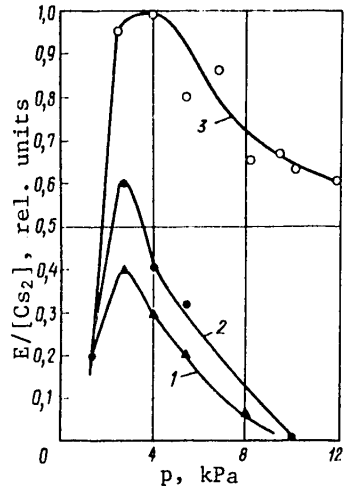

Fig. 5.4. Pressure dependence of lasing energy (C = 0.2 μF, V = 20 kV, CS_2/O_2 = 2/25): 1--CS_2/O_2; 2--$CS_2/O_2/N_2$; 3--CS_2/O_2/He

a chemical laser with longitudinal circulation but with transverse discharge is shown in Fig. 5.3 [Ref. 14], where a cylindrical discharge tube analogous to those shown in Fig. 5.1 and 5.2 with longitudinal optical cavity with inlet of the gas mixture and evacuation is equipped with transverse discharge electrodes. Reactions are initiated by discharge of a capacitor of 0.02 μF charged to 20 kV through a resistor network (each resistor is ~100 Ω). This chemical laser operated both in the gas-static state and with continuous circulation of the mixture.

Fig. 5.4 shows data on the way that lasing energy depends on the pressure of the mixture. The energy of the lasing pulse is plotted in relative units along the axis of ordinates, divided by the CS_2 concentration. Maximum pulse energy in the absence of a diluent (curve 1) was reached at a pressure of

2.66 kPa. The ratio of concentrations CS_2/O_2 was 2/25, which is the ratio where the energy of lasing is the maximum. If He or N_2 is added to such a mixture beginning at a pressure of 1.33 kPa, there is a considerable increase in the energy of stimulated emission (curves 3 and 2 respectively). The maximum energy of stimulated emission E equal to 26 mJ was attained in a mixture with helium at a pressure of 4 kPa. The peak power was determined on the assumption that the lasing pulse is triangular. A peak power of 1 kW was attained in a mixture with helium at pressure of 4 kPa. Under these conditions the pulse duration is ~40 μs and decreases with increasing pressure.

The wavelengths of transitions with stimulated emission are situated in the band from 4.7 to 5.7 μm. Spectral measurements were made with constant circulation of the mixture of $CS_2/O_2/N_2 = 2/25/50$ at pressure of 4 kPa and pulse recurrence rate of 2 Hz. Seventy-nine lines were recorded, identified as transitions of the $\mathcal{P}$-branch as vibrational numbers changed from $v = 13 \rightarrow v = 12$ to $v = 2 \rightarrow v = 1$. A definite sequence was observed in line emission, which can be attributed to cascade transitions.

There are two possible mechanisms of population inversion when the combustion of the mixture is initiated by an electric spark. In the first it is assumed that simultaneous dissociation of both oxygen and hydrogen disulfide is possible with subsequent direct formation of excited CO molecules, i. e.

$$CS_2 = CS + S; \tag{5.2}$$

$$O_2 = 2O; \tag{5.3}$$

$$CS + O = CO^* + S\ (-313\ \text{kJ/mole}). \tag{5.4}$$

If inversion is produced by a spark-initiated combustion chain reaction, an alternative possibility is the following system of reactions:

$$O + CS_2 = CS + SO; \tag{5.5}$$

$$CS + O = CO^* + S\ (-313\ \text{kJ/mole}); \tag{5.4}$$

$$CS + O_2 = CO^* + SO\ (-339\ \text{kJ/mole}); \tag{5.4a}$$

$$S + O_2 = SO + O. \tag{5.6}$$

When photodissociation is used for initiating reactions, it is not possible to create the same initial concentration of oxygen atoms as in an electric discharge. In an electric discharge, there may be fairly high concentrations of atoms of O and CS radicals, so that the principal role is played by reaction (5.4), whereas the major role is played by reaction (5.4a) in the case of photodissociation.

The outlook for chain reactions in chemical lasers is pointed out in Ref. 20, 21, and a kinetic scheme of such reactions is given in Ref. 22. Lasing was first achieved on components H_2 and F_2 with initiation of a chain reaction by an electric discharge in Ref. 23. Such a reaction was produced by both discharge and photopulse in Ref. 24, and this reaction was then studied in Ref. 25-28. The characteristics of HF chemical lasers excited by emission of a pulsed CO_2 laser were studied in Ref. 29.

Operation of chemical lasers on a branched chain reaction is possible with the use of components ClF or ClF_3 with H_2 or CH_4 [Ref. 30]. Each of these fluoride compounds yields an atom of fluorine upon photodissociation. The presence of a chlorine atom creates additional advantages. Of even more importance is the fact that there is a potential capability of amplification of emission based on a branch chain reaction in the system with ClF_3.

However, these initial substances react at room temperature with H_2 and CH_4, and therefore premixing of the initial substances with subsequent photoinitiation under ordinary conditions is impossible. This difficulty is eliminated in the continuous-flow system in which the time of spontaneous development of a reaction after mixing is minimized.

To reduce this time, the components are carefully purified of contaminants, and HF in particular. The reagents are kept from contact with glass, the construction utilizes stainless steel, copper or glass with conditioning at a ClF_3 pressure of 33.3 kPa for several hours. Because of the considerable chemical activity of ClF and ClF_3, the reacting gases are admitted to the working tube through separate inlets, and a continuous flow is maintained (about 100 μmole/s).

Besides, both reacting gases of the mixture are precooled before mixing by passing them through stainless steel cooling coils directly preceding the inlet to the tube.

As a result of the research in Ref. 30, lasing was achieved in HF in all systems; however, induced emission on HCl was recorded only for mixtures ClF/H_2 and ClF_3/H_2

Operation of quasicontinuous chemical lasers on premixed components H_2, F_2 is possible also with a rapid-action system of periodic gas admission. For example, in Ref. 31 the initial mixture newly admitted to the resonator cavity was kept from igniting upon contact with the already reacted gas volume by setting up a buffer zone of unreacted gas between the reacted volume of gas and the fresh mixture. This was accomplished by a feed system utilizing brief interruptions of the flow of H_2 while F_2 and He were supplied continuously.

A diagram of such a system is shown in Fig. 5.5. It is based on bistable fluidic controllers 1 without moving parts that operate at a speed of 1 ms on a jet flowing from an interrupter in the form of a disk 2.

Gases H_2 and He enter regulators 1 through sonic nozzles 3. The components go to mixing chamber 4, and thence into the vicinity of resonator 5. The interrupter controls both regulators 1, and activation of the flashlamp for photoinitiation of the reaction. Photomultiplier monitoring of the time dependence in the resonator cavity showed reliable operation of such a supply system.

Another chemical laser with circulation of premixed components is one based on a mixture of CS_2/O_3 [Ref. 32]. In such a mixture the reagents are prematurely depleted during the dark reaction, and therefore the chemical laser operates with continuous circulation of the reagents. Fig. 5.6 shows a diagram of a facility on which an investigation was made of the energy characteristics of radiation of a CO chemical laser based on a CS_2/O_3 mixture. Quartz working tube 1 (1 m long and 12 mm in diameter) is fitted with CaF_2 windows oriented at the Brewster's angle.

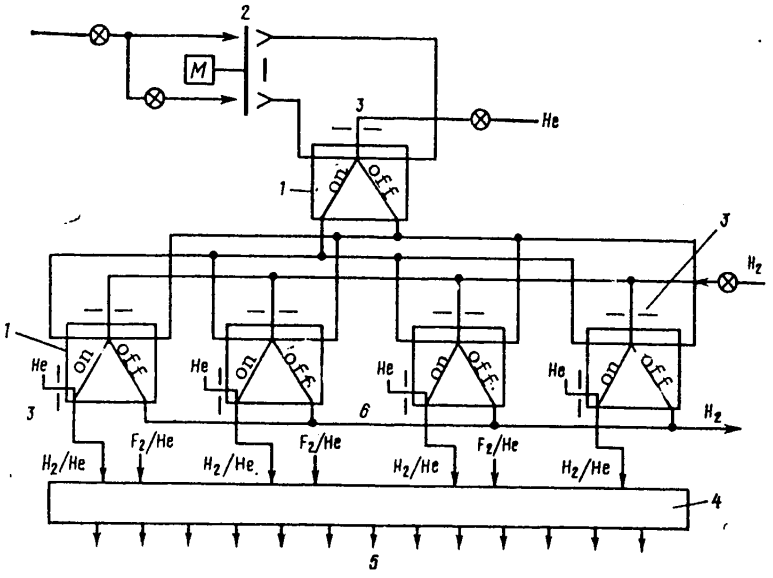

Fig. 5.5. Fast-acting system of gas admission: 1--bistable fluidic controllers; 2--interrupter; 3--sonic nozzles; 4--mixing chamber; 5--outlet to cavity; 6--H_2 outlet

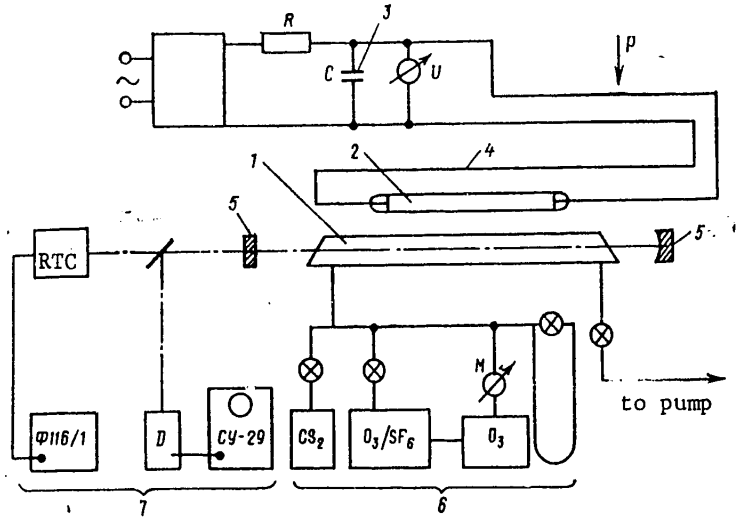

Fig. 5.6. Diagram of facility for studying the energy characteristics of chemical lasers: 1--working tube; 2--photoinitiating lamp; 3--electric capacitor; 4--network of return lines; 5--mirrors; 6--component feed system; 7--measurement system

Two IFP-20000 xenon flashlamps 2 connected in parallel (one is shown in the diagram) with reduced xenon pressure (1.33-2.66 kPa) were supplied by capacitor 3 (15 μF, 25 kV, 4.7 kJ). To reduce the inductance of the electric circuit, the wiring was done with busbars, and the flashlamps were placed in return-line network 4. This increases the maximum power contributed to lamp 2. The optical cavity 2 m long was formed by two mirrors 5, one with radius of curvature of 5 m having a dense gold coating, while the other was flat and could be interchanged to vary the reflectivity. Results were recorded by a photoresistor and radiation thermocouple [RTC] in measurement system 7.

Lasing was observed on carbon disulfide with pure ozone only at low pressure. Increasing the pressure leads to explosion of the mixture in the tube and disruption of lasing. Diluting the mixture with argon or helium increased the specific heat of the mixture and slowed down the dark-reaction depletion of ozone. The addition of a diluent with higher specific heat--sulfur hexafluoride--is conducive to an appreciably higher output energy (Fig. 5.7), and stimulated emission was improved by a further increase in SF_6 pressure. The addition of nitrous oxide increases output energy by a factor of 1.5 (Fig. 5.8). On the other hand, adding CO and OCS is detrimental to lasing [Ref. 32].

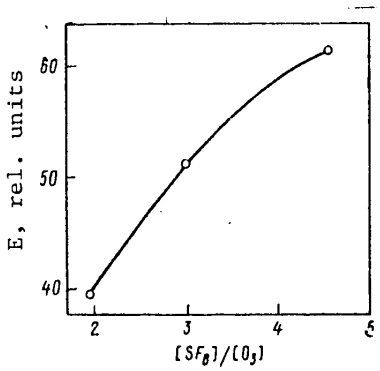

Fig. 5.7. Influence that relative expenditure of sulfur hexafluoride has on the energy of stimulated emission (pressure [kPa]: CS_2--0.8; O_3--1.33; N_2O--1.6; pumping energy 2 kJ)

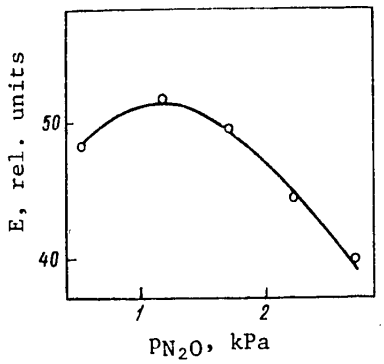

Fig. 5.8. Energy of stimulated emission as a function of N_2O pressure (pressure [kPa]: CS_2--0.53; O_3--0.93; SF_6--4.66)

The operation of the chemical laser was optimized with respect to the influence of the initiation energy $E_{I_{max}}$ on output energy E. Fig. 5.9 shows two curves plotted for two pressures of the working mixture. There is a pronounced maximum. The optimum initiation energy increases with falling pressure.

The investigated CS_2/O_3 laser has a power output as high as the CO electroionization laser operating at room temperature, and is an order of magnitude better with respect to efficiency normalized to the energy investment [Ref. 33]. The use of this mixture in continuous CO chemical lasers eliminates the difficulties associated with instability of the CS_2/O_3 mixture. With the proper rate of circulation of reagents, such a chemical laser can provide output power from the cross

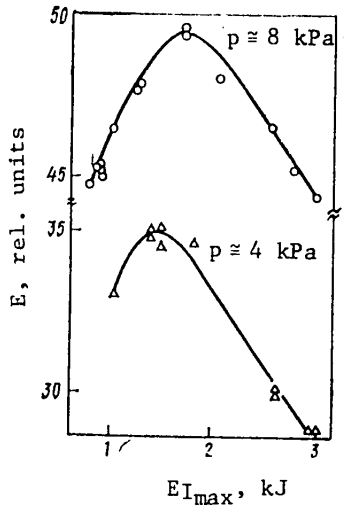

Fig. 5.9. Dependence of energy of stimulated emission on pumping energy: mixture composition $CS_2/O_3/N_2O/SF_6 = 3/5/6/15$

section of the flow of up to 45 W/cm^2. The efficiency of the system is determined solely by the efficiency of the pumping lamps, and may reach 1% [Ref. 32].

§5.2. Chemical Lasers With Subsonic Mixing of Components

Purely Chemical Subsonic Lasers. A purely chemical laser is one in which quantum-mechanical excitation and stimulation of emission are the result of chemical reactions alone, without any external sources of energy, i.e. even without preliminary external initiation of the reaction. In such a laser, the process is so rapid that it competes successfully with relaxation that quenches molecules excited in the course of the reaction. Formation of these molecules is possible in exchange reactions of atoms or radicals with molecules. However, the production of reagents in the atomic state in the process of a single act requires additional expenditures of energy, and consequently is energetically disadvantageous. Therefore reactions with a long chain of the $H_2 + F_2$ type are used, and atoms or radicals are used as a seed component.

A purely chemical cw laser was first produced in Ref. 34, 35 with quasiresonant transfer of vibrational energy from the excited molecules formed in the reaction to the cold working molecules [Ref. 36], and without external sources of excitation [Ref. 37]. The quantum-mechanical effect of stimulated emission is obtained for example in a chain reaction of deuterium and fluorine with transfer of vibrational quanta from excited molecules of deuterium fluoride to molecules of CO_2 [Ref. 38], the scheme of which for the case of photoinitiation of the reaction was considered in §4.1. This reaction has the advantage of realization of a long optical chain. The seed component is NO. The sequence of reactions in such a chain as the reagents are introduced for mixing into the subsonic stream is shown in Fig. 5.10.

The specific mechanism of setting up inversion is determined in large measure by the exchange of vibrational energy between molecules, and subsequent redistribution of energy by vibrational levels. For example, the vibrational excitation of HF molecules formed in the reaction

$$F + H_2 \rightarrow HF\ (v = n) + H, \qquad (5.7)$$

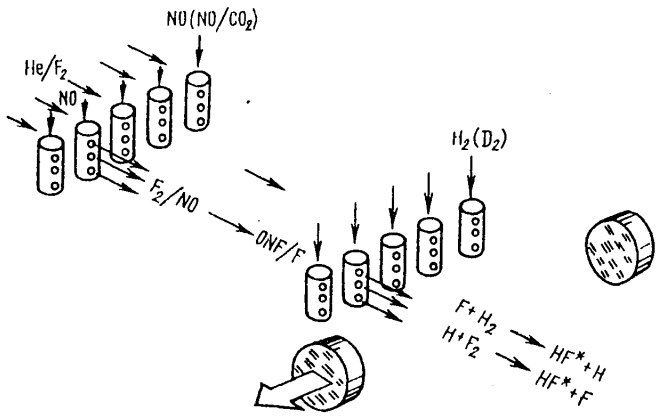

2.7 μm--HF
3.8 μm--DF
10.6 μm--DF + CO_2, HF + CO_2

Fig. 5.10. Diagram of reagent input in a purely chemical laser with transverse circulation

where n = 1, 2 or 3, is very rapidly redistributed over many levels by near-resonant processes of exchange of a vibrational quantum:

$$HF(v=n)+HF(v=m)\rightarrow HF(v=n-1)+HF(v=m+1). \tag{5.8}$$

The relative rate of processes (5.7) and (5.8) determines the possibility of lasing onset on HF molecules in the region of 2.7 μm as a result of total or partial inversion. And this is what determines the characteristics of chemical lasers: the V-R lasing spectrum, emission power, gain and optical efficiency. Besides, the vibrational excitation received by HF molecules as a result of reaction (5.7) may lead to total inversion of CO_2 and to onset of lasing on 10.6 μm as a result of the processes

$$\left.\begin{aligned} &HF(v=n)+CO_2(00^00)\rightarrow HF(v=n-1)+CO_2(10^01);\\ &CO_2(10^01)+CO_2(00^00)\rightarrow CO_2(10^00)+CO_2(00^01). \end{aligned}\right\} \tag{5.9}$$

When deuterium is used, the main reactions are [Ref. 39]:

$$F_2+NO\rightarrow ONF+F\quad(-75{,}2\ \text{kJ/mole}); \tag{5.10}$$
$$F+NO\rightarrow ONF\ (-238\ \text{kJ/mole}); \tag{5.11}$$
$$F+D_2\rightarrow DF(v=n)+D\ (-129{,}5\ \text{kJ/mole}); \tag{5.12}$$
$$D+F_2\rightarrow DF(v=n)+F\ (-414\ \text{kJ/mole}); \tag{5.13}$$
$$D+ONF\rightarrow DF(v=n)+NO\ (-326\ \text{kJ/mole}); \tag{5.14}$$
$$DF(v=n)+DF(v=m)\rightleftarrows DF(v=n-1)+DF(v=m+1); \tag{5.15}$$
$$DF(v=n)+M\rightleftarrows DF(v=n-1)+M; \tag{5.16}$$
$$DF(v=n)+CO_2(00^00)\rightleftarrows DF(v=n-1)+CO_2(00^01); \tag{5.17}$$
$$CO_2(00^01)+M\rightleftarrows CO_2(nm^l0)+M; \tag{5.18}$$
$$CO_2(10^00)+CO_2(00^00)\rightleftarrows 2CO_2(01^10); \tag{5.19}$$
$$CO_2(01^10)+M\rightleftarrows CO_2(00^00)+M, \tag{5.20}$$

where M = DF, NO, He, F_2, D_2, ONF, CO_2, F or D. When deuterium is replaced by hydrogen, equation (5.9) must be substituted for (5.17).

To illustrate how energy is transferred from vibrationally excited HCl, HF, DF, HI or HBr to CO_2 (00°1), Fig. 5.11 shows a diagram of the vibrational levels of

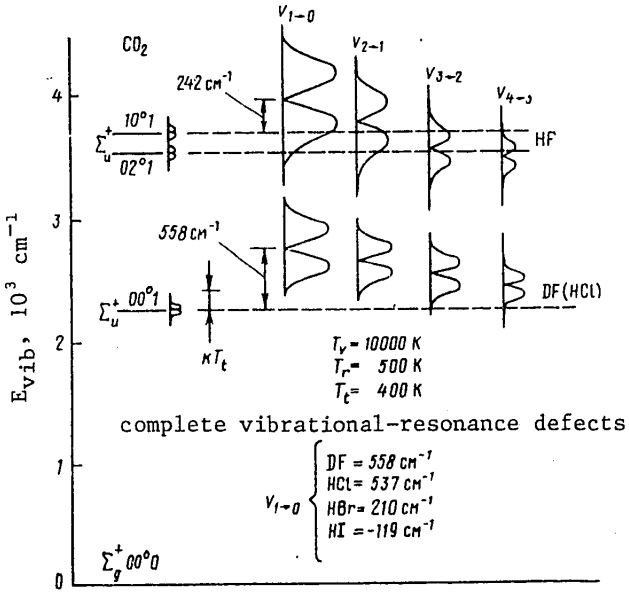

Fig. 5.11. Diagram of vibrational levels of molecules of CO_2 and hydrogen halides

these molecules. The left part of the diagram shows the levels (00°0), (00°1), (10°1) and (02°1) of CO_2. The right-hand part shows the energies corresponding to V-R transitions of DF (very close to HCl) and HF in bands $1\to0$, $2\to1$, $3\to2$ and $4\to3$. For the assumed values of vibrational and rotational temperatures, Fig. 5.11 shows the qualitative relative distribution of molecules with respect to V-R states as a function of the defects of resonances, whose values are indicated for the band $1\to0$.

Fig. 5.12. Diagram of subsonic chemical laser with reagent mixing and energy transfer: 1--F_2 and He injectors; 2--CO_2 and NO injectors; 3--D_2 or H_2 injectors; 4--NaCl Brewster windows; 5--spherical mirror (radius of curvature 10 m); 6, 7--flat mirrors; 8--semi-transparent spherical mirror (radius of curvature 10 m); 9--section for blowing nitrogen over the mirrors; 10--output emission of chemical laser; 11--flow channel

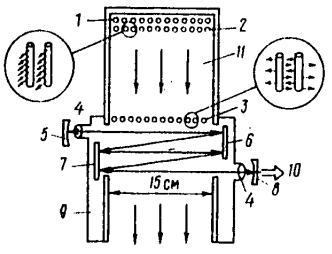

Fig. 5.12 shows a diagram of a chemical laser that works on reactions (5.10)-(5.20) under transverse flow conditions [Ref. 38].

The operation of this laser is as follows. Premixed F_2 with He and NO with CO_2 are admitted to the upper part of flow channel 11 with cross section of 1 x 15 cm through two sets of gas-mixing injector tubes 1 and 2. The gases enter the tubes through lines fastened in the upper part of channel 11. The gases are mixed rapidly (within about 50 μs), and then the necessary concentration of fluorine atoms is set up in the reactions (5.10) and (5.11). Deuterium or hydrogen is injected into the flow through tubes 3 that are analogous to the tubes in the first two rows of injectors, except for the fact that the gas from tubes 3 exits at a right angle to the flow through staggered orifices.

A five-pass optical cavity with axis directed across the flow ensures selection and extraction of energy from a region situated at a distance of from 0.5 to 6 cm from injectors 3. To eliminate the possibility of parasitic lasing directly on flat mirrors 6, 7, these mirrors are slightly misaligned. Streams of dry nitrogen are directed along the side walls of channel 11 to prevent the mirrors from coming into contact with the chemically active components of the flow. The NaCl Brewster windows are installed to enable use of external spherical mirrors. All mirrors are water-cooled. The opaque mirrors that are not intended for transmitting radiation are covered with metal-dielectric coatings with reflectivity of 99.4%. The output mirrors are made on a Ge substrate 3 mm thick with dielectric coating, and have reflectivity from 10 to 50%. The optical path between mirrors with radius of curvature of 10 m is 1.8 m.

The specific construction of the described chemical laser design requires a study of the mutual relations between all parameters, and optimization of these relations. For example, selection of the evacuation system involves the optimum pressure in the cavity, chemical efficiency is related to the specific consumption of reagents, the dimensions of the chemical laser are related to optimization of the structure and composition of the working gas mixture. It is desirable to maximize the pressure in the cavity, as this simplifies the construction of the evacuating system. Increasing the chemical efficiency involves a reduction in the expenditure of reagents per unit of emission power. Optimizing the composition and flowrate of the mixture to maximize power leads to the possibility of reducing the dimensions of the cavity and of the entire chemical laser.

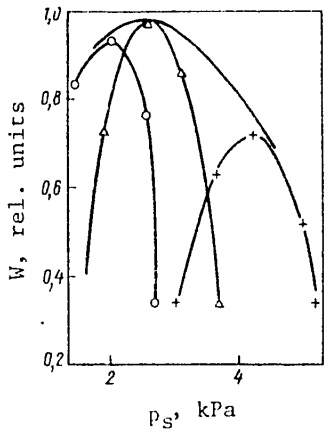

Fig. 5.13. Relative output power of subsonic chemical laser with energy transfer ($DF-CO_2$) as a function of static pressure in the cavity p_S at different flowrate concentrations of NO, mole/s: o--0.011; Δ--0.007; +--0.002. Enveloping curve--change in lasing power with change of pressure in the cavity at the optimum NO concentration

Fig. 5.13 shows the typical dependence of output emission power W on the pressure of the mixture in the cavity p_s [Ref. 40]. Here the change in output power with change in total pressure of the mixture in the cavity depends on the molar concentration of radicals NO introduced into the mixture. It can be seen that the optimum total pressure of reagents in the cavity that corresponds to maximum lasing power depends on the NO concentration. Increasing the pressure of the mixture leads to a reduction in molar concentration of NO in inverse proportion to p_s^2. Fig. 5.13 also shows that there is an optimum pressure of the mixture (2.26 kPa) and an optimum flowrate of NO (7 mole/s) that maximize the output power of stimulated emission.

The nature of the distribution of the relative population n_v/n of the upper level of CO_2 (00°1) in the vicinity of the cavity x_c and beyond this region in the x-direction downstream beginning with the H_2 (D_2) injector is shown in Fig. 5.14.

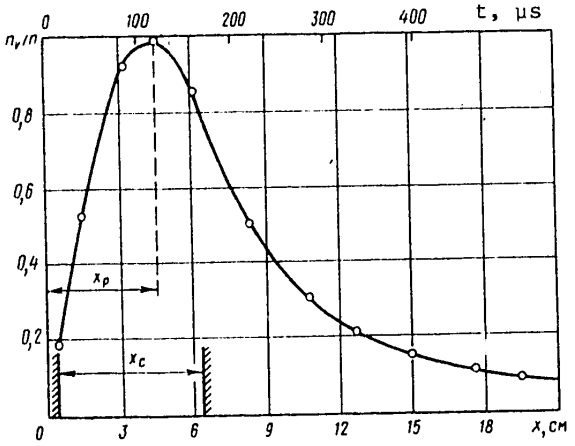

Fig. 5.14. Distribution along the x-axis of the relative population of the upper level of CO_2(00°1) n_v/n

Increasing the flowrate of NO accelerated the chain reaction, intensified 4.3 μm radiation and reduced x_p--the distance to the peak of the relative population, and accordingly the maximum emission intensity.

By way of example, let us cite some data on lasing powers W and chemical efficiencies η_x of purely chemical subsonic lasers with transverse circulation (Table 5.1).

Systems of purely chemical subsonic lasers have also been developed with longitudinal pumping [Ref. 42, 43]. A diagram of such a chemical laser is shown in Fig. 5.15 [Ref. 43]. Reactions (5.12), (5.13) and (5.17) were carried out in Teflon tube 1. The length of the tube was 150 mm, and inside diameter was 8 mm. Reaction (5.10) took place in a flow of $He/F_2/NO$ in copper connecting tube 2 on a section 35 cm

TABLE 5.1

Values of W and η_x according to various references

Parameter	Reference		
	[40]	[38]	[41]
W, watts	560	160	19
η_x, %	4	4,6	4,2

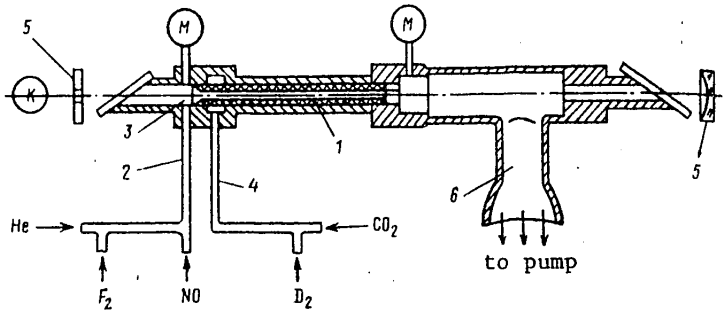

Fig. 5.15. Purely chemical laser with longitudinal circulation: 1--working reactor tube; 2--inlet of $He/F_2/NO$ mixture; 3--end face of the reactor; 4--inlet of CO_2/DO_2 mixture; 5--mirrors; 6--branch for evacuation of gas

long, and the resultant gas mixture was fed to the end face of the reactor 3. Connecting tube 4 was used for inlet of gas mixture CO_2/D_2. This mixture was injected into the reaction space through a number of orifices around the perimeter close to the end face 3 of Teflon tube 1. A semiconfocal cavity was formed by gold-coated mirror 5. The stimulated emission was coupled out on the side of the flat mirror through an orifice 1 mm in diameter. The pressure at the inlet to the reaction space under the conditions of the experiment was 2-2.66 kPa. To ensure adequate velocity of the gas stream through reaction tube 1, it was connected to the ballast tank through larger-diameter tube 6. This provided an average flow velocity of ~200 m/s.

The flowrates of working components of the mixture that are optimum with respect to radiation power were experimentally determined in Ref. 43 [mmole/s]: NO--0.04; F_2 ~ 0.451 D_2--0.37; CO --1.65; He--5.07. Fig. 5.16 shows how the power of a cw chemical laser with longitudinal circulation depends on gas flowrates. Since the

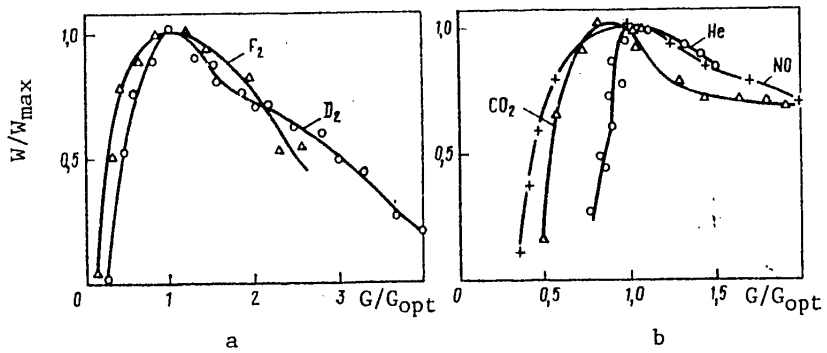

Fig. 5.16. Power of cw chemical laser as a function of gas flowrate for reagents:
a--of reaction (5.12), (5.13); b--of reaction (5.11), (5.17, (5.18)

output power of purely chemical cw lasers is appreciably dependent on the rate of mixing of initial reagents, the conditions of reagent mixing in Ref. 43 were altered by reducing the diameter of the injection orifices. For example at an orifice diameter of d = 1 mm the pressure differential between the injected fluid and the reaction space was $\Delta p = 1.33$–2 kPa, while at d = 0.35 mm and retention of the same gas flowrate, $\Delta p \sim 0.1$ MPa. A reduction in the diameter of the orifices increased the velocities of the injected jets, i. e. it improved the conditions of mixing of the components. An imporvement in mixing conditions at d = 0.35 mm led to an increase in the power of cw emission by approximately a factor of four to 2.1 W.

Electric-Discharge Subsonic Chemical Lasers. Amplification of radiation in the continuous mode due to chemical reactions excited by an electric discharge was first achieved in reactions of exchange type [Ref. 44]. The reaction took place in a stream of a mixture of H_2 and halide, vibrationally excited molecules of hydrogen halides being generated under conditions of low pressures of 1.33–0.13 Pa:

$$H + Cl_2 \rightarrow HCl^* + Cl; \quad (5.21)$$

$$H + Br_2 \rightarrow HBr^* + Br; \quad (5.22)$$

$$Cl + HI \rightarrow HCl^* + I. \quad (5.23)$$

At higher pressures--from 0.66 to 2 kPa--a chemical laser operated [Ref. 45, 46] in which atoms of F were produced in an electric discharge in a gas mixture of He, O_2 and SF_6. Then the SF_6 was mixed with hydrogen that fed into the flow region upstream along the axis of the transverse optical cavity.

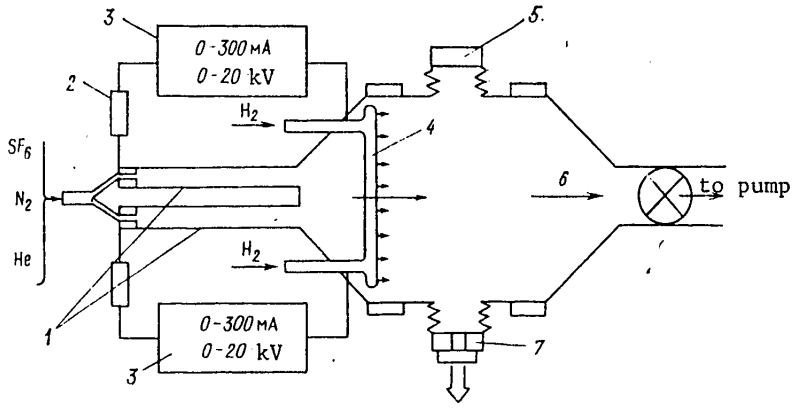

Fig. 5.17. Diagram of subsonic cw electric-discharge HF chemical laser with transverse circulation and mixing of reagents: 1--Pyrex discharge tubes; 2--ballast resistors for discharge stabilization; 3--discharge power supply; 4--injection tube; 5--opaque mirror; 6--gas flow; 7--mirror with hole for coupling out the radiation

Fluorine atoms have also been produced in a dc discharge in a mixture of N_2, He and SF_6 [Ref. 47], after which these atoms were reacted in the same way with H_2 or D_2.

The facility described in Ref. 47 is diagrammed in Fig. 4.17. A characteristic feature of this installation is that the location of the injection tube can be changed. Gas mixing, chemical reactions and lasing take place in a flow with cross section of 30 x 1.25 cm. The optical cavity is formed by mirrors with radius of curvature of 2 m separated by a distance of 45 cm. Emission is coupled out of the cavity through a hole with diameter of 5 mm in one of the mirrors.

The typical gas flowrate [mmole/s]: H_2--3, N_2--20, He--10, the flowrate of SF_6 varied from 3 to 20. Increasing the amount of SF_6 in the mixture led to an increase in the impedance of the discharge, and consequently in the power consumption. Adding N_2 to the mixture also increased power consumption since there was a rise in the voltage drop across the discharge. Helium was added to the mixture to stabilize the discharge and reduce the gas temperature.

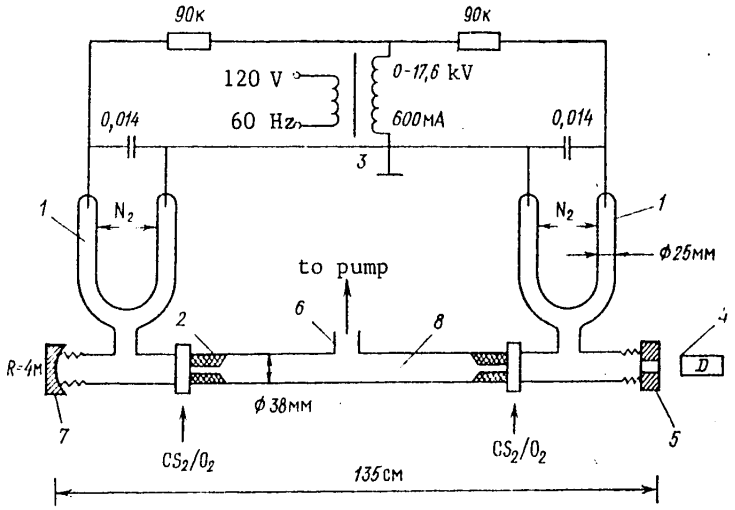

Fig. 5.18. Diagram of electric-discharge chemical laser with longitudinal mixing of reagents: 1--discharge tubes with inlet of N_2; 2--injectors with inlet of CS_2/O_2 mixture; 3--electric supply for the discharge; 4--radiation detector; 5--flat mirror; 6--gas outlet with evacuation rate of 5 m^3/min; 7--spherical mirror; 8--working reactor tube

At an evacuation rate of 0.236 m^3/s, the pressure in the flow in the intermixing region was about 0.7 kPa, and the velocity of the flow was about $4 \cdot 10^3$ cm/s (according to estimates, the speed of sound in the mixture is $7 \cdot 10^4$ cm/s). Under these conditions, adequate efficiency of operation of the chemical laser was reached only when the tube through which H was injected was located in the vicinity of 2 ± 0.5 cm upstream from the cavity axis. From this we can estimate the lifetime of the excited gas mixture at about 3.6 μs -- the upper limit of the lifetime of excited HF molecules associated with the specific conditions in the given facility. The HF makes up a small fraction of the total number of particles, and the temperature of the mixture is approximately 150°C. A relatively short time for the mixture to stay in the optical cavity is useful, since HF molecules that are in the ground

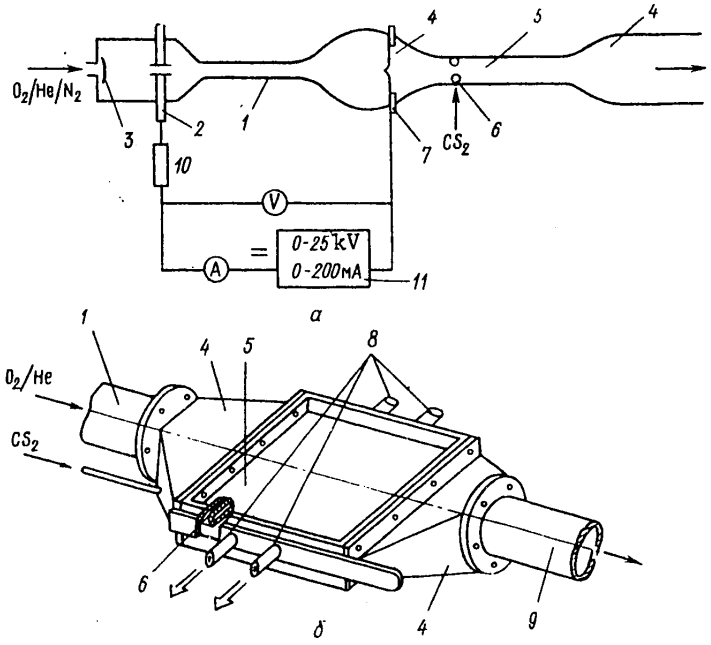

Fig. 5.19. Subsonic electric-discharge chemical laser with transverse flow: 1--discharge section; 2--anode; 3--mixer; 4--adapters; 5--working channel; 6--injectors with CS_2 inputs; 7--cathode; 8--resonators; 9--branch pipe for gas outlet; 10--ballast resistor; 11--discharge supply source

state are carried off with the flow out of the cavity, and consequently there is the possibility of achieving lasing on transition (1-0), in contrast to systems in which the gas flow is directed parallel to the axis of the cavity.

The power of stimulated emission of this kind of HF chemical laser depended on the electric power of the supply. The maximum power of 5.5 W with lasing on HF corresponds to intensity of stimulated emission of 700 W/cm for beam diameter of about 1 mm. DF lasing power is about half this level under analogous conditions. The ratio of the energy of stimulated emission to the electrical energy expended on initiating the reaction (called the electrical efficiency of electric-discharge chemical lasers) was about 0.1%.

By using separate discharge tubes and longitudinal circulation of the reagents, a chemical laser has been made that is based on CS_2/O_2 and nitrogen [Ref. 9, 48] (Fig. 5.18). When N_2 is dissociated in the electric discharge in tubes 1, atoms of N are formed which are then mixed with CS_2/O_2 in the Teflon injectors 2 inside the optical cavity longitudinal to the flow that is formed by flat mirror 5 and spherical mirror 7. The radiation is coupled out to InSb detector 4 through an aperture in the flat mirror.

Here there are two possible paths of initiation of the reaction. One is by dissociation of N_2, and the other is by dissociation of O_2, in the case where discharge

tube 1 is filled with a mixture of O_2 and He. It was found in Ref. 48 that increasing the flowrate of O_2 or N_2 raises the output power of the chemical laser. The reactions that take place in such a laser are similar to those in the CO photochemical laser described in Ref. 7.

A subsonic electric-discharge chemical laser with transverse flow operates on an analogous mixture [Ref. 49]. Fig. 5.19 shows a schematic (a) and the outside view (b) of this laser. The discharge section is made of Pyrex tube 1, at the inlet of which is copper disk anode 2 with central orifice for passing a mixture of gases O_2, He, N_2 coming from mixer 3. From discharge section 1 (90 cm long, 2.5 cm in diameter) the gas stream passes through adapter 4 into the section of rectangular working channel 5 (50.8 x 30.5 x 1.3 cm) with adjustable positioning of injectors 6 for introducing CS_2. The reaction-initiating discharge takes place between anode 2 and cathode 7. Adapters 4 and channel 5, made of copper and stainless steel respectively, are water-cooled. Transverse resonators 8 are installed on channel 5. The gas is evacuated through outlet 9. Ballast resistor 10 is used to stabilize the discharge.

A power of 4.5 W was achieved in such a chemical laser with flowrates of 7.7, 33.4 and 2.4 g/m for He, O_2 and CS_2 respectively at a total pressure of 0.72 kPa, discharge power of 800 W, and distance between the CS_2 injector and the optical axis of the resonator of 1.5 cm. The electrical efficiency was 0.56%, and the chemical efficiency was 2.7%. Fig. 5.20 shows curves for the output power W_{out} as a function of the invested power W_{inv} and partial pressures p_i of O_2 and He (the unstable discharge region is shaded).

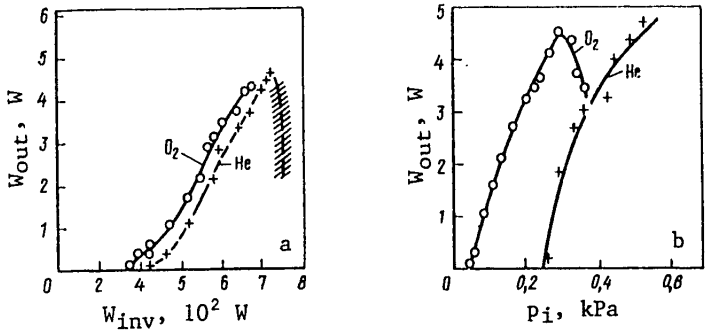

Fig. 5.20. Output power of chemical laser as a function of invested energy (a) and partial pressures of O_2 and He (b)

The described chemical laser [Ref. 49] operates with greater efficiency than similar lasers described in Ref. 8 and 11. This can apparently be attributed to the capability for optimizing the position of the CS_2 injector in the resonator cavity. Another factor is in the effect of reduced rotational temperature of CO.

Similar in design to the chemical laser depicted in Fig. 5.19 is the miniature cw HF (DF) subsonic electric-discharge chemical laser shown in Fig. 5.21. The

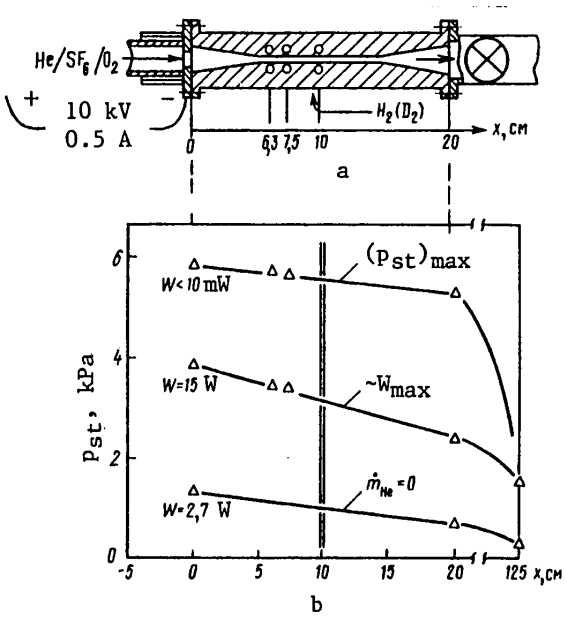

Fig. 5.21. Channel of a miniature subsonic electric-discharge chemical laser (a) and pressure distribution p_{st} at different powers W of stimulated emission (b)

parameters of this laser were studied in Ref. 50 as a function of the mass flowrate $\dot{m}$ of components of the working mixture SF_6/H_2 $(D_2)/He/O_2$. The small overall size of the chemical laser is due to the comparatively small dimensions of the channel (20 x 10 x 3 cm). BaF_2 Brewster windows are installed in the side walls of the channel so that the optical axis passes 1 mm downstream from the orifices of the H_2 injector. The cavity was formed by mirrors placed 40 cm apart: a flat mirror and an interchangeable spherical mirror with radius that could be varied from 1 to 10 m. Some results of investigation of such a miniature chemical laser are shown in Fig. 5.21 and 5.22.

An electrodeless discharge is also used to get active atoms that initiate a reaction. An advantage of such a discharge over a conductive discharge for initiating a reaction in chemical lasers is the fact that it enables production of fluorine atoms in the large volumes of plasma microwave oscillators with more uniform distribution of these atoms in the discharge space. Radio-frequency emission [Ref. 51] or microwave radiation [Ref. 52] is used for dissociation of SF_6 or F_2 in chemical lasers.

Fig. 5.23 shows diagrams of a quasi-cw chemical laser with microwave initiation of the reaction and the working chamber of this laser. The working chamber 1 shown in Fig. 5.23b is made of a one-piece aluminum block. In this chamber the main channel for flow of the active medium (indicated by the arrows) has dimensions of: height 6.4 mm, width 5 cm, length 7.5 cm. Perpendicular to this channel is an optical channel with the same cross section enabling adjustment of the resonator axis along the flow of active medium, this axis being perpendicular to the flow.

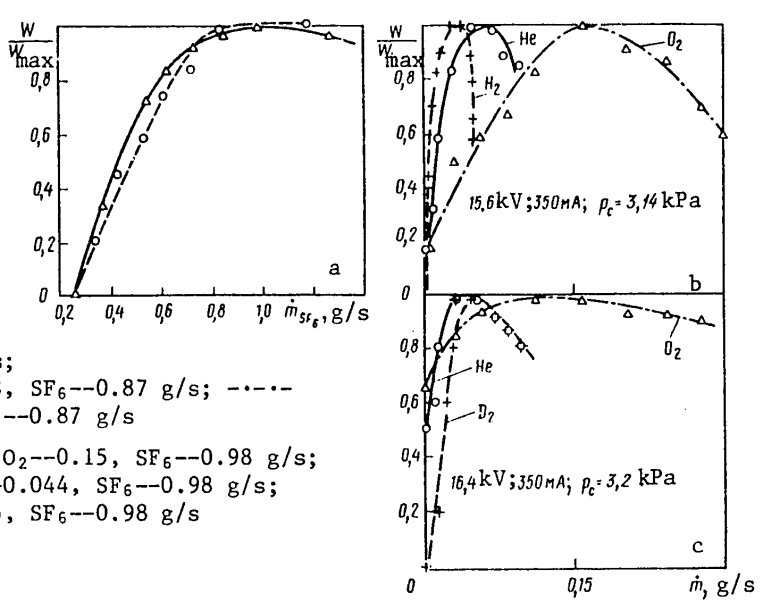

Fig. 5.22. Working characteristics of miniature chemical laser:
a——16.4 kV, 350 mA, $\dot{m}$: He--0.0405, D_2--0.044, O_2--0.150 g/s; p_s = 3.2 kPa; ----15.6 kV, 350 mA, $\dot{m}$: He--0.054, H_2--0.03; O_2--0.18 g/s; p_s = 3.14 kPa

b--$\dot{m}$: ---- He--0.054, O_2--0.18, SF_6--0.87 g/s; —— H_2--0.03, O_2--0.18, SF_6--0.87 g/s; -·-·- He--0.54, H_2--0.03, SF_6--0.87 g/s

c--$\dot{m}$: —— D_2--0.044, O_2--0.15, SF_6--0.98 g/s; -·-·- He--0.0405, D_2--0.044, SF_6--0.98 g/s; ---- He--0.04, O_2--0.15, SF_6--0.98 g/s

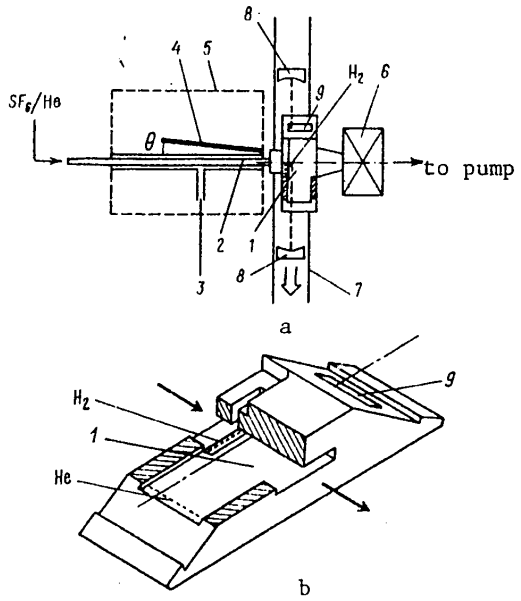

Fig. 5.23. Diagrams of quasi-cw chemical laser with microwave initiation of reaction (a) and the working chamber of this laser (b): 1--working chamber; 2--quartz plasma tube; 3--air-cooling inlet; 4--microwave plasma generator; 5--microwave radiation shield; 6--gate; 7--optical bench; 8--mirrors; 9--Brewster windows

Placed above and below the inlet to the main channel are H_2 injectors with a number of orifices 0.1 mm in diameter. The two rows of transverse H_2 jets meet the F atoms contained in the main gas stream of reagents.

The inlet of the working chamber of the chemical laser is connected through a transitional section to quartz plasma tube 2 with inside diameter of 13 mm. In this tube, helium-diluted SF_6 is dissociated in the field of a source of microwave radiation [Ref. 53] with power of 1.2 or 2.5 kW at a frequency of 2.45 GHz. The energy of the microwave emission was injected in pulses with frequency of 120 Hz. For optimum transfer of the energy of microwave emission inside the plasma tube, and to attain uniform electrodeless discharge therein, this tube and the source of microwave emission were placed side by side at some adjustable angle θ.

The cavity was formed by two mirrors: one with radius of curvature of 10 m was gold-coated, and the other with radius of curvature of 4 m was made of germanium with dielectric coating having a transmission factor of 4% in the wavelength region from 1.9 to 3.3 μm. The distance between the mirrors was 43 cm. The Brewster's windows were shielded by helium jets from the diffusion of HF molecules out of the main flow of active medium. Without this protection, the emission power of the chemical laser was cut approximately in half due to absorption of radiation by HF molecules in the ground state. Upon attainment of stimulated emission, the flowrates of the gas components were adjusted to optimize emission power W. The optimum proportion of flowrates: helium flow for shielding the windows--6 mmole/s; main helium flow--21 mmole/s; SF_6--0.4 mmole/s; H_2--4 mmole/s. Total pressure in the working chamber--133 Pa.

The design of the given chemical laser enables optimization of not only the flowrate of components in the stream, but also the angle θ, the distance x_c of the optical axis from the H_2 injector, the angle of turn ϕ of this axis relative to the axis of the flow. Graphs of such relations are shown in Fig. 5.24, 5.25.

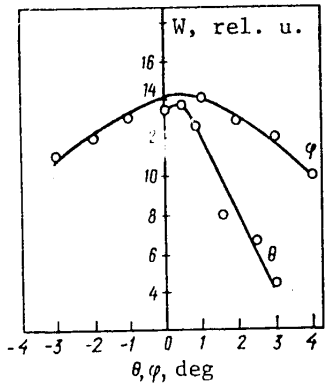

Fig. 5.24. Relative power of chemical laser as a function of angles of turn ϕ and θ

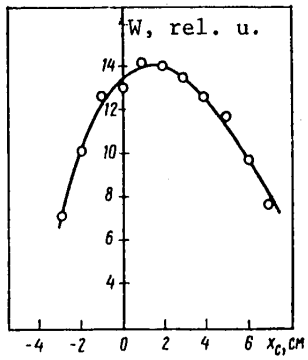

Fig. 5.25. Relative power of chemical laser with transverse circulation as a function of the distance of the optical axis from the H_2 injector

As a result of optimization in Ref. 53 at a power of 2.5 kW for the microwave source, the maximum emission power for all transition lines was 560 mW, with a corresponding figure of 290 mW at a power of 1.2 kW for the microwave source.

Chemical lasers with transverse flow have operated with a source of electrodeless discharge in the rf band on both HCl [Ref. 54] and HF, DF [Ref. 55]. Here the source of fluorine atoms is a discharge in He/F_2 inside a water-cooled quartz tube at a frequency of the electromagnetic field of the source of 21 MHz. The activated flow passes from the discharge region through a number of small channels matched to the outlets of the secondary-flow injectors. The primary flow of He/F_2 and F is discharged with sonic velocity and mixes with the secondary flow of H_2 (D_2). The cross section of the discharge nozzle (3 x 0.5 cm) determines the dimensions of the flow in which the optical axis of the resonator is located 0.5 cm downstream from the nozzle tip. Optimum flowrates in this chemical laser are 2, 0.3 and 0.1 mmole/s for He, F_2 and H_2 (D_2) respectively. The pressure in the resonator is about 130 Pa. Radiation power on all lines is 0.3 W for the HF laser and 0.12 W for the DF laser.

Microwave initiation of the reaction has also been studied in a CO chemical laser with subsonic flow transverse to the optical axis of the cavity [Ref. 49, 56-58]. The following conditions of efficient operation of a CO chemical laser, including conditions that are characteristic of chemical lasers operating on other active media have been formulated as a result of research.

1. High degree of dissociation and production of active atoms, in the given case oxygen atoms.

2. Rapid mixing of flows of O/O_2 with CS_2.

3. Adequate input of diluent to regulate the rise in temperature in an exothermic chemical reaction.

4. Organization of flow geometry to ensure effective interaction with the optical field of the resonator.

5. Rapid transport of chemically excited CO into the optical field and rapid removal.

Ref. 56 describes a chemical laser in which atomic oxygen is formed in the process of dissociation of O_2 when a mixture of O_2/He is passed through a high-frequency discharge region. The cross section of such a chemical laser is shown in Fig. 5.26. The discharge was excited in quartz tube 2 intersecting waveguide 3 connected to the output of a magnetron (2.45 GHz, 1 kW) at an angle of $\theta = 10°$. The O/O_2/He mixture flowed from the discharge region to oxygen injector 4. The flowrate G_0 of atomic oxygen through the region of the resonator was measured by titration of the working mixture with injected NO_2 additive. Fig. 5.7 shows the dependence of G_0 on the pressure p_s in the cavity as plotted for fixed flowrates of O_2, He and H_2. A small amount of H_2 (0.0215 mmole/s) was added to the O_2/He mixture at the inlet to the discharge gap.

Experiments have shown that at a pressure of the mixture of 1.33 kPa, such an additive doubles the degree of dissociation of O_2. The flowrates of atomic oxygen at

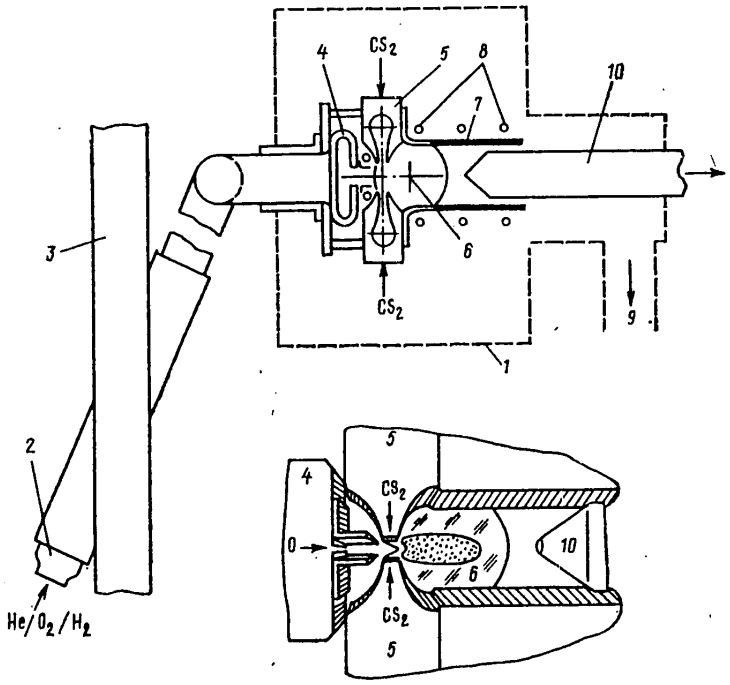

Fig. 5.26. Diagram of chemical laser with dissociation of O_2 in a high-frequency discharge: 1--evacuated space; 2--quartz discharge tube (diameter 2.7 cm, wall thickness 0.1 cm); 3--waveguide; 4--oxygen injector; 5--CS_2 injector; 6--resonator; 7--nozzle; 8--cooling water; 9--evacuation; 10--mass-spectrometer sensor for flow (with orifice on the axis Ø 0.1 mm)

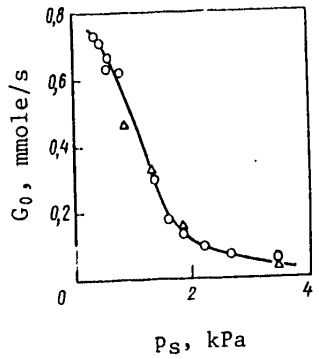

Fig. 5.27. Flowrate of atomic oxygen in the active region as a function of pressure in the cavity: ○--NO_2 inlet after the dissociator; △--NO_2 inlet through the CS_2 injector; W = 1.4 kW; G_{O_2} = 5.6; G_{H_2} = 20.8; G_{He} = 0.0215 mmole/s

the outlet from the discharge tube was the same as at the inlet to the cavity. There was little change in the value of G_0 with increasing O_2 flowrates from 1 to 7 mmole/s, and He flowrates from about 13 to 21 mmole/s.

The injection system shown in Fig. 5.26 included one atomic oxygen injector and two CS_2 injectors arranged transversely to the oxygen injector. The two-dimensional injectors and the system for evacuating the working mixture had a length of 50 cm along the optical axis of the cavity. The brass CS_2 injectors were water-cooled.

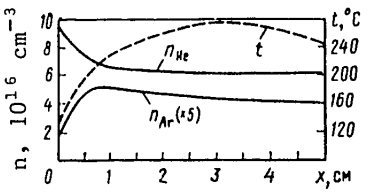

Fig. 5.28. Distribution of Ar and He concentrations along the direction of circulation in the chemical laser

The density profiles of the flows of working gases were measured by a mass-spectrometric unit in which the sensor could be shifted along the direction of circulation of the gas (x-axis). Fig. 5.28 shows the measured distributions of Ar and He concentrations along the direction of circulation. The point of intersection of injected flows of O and CS_2 was taken as the zero point. Also shown is the distribution of temperature of the gas mixture. The temperature was measured by a thermocouple placed 2 cm away to the side of the mass-spectrometer sensor. Since Ar was used as a diluent of the CS_2 stream, and He was contained in the O/O_2 flow, the density profiles of the flows of Ar and He could be used to determine the degree of intermixing of the primary (O/O_2/He) and secondary (CS_2/Ar) flows. It can be seen from Fig. 5.28 that complete intermixing of these flows under the conditions of the experiment had already been attained at a distance of about 0.9 cm.

Excited CO* molecules in a continuous chemical laser operating on an $O/O_2/CS_2$ mixture are formed in reactions already considered in section 5.1:

$$O + CS_2 \rightarrow CS + SO; \quad (5.5)$$

$$O + CS \rightarrow CO^* + S. \quad (5.4)$$

Since the working mixture of gases usually contains a large amount of molecular oxygen, sulfur is quickly oxidized:

$$S + O_2 \rightarrow SO + O. \quad (5.6)$$

In analysis of the chemical kinetics of such a mixture of reagents and modeling of chemical lasers based on a mixture of $O/O_2/CS_2$, it is usually only reactions (5.4)-(5.6) that are considered. Sometimes the reaction

$$SO + O_2 \rightarrow SO_2 + O, \quad (5.24)$$

is also taken into consideration, but estimates have shown that the rate of this reaction at $T \cong 500$ K is considerably less than the rate of other reactions.

In order to determine which reactions take place in the active medium of a chemical laser operating on a mixture of $O/O_2/CS_2$, a mass spectrometer was used in Ref. 56

to study the composition of the working gas mixture in operation of a chemical laser under optimum excitation conditions. Measurements were made at the point x = 1.5 cm.

Mass-spectrometric and flowrate studies of the composition of the working gas mixture led to the following conclusions: 1) CS_2 is efficiently converted to CO in the reagent system used; 2) reactions in which SO_2 and S_2O molecules are formed take place quite rapidly; 3) reactions in which SO molecules participate take place intensively in the gas mixture.

The optimum parameters of the investigated subsonic CO chemical laser with microwave initiation of the reaction are given in Table 5.2

TABLE 5.2

Optimum parameters of subsonic CO chemical laser [Ref. 56]

Parameter	Cavity with opaque mirrors	Cavity with pervious output mirror
Power, watts	28.2	22.0
Flowrates of $O_2/He/CS_2/N_2O$, mmole/s	5.59/19.9/0.58/3.11	12.6/21.5/0.50/4.0
Total mass flowrate, g/s	0.44	0.70
Specific power, J/g	65.5	31.4
Chemical efficiency, %	21.1	18.7

Here the power for a cavity with opaque copper mirrors was determined from the heating of the mirrors, and the chemical efficiency was calculated from the expression

$$\eta_x = \frac{W_{out}}{G_{CS_2} \Delta H_e f_v}, \tag{5.25}$$

where W_{out} is the power expended on excitation of vibrational levels of CO; G_{CS_2} is the flowrate of CS_2 [mole/s]; $\Delta H_e = -356$ kJ/mole is the specific heat of reaction O + CS; $f_V = 0.66$ is the fraction of pumping energy expended on excitation of vibrational levels of CO molecules.

The optimum parameters of a CO chemical laser with transverse pumping can be increased by adding trace gases to the flow [Ref. 56, 59]. The dopant gases are added to the mixture for example through CS_2 injectors. Dopants may produce various effects. First of all, they bind atomic oxygen if their reaction rate with the oxygen atom is of the same order as the rate of the reaction $CS_2 + O$. This is observed for example with addition of OCS. Secondly, dopants may take part in deactivation of CO* molecules. For example, molecules of OCS, NO, N_2O and CO have high rates of V-V exchange with CO molecules. Finally, in this injection system the addition of practically any gas initially at low densities of dopant flow improves intermixing of the reagents, and consequently increases radiation power. At high dopant flow densities the homogeneity of the primary flow of working gases is disrupted, leading to a rapid drop of radiation power. This limits the admissible flow density of inert dopants such as argon.

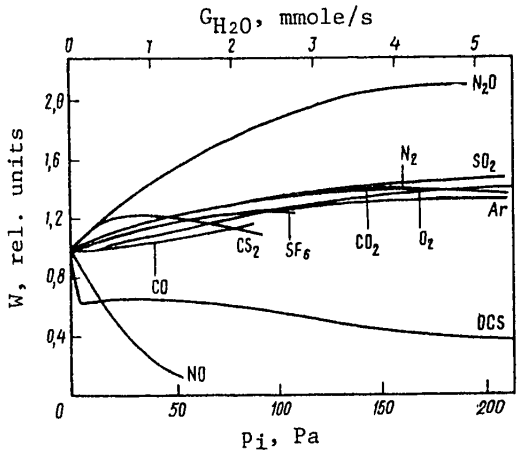

Fig. 5.29. Relative power of stimulated emission as a function of partial pressure of additives of different gases

Fig. 5.29 shows the way that the measured emission power in relative units depends on the partial pressure p_i of different additives.

The gas N_2O was found to be the best additive; radiation power was doubled when this additive was injected into the mixture. The introduction of additives changes the spectral distribution of radiation power by changing the rates of V-V relaxation of CO* molecules excited to different vibrational levels. In collisions

$$\mathrm{CO}(v)+\mathrm{M}\xrightarrow{P_v}\mathrm{CO}(v-1)+\mathrm{M} \tag{5.26}$$

(M is a molecule of additive, P_v is the probability of a collision with energy transfer) there may be either an increase of inversion on transition $v \to v-1$ (without a reduction in the overall population of levels v and v - 1) at $P_v < P_{v-1}$, or a reduction of inversion at $P_v > P_{v-1}$.

Such changes in the distribution of populations of vibrational levels, and consequently in the gains on different transitions are primarily responsible for the observed changes in the lasing spectrum. The overall optical gain when additives are used can be expressed as

$$g(G_M) = g_0|_{G_M=0} + \Delta g^M_{gd}(G_M) + \Delta g^M_{coll}(G_M) + \Delta g^M_{optc}(G_M), \tag{5.27}$$

$$g_0 = \exp(\alpha_0 L) - 1, \tag{5.28}$$

where α_0 is specific gain; L is the length of the amplification region; G_M is the molar flowrate of additive M; Δg^M_{gd}, Δg^M_{coll} and Δg^M_{optc} are the changes in the optical gain due to the action of M on gasdynamic mixing, due to molecular collisions, and due to absorption of radiation by additive M respectively.

In Ref. 59, G_M was taken as the independent variable, and estimates were made of the components in the total optical gain in (5.27). It was found that the term Δg^M_{optc} can be disregarded, and Δg^M_{gd} can be experimentally isolated by injecting an

inert additive with negligible collisional effects into the flow. This also enables determination of the remaining component Δg^{M}_{coll}.

The results of such an estimate [Ref. 59] are shown in Table 5.3, summarizing the influence of a number of gas additives on the gain of a CO chemical laser.

TABLE 5.3

Influence of gas additives on the gain of a CO chemical laser

Additive	Lower levels 3→2-5→4	Intermediate levels 6→5-9→8	Upper levels 10→9-13→12
N_2	*n*	*n*	*n*
SO_2	*n*	*n*	*q*
H_2	*n*	*n*	*q*
HF	*e*	*q—Q*	*Q*
CF_4	*e*	*q—Q*	*Q*
CCl_2F_2	*e*	*e—q*	*Q*
CO	*Q*	*q—e*	*e*
OCS	*Q*	*Q*	*e—Q*
N_2O	*e*	*e—n*	*n—q*
NO	*E*	*e—Q*	*Q*

Notation: n--neutral; e--weak intensification; q--weak inhibition; E--strong intensification; Q--strong inhibition

It can be seen from the table that inversion on lower levels is intensified by additive N_2O, while inversion on intermediate levels is inhibited by additive NO. Another important effect of adding NO shows up in the collisionally induced cascade of population from the upper to the lower levels. This effect is typical of the pumping reaction O+CS in CO chemical lasers.

The graph of Fig. 5.29 and Table 5.3 show that the spectrum of output radiation and the overall output power can be controlled by introducing certain additives in CO chemical lasers. For example N_2O enhances the total output power of chemical lasers with transverse flow by about 50%. Such power enhancement is due to a slight increase in gain on the lower and intermediate energy levels without appreciable quenching on high levels.

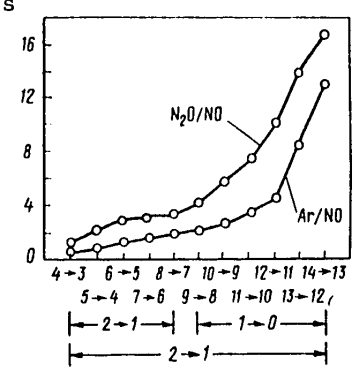

Fig. 5.30. Output power of chemical laser on different transitions with introduction of NO additive

It should be noted that the amplification characteristics of CO chemical lasers are not very sensitive to many gas additives, and this relaxes the requirements for diluents, and expands the range of both diluents and reagents such as those used for fuel of chemical lasers. It is also typical that the total power drops rapidly in a multilevel

cascade chemical laser with a reduction in the length of the cascade [Ref. 59] as can be seen from Fig. 5.30.

§5.3. Flame Lasers

The Flame Model. Flame chemical lasers include devices in which induced radiation is obtained with free combustion of the initial reagents in a flare. This gives a continuous laser on a self-maintained flame. Such a self-maintained system is an example of a purely chemical laser that does not require electric or other power for support of the process except as for a system for feeding the reagents and evacuating the combustion products, or for igniting the flare.

Ref. 60 considers two gases A and B that enter into a chemical reaction with each other after they have been brought into contact in a common space. The reacting mixture is in motion and has a total pressure of some hundreds of Pa. It is assumed that one of the newly produced types of molecules is partly or completely in the excited state. It is further assumed that there are two energy levels corresponding to the reaction

$$\left.\begin{aligned} A + B \xrightarrow{k_1} C_1 + \ldots, \\ A + B \xrightarrow{k_2} C_2 + \ldots, \end{aligned}\right\} \tag{5.29}$$

where k_1 and k_2 are specific rate constants of the second-order reaction, subscripts 1 and 2 denote the lower and upper quantum state of C respectively. The concentration of molecules in states 1 and 2 (n_1 and n_2 respectively) is determined by the radiating transitions characterized by lifetime τ_{12}. The influence of relaxation and damping processes is disregarded.

Approximate solution of the rate equations leads to the following expression for the steady-state population difference, incorporating the characteristic rate constants for the different processes:

$$\left(\frac{n_2 - n_1}{n_0}\right)_{\max} \simeq (f_2 - f_1)\,\frac{\tau_M}{\tau_M + \tau_p} - \frac{1}{\tau_{12}}\left[\tau_M - \tau_p \ln\left(1 + \frac{\tau_M}{\tau_p}\right)\right], \tag{5.30}$$

where n_0 denotes identical initial concentrations of gases A and B; $f_{1,2} = k_{1,2}/(k_1 + k_2)$; $\tau_p = 1/n_0 (k_1 + k_2)$; τ_M is the time over which the difference $n_2 - n_1$ reaches the maximum value. Obviously, population inversion occurs only when $k_2 > k_1$. The pumping conditions can be obtained by comparing the population difference with the threshold conditions

$$n_2 - n_1 \geqslant \Delta N_{\text{vib}} \tag{5.31}$$

where

$$\Delta N_{\text{vib}} = 8\pi c \frac{1-r}{l}\,\tau_{12}\,\omega^2 \frac{\Delta\omega}{\omega} \text{ [Ref. 61]} \tag{5.32}$$

c is the speed of light, ω is the wave number of the transition between C_1 and C_2, $(1 - r)$ and l are determined by the properties of the resonator of the chemical laser. Thus the requirement for the relative reaction rate is defined by the expression

$$f_2 - f_1 \geqslant \frac{\Delta N_{vib}}{n_0} \frac{\tau_p + \tau_M}{\tau_M} + \frac{\tau_p + \tau_M}{\tau_{12}} \left[1 - \frac{\tau_p}{\tau_M} \ln\left(1 + \frac{\tau_M}{\tau_p}\right)\right]. \quad (5.33)$$

If we assume that the parameters of the system are $\omega = 2 \cdot 10^3$ cm^{-1}, $\Delta\omega/\omega = 10^{-6}$, $1 - r = 10^{-2}$, $l = 10$ cm, $\tau_{12} = 10^{-2}$ s, $n_0 = 10^{16}$ cm^{-3}, $\tau_M = 10^{-3}$ s, then τ_p may vary over a range of 10^{-2}-10^{-4} s without causing great changes in pumping conditions, i. e. the $f_2 - f_1$ vary from $6 \cdot 10^{-2}$ to $9 \cdot 10^{-2}$. The reaction rate constants associated with these values of τ_p have values of 10^{-14}-10^{-12} cm^3/s, or 10^7-10^9 (mole·s)$^{-1}$.

To bring about conditions under which stimulated emission from a flame becomes possible, it is important to have detailed data on the magnitude of absorption for different states of the flame. An oxyacetylene flame was considered as the flame quantum system in Ref. 69. It is well known that the reaction zone of this flame emits in the visible and ultraviolet regions of the spectrum, part of this emission being chemical rather than thermal [Ref. 62]. The studies were done on low-pressure oxyacetylene flames burning at pressures of 0.1-2 kPa. Particular attention was given to determination of the population of energy levels of such components as C_2 and CH. At a total pressure of 0.66 kPa, absorption bands (0-0) and (1-1) of C_2 were observed together with five bands of the (1-0) sequence. The lower limits for the absorption coefficients were calculated:

$$(0—0),\ 7 \cdot 10^{-4}\ \text{см}^{-1};\ (1—1),\ 2 \cdot 10^{-4}\ \text{см}^{-1};\ (1—0),\ 2 \cdot 10^{-4}\ \text{см}^{-1};$$
$$(2—1),\ 3 \cdot 10^{-4}\ \text{см}^{-1};\ (3—2),\ 3 \cdot 10^{-4}\ \text{см}^{-1};\ (4—3),\ 2 \cdot 10^{-4}\ \text{см}^{-1};$$
$$(5—4),\ 1 \cdot 10^{-4}\ \text{см}^{-1}.$$

Observation of higher vibrational components, in particular of the (1-0) sequence, showed a greater degree of vibrational excitation of the $X'^3\Pi_u$ state of C_2 under the selected conditions of the experiment. The same is implied by the distribution of intensity in sequence (1-0) with observation of radiation from the $A^3\Pi_g$ state.

Absorption for CH is obtained in the region of 430 nm. The effect is very slight, and depends in large measure on the state of the flame. In Ref. 53 an experimental determination was made of optical gain of a freely burning oxyacetylene flame in the pressure range of 0.4-2 kPa, the lower pressure limit being determined by the conditions of flame cutoff, and the upper limit--by the conditions of reduction in flare volume, increase of energy release and so on.

It was established by the measurements that amplification of radiation takes place directly in the flame front in some optimum range of flare parameters. It was shown that in the oxyacetylene flame an appreciable part of the CO is produced in the nonthermal vibrationally excited state. This agrees with the results of studies of the kinetics of the oxygen-acetylene reaction in Ref. 64-66. However, in Ref. 63 lasing was not achieved in an oxyacetylene flame since not a single transition had a gain greater than the losses in the cavity, equal to about 5%. Obviously a more promising mixture is CS_2/O_2, which was used for the first flame chemical lasers [Ref. 67].

Examples of Realization of Flame Chemical Lasers. Side by side with the conditions that are conducive to development of flame chemical lasers such as the presence of a self-maintained process and the absence of a need for energy sources, there

are also difficulties. These include the high flame temperature that reduces gain, and the fact that only a few of the large number of high-temperature chemical reactions participate in the mechanism of pumping of upper energy levels.

Besides, the rates of propagation of fuel-oxygen flames are unusually slow--from a few centimeters to several meters per second, and because of this there is a limit for increasing the volumetric efficiency of flame chemical lasers. Nonetheless, flame lasers are attractive for simplicity of construction, zero or small expenditures of energy from an outside source, since branched chain reactions are realized in the chemical laser itself. Such reactions maintain the equilibrium concentration of intermediate active centers, making up their losses from the flame due to diffusion and reactions that take place in the flame itself. The rates of these branched chain reactions to a considerable extent determine the success of using a specific system as a flame chemical laser. In making a flame laser, it is usually desirable for the chain reactions to be as rapid as possible and to have minimum activation energies.

The possible reactions in a CS_2/O_2 flame at low pressure [Ref. 67] are analogous to (5.4)-(5.6), (5.24).

To achieve lasing, as has already been pointed out, a high temperature is undesirable as this reduces amplification and is conducive to relaxation within the flame itself. Since the degree of impact relaxation depends strongly on the rate of flame propagation, which determines the time of interaction of molecules, and consequently the number of collisions within the resonator of the chemical laser, the most advantageous systems are those with rapid kinetics of all processes, which in turn presupposes a high rate of propagation.

To reduce the temperature and impact relaxation rate in the flame, it is desirable to work at lower pressures. The results of experiments with chemiluminescence at an overall pressure of 66-80 Pa in a CS_2/O_2 flame were reported in Ref. 68, where it was assumed that inversion exists on certain V-R transitions of CO. At higher pressures [Ref. 69] it was found that in a freely burning CS_2/O_2 flame the amplification on V-R transitions of CO in bands 8-7, 9-8, 10-9 amounts to about two percent.

Although the designs of flame chemical lasers differ in details, they are basically quite similar. A general design of such a chemical laser is shown in Fig. 5.31. Burner 1 is installed so that it can be moved vertically in vacuum chamber 3 equipped for cooling 2. Above the burner is a fine-mesh screen 4. Cavity mirrors 5 are placed in the direction of the optical axis passing through the reaction zone. The position of the reaction zone relative to the axis of the cavity is shifted by mechanism 6, enabling measurement of the gain at any flame height. In Ref. 67 the burner was made in the form of a row of parallel tubes. Each tube was 60 mm long and 6 mm in outside diameter, and had 50 orifices

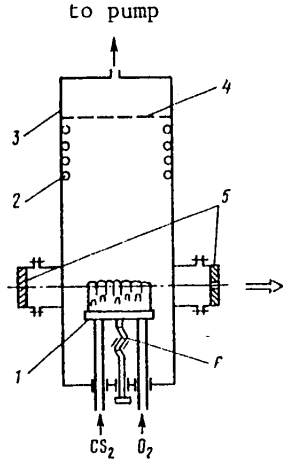

Fig. 5.31. Diagram of flame chemical laser: 1--burners; 2--cooling; 3--evacuated chamber; 4--screen; 5--mirrors; 6--burner shifting mechanism

1 mm in diameter. Alternate tubes injected CS_2 and O_2. The dielectric mirrors of the resonator had reflectivity of 99.2%. Emission was coupled out through a 0.5 mm hole in one of the mirrors. Estimates gave total losses of no more than 3% in the resonator. The output radiation was modulated by a frequency of 150 Hz and detected by an Au-Ge detector at 77 K. Measurements were made by a tunable amplifier. A CO_2 electric-discharge laser was set up inside the cavity outside of the flame zone. With this laser switched on, the cavity was tuned and the amplification was measured. A vacuum chamber 120 cm in diameter and 270 cm long was connected to a vacuum pump with capacity of 9 m^3/min. The flame was ignited by a glow discharge located a few cm above the burners. Combustion continued independently after ignition.

At pressures below 266 Pa, the blue luminescence of the flame was diffuse and homogeneous. As the O_2 pressure was increased while holding the CS_2 pressure constant, beginning at a ratio of $p_{CS_2}/p_{O_2} = 0.5$, the flame broke up into several hundred tongues uniformly distributed in the upper part of the burners. To achieve appreciable amplification, the boundaries of the flame had to be raised somewhat, which was accomplished by further increasing the O_2 pressure. Lasing occurred at pressures of O_2 of 1.2 kPa and CS_2 of 80 Pa, the flame being inhomogeneous with signs of some spatial instability. Lasing was interrupted with a slight change in CS_2 pressure by about 13 Pa.

The emission spectrum was determined by a monochromator. Continuous lasing in Ref. 67 was observed on three transitions of CO with wavelengths of 5.216, 5.297 and 5.421 μm. The measured total output power of stimulated emission was 1 mW.

The initial components in flame chemical lasers of the type shown in Fig. 5.31 are mixed either directly in the reaction vessel or in a special mixer installed at the inlet of gases to the burner or in a feed line.

In Ref. 70, nitrous oxide N_2O was added to the reaction mixture of CS_2/O_2 in the flame laser to increase the gain. Different versions of premixing of the components were used: either two of them N_2O/O_2, or all three components $CS_2/O_2/N_2O$. In the case of separate delivery of the N_2O/O_2 mixture and carbon disulfide, the power of coherent radiation was approximately half the level for delivery of the three-component mixture, which is due to inadequate mixing in the reaction region of the resonator cavity.

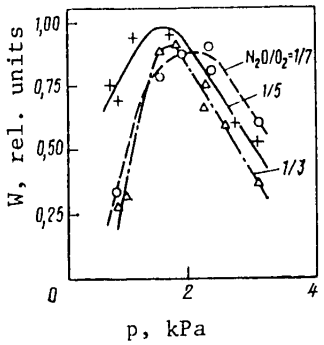

Fig. 5.32. Power W of stimulated emission as a function of pressure in the evacuated chamber

Investigations of the optimum conditions of operation of chemical lasers based on $CS_2/N_2O/O_2$ mixture with respect to pressures and the relative content of components of the reaction mixture have shown that these conditions are similar for a mixture prepared beforehand and held in the mixer for 3-4 hours and for a mixture freshly prepared by mixing the streams in the mixer at the inlet to the burner. For the latter case, Fig. 5.32 shows typical dependences of the power of stimulated emission on the pressure of the mixture in the evacuated chamber. Power maxima lie in a range of 2-2.66 kPa. The reduction of emission power in regions of lower and higher pressures relative to the maximum can be attributed respectively to a reduction in the density of inverse population in the cavity, and an increase in the rates of relaxation processes that equalize the nonequilibrium distribution with respect to vibrational levels of the CO molecules. The dependence of lasing power on the composition of the mixture is characterized by curves with maxima in the region satisfying the ratio

$$\frac{c_{N_2O}}{c_{N_2O/O_2}} \approx 1.10\text{-}0.13 \qquad (5.34)$$

There is also an optimum ratio with respect to CS_2 concentration.

CO chemical lasers typically operate with small additives of N_2O (Fig. 5.33). As N_2O is added to the mixture, the radiation power increases sharply as compared with that in the state $c_{N_2O} = 0$ even at a ratio $c_{N_2O}/c_{O_2/N_2O} = 1/240$, and the power rises nearly linearly upon a further increase in this ratio. The abrupt change in lasing power at low relative concentrations of N_2O, in the opinion of the authors of Ref. 70, cannot be explained by the peculiarities of the mechanism of vibrational exchange of energy [see, for example, Ref. 69]. At such low N_2O concentrations as $(3\text{-}5)\cdot10^{15}$ cm^{-3} the main contribution to vibrational relaxation of CO molecules with concentration of the order of 10^{16} cm^{-3} is from CO-CO collisions in which the probability of exchange of vibrational energy is two to four times as high as in CO-N_2O collisions. It is assumed in Ref. 70 that the abrupt increase in radiation power with small additives of N_2O is due to dissociation of these molecules in the zone of a flame with temperature of the order of 1200 K. Actually, calculation of the equilibrium constant for

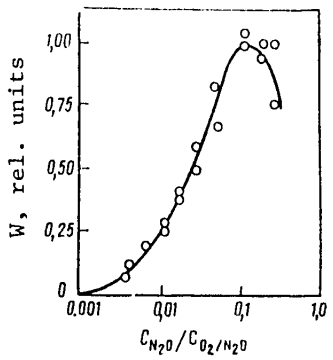

Fig. 5.33. Power of stimulated emission as a function of the relative concentration of N_2O

$$N_2O \rightleftarrows N_2 + O \qquad (5.35)$$

at n_{N_2O} of $3(10^{15}\text{-}10^{17})$ cm^{-3} gives nearly complete dissociation of N_2O molecules at 1000-1200 K. An increase in n_0 intensifies the process of formation of CO* in the course of the reaction

$$CS + O \rightarrow CO^* + S \qquad (5.36)$$

and consequently increases the power of stimulated emission.

Use of a burner with spacing between injection orifices for fuel and oxygen equal to 1.3 mm with special screens provided rapid mixing of gases on its surface [Ref. 71]. A burner of this kind was used in the investigation of working characteristics of a flame laser on CS_2/O_2 and of the way that these characteristics are influenced by additives of He, SF_6, N_2O, CO, CO_2, N_2, SO_2 and NO_2. The resultant dependence of power on CS_2 flowrate is shown in Fig. 5.34. Maximum radiation power of 0.6 W was attained in operation of a chemical laser on a mixture of $CS_2/O_2/N_2O$ with corresponding molar flowrates of 3, 9, 110 and 7.6 mmole/s.

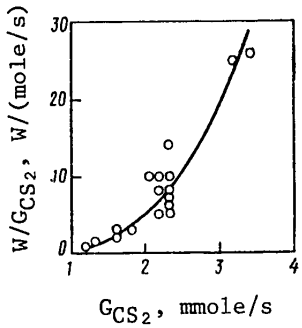

Fig. 5.34. Dependence of power of a flame laser on CS_2 flowrate. Distance of optical cavity from burner 1.1 cm

Considerably higher output radiation powers of flame chemical lasers were obtained in Ref. 72-74--of the order of 10-25 W with specific energy of 13 J/g and chemical efficiency of 2.5%. Powers measured in the tens of watts have also been attained in systems with predissociation of the reagents, and estimates have been made of the parameters and working conditions of plasma chemical lasers in the kilowatt range [Ref. 75].

§5.4. Subsonic Lasers Based on Metal Vapor

When Ba, Ca and Mg are burned in mixtures of $N_2O/He/CO_2$, amplification of emission is observed on the transition 00°1-10°0 of CO_2. On this same transition in Ref. 76, continuous lasing was achieved upon ignition of Mg vapor in a mixture of N_2O/CO_2. Pumping was by the fast exothermic reaction

$$Mg + N_2O \rightarrow MgO + N_2, \qquad (5.37)$$

during which MgO molecules are formed in state $B^1\Sigma$.

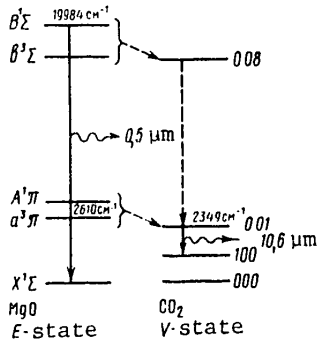

Fig. 5.35. States of MgO and CO_2 with possible E-V transitions

Among the various possible schemes of energy transfer from reaction products to CO_2 molecules, the most probable is the transfer of energy of excited electronic states of the MgO molecule to vibrational levels of the ground electronic state of the CO_2 molecule (E-V transfer). Such a process can take two paths: directly from levels $B^1\Sigma$ and $b^3\Sigma$ to high vibrational levels of CO_2, or after decay of the excited $B^1\Sigma$ state of MgO to state $A^1\Pi$ (3563 cm^{-1}) and subsequent population due to internal conversion of metastable level $a^3\Pi$ (2610 cm^{-1})--to level 00°1 of CO_2 (2349 cm^{-1}). Both possible schemes are shown in Fig. 5.35.

V-V transfer of energy from MgO and N_2 to CO_2 is improbable since the vibrational levels of MgO are about 760 cm^{-1} apart [Ref. 77] and do not coincide with CO_2 levels, and the N_2 molecule formed in the reaction

$Mg + N_2O$ is practically unexcited. Formerly E-V quenching of excited electronic states has been observed in mixtures of Na, Rb, Cs and Hg with H_2, and Na with N_2 [Ref. 78, 79].

The results of measurement of the gain in flames show that a more probable process of E-V transfer is a transition between high levels since the addition of nitrogen increased the gain on transition 00°1-10°0 [Ref. 76]. If excitation had been transferred directly to the upper level, the addition of nitrogen would have meant that a part of the energy would go to level v = 1 of N_2, and the population of level 00°1 should have been reduced. On the other hand, if level 00°1 is populated as a result of V-V relaxation of upper vibrational levels, then all the energy that goes to vibrational levels of nitrogen should in the final analysis reach level 00°1 of CO_2. Consequently an increase in nitrogen content in this case cannot reduce the gain.

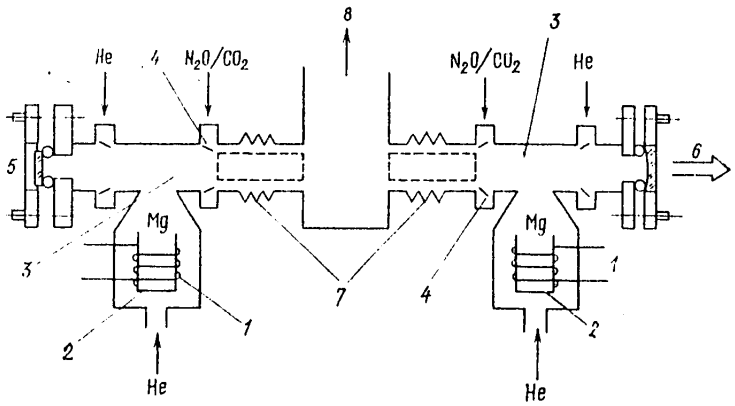

Fig. 5.36. Diagram of metal-vapor flame chemical laser: 1--heaters; 2--crucibles; 3--working tubes; 4--injectors; 5--flat mirror; 6--concave mirror; 7--bellows; 8--evacuation channel

The construction of a subsonic chemical laser based on metal vapor is shown in Fig. 5.36, and in many ways is similar to those used in Ref. 35, 80.

Heating of metallic magnesium in aluminum crucibles 2 (2.5 cm deep, 2.5 cm inside diameter) by tungsten heaters 1 produces Mg vapor that is carried by a stream of He into tube 3. A mixture of CO_2/N_2O is introduced into the Mg/He stream through radially placed injectors 4 at the inlet to the active region. Additional low-intensity streams of helium are introduced into tube 3 close to mirrors 5 and 6 to prevent the reaction products from reaching them. The reaction itself takes place inside stainless steel bellows 7 (inside diameter 1.9 cm, length 7.6 cm). Two such units are connected into a single channel with common exhaust 8.

The cavity is formed by a flat opaque mirror 5 on a silicon substrate, and a concave mirror 6 with reflectivity of 98% on a germanium substrate (dielectric mirrors were used). The mirrors were 12.7 mm in diameter and separated by a distance of 65 cm. The position of the mirrors was stabilized by three Invar rods. Coarse

and fine adjustment of the cavity was provided by gas-discharge excitation of lasing on CO_2 and N_2O respectively in this same tube 3.

The crucibles usually held 1.5 g of Mg each, which was vaporized within 3 minutes at a heater power of 300 W. About 50% of the resultant Mg vapor reached the active region (the rest condensed on the walls), and uniform blue-green chemiluminescence filling the entire cross section of tube 3 arose close to injectors 4. Chemiluminescence in the vicinity of ~0.5 μm corresponding to transition of MgO from state $B^1\Sigma$ to the ground state exists over a length of ~1 cm at a flowrate of 1400 cm/s, and consequently the time of mixing of the gas mixture was ~1 ms. The bellows within which chemiluminescence takes place are practically unheated.

Maximum power of stimulated emission was 5 mW, and was reached under the same conditions where gain was maximum in the absence of mirrors ($\sim 10^{-2}$ cm^{-1}). The maximum was observed at a total pressure in the tube of ~1.33 kPa and with proportions of the partial flowrates of gases of $He/N_2/N_2O/CO_2/Mg = 50/15/15/15/5$.

In Ref. 76 it is noted that many effects that determine the operation of the described chemical laser are still unexplained. For example the rate of deactivation of excited molecules of CO_2 and N_2 by atoms of alkali metals is fairly low, and therefore the only channel of losses in the tube is extraction of radiation through the output mirror. The radiation power should be 0.5 W/cm^3, which corresponds to a yield of one photon on a wavelength of 10.6 μm for every Mg atom that enters the active region. However, considerably weaker lasing is observed in the experiment, which may be a consequence of either resonant absorption of radiation by the thermalized reaction products, or the presence of additional intracavity losses due to scattering of radiation by Mg particles of 1 μm size produced when it evaporates. E-V quenching of luminescence of atoms and molecules that are the products of exothermic chemical reactions determines lasing parameters in other gas mixtures as well. For example, in an $N_2O/CO/Na$ flame the vibrational levels of CO that are resonant with respect to electronic state 3p of the Na atom are nonequilibrium-populated [Ref. 81]; in flash photolysis of mixtures of CO_2/N_2O, CO_2 lasing is observed that is most likely excited by energy transfer from high electronic levels of the NO molecule that is one of the products of photolysis [Ref. 82].

The investigation of chemical lasers excited by E-V transfer is of great interest since it enables us to find molecules such as MgO that are formed in the course of exothermic reactions and store energy on metastable electronic levels. Molecules of this type are the basis for chemical lasers that emit in the visible region of the spectrum. Some problems that are associated with design and development of chemical lasers that radiate in the visible range on electronic transitions, in particular in the process of the gas-phase reaction $Ba + N_2O \rightarrow BaO^* + N_2$ and others are examined in survey articles 83 and 84. Ref. 31, 85 deal with processes in flame chemical lasers with periodically repeated pulses.

REFERENCES

1. Ultee, C. J., "Compact Pulsed HF Laser", REV. SCI. INSTRUM., Vol 12, No 8, 1971, pp 1174-1176; "Premixed CW Electric-Discharge CO Chemical Lasers", APPL. PHYS. LETT., Vol 19, No 12, 1971, pp 535-537.

2. Deutsch, T. F., "molecular Laser Action in Hydrogen and Deuterium Halides", APPL. PHYS. LETT., Vol 10, 1967, pp 234-236.

3. Ultee, C. J., "Pulsed Hydrogen Fluoride Laser", IEEE J. QUANT. ELECTRON., Vol 6, 1970, pp 647-648.

4. Parker, J. H., Pimental, G. C., "Vibrational Energy Distribution Through Chemical Laser Studies: I. Fluorine Atoms Plus Hydrogen or Methane", J. CHEM. PHYS., Vol 51, 1969, pp 91-96.

5. Polanyi, J. C., Tardy, D. C., "Energy Distribution in the Exothermic Reaction $F+H_2$ and the Endothermic Reaction $HF+H$", J. CHEM. PHYS., Vol 51, No 12, 1969, pp 5717-5719.

6. Gordon, Ye. B., Pavlenko, V. S., Moskvin, Yu. L. et al., "Kinetics of Pulsed Chemical CO Laser With Photoinitiation Based on the Reaction of Oxidation of Carbon Disulfide", ZHURNAL EKSPERIMENTAL'NOY I TEORETICHESKOY FIZIKI, Vol 63, No 4, 1972, pp 1159-1172.

7. Pollack, M. A., "Laser Oscillation in Chemically Formed CO", APPL. PHYS. LETT., Vol 8, 1966, pp 237-238.

8. Arnold, S. J., Kimbell, G. H., "Chemical Laser Action in Electrically Pulsed Flowing CS_2-O_2 Mixture", APPL. PHYS. LETT., Vol 15, 1969, pp 351-353.

9. Wittig, C., Hassler, J. C., Coleman, P. D., "Carbon Monoxide Chemical Laser Utilizing a Fast Flow System", APPL. PHYS. LETT., Vol 17, 1970, pp 117-118.

10. Suart, R. D., Kimbell, G. H., Arnold, S. J., "Continuous-Wave Stimulated Emission in Flowing Carbon Disulfide Oxygen Mixtures", CHEM. PHYS. LETT., Vol 5, 1970, pp 519-520.

11. Jeffers, W. Q., Wiswall, C. A., "A Transverse-Flow CO Chemical Laser", APPL. PHYS. LETT., Vol 17, 1970, pp 67-69.

12. Jacobson, T. V., Kimbell, G. H., "Transversely Spark-Initiated Chemical Laser With High Pulse Energies", J. APPL. PHYS., Vol 41, No 13, 1970, pp 5210-5212.

13. Alain, L., Nicole, L. S., "Etude d'un laser a oxyde de carbone forme chimiquement", COMPT. REND. ACAD. SCI., Vol 271, No 25, 1970, pp 1212-1215.

14. Ahlborn, B., Gensel, P., Kompa, K. L., "Transverse-Flow Transverse-Pulsed Chemical CO Laser", J. APPL. PHYS., Vol 43, 1972, pp 2487-2489.

15. Lin, M. C., "Chemical Lasers Produced from $O(^3P)$ Atom Reactions. III. 5 μm CO Laser Emission From the O+CH Reaction", J. Chem. Kinetic., Vol 6, No 1, 1974, pp 1-14.

16. Rosenwaks, S., Smith, I. W. M., "Laser Emission From Carbon Monoxide Formed in the Flash-Initiated Reactions of $O(^3P)$ Atoms With Carbon Monosulfide and Selenide", TRANS. FARADAY SOC., Vol 69, No 9, 1973, pp 1416-1424.

17. Tsuchiya, S., Nielsen, N., Bauer, S. H., "Lasing Action and the Relative Population of Vibrationally Excited Carbon Monoxide Produced in Pulse-Discharged Carbon Disulfide-Oxygen-Helium Mixtures", J. PHYS. CHEM., Vol 77, No 20, 1973, pp 2455-2464.

18. Lin, M. C., "Chemical CO and CO_2 Lasers Produced From the $CH+O_2$ Reaction", J. CHEM. PHYS., Vol 61, No 5, 1974, pp 1835-1843.

19. Tiee, J. J., Quick, C. R. Jr., Harper, C. D. et al., "High-Energy Pulsed CO Chemical Laser", J. APPL. PHYS., Vol 46, No 12, 1975, pp 5191-5193.

20. Orayevskiy, A. N., "Onset of Negative Temperatures During Chemical Reactions", ZHURNAL EKSPERIMENTAL'NOY I TEORETICHESKOY FIZIKI, Vol 45, No 2(8), 1963, pp 177-179.

21. Tal'roze, V. L., "Stimulated Emission of Coherent Induced Radiation in Chemical Reactions", KINETIKA I KATALIZ, Vol 5, No 1, 1964, pp 11-27.

22. Orayevskiy, A. N., "Chemical Laser Based on Branched Reactions", ZHURNAL EKSPERIMENTAL'NOY I TEORETICHESKOY FIZIKI, Vol 55, No 4(10), 1968, pp 1423-1429.

23. Batovskiy, O. M. et al., "Chemical Laser Operating on Branched Chain Reaction of Fluorine With Hydrogen", PIS'MA V ZHURNAL EKSPERIMENTAL'NOY I TEORETICHESKOY FIZIKI, Vol 9, No 6, 1969, pp 341-343.

24. Basov, N. G., Kulakov, L. V., Markin, Ye. P. et al., "Emission Spectrum of Chemical Laser on Mixture H_2+F_2", PIS'MA V ZHURNAL EKSPERIMENTAL'NOY I TEORETICHESKOY FIZIKI, Vol 9, No 11, 1969, pp 613-617.

25. Hess, L. D., "Pulsed Laser Emission Chemically Pumped by the Chain Reaction Between Hydrogen and Fluorine", J. CHEM. PHYS., Vol 55, 1971, pp 2466-2473.

26. Basov, N. G., Galochkin, V. T., Igoshin, V. I. et al., "Spectra of Stimulated Emission in Hydrogen-Fluorine Reaction Process and Energy Transfer From DF to CO_2", APPL. OPTICS, Vol 10, No 8, 1971, pp 1814-1820.

27. Dolgov-Savel'yev, G. G., Polyakov, V. A., Chumak, G. M., "Stimulated Emission in the 2.8 μm Region on Vibrational-Rotational Transitions of the HF Molecule", ZHURNAL EKSPERIMENTAL'NOY I TEORETICHESKOY FIZIKI, Vol 58, No 4, 1970, pp 1197-1203.

28. Basov, N. G., Markin, E. P., Nikitin, A. I. et al., "Branching Reactions and Chemical Lasers", IEEE J. QUANT. ELECTRON., Vol QE-6, 1970, pp 183-184.

29. Galochkin, V. T., Zavorotnyy, S. I., Kosinov, V. N. et al., "Investigation of the Characteristics of a Chemical HF Laser Excited by Emission of a Pulsed CO_2 Laser", KVANTOVAYA ELEKTRONIKA, Vol 3, No 1, 1976, pp 125-130.

30. Krogh, O. D., Pimental, G. C., "Chemical Lasers From the Reactions of ClF and ClF_3 With H_2 and CH_4: a Possible Chain-Branching Chemical Laser", J. CHEM. PHYS., Vol 56, No 2, 1972, pp 969-975.

31. Woodroffe, J. A., Limpaecher, R., "Pulsed H_2-F_2 Laser Flame-Out", APPL. PHYS. LETT., Vol 30, No 4, 1977, pp 195-196.

32. Bashkin, A. S., Orayevskiy, A. N., Tomashev, V. N. et al., "Chemical CO Laser on $CS_2 + O_3$ Mixture With Photoinitiation", KVANTOVAYA ELEKTRONIKA, Vol 3, No 2, 1976, pp 362-368.

33. Lacina, W. B., Mann, M. M., "Transient Oscillator Analysis of a High-Pressure Electrically Excited CO Laser", APPL. PHYS. LETT., Vol 21, No 5, 1972, pp 224-226.

34. Cool, T. A., Stephens, R. R., Falk, T. J., "A Continuous-Wave Chemically Excited CO_2 Laser", INT. J. CHEM. KINETICS, Vol 1, 1969, pp 495-497.

35. Cool, T. A., Falk, T. J., Stephens, R. R., "DF-CO_2 and HF-CO_2 Continuous-Wave Chemical Laser", APPL. PHYS. LETT., Vol 15, 1969, pp 318-320.

36. Basov, N. G., Mikhaylov, V. G., Orayevskiy, A. N., Shcheglov, V. A., "Thermal Methods of Laser Excitation", ZHURNAL TEKHNICHESKOY FIZIKI, Vol 37, No 2, 1967, pp 339-348.

37. Cool, T. A., Stephens, R. R., "A Chemical Laser by Fluid Mixing", J. CHEM. PHYS., Vol 51, 1969, pp 5175-5176.

38. Cool, T. A., Shirley, J. A., Stephens, R. R., "Operating Characteristics of a Transverse-Flow DF-CO_2 Purely Chemical Laser", APPL. PHYS. LETT., Vol 17, 1970, pp 278-281.

39. Shirley, J. A. et al., "Purely Chemical Laser Operation in the HF, DF, HF-CO_2 and DF-CO_2 Systems", AIAA PAPER, No 27, 1971, p 9.

40. Cool, T. A., "The Transfer Chemical Laser: a Review of Recent Research", IEEE J. QUANT. ELECTRON., Vol QE-9, No 1, 1973, pp72-83.

41. Brunet, H., Mabru, M., "Etude d'un laser chemique DF-CO_2 utilisant un ecoulement gazeux transversal", COMPT. REND. ACAD. SCI., Vol 272, 1971, pp 232-235.

42. Cool, T. A., Stephens, R. R., "Efficient Purely Chemical CW Laser Operation", APPL. PHYS. LETT., Vol 16, 1970, pp 55-58.

43. Basov, N. G., Gromov, V. V., Koshelev, Ye. L. et al., "DF-CO_2 CW Laser", PIS'MA V ZHURNAL EKSPERIMENTAL'NOY I TEORETICHESKOY FIZIKI, Vol 13, 1971, pp 496-498.

44. Anlauf, K. G., Kuntz, P. T., Maylotte, D. H. et al., "Energy Distribution Among Reaction Products", DISCUSS. FARADAY SOC., Vol 44, 1967, pp 183-193; "Vibrational Population Inversion and Stimulated Emission From the Continuous Mixing of Chemical Reagents", PHYS. LETT., Vol 24A, No 4, 1967, pp 208-210.

45. Wang C. P., "Frequency Stability of CW HF Chemical Laser", J. APPL. PHYS., Vol 47, No 1, 1976, pp 221-223.

46. Wang, C. P., Varwing, R. L., "Longitudinal Mode Beat Intensities in a CW HF Chemical Laser", APPL. PHYS. LETT., Vol 29, No 6, 1976, pp 345-347.

47. Hinchen, J. J., Banas, C. M., "CW HF Electric Discharge Mixing Laser", APPL. PHYS. LETT., Vol 17, No 9, 1970, pp 386-388.

48. Hirose, Y., Hassler, J. C., Coleman, P. D., "A CW CO Chemical Laser From the Reaction of Active Nitrogen With $O_2 + CS_2$", IEEE J. QUANT. ELECTRON., Vol QE-9 No 1, 1973, pp 114-116.

49. Ultee, C. J., Bonczyk, P. A., "Performance and Characteristics of a Chemical CO Laser", IEEE J. QUANT. ELECTRON., Vol QE-10, No 2, 1974, pp 105-110.

50. Spencer, D. J., Beggs, J. A., Mirels, H., "Small-Scale CW HF(DF) Chemical Laser", J. APPL. PHYS., Vol 48, No 3, 1977, pp 1206-1211.

51. Stephens, R. R., Cool, T. A., "A Continuous-Wave Chemical Laser for Laser-Induced Fluorescence Studies", REV. SCIENT. INSTRUM., Vol 42, No 10, 1971, pp 1489-1494.

52. Rosen, D. I. Sileo, R. N., Cool, T. A., "A Spectroscopic Study of CW Chemical Lasers", IEEE J. QUANT. ELECTRON., Vol QE-9, No 1, 1973, pp 163-167.

53. Gagne, J. M., Mah, S. Q., Conturie, Y., "Transverse-Flow Quasi-CW HF Chemical Laser: Design and Preliminary Performance", APPL. OPTICS, Vol 13, No 12, 1974, pp 2835-2839.

54. Glaze J. A., Finzi, J., Krupke, W. F., "A Transverse Flow CW HCl Chemical Laser", APPL. PHYS. LETT., Vol 18, 1971, pp 173-175.

55. Glaze, J. A., "Gain and Spectral Characteristics of a CW HF/DF Chemical Laser", APPL. PHYS. LETT., Vol 19, No 5, 1971, pp 135-136.

56. Jeffers, W. Q., Wiswall, C. E., "Experimental Studies of the $O/O_2/CS_2$ CW CO Chemical Laser", IEEE J. QUANT. ELECTRON., Vol QE-10, No 12, 1974, pp 860-869.

57. Suart, R. D., Dawson, P. H., Kimbell, G. H., "CS_2/O_2 Chemical Laser: Chemistry and Performance Characteristcs", J. APPL. PHYS., Vol 43, 1972, pp 1022-1032.

58. Foster, K. D., "Initial Distribution of CO From the Reaction $O + CS \rightarrow CO^* + S$", J. CHEM. PHYS., Vol 57, 1972, pp 2451-2455.

59. Jeffers, W. Q., Wiswall, C. E., Ageno, H. Y., "Gas Additive Effects in CO Chemical Lasers", IEEE J. QUANT. ELECTRON., Vol QE-12, No 11, 1976, pp 693-697.

60. Bleekrode, R., Nieuwport, W. C., "Flame Laser: Model and Some Preliminary Experimental Results", APPL. OPTICS, 1965, Suppl. No 2, pp 179-180.

61. Shawlow, A., Townes, C. H., "Infrared and Optical Masers", PHYS. REV., Vol 112, No 6, 1958, pp 1940-1949.

62. Gaydon, K. G., "The Spectroscopy of Flames", London, Chapman and Hall, 1957.

63. Searles, S. K., Djeu, N., "Gain Measurements on CO P-Branch Transition in a C_2H_2-O_2 Flame", IEEE J. QUANT. ELECTRON., Vol QE-9, No 1, 1973, pp 116-120.

64. Clough, P. N., Schwartz, S. E., Thrush, B. A., "Infrared Chemiluminescence From Carbon Monoxide in the Reactions of Atomic Oxygen with Acetylene and Carbon Suboxide", PROC. ROY. SOC., Vol 317A, 1970, pp 575-586.

65. Greek, D. M., Melliar-Smith, C. M., Jonathan, H., "Infrared Emission From the Reaction of Atomic Oxygen With Acetylene", J. CHEM. SOC., Vol 1970A, 1970, pp 646-651.

66. Gutman, D., Matsuda, S., "Shock-Tube Study of the Acetylene-Oxygen Reaction. I. CH ($A^2\Delta \rightarrow X^2\Pi$) Chemiluminescence and CO Production During the Induction Period", J. CHEM. PHYS., Vol 52, 1970, pp 4122-4132.

67. Pilloff, H. S., Searles, S. K., Djeu, N., "CW CO Laser From the CS_2-O_2 Flame", APPL. PHYS. LETT., Vol 19, No 1, 1971, pp 9-11.

68. Foster, K. D., Kimbell, G. H., "Vibrational Population Inversion of CO in a Free-Burning CS_2/O_2 Flame", J. CHEM. PHYS., Vol 53, No 6, 1970, pp 2539-2541.

69. Suart, R. G., Arnold, S. J., Kimbell, G. H., "Power Enhancement of a CO Chemical Laser by the Action of Vibrationally Cool Gases", CHEM. PHYS. LETT., Vol 7, No 3, 1970, pp 337-340.

70. Dudkin, V. A., Librovich, V. B., Rukhin V. B., "Investigation of a Chemical CO Laser Based on a Carbon Disulfide Flame" in: "Khimicheskaya fizika protsessov goreniya i vzryva. Kinetika khimicheskikh reaktsiy" [Chemical Physics of Processes of Combustion and Explosion. Kinetics of Chemical Reactions], Chernogolovka, Institute of Chemical Physics, USSR Academy of Sciences, 1977, pp 13-16.

71. Searles, S. K., Djeu, "Characteristics of a CW CO Laser Resulting from a CS_2-O_2 Additive Flame", CHEM. PHYS. LETT., Vol 12, No 1, 1971, pp 53-56.

72. Linevsky, M. J., Carabetta, R. A., "Continuous-Wave (CW) Laser Power From Carbon Disulfide Flames", APPL. PHYS. LETT., Vol 22, No 6, 1973, pp 288-291.

73. Foster, K. D., Kimbell, G. H., Snelling, D. R., "Near Single-Line Operation of a Free-Burning $CS_2/O_2/N_2O$ Flame Laser With a Nondispersive Optical Cavity", IEEE J. QUANT. ELECTRON., Vol QE-11, No 6, 1975, pp 253-258.

74. Solimeno, S., "Chemical Lasers", PHYS. BULL., Nov, 1974, pp 517-520.

75. Jeffers, W. Q., Ageno, H. Y., Wiswall, C. E., "CO Chain Reaction Chemical Laser. I. Experimental", J. APPL. PHYS., Vol 47, No 6, 1976, pp 2509-2510.

76. Bernard, D. J., "CW Chemical Transfer CO_2 Laser", APPL. PHYS. LETT., Vol 26, No 10, 1975, pp 542-544.

77. Schamps, J., Lefebvre-Brion, H., "Vibrational Relaxation of N_2 and CO_2(001) by Alkali Metal Atoms", J. CHEM. PHYS., Vol 61, No 5, 1974, pp 1652-1657.

78. Lee, P. H. et al., "Direct Observation of Vibrationally Excited Hydrogen Produced by Collisional Energy Transfer From Electronically Excited Sodium, Rubidium, Cesium and Mercury", J. PHOTOCHEM., Vol 2, No 2, 1973, pp 165-172.

79. Krause, H. E., Fricke, J., Fite, M. L., "Excitation of Na D-Line Radiation in Collisions of Sodium Atoms With Internally Excited H_2, D_2 and N_2", J. CHEM. PHYS., Vol 56, No 9, 1972, pp 4593-4605.

80. Benard, D. J., Benson, R. C., Walker, R. E., "N_2O Pure Chemical CW Flame Laser", APPL. PHYS. LETT., Vol 23, No 2, 1973, pp 82-84.

81. Walker, R. E. et al., "Vibrational Disequilibrium in a Low-Pressure Sodium Catalyzed Carbon Monoxide Nitrous Oxide Flame", CHEM. PHYS. LETT., Vol 20, 1973, pp 528-533.

82. Lin, M. C., "Photoexcitation and Photodissociation Lasers. Part I. Nitric Oxide Laser Emissions Resulting from $C(^2\Pi) \rightarrow A(^2\Sigma^+)$ and $D(^2\Sigma^+) \rightarrow A(^2\Sigma^+)$ Transitions", IEEE J. QUANT. ELECTRON., Vol QE-10, No 6, 1974, pp 516-521.

83. Jones, C. R., Broida, H. P., "Chemical Lasers in the Visible", LASER FOCUS, Vol 10, No 3, 1974, pp 37-47.

84. Benard, D. J., "Sensing Chemically Excited Metastable Populations by CO_2 Laser Gain Measurements" in: "Electron Transit Lasers", Cambridge Massachusetts, London, MIT Press, 1976, pp 60-67.

85. Limpaecher, R., Woodroffe, J. A., "Flameout in Repetitively Pulsed Chemical Lasers", AIAA JOURN., Vol 15, No 11, 1977, pp 1612-1616.

CHAPTER 6: SUPERSONIC CHEMICAL LASERS

§6.1. Diffusion Chemical Lasers With Thermal Initiation of the Reaction

Working Principles and Design Diagrams of Supersonic Chemical Lasers. Feasibility studies were done in Ref. 1-10 on achieving inverse population in gases by thermal methods of excitation: rapid heating or rapid adiabatic cooling. In particular, it was shown in Ref. 6-10 that a high-velocity flow of a two-component gas mixture in a Laval nozzle can be used to get inverse population of molecules for operation of a cw laser in the infrared range. If the components used in the mixture are capable of chemical reaction, then gas dynamics, chemical reaction and optical radiation, and convective transfer as well when the components are preseparated, can convert the energy of the chemical reaction to energy of excitation of molecules.

In supersonic flows, it is possible to bring about conditions for the most efficient conversion of the energy of the chemical bond to energy of coherent induced radiation with fairly high rates of transfer of components into the reaction zone and with weak reverse diffusion out of the reactive zone and low collisional deactivation in the active medium for the time preceding stimulated emission. The production of such flows in turn requires high-temperature heating of the gas mixture, which can be utilized at the same time for dissociation of the medium into chemically active centers, i. e. for thermal initiation of a reaction in supersonic chemical lasers.

Here as well, just as in the case of subsonic chemical lasers, the chemical reaction can also be initiated by the process of combustion, electric discharge, such as a

microwave induction discharge, or shock-wave initiation. The design peculiarities of the chemical laser determine which methods of initiating the chemical reaction will be used in processes that take place in supersonic chemical lasers.

The working principle of a supersonic diffusion chemical laser with thermal initiation of the chemical reaction is based on sequential realization of the following processes:

heating of the heat-transfer fluid to a temperature that ensures the required degree of dissociation of the chemical reagent;

mixing of the chemical reagent with the heat-transfer fluid, and dissociation of this reagent into chemically active centers in the mixing process;

acceleration of the mixture of heat-transfer fluid and chemically active centers to supersonic velocity;

injection and diffusion of fuel molecules into the supersonic mixture flow that enter into a pumping reaction with the chemically active centers that are in the flow;

excitation in a downstream resonator of the process of stimulated emission by the active molecules formed in the pumping process.

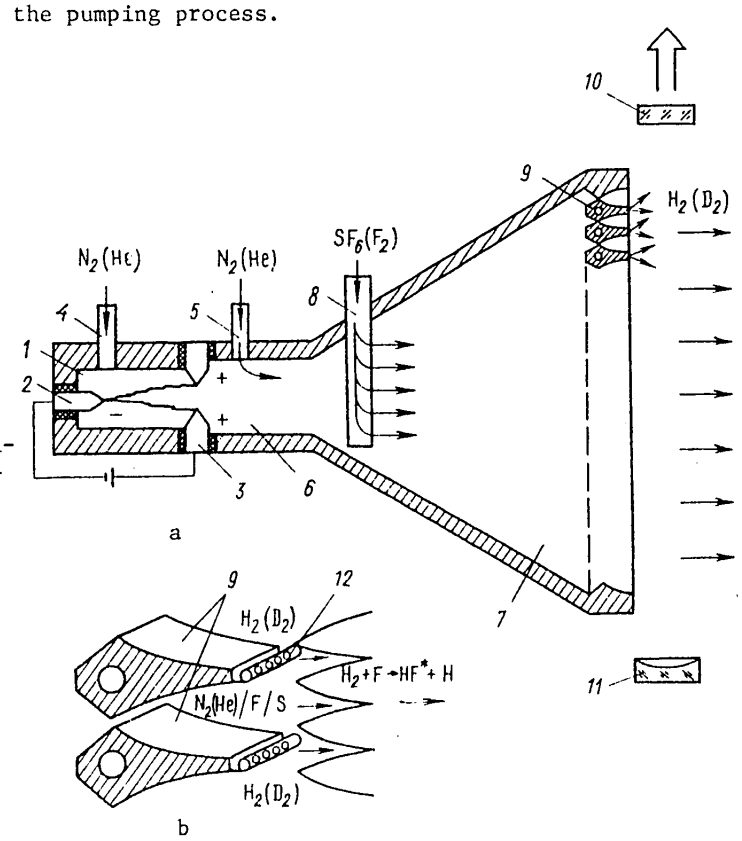

Fig. 6.1. Diagram of supersonic chemical laser with thermal initiation of the reaction: a--laser construction; b--element of nozzle array and flow scheme; 1--electric discharge chamber; 2--cathode; 3--anode; 4--inlet for heat-transfer gas; 5--auxiliary coolant injector; 6--secondary chamber; 7--expansion head; 8--injector of chemical reagent (oxidant); 9--supersonic nozzle module; 10--semitransparent or apertured mirror for extraction of radiation; 11--opaque mirror; 12--fuel injector

These processes are realized for example in the supersonic diffusion chemical laser design shown schematically in Fig. 6.1 [Ref. 11-13]. In this cw laser with thermal initiation of the reaction, N_2 or He is heated by an electric arc and then mixed with SF_6 producing dissociation that results in F atoms in expansion head 7 according to reaction (5.1).

Inversion is produced when H_2 or D_2 diffuse into the supersonic flow containing F atoms. As it passes through the nozzle array, the gas is accelerated to supersonic velocities, and H_2 is injected into this stream. In analogy to process (5.1) as a result of the pumping reaction

$$F + H_2 \rightarrow HF(v) + H\ (-134\ \text{kJ/mole},\ v \leqslant 3) \qquad (6.1)$$

vibrationally excited HF is formed. The HF molecules approach the state of thermodynamic equilibrium thanks to induced radiation and processes of collisional deactivation. The latter can be written in the form

$$HF(v) + M \rightarrow HF(v-1) + M; \qquad (6.2)$$

$$HF(v) + M(v') \rightarrow HF(v-1) + M(v'+1), \qquad (6.3)$$

where (6.2) and (6.3) are respectively V-T and V-V collisions. Gasdynamic and energy parameters obtained in chemical lasers [Ref. 12, 13] are summarized in Table 6.1. (Hereafter the subscript "0" denotes gas parameters in an electric discharge chamber, while subscript "j" denotes gas parameters at the outlet from the nozzle module.)

TABLE 1.6

Example of the gasdynamic and energy parameters of a supersonic diffusion chemical laser

$\dot{m}_{SF_6}$, g/s	W, watts	Conditions in prechamber				η_x, %
		T_0, K	$(p_F/p)_0$	G_F, mole/s	$\frac{G_F}{6G_{SF_6}}$	
0,105	90	4150	0,014	0,00431	1,00	15,8
0,203	167	3970	0,0267	0,90833	1,00	15,2
0,297	236	3870	0,0387	0,0122	1,00	14,7
0,400	293	3660	0,0513	0,0164	1,00	13,5
0,505	357	3510	0,0639	0,0207	1,00	13,1
0,600	415	3400	0,075	0,0246	1,00	12,8
0,800	514	3200	0,0976	0,0328	1,00	11,9
1,00	586	2920	0,116	0,0396	0,96	11,2
1,25	648	2680	0,135	0,0473	0,92	10,4
1,40	692	2580	0,145	0,0515	0,90	10,2
1,60	722	2480	0,153	0,0548	0,83	10,0
1,80	738	2400	0,155	0,0555	0,75	10,1
2,00	732	2360	0,156	0,0560	0,68	9,9
2,20	710	2320	0,157	0,0564	0,62	9,7

Constant conditions were: $\dot{m}_{N_2} = 8.5$ g/s, $\dot{m}_{H_2} = 1.0$ g/s, $p_0 = 0.166$ MPa, beam power 42.5 kW, Mach number $M_j = 4.4$,

$$T_j = 0{,}205\ T_0;\ p_j = 3{,}92 \cdot 10^{-3}\ p_0;\ u_j = 2{,}03 \cdot 10^3 \times$$

$$\times (T_0/2500)^{1/2}\ \text{m/s};\ (c_F)_j = 1{,}55 \cdot 10^{-7} \cdot (p_F/p)_0\ (2500/T_0)\ \text{mole/cm}^3.$$

In order to get efficient conversion of the energy of the chemical bond to energy of coherent induced emission it is necessary that the rate at which H_2 diffuses into the flow, and the rate of pumping reaction (6.1) must be greater than the rate of collisional deactivation (6.2), (6.3). These rates can be estimated

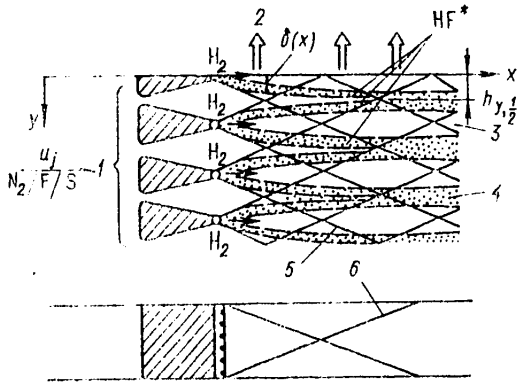

Fig. 6.2. The process of supersonic diffusion of fuel: 1—supersonic nozzles; 2—stimulated emission; 3—hydrogen-filled space; 4—region of mutual diffusion of components; 5—shock waves formed by the chemical reaction; 6—shock waves reflected from the walls

representing the flow in the H_2 diffusion region as shown in Fig. 6.2, where $\delta(x)$ is the boundary of the diffusion region in the y-direction. For laminar flow we have the relation

$$\delta = k_l (Dx/u_j)^{1/2}, \tag{6.4}$$

where k_l is a constant of the order of unity. When H_2 diffuses into N_2,

$$D = 15.8 \cdot 10^{-4}\, T_j^{3/2}\, p_j^{-1} \text{ m/s} \tag{6.5}$$

(T_j is in K, p_j is in Pa). Let $h_{y,\frac{1}{2}}$ be the half-width of the flow (see Fig. 6.2) in the characteristic diffusion length $x = L_D$ will correspond to $\delta = h_{y,\frac{1}{2}}$ and we get from equations (6.4), (6.5), expressing u_j in terms of the Mach number M_j:

$$\frac{T_j p_0}{T_0 p_j}\left(\frac{\mu}{28}\right)^{1/2}\left(\frac{k_l}{2}\right)^2 \frac{T_0}{2500}\left(\frac{10^4}{p_0}\right) h_{y,1/2}^{-2} L_D \sim M_j, \tag{6.6}$$

where μ is molar mass.

As the reagents are mixed at $x = 0$, the rate of initial development of process (6.1) can be represented as

$$u_j (dc_F/dx)_{x=0} = -(k_f c_{H_2} c_F)_{x=0}. \tag{6.7}$$

The characteristic length of the reaction along the flow is determined by the re-

$$L_R = \left[\frac{c_F}{dc_F/dx}\right]_{x=0}. \tag{6.8}$$

Here L_R is the longitudinal distance that must be covered by the flow for all F atoms to be reacted if the overall reaction rate remains at the original level. If we use a local partial pressure of atoms of F equal to $p_F = 8 \cdot 10^6 c_F T$, then we get from (6.7) and (6.8)

$$\left(\frac{\mu}{28}\frac{1,4}{\gamma}\right)^{1/2}\left[\frac{c_{H_2}}{c_F}\frac{5,0}{M}\frac{p_F}{10^4}\right]_j L_R \sim \frac{T_j^{3/2}}{k_f}. \tag{6.9}$$

The first member includes parameters that characterize the operating conditions of the supersonic diffusion chemical laser, and the second member of (6.9) is the function T_j, where

$$k_f = 12,0 \cdot 10^{13} \exp\left[-1710/(1,987\ T_j)\right]. \tag{6.10}$$

The relations $L_D = f_1(M_j)$ and $L_R = f_2(T_j)$ are used to evaluate L_D and L_R in order of magnitude, assuming that $k_f/k_b \gg 1$ for typical operating conditions of the supersonic diffusion chemical laser. If in this event $L_D/L_R \ll 1$, then it can be assumed that H_2 has been completely diffused into the flow at $x = 0$, and the reaction zone should be treated as in a one-dimensional flow. On the other hand, if $L_D/L_R \gg 1$, the reaction zone is due to diffusion mixing. For typical working conditions of a supersonic diffusion chemical laser with the parameters indicated in Table 6.1, when $T_j = 500$ K, $M_j = 4.4$, it follows [Ref. 12] that $L_D \approx 4$ cm and $L_R \approx 0.4$ cm. This means that the reaction zone is determined by supersonic diffusion of components.

The component mixing pattern depends on the nozzle module design that is used. Fig. 6.3 shows some of the most widely used nozzle configurations. Ref. 14 points out the advantages of nozzle blocks of axisymmetric matrices over slit injectors due to ease of manufacture, better initial mixing characteristics and small size of the nozzle at the outlet (2-3 mm).

Of greatest interest is the investigation of such parameters of the supersonic diffusion chemical laser as power W and chemical efficiency η_x. A study was done in Ref. 12 on the way that these parameters are affected by changes in flowrates of the components of the working mixture and the distance x_c of the optical axis of the cavity from the outlet tip of the nozzle, as well as by various gas additives.

Fig. 4 shows how the chemical efficiency and power of stimulated emission of an HF supersonic diffusion chemical laser depend on mass flowrate $\dot{m}_{SF_6}$ at constant flowrates of N_2 and H_2 and fixed flow

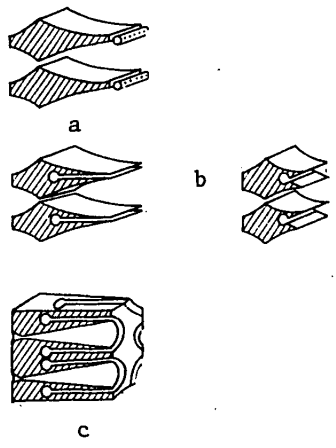

Fig. 6.3. Nozzle designs: a--with perforated tubes; b--with slit feed; c--with annular feed of the component

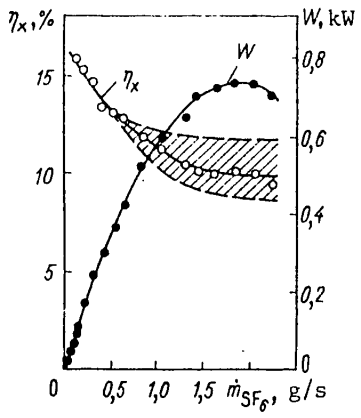

Fig. 6.4. Chemical efficiency and lasing power as dependent on mass flowrate of SF_6 at constant mass flowrates $\dot{m}_{N_2} = 8.5$ g/s and $\dot{m}_{H_2} = 1.0$ g/s

parameters. Power was measured in a cavity with opaque mirrors at $x_c = 1.9$ cm, radius of curvature of the mirrors was 1.15 m, distance between mirrors was 1 m. The chemical efficiency of the supersonic diffusion chemical laser was determined from the relation

$$\eta_x = \frac{W\ (\text{kW})}{133 G_F\ (\text{mole/s})} \cdot 100. \qquad (6.11)$$

Equation (6.11) is the ratio of the actual lasing power to the power that is theoretically attainable on the basis of reaction (6.1). Chemical efficiency decreases from 16 to 8-10% at maximum power. The shaded region in Fig. 6.4 corresponds to the spread of data on chemical efficiency obtained as a result of a large number of experiments. This scatter is due to errors in evaluation of G_F associated with determination of the concentration of SF_6, and errors in determination of the electrical energy transferred to the gas by the arc. At low SF_6 flowrates, such errors are lower since under these conditions the SF_6 is almost completely dissociated, and the flowrate G_F corresponds to the flowrate of SF_6. A reduction in chemical effieicncy with increasing G_F may be due to an increase in HF-HF collisional deactivation.

Lasing power increases with an increase in SF_6 flowrate, and reaches a maximum at $\dot{m}_{SF_6} = 1.8$ g/s. The maximum is due to a lowering of chemical efficiency and a reduction in the dissociation of SF_6 ($G_F/6G_{SF_6}$) at large SF_6 flowrates. At maximum power the flowrate of H_2 is nine times as high as the stoichiometric value required for reaction (6.1), i. e. $G_{H_2}/G_F = 9$. A reduction in the flowrate of H_2 reduces the lasing power due to a corresponding reduction in the rate of diffusion of H_2 into the supersonic flow.

The parameters of the supersonic diffusion chemical laser can also be optimized by changing the materials of the heat-transfer fluid and additives, and their flowrates. Since SF_6 is incompletely dissociated even when lasing power is maximized, the power can be increased by additional injection of oxygen into the high-pressure chamber. For example at $T_0 \sim 2000$ K, $p_0 \sim 0.1$ MPa, another source of fluorine atoms in addition to (6.1) could be the reaction

$$SF_4 + O_2 \rightarrow SO_2F_2 + 2F. \qquad (6.12)$$

In Ref. 15, in addition to investigating the effect of O_2 additives, the authors studied the change in parameters of an HF supersonic diffusion chemical laser when He was substituted for N_2 as the heat-transfer agent. The data found at $x_c = 1.9$ cm (see Fig. 6.4) are compared in Fig. 6.5 with other conditions of operation of the HF supersonic diffusion chemical laser. The comparison shows that adding a small amount of oxygen to the heat-transfer agent increases power emission by 20-30%. Probably this is due to the effect of reaction (6.12). A supersonic diffusion chemical laser with helium as the heat-transfer fluid has higher parameters than

when nitrogen is used. Typically, the use of helium makes the emission powers nearly identical in HF and DF supersonic diffusion chemical laser, whereas when nitrogen is used as the heat-transfer fluid, the maximum power of the DF laser is only 70% compared with that of the HF laser [Ref. 15].

As has already been pointed out, the characteristics of flow chemical lasers are determined by competing processes: formation of excited molecules, interdiffusion of two flows with reagents such as H_2 and F, and deactivation of the excited molecules by collisional processes. It can be assumed that the process of formation of HF* is fast compared with the other two. If the diffusion time is less than the deactivation time, chemical and quantum-mechanical processes must be controlled by the deactivation process, and the processes in the chemical laser are not dependent on mixing. In the case where the deactivation time is less than or comparable with the diffusion time, the quantum-mechanical effect of stimulated emission decreases owing to absorption during the time preciding total expenditure of the reagents.

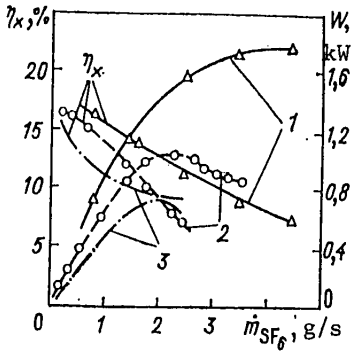

Fig. 6.5. Lasing power and chemical efficiency as functions of the mass flowrate of SF_6

Mixture	$\dot{m}$, g/s	Curves	Ref.
$He/H_2/O_2$	2,06/1,25/0,75	1	[14]
$N_2/H_2/O_2$	8,5/1,0/0,4	2	[12,15]
As in Fig. 6.4		3	[14]

Parameters of a transverse-flow chemical laser with microwave initiation of the reaction increase considerably in an accelerated flow. Fig. 6.6 shows an improvement in a fromer subsonic design made in Ref. 16. Zone A between the microwave discharge region and the H_2 injectors contains a mixture of fluorine atoms, inert gas and products of SF_6 dissociation. Hydrogen accelerated at the nozzle inlet in zone B diffuses quite rapidly into the fluorine jet. A homogeneous mixture of fluorine and molecular hydrogen is formed. Formation of HF(v) occurs in zone C by reaction (6.1). Stimulated emission is coupled out of the cavity with distance of 40 cm between mirrors.

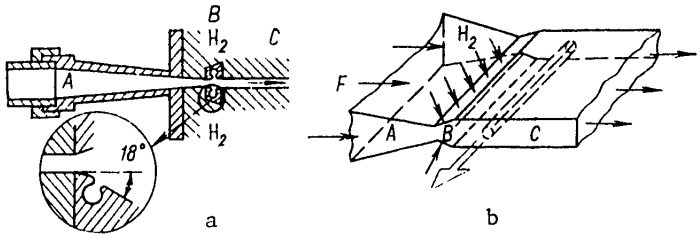

Fig. 6.6. Diagram of working chamber (a) and gas inlet (b) in HF diffusion chemical laser

In such a chemical laser, the power W of stimulated emission increases linearly with an increase in the ionization potentials of the inert gas additives. The higher their ionization potential, the higher will be the average electron energy, and hence the greater the dissociation of SF_6 at inelastic electron collisions in accordance with

$$SF_6 + e \rightarrow SF_i + (6 - i)\,F + 2e \quad (i = 1, \ldots, 6). \tag{6.13}$$

In Ref. 17, this increase in W is attributed to a mechanism of electron-impact dissociation of SF_6 according to which as many as three fluorine atoms are produced from a single electron with kinetic energy close to the ionization potential of He, while only one fluorine atoms is formed from a single electron with kinetic energy close to the ionization potential of Ar. On the other hand, there is a linear relation between W and the injected microwave power. The strong dependence of W on additives of inert gases and the weak dependence on O_2 additive shows that the dissociation of SF_6 with formation of chemically active centers--F atoms--takes place due to electronic collisions. On the other hand, atoms with a metastable state cannot contribute to dissociation when Kr and Ar are used, and their contribution is small in He.

The efficiency of chemical lasers increases considerably in the case of repeated use of chemically active centers such as oxygen atoms as a result of a chain reaction comprising (5.4) and (5.6):

$$\left.\begin{aligned} O + CS &\rightarrow CO^* + S, \\ S + O_2 &\rightarrow SO + O. \end{aligned}\right\} \tag{6.14}$$

Here CS is the fuel, O and S are the active centers.

The efficiency of repeated utilization of each atom in a fuel-oxidant mixture is measured by the average length of the chain

$$l^* = G_{CO}^{end}/G_O^{beg}. \tag{6.15}$$

Here G_{CO}^{end} is the flowrate of CO at the outlet of the cavity, G_O^{beg} is the flowrate of the oxygen atoms that initiate the reaction. In essence, l^* is the average number of cycles of the pumping reaction with participation of an oxygen atom until it is lost in some quenching reaction such as $O + OCS \rightarrow CO + SO$.

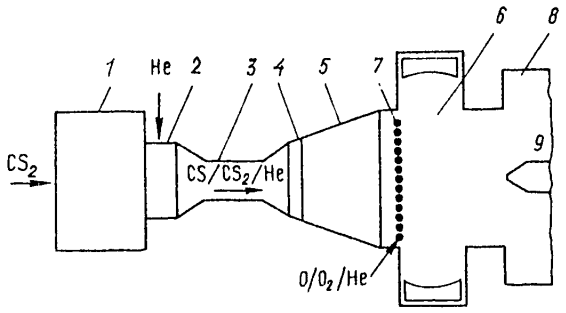

Fig. 6.7. Diagram of CO diffusion chemical laser: 1--electric heater; 2--supersonic nozzle module; 3--supersonic diffuser; 4--annular injector; 5--transition section; 6--resonator; 7--rows of orifices; 8--tubing; 9--mass spectrometer

Chain reaction (6.14) is realized in the experimental facility shown in Fig. 6.7. A stream of CS_2 flows through electric heater 1 in which the CS_2 molecules are

thermally dissociated into CS and S. Heating temperature is about 2400°C. The flowrate of CS reaches 1 mmole/s, and the ratio of molar concentrations of CS and CS_2 at the heater outlet is 2.2. The temperature of the gas flow is reduced and the pressure is increased by injecting helium into the hot CS/CS_2 gas through supersonic nozzle 2, and passing the resultant mixture through supersonic diffuser 3.

At the output of the diffuser is annular injector 4 that enables homogeneous introduction of various dopants into the flow. Before entering cavity 6, the flow passes through transition section 5 with change in cross section from circular to rectangular (height 0.95 cm, length along the optical axis 9.84 cm). In the wedge-shaped region (length along the direction of flow equal to 15 cm), the flow is accelerated and expands from 0.95 to 3 cm.

The pumping reaction is initiated at the inlet to the cavity by injecting a mixture of $O/O_2/He$ into the flow of $CS/CS_2/He$ at sonic velocity through two rows of apertures 7 located opposite each other (diameter of the holes 1.5 mm, distance between centers 2.0 mm, 48 holes in a row). At the outlet from the active region, the gas flow enters a large section of branched tubing 8, the chemical composition of the flow in this region being determined by quadrupole mass spectrometer 9 (the measurement technique is analogous to that used in Ref. 18).

Principles of achieving lasing with the use of low-toxicity reagents that are convenient to handle have been worked out, and the operation of continuous chemical lasers with high flowrate of reagents has been modeled on compact shock-wave chemical lasers as well, for example of the type of a shock tube with supersonic nozzle and mixing of the flow at the outlet of this nozzle with fuel injection [Ref. 19]. In a device of this kind (Fig. 6.8) the dissociation of oxygen takes place in three-section tube 1 behind the shock wave reflected from the constriction at the inlet to nozzle 2.

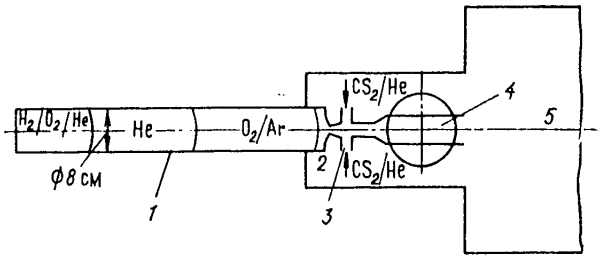

Fig. 6.8. Diagram of chemical laser with shock-wave initiation of the reaction:
1--three-section tube; 2--nozzle; 3--injector; 4--cavity; 5--receiver

The supersonic wedge-shaped nozzle with critical cross section of 0.3 x 70 mm was equipped with injector 3 in its flared section. The flow was ejected into the cavity of resonator 4 communicating with receiver 5.

A mixture of oxygen and argon was admitted to the low pressure chamber separated from the nozzle by a diaphragm. The injected gas, a mixture of CS_2/He was fed through an electromagnetic valve that opened 5 ms after triggering of the shock

tube and had an opening time of less than 0.5 ms. Discharge of the $O/O_2/Ar$ mixture from the shock tube began within 3 ms after opening of the valve. To prevent contamination, the mirrors of the cavity were blown with helium through another solenoid valve synchronized with triggering of the device.

Another shock-wave design of a chemical laser with mixing of reagents was proposed in Ref. 20, where the mixture was heated in the configuration of shock waves reflected from the constriction at the inlet of the supersonic continuous flow to the resonator cavity, with chemical reaction

$$N_2 + CF_3I + Q \rightarrow CF_3 + I^* + N_2. \qquad (6.16)$$

The excited atom of iodine in the vicinity of the resonator produces a photon downstream $I^* \rightarrow I + h\nu$.

The cited examples of shock-wave chemical lasers should be supplemented by the method proposed in Ref. 21 for shock-wave initiation of a reaction, and the attainment within 1.8 ms of continuous operation of a supersonic diffusion chemical laser in reflected shock-wave geometry [Ref. 22] in a mixture of F_2/HCl. In this wave fluorine was partly dissociated $F_2 + M \rightarrow 2F + M$, and then the resultant flow expanded in a nozzle with Mach number $M = 4$. HCl expanded in a nozzle with $M = 2$ to a static pressure identical to this flow. The gas streams were mixed in a two-dimensional diffusion zone with reaction $F + HCl \rightarrow HF^* + Cl$, and the output power was generated in an optical cavity transverse to the flow. The supersonic diffusion chemical laser also uses the pumping reaction $Cl + HI \rightarrow HCl^V + I$. In this case, $\eta_X \approx 3.5\%$ for mixture $He/ClO_2/NO/HI$.

The thermal energy required for a supersonic diffusion chemical laser is also obtained by combustion in a high-pressure chamber [Ref. 23] into which part of the flow of F_2 is injected to react with H_2 and attain a temperature that ensures dissociation of the remainder of the F_2.

An attempt to combine electric heating in a high-pressure chamber with combustion at the nozzle outlet is described in Ref. 24. The action of a discharge temperature of about 6000 K was used to convert N_2 into a stream of active nitrogen in the form of a mixture of vibrationally and electronically excited molecules. This mixture expanded through a nozzle into the reaction chamber at a velocity of up to 15 km/s. The pressure in the chamber was about 1.33 kPa. A bright flame appeared at the nozzle outlet when carbon disulfide was injected into the supersonic flow of active nitrogen. Analysis of the chemiluminescence of radiation of this flame showed a photon yield of 18.5% for CN $A^2\Pi \rightarrow X^2\Sigma^+$ radiation when C_2F_4 was used as the reagent. Estimates in Ref. 24 showed that under conditions of vibrational cooling of the populations of electronically excited states it is possible to attain a positive gain in such a system.

In Ref. 25, a mixture of oxygen and argon was heated to temperatures in the range of 1000-4000 K at a pressure of 20-50 kPa in an electric-discharge chamber and the resultant supersonic flow with oxygen atoms was injected with a $Cs_2/Ar/He$ mixtuer at the nozzle outlet. This ensured efficient production of CO* and lasing in a cavity transverse to the flow with power of 34 W in the band of V-R transitions from 4.9 to 5.7 μm.

The search for substances that are convenient to handle for producing chemically active centers has led in particular to the use of liquid fuels such as toluene ($C_6H_5 \cdot CH_3$) or C_6F_6 that react with NF_3 [Ref. 26]. In such a liquid-fuel supersonic diffusion chemical laser, burning of the reagents produces excited fluorine, which after dilution with helium expands through nozzles from 0.3-1 MPa in the combustion chamber to 0.133-1.33 kPa in the resonator cavity. In the nozzles, the fluorine-containing flow is mixed with the injected deuterium, and the resultant excited molecules of DF* produce lasing of up to 8 kW for 120 s.

§6.2. Supersonic Chemical Lasers With Energy Transfer

A method of getting stimulated emission in the cw mode with an auxiliary component was proposed in Ref. 7, 27. Such a purely chemical laser in which the rapid exchange of reagents enables the use of components that react at a high rate without any initiation was first proposed in Ref. 28. The process is based on the reaction of D_2 (H_2) with F_2 with subsequent transfer of the energy of excitation to CO_2, i. e. the same reaction (5.9) as in the chemical lasers described in §4.1 and §5.2. Examples of other reactions are given in Ref. 29.

The gasdynamic laser described in Ref. 2, 6 is an example of a device that is capable of operation at rather high static pressures in a resonator with the capability of restoring the static pressure to the atmospheric level at the diffuser outlet. In the case of a supersonic chemical laser the use of an analogous open-cycle gasdynamic laser would enable elimination of the complicated system for evacuation of depleted gases that is required for maintaining low pressure in the resonator.

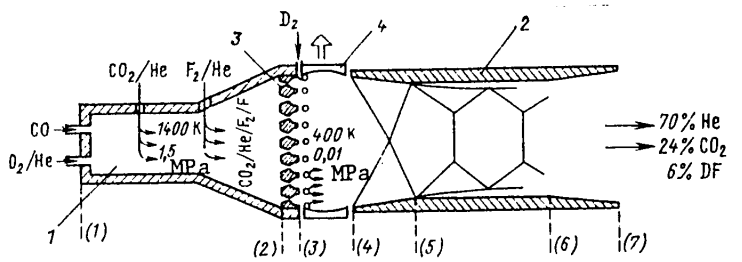

Fig. 6.9. Diagram of supersonic chemical laser with energy transfer: 1--combustion chamber; 2--diffuser; 3--nozzle module; 4--resonator mirrors; figures in parentheses (1)-(7) denote cross sections of the laser channel

The hybrid supersonic chemical laser design described in Ref. 30 (Fig. 6.9) is analogous to the CO_2 gasdynamic laser of Ref. 31 in flow conditions. This design is in principle the same as shown in Fig. 6.1, but the electric-discharge chamber is replaced by combustion chamber 1, and supersonic diffuser 2 is installed at the flow outlet. The flow passes through nozzles 3 and a resonator formed by mirrors 4. Approximately half the gas flowrate is provided by the combustion chamber where CO is burned in helium-diluted oxygen that can reach a temperature of 1400 K at pressure of 1.5 MPa. The hot gases at the outlet to the supersonic nozzle module form a mixture of He, CO_2, F_2 and F. Upon passage through the nozzle, this mixture is accelerated to supersonic velocity, mixed with deuterium and enters the cavity. A pressure of about 8 kPa can be attained in the resonator by selection of the parameters in the nozzle. The diffuser installed after the resonator brings the

static pressure to the atmospheric level. A total output power of stimulated emission of more than 500 W at $\eta_X = 3\%$, specific power of about 30 kW/(kg·s) and pressure in the resonator cavity of $p_c = 3$ kPa was achieved on a small model of a supersonic hybrid chemical laser in Ref. 30.

A large-scale DF/CO_2 chemical laser with energy transfer has been realized in subsonic (IRIS-I) and supersonic (IRIS-II) versions [Ref. 32]. Nitric oxide mixed with carbon dioxide was used as the fuel, and helium-diluted fluorine was the oxidizer. These two versions differ from one another only in the supersonic nozzles in the IRIS-II to accelerate the flow to Mach numbers M = 1.75. Such a Mach number is attained as a result of expansion of 6:1, which is due in turn to the pressure in the combustion chamber and resonator cavity. The pressure in the combustion chamber should be no greater than about 13 kPa to minimize the formation of NOF, which appreciably reduces the output characteristics of chemical lasers, but should be greater than 2kPa in the resonator cavity to support the chemical reactions. The output powers attained in the subsonic and supersonic modes are respectively equal to approximately 5-15 kW at pressure in the cavity $p_c = 8$-4.7 kPa, and 6-7.7 kW at $p_c = 1.8$ kPa.

Thus a considerable constraint on operation of both subsonic and supersonic hybrid chemical lasers is that they are capable of stimulated emission only at resonator pressures below 8 kPa. However, it has been found that a radical change in the current concepts of designs of supersonic chemical lasers and of their operating conditions enables development of chemical lasers with resonator pressures exceeding 27 kPa [Ref. 33]. What distinguishes the design of such a laser from conventional supersonic lasers is that they use a single nozzle rather than a block of many small nozzles, and that the gas in the high-pressure compartment is at room temperature as contrasted with chemical lasers with electric-arc heating or combustion to produce atomic fluorine.

Let us examine in more detail this chemical laser that is so unusual compared with established concepts (see Fig. 6.10). The primary gas flow consists of a mixture of $F_2/CO_2/He$ formed in mixing compartment 1. This primary room-temperature flow passes through grid 2 that is designed for breaking up large-scale eddies in the flow. Downstream is injector 3 for gases NO and D_2 with outlet placed along the axial line of two-dimensional nozzle 4 with ratio of areas of the outlet tip and the critical cross section equal to 1.14. This gives a Mach number of the flow at the nozzle outlet of about 1.5. Dimensions of the outlet tip are 1.488 x 4.445 cm with the longer side in the direction of the axis of cavity 5. The NO/D_2 mixture is injected into the primary flow inside the nozzle through 20 tiny tubes with inside diameter of 0.122 cm and outside diameter of 0.183 cm, each terminating in 17 orifices with diameter of 0.024 cm. These orifices ensure discharge of the gas at a maximum angle of 20° to the direction of the primary flow. The entire unit is made of aluminum and Teflon.

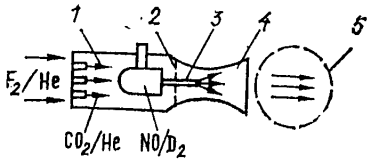

Fig. 6.10. Design of hybrid supersonic chemical laser with elevated pressure in the resonator: 1--mixing compartment; 2--grid; 3--injector; 4--two-dimensional nozzle; 5--resonator

The jet is discharged into the large chamber of the resonator, which is evacuated by a machenical pump. The two gold-coated mirrors were water-cooled and had dimensions of 10 x 10 cm, forming a cavity with opaque mirrors for measuring the power of optical radiation on a wavelength of 10.6 μm.

In the immediate vicinity of the jet are helium feed tubes for preventing strongly absorbent CO_2 (100) in the hot ambient gas from getting into the path of the stable resonator.

A curved mirror was incorporated into the design that could be moved to determine the change in power as a function of the position of the optical axis.

When the NO/D_2 gas is mixed with the primary flow, fluorine atoms are produced in the reaction $F_2 + NO \rightarrow F + NOF$. These fluorine atoms then excite the DF chain considered in detail in §4.1:

$$F + D_2 \rightarrow DF^* (v) + D;\ D + F_2 \rightarrow DF^* (v) + F,$$

and the excited DF(v) pumps the CO_2 to state (001) which then yields the quantum-mechanical effect of stimulated emission. An increase in the efficiency of this effect requires a large CO_2 concentration. Without CO_2, the excited DF is collisionally deactivated too rapidly, and the lasing effect does not arise.

Power measurements using a resonator with opaque mirrors showed some gain of 0.7 cm^{-1}. A power of 1.45 kW was measured in a chemical laser with optical axis located 3.89 cm downstream from the nozzle tip. This power corresponds to $\eta_X = 1.9\%$. Under such conditions, the pressure in the prechamber was 84 kPa, and in the resonator proper--31 kPa. The flow in the jet consisted of 5.29 g/s F_2, 57.8 g/s CO_2, 15.1 g/s He, 1.61 g/s D_2 and 1.53 g/s NO. It should be noted that these mass flowrates, resonator pressure, and position of the optical axis were not the optimum for maximizing power.

Hybrid supersonic chemical laser designs can also be developed on the basis of dissociation of molecular deuterium in a mixture with argon behind a reflected shock wave [Ref. 34]. On the facility shown in Fig. 6.8, lasing was also achieved on a mixture of $D_2/O_3/CO_2$ in the quasi-cw mode. The mixture of $D/D_2/Ar$ obtained behind the reflected shock wave flowed through a flat wedge-shaped supersonic nozzle into the injector, where it was mixed with a subsonic flow of a mixture of ozone, carbon dioxide and helium fed through a solenoid valve. Mixing of the flows led to the basic reactions:

$$D + O_3 \rightarrow OD^* (v) + O_2;$$
$$OD^* (v) + CO_2 (00^00) \rightarrow OD^* (v - 1) + CO_2 (00^01).$$

From the mixing chamber of the injector, the flow entered the region of the resonator with transverse optical axis. The operating time of such a chemical laser was determined by the discharge time of the gas heated behind the reflected shock wave, and amounted to 4.5 ms. Lasing duration was nearly four times as long as the time of existence of the quasi-steady state behind the reflected shock wave front.

Lasing was obtained under the following conditions: initial pressure of the mixture $D_2/Ar = 1/15$ in the low-pressure channel of the shock tube was 9 kPa; velocity of the incident shock wave--1.48 km/s; pressure of the mixture $O_3/CO_2/He = 1/3/17$ in the valve at the instant of beginning of discharge was 50 kPa. The cavity was made up of an opaque spherical mirror with radius of curvature of 3 m coated with gold, and a flat dielectric output mirror with transmission of ~1%.

Under the given conditions, lasing was achieved with peak power of 1.5 W at an average power equal to 0.4 W over 4.5 ms. Control experiments with elimination of deuterium or ozone from the mixtures were done to prove the chemical mechanism of formation of inverse population of CO_2 molecules. Lasing was absent in both cases. Lasing was achieved when hydrogen was substituted for deuterium, although the emission power in this case was considerably weaker.

§6.3. Chemical Gas-Dynamic Lasers

The actual conditions of processes in gasdynamic lasers often result in chemical reactions, depending on the method of producing the working gas and the laser design, especially in cases where the gasdynamic lasers design is optimized by using special mixtures, fuel ignition, gas mixing, and stimulation of certain chemical reactions [Ref. 35]. Chemical gasdynamic lasers may include for example devices in which nonequilibrium chemical combustion reactions form vibrationally excited molecules used as the working medium of gasdynamic lasers [Ref. 36]. For example when CO is burned in air, vibrationally excited CO_2 molecules are formed with vibrational temperatures exceeding the gas temperature. When CO or hydrocarbons are burned, more than 20% of the heat is emitted in the infrared region. Part of this emission is the 4.4 μm V-R band that is used to pump energy to the upper energy level [Ref. 37]. Excited CO_2 molecules may also be formed as a result of additional burning of the mixture in the nozzle. For example, Fig. 6.11 shows a diagram of a cw chemical laser of this type with supersonic flow of material that operates on a chemical reaction with nontoxic products. The device uses the reaction of oxidation of $CO + 0.5O_2$ in a mixture of $CO/0.5O_2/H_2/He$.

The working mixture was admitted to combustion chamber 2, after which it was ignited by a spark. Pneumoelectric valve a enabled admission of the ignited mixture to nozzle 3 at nearly any instant of the ignition process.

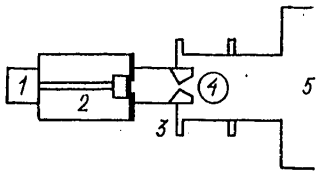

Fig. 6.11. Diagram of chemical combustion laser: 1--pneumoelectric valve; 2--combustion chamber; 3--nozzle; 4--resonator; 5--receiver

The purely gasdynamic mode was studied in addition to the chemical-gasdynamic mode for purposes of comparison. It was found that the power in the former case drops considerably when the combustion chamber is opened on the leading edge of the ignition front, which is responsible for the most intense combustion of the mixture. A drop in power can be attributed to the fact that there is an insufficient amount of CO_2 and the temperature is low on the leading edge in the mixture.

In contrast to the gasdynamic mode, in the chemical-gasdynamic mode the maximum power was realized in just that region where the conditions for thermal pumping

are far from optimum. Maximum power in this case is observed when the combustion chamber is opened on the leading edge of the ignition front where the temperature is 600-900 K. When the chamber is opened on the trailing edge, lasing is absent even at the same temperatures. Thus the given experiment shows that the excited CO_2 molecules are formed due to additional burning of the mixture in the nozzle.

When the resonator axis was moved away from the critical cross section of the nozzle the power reduction was much smoother than in the gasdynamic mode, which can also be explained only by formation of excited CO_2 molecules due to a chemical reaction in the cavity region. The power W_1 of the chemical laser was slightly higher than the power W_2 of the gasdynamic laser ($W_1/W_2 \approx 1.25$) with the same mixture caloricity. The use of chemical reactions for additional pumping of gasdynamic lasers based on products of the reaction of carbon monoxide with nitrous oxide was also studied in Ref. 39. It was shown that the gain in the temperature region of 1500-2000 K is appreciably higher for the reacting mixture than for the premix that simulates the products of the same chemical reaction.

§6.4. Analysis of the Efficiency of Diffusion Chemical Lasers

Particulars of Analysis of Chemical Lasers of Diffusion Type. The energy of the chemical reaction in cw diffusion chemical lasers is only partly used. For example the chemical efficiency of conversion of the energy of reagents to the energy of radiation is no more than 10-20%, and the total efficiency with consideration of expenditures such as those of thermal energy for preparation of the mixture is still rather low: $\eta \leqslant 2$-3%. This is due to the fact that there is an equilibrium store of vibrational energy in the presence of radiation, and this does not permit conversion of the total vibrational energy of the molecules to the energy of a radiation field even in the absence of V-T relaxation. Another factor is rapid relaxation of the working molecules on reaction products and incomplete mixing of the reagents in the resonator cavity during the cycle of stimulated emission. The necessity for simultaneous consideration of these factors considerably complicates theoretical analysis of operation of cw diffusion chemical lasers.

In the supersonic diffusion chemical laser inversion is formed either as a result of direct chemical interaction upon diffusion of a single component like H_2 into a supersonic jet that contains another diluent component (He) [Ref. 15], or as a result of energy transfer to an auxiliary reagent like CO_2 [Ref. 27, 40]. In the diffusion mode the time of convective travel of the reacting particle (τ_{conv}) must be greater than the time of diffusional travel of the particle τ_d, i. e.

$$\tau_{conv} > \tau_d. \tag{6.17}$$

Introducing the Schmidt number Sc and the Reynolds number Re, and assuming [Ref. 41] $\tau_{conv} = l_\parallel/u$, $\tau_d = l_\perp^2/D$, where $l_\parallel$ and $l_\perp$ are characteristic longitudinal and transverse dimensions of the channel, D is the coefficient of diffusion, u is the characteristic flow velocity, we get

$$\mathrm{Sc\,Re} < l_\parallel/l_\perp. \tag{6.18}$$

In the case of a purely diffusional mode we have $\mathrm{ScRe} \ll 1$, i. e. for example $\mathrm{ScRe} \lesssim 0{,}1$.

For continuous lasing it is necessary that the lasing time τ be greater than the transit time of the reagents τ_c, i. e. $\tau > \tau_c = l_\parallel/u$, whence $u > l_\parallel/\tau$.

For the minimum value of $l_\parallel = 1$ cm and $\tau = 10^{-4}$–10^{-5} s, typical of pulsed chemical lasers at pressures of the reagents up to a few kPa we have

$$v > 10^4\text{–}10^5 \text{ cm/s}.$$

As a rule, the longitudinal dimension of the channel is greater than 1 cm, and τ decreases with increasing pressure and specific lasing power. Therefore, successful operation of actual cw chemical lasers requires high-velocity flows of reagents moving at the speed of sound or faster. These high velocities on the one hand create additional technical difficulties associated with the need for having powerful evacuating systems, and on the other hand enable the use of components that react with one another rapidly upon mixing without any initiation.

Besides, efficient operation requires that the time τ_d of mixing of components and the time τ_x of the chemical reaction be less than the time of collisional relaxation τ_p, i. e.

$$\tau_d, \tau_x < \tau_p.$$

For a purely chemical laser operating without preliminary external initiation, suitable from this standpoint are exchange reactions of atoms or radicals with molecules as considered in Chapter 2, but it is more advantageous to use chain reactions such as the $H_2 + F_2$ type, and to introduce additional reagents for the original initiation of the reaction that react with the main component and yield seed atoms or radicals.

Laminar Mixing Model. In theory, the highest efficiency of a supersonic diffusion chemical laser can be realized at comparatively low pressures in the cavity and at low Reynolds numbers, i. e. with laminar flow conditions. However, in actual cw chemical lasers, where high pressures are used, the rate of laminar mixing becomes inadequate to compete with deactivation of excited particles. As a consequence, more rapid--turbulent--mixing becomes desirable. A solution can be found [Ref. 41] for linear differential equations of multicomponent diffusion with consideration of nondiagonal diffusion components:

$$\frac{\partial n_l}{\partial t} + \mathbf{u}\nabla n_l - \sum_{k=1}^{p} D_{lk}\nabla^2 n_k + \alpha_{sl} n_l = 0. \tag{6.19}$$

Here $\vec{u}$ is the mean velocity vector of the flow, α_{si} are the dissipative coefficients, D_{ik} are coefficients of diffusion that are related by Onsager laws.

On the basis of (6.18), the second term in (6.19) can be disregarded for the purely diffusional mode. Besides, when the inequality

$$|\alpha_{sl} - \alpha_{sk}| < \tau_d^{-1} \tag{6.20}$$

is met, which is often the case in practice, we can disregard differences in the dissipative coefficients, and then instead of (6.19) we have

$$\frac{\partial n_i}{\partial t} = \sum_{k=1}^{p} D_{ik} \nabla^2 n_k - \alpha_s n_i. \tag{6.21}$$

This sum of equations is reduced to a system of p independent equations by diagonalization of matrix D. Multiplying the equations of system (6.21) by the elements g_{ij} of auxiliary nonsingular square matrix g, summing with respect to i and substituting subscript k for i in terms with simple summation, we get

$$\frac{\partial}{\partial t} \sum_{k=1}^{p} g_{kj} n_k = \operatorname{div} \operatorname{grad} \sum_{k=1}^{p} n_k \sum_{i=1}^{p} g_{ij} D_{ik} - \alpha_s \sum_{k=1}^{p} g_{kj} n_k, \quad j = 1, 2, \ldots, p. \tag{6.22}$$

Introducing the notation

$$G_j = \sum_{k=1}^{p} g_{kj} n_k, \quad H_j = \frac{1}{g_{kj}} \sum_{i=1}^{p} g_{ij} D_{ik}, \tag{6.23}$$

we get from (6.22)

$$\partial G_j / \partial t = H_j \nabla^2 G_j - \alpha_s G_j. \tag{6.24}$$

The elements of matrix H are found from the condition

$$\det (D_{ik} - H \delta_{ik}) = 0, \tag{6.25}$$

and the solution of system of equations (6.21) is

$$n_i = \sum_{j=1}^{p} g_{ij}^{-1} G_j, \tag{6.26}$$

where the g_{ij}^{-1} are elements of inverse matrix g^{-1}.

Ref. 41 gives the reduction of this problem of multicomponent convective diffusion with consideration of the geometry of the system. It is shown for an HF amplifier of diffusion type that a gain in the output power of a chemical laser is possible with asymmetric injection of reacting molecules.

Turbulent Mixing. The description of macroscopic characteristics of turbulent mixing is based on time-averaged Navier-Stokes equations. Representing each quantity f as a sum of time-averaged $\bar{f}$ and pulsation f' components

$$f = \bar{f} + f' \quad (\bar{f}' = 0), \tag{6.27}$$

we get equations of conservation of mass, momentum, enthalpy of the mixture and mass of an individual component:

$$\partial \bar{\rho} \tilde{u}_j / \partial x_j = 0; \tag{6.28}$$

$$\bar{\rho} \tilde{u}_j \frac{\partial \tilde{u}_i}{\partial x_j} + \frac{\partial \bar{p}}{\partial x_i} + \frac{\partial}{\partial x_j} \left(\overline{\rho u_i'' u_j''} - \overline{P_{ij}^L} \right) = 0; \tag{6.29}$$

$$\bar{\rho} \tilde{u}_j \frac{\partial \tilde{h}_e}{\partial x_j} - \tilde{u}_j \frac{\partial \bar{p}}{\partial x_j} + \frac{\partial}{\partial x_j} \left(\overline{\rho u_j'' h_e''} + \overline{q_j^L} - \sum_s h_{f,s} \overline{\rho Y_s D_{sj}^L} \right) -$$

$$- \overline{P_{ij}^L} \frac{\partial \tilde{u}_i}{\partial x_j} - \overline{u_j'' \frac{\partial p}{\partial x_j}} - \overline{P_{ij}^L \frac{\partial u_i''}{\partial x_j}} = - \sum_s h_{f,s} \bar{w}_s; \tag{6.30}$$

$$\bar{\rho}\tilde{u}_j\frac{\partial\tilde{Y}_s}{\partial x_j}+\frac{\partial}{\partial x_j}\left(\overline{\rho u_j'' Y_s''}+\overline{\rho Y_s D_{sj}^L}\right)=\bar{w}_s. \tag{6.31}$$

Here Y_s is the mass fraction of component s, D_{sj}^L, P_{ij}^L, q_j^L are the rate of diffusion, the stress tensor and the thermal flux for laminar flow, w_s is the rate of chemical reaction of component s.

In fully developed turbulent flow, the laminar transport coefficients are negligible compared with the turbulent coefficients.

In the simplest approximation of an incompressible turbulent boundary layer with consideration of component of velocity v directed along the y-axis, we have

$$\left.\begin{aligned}-\overline{\rho u'' v''}=\eta^T\frac{\partial\tilde{u}}{\partial y},\ \overline{\rho v'' h_e''}=-\frac{\eta^T}{\mathrm{Pr}^T}\frac{\partial\tilde{h}_e}{\partial y};\\ \overline{\rho v'' Y_s''}=-\frac{\eta^T}{\mathrm{Sc}^T}\frac{\partial\tilde{Y}_s}{\partial y}.\end{aligned}\right\} \tag{6.32}$$

Here the numbers Pr^T, Sc^T are taken as constant, and turbulent viscosity η^T is determined by the mixing length l or excess shear velocity $|\tilde{u}_{\max}-\tilde{u}_{\min}|$:

$$\eta^T=C_1\bar{\rho}l^2\left|\frac{\partial\tilde{u}}{\partial y}\right|; \tag{6.33}$$

$$\eta^T=C_2\bar{\rho}\delta\left|\tilde{u}_{\max}-\tilde{u}_{\min}\right|, \tag{6.34}$$

where δ is the thickness of the boundary layer.

For heterogeneous mixing, agreement with experiment is better at

$$\eta^T=C_3\bar{\rho}_\infty\tilde{u}_\infty\delta^*, \tag{6.35}$$

where $\delta^*=\int_{-\infty}^{\infty}\left|1-\frac{\bar{\rho}\tilde{u}}{\bar{\rho}_\infty\tilde{u}_\infty}\right|dy$, and coefficients C_1, C_2, C_3 in (6.33)-(6.35) are determined from experiment.

Amplification of Radiation in the Flame-Front Model. In analytical description of the hydrodynamics and optical properties of chemical lasers with diffusion, convection and chemical reactions, the presence of nonequilibrium distribution of populations can be accounted for if we consider each long-lived vibrational level of the active molecule as an individual component of the mixture. To do this within the framework of the flame-front model, Ref. 43 uses laminar boundary layer equations that take consideration of chemical reactions with formation of excited particles and radiation. These equations disregard the axial pressure gradient, and assume that $D_{ij}=D$, and the Lewis number $\mathrm{Le}=\rho Dc_p/\lambda=1$, which is true for most gases. Then from (3.38)-(3.41):

$$\partial\rho u/\partial x+\partial\rho v/\partial y=0; \tag{6.36}$$

$$\rho u\frac{\partial u}{\partial x}+\rho v\frac{\partial u}{\partial y}=\frac{\partial}{\partial y}\eta\frac{\partial u}{\partial y}; \tag{6.37}$$

$$\rho\left(u\frac{\partial h_e}{\partial x}+v\frac{\partial h_e}{\partial y}\right)=\frac{\partial}{\partial y}\left\{\frac{\eta}{\mathrm{Pr}}\left[\frac{\partial h_e}{\partial y}+(\mathrm{Pr}-1)\frac{1}{2}\frac{\partial(u^2)}{\partial y}\right]\right\}; \tag{6.38}$$

$$\rho\left(u\frac{\partial Y_i}{\partial x}+v\frac{\partial Y_i}{\partial y}\right)=\frac{\partial}{\partial y}\left(\rho D\frac{\partial Y_i}{\partial y}\right)+w_i,\ i=0,1,\ldots,n-1; \tag{6.39}$$

$$p=\rho RT\sum_i(Y_i/\mu_i), \tag{6.40}$$

where $\mathrm{Pr}=\eta c_p/\lambda;\ c_p=\sum_i Y_i c_{pi}$.

By analogy with (1.22) and (1.6), for N chemical reactions of n gas components we have

$$w_i=\mu_i\sum_{j=1}^{N}(r'_{ij}-r_{ij})\left[k_{fj}\prod_{k=0}^{n-1}(c_k)^{r_{kj}}-k_{bj}\prod_{k=0}^{n-1}(c_k)^{r'_{kj}}\right],\ j=1,\ldots,N. \tag{6.41}$$

If the transfer coefficients are expressed in terms of the flow parameters, then equations (6.36)-(6.40) with consideration of (6.41) are equations for the unknowns ρ, u, v, h_e, T and Y_i.

For solution, we convert to variables x, and

$$\tilde{y}=\left(\frac{u_\infty}{2D_\infty x}\right)^{1/2}\int_{y_f(x)}^{y}\frac{\rho(x,\bar{y})}{\rho_\infty}d\bar{y}. \tag{6.42}$$

Based on the definition of the stream function, we get an expression for the flow velocity, and for the corresponding boundary conditions we seek the solution of (6.36)-(6.40) under the conditions:

$$K_p=(k_b/k_f)_p\to 0;\ x/x_p\to\infty,\ (x/x_{cd})^2\ll 1.$$

Here x_p and x_{cd} are the respective characteristic distances of chemical pumping and deactivation. As a result, expressions were found in Ref. 43 for the power per unit of area of the flow, and for the chemical efficiency, showing qualitative agreement between theory and experiment. At low temperature, when collisional deactivation can be disregarded as compared with radiational deactivation, calculation shows that the chemical efficiency should exceed 30%; however, effects of collisional deactivation reduce efficiency to 10-20% for a time of H_2 diffusion that is comparable to the time of collisional deactivation of HF.

Simplified Analysis of a Saturated Chemical Amplifier Based on Analytical Solution [Ref. 44]. In analysis of coordinates x (along the direction of flow velocity $\vec{u}$) versus y (in the direction of propagation of emission) we use the equations

$$\frac{\partial}{\partial y}I^{v,J_v-1}_{v-1,J_v}=G^{v,J_v-1}_{v-1,J_v}I^{v,J_v-1}_{v-1,J_v}\quad(v=1,2,\ldots,m); \tag{6.43}$$

$$\frac{\partial}{\partial x}(n_v y_f)=y_f\left\{P_v\frac{n_F}{x_x}+Q_{VT}(v)+Q_{VV}(v)+\frac{1}{u}\left[\alpha^{v+1,J_{v+1}-1}_{v,J_{v+1}}\times\right.\right.$$

$$\left.\left.\times I^{v+1,J_{v+1}-1}_{v,J_{v+1}}-\alpha^{v,J_v-1}_{v-1,J_v}I^{v,J_v-1}_{v-1,J_v}\right]\right\}\quad(v=0,1,\ldots m); \tag{6.44}$$

$$\frac{d}{dx}(n_F y_f)=N_0\frac{dy_f}{dx}-\frac{n_F y_f}{x_x}. \tag{6.45}$$

Here $I_{v,J}^{v',J'}$ is the intensity of radiation on transition $v', J' \to v, J$; n_v, n_F, N_0 are the respective concentrations of HF molecules on the v-th vibrational level, F atoms in the active zone within the surface of the flame front $y_f(x)$, and the initial concentration of F atoms in the flow; $\alpha_{v,J}^{v',J'} = \sigma_{v,J}^{v',J'}(n_v - \beta_{J_v} n_{v-1})$ is the specific gain in the active zone on transition $v', J' \to v, J$; $\beta_J = \exp\left(-\frac{2\theta_{rot} J}{T}\right)$; $\sigma_{v,J}^{v',J'}$ is the cross section of the induced transition; $G_{v,J}^{v',J'} = y_f \alpha_{v,J}^{v',J'}/h_y$ is the gain averaged over the height h_y of the jet; P_V is the probability of population of the v-level of the HF molecule in the course of the reaction; k_X is the rate constant of the chemical reaction; m is the number of the higher vibrational level that is populated during the reaction (m = 3 for HF chemical lasers); the Q_{VV} and Q_{VT} terms describe V-V exchange and V-T relaxation of the HF molecules.

For purposes of simplification, it is assumed that

$$I_{1,0} = I_{2,1} = \ldots = I_{m,m-1} = I/m, \text{ where } I = \sum_{v=1}^{m} I_{v,v-1}^{J};$$

$$\alpha_{v,v-1} = \alpha_{v+1,v} \quad (v = 1, 2, \ldots, m-1);$$

$$J_{1,0} = J_{2,1} = \ldots = J_{m,m-1} = \ldots = J.$$

For the density of vibrational quanta $q_V = \sum_{v=0}^{m} v n_v$ under the given assumptions we get

$$q_V = N\varepsilon_J + B_J \alpha/\sigma_{1,0}, \tag{6.46}$$

where

$$B_J = \frac{1}{m(1-\beta_J)} \sum_{v=1}^{m} \left(\frac{\sigma_{1,0}}{\sigma_{v,v-1}}\right)\left[v - (m+1)\frac{\beta_J^{m+1}}{1-\beta_J^{m+1}}\left(\frac{1}{\beta_J^v} - 1\right)\right];$$

$$\alpha = \sum_{v=1}^{m} \alpha_{v,v-1}^{J}; \quad \varepsilon_J = \frac{\beta_J}{1-\beta_J}\left[1 - (m+1)\beta_J^m\left(\frac{1-\beta_J}{1-\beta_J^{m+1}}\right)\right].$$

The values of m = 1, β_J = 1 correspond to a two-level medium. From (6.44), (6.46) we get an equation for $\alpha(J)$:

$$\frac{d}{dx}(\alpha y_f) = y_f\left\{\frac{\sigma_{1,0}}{B_J}\left(\frac{\varepsilon_X - \varepsilon_J}{x_X} + \frac{\varepsilon_J}{x_{VT}}\right) n_F - \frac{\sigma_{1,0}}{B_J}\frac{N_0}{x_{VT}}\varepsilon_J - \alpha\left[\frac{1}{x_{VT}} + \frac{\sigma_{1,0} I}{muB_J}\right]\right\}, \tag{6.47}$$

where $x_{VT} = u/(\sum_i k_{VT_i} n_i)$ is the characteristic length of the zone of V-T relaxation; $\varepsilon_X = \sum_{k=1}^{m} k P_k$ is the reserve of vibrational energy (per molecule) that is created in the course of the reaction (for the reaction $F + H_2$ $\varepsilon_X \approx 2{,}1$).

For the coordinate of the surface of the flame front in laminar mixing

$$y_f(\xi) = \begin{cases} h_y\sqrt{\xi/\xi_d}, & (\xi < \xi_d); \\ h_y, & (\xi > \xi_d) \end{cases} \tag{6.48}$$

$\left(\xi=\frac{x}{x_{VT}}, \xi_d=\frac{x_d}{x_{VT}}, x_d \text{ is the characteristic diffusion length}\right)$.

From (6.47) with consideration of (6.46) and (6.48) we have

$$\frac{\alpha y_f}{h_y}\left(\frac{\sqrt{\xi_d}}{\sigma_{1,0}N_0\gamma_J}\right)=\begin{cases}\dfrac{\varepsilon_\zeta D(\sqrt{\zeta\xi})}{(t-\zeta)\sqrt{\zeta}}-\dfrac{\sqrt{\xi}}{t}+\left(\dfrac{1}{t}-\dfrac{\varepsilon_\zeta}{t-\zeta}\right)\dfrac{D(\sqrt{t\xi})}{\sqrt{t}}, \\ \qquad \xi\leqslant\xi_d; \\ \dfrac{\varepsilon_\zeta D(\sqrt{\zeta\xi_d})}{(t-\zeta)\sqrt{\zeta}}\exp[-\zeta(\xi-\xi_d)]-\dfrac{\sqrt{\xi_d}}{t}+\left(\dfrac{1}{t}- \\ -\dfrac{\varepsilon_\zeta}{t-\zeta}\right)\dfrac{D\sqrt{t\xi_d}}{\sqrt{t}}\exp[-t(\xi-\xi_d)],\ \xi>\xi_d.\end{cases} \tag{6.49}$$

Here

$$D(z)=\exp(-z^2)\int_0^z\exp(x^2)\,dx \tag{6.50}$$

is the Dawson integral;

$$\zeta=\frac{x_{VT}}{x_x};\ \gamma_J=\frac{\varepsilon_J}{B_J};\ \varepsilon_\zeta=1+\zeta\left(\frac{\varepsilon_x}{\varepsilon_J}-1\right);\ t=1+x_{VT}\sigma_{1,0}\frac{I}{m\omega B_J}.$$

In the case of instantaneous reaction on the flame front $x_x\to 0$, $\xi\to\infty$, then

$$\frac{\alpha y_f}{h_y}\left(\frac{\sqrt{\xi_d}}{\sigma_{1,0}N_0\gamma_J}\right)=\begin{cases}\left(\dfrac{1}{t}+\dfrac{\varepsilon_x}{\varepsilon_J}-1\right)\dfrac{D(\sqrt{t\xi})}{\sqrt{t}}-\dfrac{\sqrt{\xi}}{t},\ \xi\leqslant\xi_d; \\ \left(\dfrac{1}{t}+\dfrac{\varepsilon_x}{\varepsilon_J}-1\right)\dfrac{D(\sqrt{t\xi_d})}{\sqrt{t}}\exp[-t(\xi-\xi_d)]-\dfrac{\sqrt{\xi_d}}{t},\ \xi>\xi_d.\end{cases} \tag{6.51}$$

In the absence of radiation I = 0 (t = 1 is the unsaturated gain of the medium), the width of the inversion zone is

$$\Delta x_{inv}\approx x_{VT}\frac{\varepsilon_x}{2\varepsilon_J}\approx x_{VT}\frac{1-\beta_J}{\beta_J\left[1-(m+1)\beta_J^m\dfrac{(1-\beta_J)}{1-\beta_J^{m+1}}\right]}. \tag{6.52}$$

It can be seen from this that in a multilevel medium with partial inversion ($\beta_J<1$) the width of the inversion zone is considerably greater than in a two-level medium ($m=\varepsilon_x=\beta_J=1$), where $\Delta x_{inv}\approx x_{VT}$.

At high radiation intensity ($t\gg1$), relation (6.51) enables determination of the width of the inversion zone of a saturated amplifier. For $\xi>\xi_d$ the gain decreases exponentially with increasing ξ, and therefore the width of the inversion zone is bounded by the quantity ξ_d or $\Delta x_{inv}\approx x_d$. In the region $\xi\leqslant\xi_d$ for a multilevel medium

$$\Delta x_{inv}\approx\frac{1}{2}x_{VT}\left(\frac{\varepsilon_x}{\varepsilon_J}-1\right), \tag{6.53}$$

and for a two-level medium $\Delta x_{inv} \geq \frac{1}{2} x_{VT}$. Hence it is clear that even in the region $\xi \leqslant \xi_d$ in a multilevel medium the inversion zone is larger than in the two-level medium. With increasing J the inversion zone grows up to $\Delta x_{inv} = x_d$.

In the case of instantaneous reaction on the flame front, the useful normalized power W_{norm} per sq. cm of the critical cross section of the nozzle module is expressed by the relation

$$W_{norm}(\xi) = \frac{h_y \nu_J \sigma_{1,0} \gamma_J I_0 N_0 x_{VT}}{m \sqrt{\xi_d}} \left\{ \frac{1}{t^{3/2}} \left(\frac{1}{t} + \frac{e_x}{e_J} - 1 \right) \left[\sqrt{t\xi} - D\left(\sqrt{t\xi}\right) \right] - \frac{2}{3t} \xi^{3/2} \right\} \quad (\xi \leqslant \xi_d). \quad (6.54)$$

In a saturated amplifier the maximum power from the entire lasing zone is

$$W_{max}\ (\xi^*) = h_y \nu_J u N_0 e_J \sqrt{\frac{\xi^*}{\xi_d}} \left[\left(\frac{\xi_x}{e_J} - 1 \right) - \frac{2}{3} \xi^* \right], \quad (6.55)$$

whence

$$\eta_x(\xi^*) \approx \frac{N_A h_y \nu_J e_J}{Q} \left[\left(\frac{e_x}{e_J} - 1 \right) - \frac{2}{3} \xi^* \right] T \sqrt{\frac{\xi^*}{\xi_d}}. \quad (6.56)$$

We can see from (6.56) that in accordance with Ref. 45 the efficiency of a cw diffusion chemical quantum amplifier increases with an increase in the number J of the working transtion. Actually, according to calculations done in Ref. 44 by the given formulas, at T = 400 K, p = 0.66 kPa, u = 3 km/s, $n_{He}/n_F = 5$, $h_y = 0.2$ cm and $T_{He} = 100$ K, it is found that passage from J = 4 to J = 8 raises the efficiency of the chemical amplifier by a factor of 2-2.5 (from 8% to 20%). In this connection the spectrum of radiation can be shifted to higher values of the rotational number J even without using selective mirrors.

To do this, it is suggested in Ref. 44 that a working mixture be used in the master laser with a degree of dilution by an inert gas such as helium that is lower than in the amplifier itself. Then the average temperature of the lasing mixture will be higher, and therefore the frequency spectrum arriving at the amplifier input will be shifted toward values of J that do not coincide with the maximum amplification zone, but ensure higher efficiency of the chemical amplifier. However, it is possible that such an increase in efficiency will be realized only in a rather powerful amplifier with greater extent of the active medium that compensates for the reduction in gain that is due to the reduction in the cross section of the induced transition as J increases.

Numerical Study of DF Chemical Laser When Rotational Equilibrium is Violated. The assumption made in some theoretical studies about equilibrium boltzmannian distribution is unjustified. Refinements in the ideas of the role of rotational relaxation have shown that in cw chemical lasers the violation of rotational equilibrium results in a reduction in power by 20-30% [Ref. 45]. In Ref. 46 a theoretical study was done on a cw DF chemical laser without the assumption of equilibrium distribution of populations of rotational levels. It was assumed that gas dynamics and processes of mixing of reagents are described by quasihomogeneous equations along individual jets in which mixing has already occurred, and which vary in width in accordance with the formula

$$\delta l = \frac{L_c}{i} \operatorname{tg}\left(\frac{x}{L_d}\right)^{1/2}, \tag{6.57}$$

where L_c is the total length of the resonator cavity, i is the number of nozzles, L_d is the length of the mixing zone. The concentration of reagents was determined by using the equation

$$\frac{dc_s}{dx} = \frac{\dot{c}_s}{u} + (c_s^0 - c_s)\frac{dw}{wdx}, \tag{6.58}$$

where $\dot{c}_s$ is the rate of change in concentration due to chemical reactions, V-V exchange and vibrational relaxation, rotational relaxation and induced transitions. Analogous equations have also been used for the reaction products in excited V-R states of DF ($v \leqslant 4$) in excited V-states of DF ($v > 4$) and for excited D_2 molecules ($v \geqslant 1$).

It was assumed that the only pumping reaction was

$$F + D_2 \rightarrow DF(v, J) + D, \tag{6.59}$$

with integral rate constant taken from Ref. 47. The distribution of products of relaxation with respect to levels v and J is taken from Ref. 48, in accordance with which the distribution maximum for v = 1, 2, 3, 4 falls respectively to J = 13, 11, 9, 5. Numerical calculations were done for active medium F/He/HF/D_2 = 3/6/3/14 at T = 300 K, u = 2.13 km/s, pL_d = 1.66 kPa·cm, pL_c = 13.3 kPa·cm, p = 133 Pa.

High amplification on transitions of strongly rotating molecules immediately after the onset of mixing shows up experimentally in the development of lasing in this region simultaneously on several lines. Calculations of lasing intensity also show that after the beginning of mixing, lasing takes place at the same time on many lines, those lines with small J ceasing to emit with the course of time, and the maximum of the spectrum being shifted toward higher J. Amplification on purely rotational transitions of DF (v = 2) may increase considerably. For example at p = 0.66 kPa, $\alpha > 1$ cm^{-1} at distances $x \leqslant 0.3$ cm.

Violation of rotational equilibrium leads to a reduction of power in a nonselective cavity by 14%, and with selection of a single line--by 35%. According to calculations, in the case of selection of individual lines, the output power is appreciably dependent on the choice of the rate constant of rotational relaxation.

Other Numerical Studies of the Supersonic Diffusion Chemical Laser. The idealized flow pattern with laminar diffusion of a stream of H_2 of finite width into a semi-infinite stream containing fluorine and a diluent was considered in Ref. 49 in a coherent radiation field. Mises transformation was used to simplify numerical solution of equation system (3.38)-(3.41) of boundary-layer type with consideration of multicomponent diffusion, radiation and chemical reactions. At constant values of the initial velocity of the flow, temperature, width of the stream of H_2 and initial partial pressure of fluorine, direct relations were found for the pressure dependence of the integral gain and the effective specific output power of chemical lasers, and inverse relations for pressure dependence of the length of the active region and the chemical efficiency.

Similar constraints on the length of the active zone and efficiency with pressure increase due to processes of mixing of reagents in the laminar mode of operation of an HF supersonic diffusion chemical laser were found by numerical calculation in Ref. 50. However, the total efficiency of chemical lasers with consideration of thermal expenditures on mixture preparation increase in the case of operation in the mode of a chain mechanism of excitation, which is analyzed in Ref. 51 in chemical lasers with a small degree of dissociation of molecular fluorine. The comparative efficiency of different fuel compositions of chemical lasers on an H_2/F_2 mixture can be evaluated by using calculation based on an instantaneous mixing model [Ref. 52].

Numerical analysis of the efficiency of energy conversion in HF diffusion chemical lasers [Ref. 53] shows that the use of turbulent injectors in chemical lasers leads to an increase of pressure in the resonator cavity. This ensures a high rate of mixing of the components of the mixture under conditions of a turbulent flow mode.

For HF chemical lasers, especially with a chain reaction mechanism, there is typically multilevel excitation with kinetic pressures in the active zone that take place against a background of diffusion flow with gradients of the index of refraction in flow beyond the nozzle tip. Calculation of the structure of amplitude and phase diagrams of the radiation field in the near and far zones [Ref. 54] for typical conditions of operation of HF chemical lasers has shown that the use of telescopic cavities leads to an increase in the directionality of emission with moderate reductions in efficiency.

Numerical analysis of the kinetics of physical processes has also been done for a chemical-gasdynamic laser on a mixture of $CS_2/CS/O_2/O$ [Ref. 53]. Simultaneous solution of equations of chemical kinetics, vibrational relaxation and gas dynamics for a logarithmic nozzle shows that efficient chemical pumping and gasdynamic cooling should give comparatively high values of total inversion ($\sim 10^{14}$ cm^{-3}) and gain (~ 0.1 cm^{-1}).

§6.5. Open-Cycle Chemical Lasers With Pressure Recovery in the Diffuser

Since gas flow with Mach number $M > 1$ takes place at the inlet to the cavity of a supersonic chemical laser, it is possible, as pointed out in §6.2, to use a diffuser for restoring the pressure from the range of 0.66-3.33 kPa required in the resonator to 26.7-53.3 kPa at the diffuser outlet. From this level, a mechanical pump or ejector can bring the exhaust pressure up to the level that is required for example when chemical lasers work into the atmosphere [Ref. 56]. Energy expenditures on evacuation must be minimized to increase the overall efficiency. From this we can see that the requirements for pressure recovery in the diffuser are important in calculating and designing supersonic chemical lasers.

In the open-cycle chemical laser (see Fig. 6.9) the primary fuel mixture is formed on section (1)-(2) and is accelerated in nozzle (2)-(3) to supersonic velocity at low static pressure. In the cavity (3)-(4), heat release takes place in the flow as the primary and secondary mixtures burn, and in the diffuser (4)-(7) the flow is decelerated from supersonic velocities with a corresponding increase in gas pressure. A one-dimensional analysis of such a flow in chemical lasers is given for example in Ref. 57, where an examination is made of chemical and

thermochemical processes in the cavity, the hydrodynamics of the flow with consideration of the boundary layer and deceleration of the flow in a diffuser with constant cross section of the intake and throat (4)-(6), and with a subsonic expanding diffuser (6)-(7) at the outlet.

If we denote the parameters of the primary flow of oxidant by subscript p, and those of the secondary flow of fuel by subscript s, the molar flowrates of oxidant in the nozzle are G_{pF} and G_{pF_2}. The relative dissociation of fluorine is then defined as $\alpha = \frac{1}{2}G_{pF}/\hat{G}_{pF_2}$, where $\hat{G}_{pF_2} = \frac{1}{2}G_{pF} + G_{pF_2} = \hat{G}$ is a normalizing parameter that characterizes the flowrate of all fluorine in molecular form. The dilution of components i (F, F_2, D, D_2, He, DF and so on) in the cavity is described by the degree of dilution $\psi_{pi} = G_{pi}/\hat{G}$, the total dilution of the primary oxidant flow being expressed as $\psi_p = \Sigma\psi_{pi}$. The molar flowrates of F and F_2 will be $G_{pF} = 2\alpha_F\hat{G}$ and $G_{pF_2} = (1 - \alpha_F)\hat{G}$.

The normalized molar flowrate of fuel with consideration of the ratio R_c of components of the mixture in the cavity will be $G_{sD_2} = R_c\hat{G}$, and the flowrate of diluted secondary flow $\psi_s\hat{G}$. Overall molar flowrate of fuel: $G_s = \hat{G}(R_c + \psi_s)$.

The total molar flowrate at the cavity inlet (3) (see Fig. 6.9) with consideration of dilution is equal to the sum of the flowrates of fuel and oxidant:

$$G_3 = \hat{G}(1 + \alpha_F + \varphi_p + \varphi_s + R_c). \tag{6.60}$$

Since F and F_2 react completely to DF at the cavity outlet, and the diluent does not take part in the chemical process, the equality $G_{4DF} = 2\hat{G}$ is satisfied in cross section (4), and for atomic deuterium $G_{4D} = \alpha_D G_{pF} = 2\alpha_F\alpha_D\hat{G}$, where α_D is the relative dissociation of D atoms. Then the flowrate of molecular deuterium at the cavity outlet $G_{4D_2} = \hat{G}(R_c - 1 - \alpha_F\alpha_D)$, and the total molar flowrate at the cavity outlet is

$$G_4 = \hat{G}(1 + \alpha_F\alpha_D + \psi_p + \psi_s + R_c). \tag{6.61}$$

Thermochemical processes in cavity (3)-(4) are described by the expressions $H_{e3} = G_3h_{e3}$ and $H_{e4} = G_4h_{e4}$, which are equal in the adiabatic state. However, the cavity releases the power of stimulated emission $W = G_3\mu_3w_{sp}$, where μ_3 is molar mass, $w_{sp} = W/\dot{m}$ is the specific power of stimulated emission, $\dot{m}_3$ is mass flowrate. Then $H_{e3} = H_{e4} + W$ or

$$(G_4 h_{e04} - G_3 h_{e03}) + G_3\mu_3 w_{sp} = Q = \sum_i (G_{3i} h_{fi} - G_{4i} h_{fi}), \tag{6.62}$$

where h_{ji} is the specific heat of formation of the i-th component. For diluents $G_{3i} = G_{4i}$ and for F_2 and D_2 $h_{jF_2} = h_{jD_2} = 0$, therefore

$$Q = G_{pF}h_{fF} - G_{4DF}\,h_{fDF} - G_{4D}h_{fD}. \tag{6.63}$$

The specific energy release in the cavity with respect to oxidant F_2 is

$$\hat{q} = Q/\hat{G} = 2\alpha_F(h_{fF} - \alpha_D\,h_{fD}) - 2h_{fDF}. \tag{6.64}$$

From (6.60)-(6.62) we can get a relation for the specific enthalpies of deceleration of the flow in the cavity:

$$h_{e03}/h_{e03} = 1 + \frac{1}{\lambda_s}\left[\frac{\hat{q}/h_{e0p}}{1+\alpha_F+\psi_p} - \frac{\mu_3 w_{sp}}{X_p h_{e0p}}\right], \qquad (6.65)$$

where $X_p = G_p/G_3$ is the mole fraction of oxidant, h_{eop} is the specific enthalpy of deceleration of the primary flow at the nozzle outlet; λ_s is a parameter that describes the influence of the secondary flow,

$$\lambda_s = 1 + \frac{X_s h_{e0s}}{X_p h_{e0p}}. \qquad (6.66)$$

In general, as can be seen from Fig. 6.2, the flow at the nozzle outlet is inhomogeneous and may have a complicated system of compression shocks. However, these effects, which are associated with energy release and mixing, play a major role only in the inlet part of the cavity, and in the remaining part they can be disregarded. The contour of the walls on section (4)-(5) is usually smooth with a large radius of curvature, and therefore there are no large pressure gradients. Thus since transverse velocities of the flow are small throughout the entire extent of the channel compared with axial velocities, deviations from unidimensional flow can be treated as quantities of the second order of smallness. In this connection, the homogeneous flow parameters at the outlet of the nozzle array in Ref. 57 are obtained by integrating the inhomogeneous distributions across the nozzle by the method given in Ref. 58. The diffuser (4)-(6) is equipped with a throat with constant cross sectional area and length sufficient for conversion of the flow in the shock wave system from supersonic to subsonic flow, and also for equalizing inhomogeneities of the flow at the diffuser outlet. Thus the one-dimensional approximation can be used in analyzing the flow in cross section (6) as well.

The equation of momentum for the inviscid control volume I of the cavity in region (3)-(4) is written as

$$[pS(1+\gamma M^2)]_{4I} = [pS(1+\gamma M^2)]_3 + \int_3^4 p\,dS. \qquad (6.67)$$

Here the cross section of the inviscid control volume $S_{4I} = S_4 - S_\delta$, S_δ characterizes the boundary layer in the cavity determined by the thickness of displacement δ and the hydraulic diameter D_H as $S_\delta = S_4 4\delta/D_H$.

The solutions of the equations of momentum, energy and continuity give expressions for the velocity of the flow u_3, enthalpy h_{e3} and pressure p_3:

$$u_3 = Y_p u_p + Y_s u_s + \dot{m}_3^{-1}[p_p S_p + p_s S_s - p_3(S_p + S_s)]; \qquad (6.68)$$

$$h_{e3} = X_p h_{ep} + X_s h_{es} + (2\mu_3)^{-1}[Y_p u_p^2 + Y_s u_s^2 - u_3^2]; \qquad (6.69)$$

$$p_3 = \dot{m}_3 R_3 T_3/(u_3 S_3) \qquad (6.70)$$

(R is the gas constant, $h_{ej} = \sum_i \int_0^{T_j} C_{pi}\,dT$ is the enthalpy of the j-th state of the medium, for example $j = p, s, 3$; $Y_{ji} = \dot{m}_{ji}/\dot{m}_j$ is the mass fraction of component i) from

which, by iterations with the use of temperature dependences of the gas properties, we determine p_3, u_3, T_3, and then p_{03} and M_3. For the general case $p = f(S)$, the relation

$$pS^{\zeta/(\zeta-1)} = \text{const} \ (0 \leqslant \zeta \leqslant 1) \ \text{[Ref. 59]} \tag{6.71}$$

is substituted in (6.67) and an estimate is made of the pressure integral and the quantities

$$p_{4I}/p_3 = \left[\frac{\zeta + \gamma M_3^2}{\zeta + \gamma M_{4I}^2}\right]^{\zeta}; \tag{6.72}$$

$$S_{4I}/S_3 = [(\zeta + \gamma M_3^2)/(\zeta + \gamma M_{4I}^2)]^{(1-\zeta)}; \tag{6.73}$$

$$T_{4I}/T_4 = [M_{4I}(\zeta + \gamma M_3^2)/M_3(\zeta + \gamma M_{4I}^2)]^2. \tag{6.74}$$

For the stagnation pressure ratio we have

$$p_{04}/p_{03} = (p_{4I}/p_3)\left[\left(1 + \frac{\gamma-1}{2} M_{4I}^2\right) \Big/ \left(1 + \frac{\gamma-1}{2} M_3^2\right)\right]^{\gamma/(\gamma-1)}. \tag{6.75}$$

The stagnation temperature at the cavity outlet is

$$T_{04} = T_{4I}\left(1 + \frac{\gamma-1}{2} M_{4I}^2\right). \tag{6.76}$$

The expression for T_{03} will be analogous. Dividing (6.76) by T_{03} and substituting the result in (6.74), we get

$$T_{04}/T_{03} = \left[\left(1 + \frac{\gamma-1}{2} M_{4I}^2\right) \Big/ \left(1 + \frac{\gamma-1}{2} M_3^2\right)\right]\left[\frac{M_{4I}(\zeta+\gamma M_3^2)}{M_3(\zeta+\gamma M_{4I}^2)}\right]^2. \tag{6.77}$$

The ratio T_{04}/T_{03} is found from (6.65), (6.66), and equation (6.77) is solved with respect to M_{4I} at a given ζ, after which the quantities appearing in (6.72)-(6.75) are readily determined. Data of Ref. 58 can be used to convert from inviscid parameters to averaged parameters in cross section (4) with consideration of the boundary layer.

The parameters in cross sections (4) and (5) for a diffuser with throat of constant cross section and without constriction at the inlet can be taken as equal: $S_5 \approx S_4$, $M_5 \approx M_4$, $p_5 \approx p_4$, and so on. From cross section 5 to cross section 6 the flow transition from $M > 1$ to $M < 1$ takes place on a throat length of $(8\text{-}13)D_H$ through a complex system of oblique shocks identifiable with a single straight shock wave. Consequently the flow parameters in cross section (6) are calculated from the parameters in section (5) by well known expressions for a forward compression shock.

After this, the unknown pressure is determined at the diffuser outlet of the open-cycle supersonic chemical laser:

$$p_7 = p_6[1 + \delta(p_{06}/p_6 - 1)], \tag{6.78}$$

where δ is the coefficient of recovery of static pressure of the subsonic diffuser (6)-(7). Here we can assume $p_7 \approx p_{07}$ in view of the smallness of the number M_7.

The characteristics of the described diffuser can be improved by using a constricting inlet (4)-(5) as shown in Fig. 6.9 that compresses the flow and reduces the Mach number in front of throat of constant cross section (5)-(6).

The above-mentioned one-dimensional analysis of Ref. 57 agrees with the results of experimental studies of the nozzle module of a chemical laser with diffuser of constant cross sectional area of the inlet and throat. In these experiments, the pressure at the outlet of the diffuser (7) was restored to 35 kPa. The results showed linearly increasing dependence of the output pressure in the diffuser as a function of increasing pressure in combustion chamber (1)-(2). The change in temperature of the medium in the combustion chamber has a considerable effect on pressure recovery σ. For example increasing T_{02} from 1700 to 2100 K leads to a rise in p_{07} by 25%.

REFERENCES

1. Basov, N. G., Orayevskiy, A. N., "Obtaining Negative Temperatures by the Method of Heating and Cooling a System", ZHURNAL EKSPERIMENTAL'NOY I TEORETICHESKOY FIZIKI, Vol 44, No 5, 1963, pp 1742-1745.

2. Hurle, I. R., Hertzberg, A., "Electronic Population Inversions by Fluid-Mechanical Techniques", PHYS. FLUIDS, Vol 8, No 9, 1965, pp 1601-1607; "On the Possible Production of Population Inversions by Gas-Dynamic Techniques. Minutes of the 1963 Annual Meeting of the Division of Fluid Dynamics. Cambridge Massachusetts, 25-27 Nov 1963", BULL. AMER. PHYS. SOC., Vol 9, No 5, 1964, pp 582-595.

3. Wells, W. H., "Proposed Gas Maser Pumping Scheme for the Far Infrared", J. APPL. PHYS., Vol 36, No 9, 1965, pp 2838-2843.

4. Shimoda, K., "Thermally Pumped Infrared Masers", INSTITUTE OF PHYS. AND CHEM. RESEARCH, 1965, Papers 59, No 2, pp 53-68.

5. Basov, N. G., Orayevskiy, A. N., Shcheglov, V. A., "Beam Laser in the Infrared Range", ZHURNAL EKSPERIMENTAL'NOY I TEORETICHESKOY FIZIKI, Vol 4, No 2, 1966, pp 61-62.

6. Konyukhov, V. K., Prokhorov, A. M., "Inverse Population in Adiabatic Expansion of a Gas Mixture", PIS'MA V ZHURNAL EKSPERIMENTAL'NOY I TEORETICHESKOY FIZIKI, Vol 3, No 11, 1966, pp 436-439.

7. Basov, N. G., Orayevskiy, A. N., Shcheglov, V. A., "Thermal Methods of Laser Excitation", ZHURNAL TEKHNICHESKOY FIZIKI, Vol 37, No 2, 1967, pp 339-348.

8. Orayevskiy, A. N., "Population Inversion With Thermal Dissociation of Molecules in a Shock Wave", ZHURNAL EKSPERIMENTAL'NOY I TEORETICHESKOY FIZIKI, Vol 48, No 4, 1965, pp 1150-1154; "Arisal of Negative Temperatures in Chemical Reactions", Ibid., Vol 45, No 2(8), 1963, pp 177-179.

9. Makhov, G., Wieder, I., "Vibrational Excitation of the CO_2 by Transfer From Thermally Excited Nitrogen", IEEE J. QUANT. ELECTRON., Vol QE-3, No 9, 1967, p 378.

10. Basov, N. G. et al., "Obtaining Inverse Population of Molecules in a Supersonic Flow of Binary Gas in a Laval Nozzle", ZHURNAL TEKHNICHESKOY FIZIKI, Vol 38, No 12, pp 2031-2041.

11. Spencer, D. J. et al., "Preliminary Performance of a CW Chemical Laser", APPL. PHYS. LETT., Vol 16, No 6, 1970, pp 235-237.

12. Mirels, H., Spencer, D. J., "Power and Efficiency of a Continuous HF Chemical Laser", IEEE J. QUANT. ELECTRON., Vol 7, No 11, 1971, pp 501-507.

13. Spencer, D. J. et al., "Continuous-Wave Chemical Laser", INT. J. CHEM. KINETICS, Vol 1, No 5, 1969, pp 493-494.

14. Warren, W. R. Jr., "Chemical Lasers", ASTRON AND AERON., Vol 13, No 4, 1975, pp 36-49.

15. Spencer, D. J., Mirels, H., Durran, D. A., "Performance of CW HF Chemical Laser With N_2 or He Diluent", J. APPL. PHYS., Vol 43, 1972, pp 1151-1157.

16. Bertrand, L., Gagne, J. M., Mongeau, B. et al., "A Continuous HF Chemical Laser: Production of Fluorine Atoms by a Microwave Discharge", J. APPL. PHYS., Vol 48, No 1, 1977, pp 224-229.

17. Jeffers, W. Q., Ageno, H. Y., "CO Chain-Reaction Chemical Laser", APPL. PHYS. LETT., Vol 27, No 4, 1975, pp 227-229.

18. Jeffers, W. Q., Wiswall, C. E., "Experimental Studies of the $O/O_2/CS_2$ CW CO Chemical Lasers", IEEE J. QUANT. ELECTRON., Vol QE-10, No 12, 1974, pp 860-869.

19. Bashkin, A. S., Gorshunov, N. M., Kunin, Yu. A. et al., "Lasing on a CS_2-O Mixture in a Shock Tube With Supersonic Nozzle", KVANTOVAYA ELEKTRONIKA, Vol 3, No 2, 1976, pp 463-465.

20. Blackman, A. W., "Laser Device", U. S. Patent No 3566297, 3 Nov 70.

21. Basov, N. G. et al., "Dynamics of Chemical Lasers", KVANTOVAYA ELEKTRONIKA, No 2, 1971, pp 3-24.

22. Airey, J. R., McKay, S. F., "A Supersonic Mixing Chemical Laser", APPL. PHYS. LETT., Vol 15, No 12, 1969, pp 401-403;

Arnold, S. J., Foster, K. D., Snelling, D. R., "A Supersonic HCl, Chemical Laser", J. OPT. SOC. AMER., Vol 68, No 5, 1978, p 652.

23. Meinzer, R. A., "A Continuous-Wave Combustion Laser", INT. J. CHEM. KINETICS, Vol 2, 1970, p 335.

24. Capelle, G. A., Suchard, S. N., "CN* Production Efficiencies From Active Nitrogen-Hydrocarbon Flames", IEEE J. QUANT. ELECTRON., Vol QE-12, No 7, 1976, pp 417-421.

25. Boedeker, L. R., Shirley, J. A., Bronfin, B. R., "Arc-Excited Flowing CO Chemical Laser", APPL. PHYS. LETT., Vol 21, No 6, 1972, pp 247-249.

26. "Studying Liquid-Fuel Chemical Lasers, a Group at TRW Works up From 8 kW", LASER FOCUS, Vol 12, No 6, 1976, p 38.

27. Basov, N. G., Orayevskiy, A. N., "Laser", Soviet Patent No 436413, 24 Apr 67, BYULLETEN' IZOBRETENIY, No 26, 1974, p 146.

28. Cool, T. A., Stephens, R. R., Falk, T. J., "A Continuous-Wave Chemically Excited CO_2 Laser", INT. J. CHEM. KINETICS, Vol 1, 1969, pp 495-496.

29. Orayevskiy, A. N., "Chemical Lasers", KHIMIYA VYSOKIKH ENERGIY, Vol 8, No 1, 1974, pp 3-20.

30. Cool, T. A., "The Transfer Chemical Laser. A Review of Recent Research", IEEE J. QUANT. ELECTRON., Vol QE-9, No 1, 1973, pp 72-83.

31. Gerry, E. T., "Gas Dynamic CO_2 Lasers", BULL. AMER. PHYS. SOC., Vol 15, 1970, p 563.

32. Tregay, G. W. et al., "DF-CO_2 Transfer Laser Development", IEEE J. QUANT. ELECTRON., Vol QE-11, No 8, 1975, pp 672-678.

33. Emanuel, G., Gaskill, W. G., Reiner, R. J. et al., "High-Pressure Operation of a CW DF-CO_2 Transfer Laser", IEEE J. QUANT. ELECTRON., Vol QE-12, No 11, 1976, pp 739-740.

34. Bashkin, A. S., Gorshunov, N. M., Kunin, Yu. A. et al., "Supersonic CO_2 Chemical Laser Based on a Mixture of Atomic Deuterium With Ozone and Carbon Dioxide", KVANTOVAYA ELEKTRONIKA, Vol 3, No 5, 1976, pp 1142-1143.

35. Biryukov, A. S., " Kinetics of Physical Processes in Gasdynamic Lasers" in: "Teoreticheskiye problemy spektroskopii i gazodinamicheskikh lazerov" [Theoretical Problems of Spectroscopy and Gasdynamic Lasers", Moscow, Izdatel'stvo AN SSSR, Vol 83, 1975, pp 13-86.

36. Biryukov, A. S., Shelepin, L. A., "Chemical-Mechanical Molecular Laser", ZHURNAL TEKHNICHESKOY FIZIKI, Vol 40, No 12, 1970, pp 2575-2577.

37. Wieder, J., "Flame Pumping and Infrared Maser Action in CO_2", PHYS. LETT., Vol 24A, No 13, 1967, pp 759-760.

38. Basov, N. G., Gromov, V. V., Markin, Ye. P. et al., "Chemical Laser on Oxidation Reaction $CO+0.5O_2$ With Supersonic Material Flow", KVANTOVAYA ELEKTRONIKA, Vol 3, No 5, 1976, pp 1154-1155.

39. Kudryavtsev, N. N., Novikov, S. S., Svetlichnyy, I. B., "Influence of Nonequilibrium Chemical Pumping on Amplification of Radiation of CO_2 Laser in Products of Reaction of $CO+N_2O$", DOKLADY AKADEMII NAUK SSSR, Vol 231, No 5, 1976, pp 1113-1115.

40. Basov, N. G., Gromov, V. V., Koshelev, Ye. L. et al., "CW DF-CO_2 Chemical Laser", PIS'MA V ZHURNAL EKSPERIMENTAL'NOY I TEORETICHESKOY FIZIKI, Vol 13, No 9, 1971, pp 496-498.

41. Preobrazhenskiy, N. G., "Diffusion Problems That Arise in Linear Theory of Gasdynamic and Chemical Lasers", ZHURNAL PRIKLADNOY MEKHANIKI I TEKHNICHESKOY FIZIKI, No 2, 1974, pp 32-37.

42. Grohs, G. L., "Turbulent Cavity Mixing in Continuous-Wave Chemical Lasers: Status of Theory", COMBUSTION SCI. AND TECHNOLOGY, Vol 13, 1976, pp 257-267.

43. Holland, R., Mirels, H. "Flame-Sheet Analysis of CW Diffusion-Type Chemical Lasers. I. Uncoupled Radiation", AIAA JOURN., Vol 10, No 4, 1972, pp 420-428.

44. Orayevskiy, A. N., "Efficiency of CW Diffusion-Type Chemical Amplifier", KVANTOVAYA ELEKTRONIKA, Vol 3, No 9, 1976, pp 1896-1908.

45. Skifstad, J. G., Chao, C. M., "Rotational Relaxation in a Line Selected Continuous HF Chemical Laser", APPL. OPTICS, Vol 14, 1975, pp 1713-1718;

Sentman, L. H., "Chemical Laser Power Spectral Performance: a Coupled Fluid Dynamic, Kinetic and Physical Optics Model", APPL. OPTICS, Vol 17, No 14, 1978, pp 2244-2249.

46. Hall, R. J., Rotational Nonequilibrium and Line-Selected Operation CW DF-Chemical Lasers", IEEE J. QUANT. ELECTRON., Vol 12, No 8, 1976, pp 453-462.

47. Homann, K. H. et al., "Eine Methode zur Erzeugung von Fluorstammer in inerten Atmosphäre", BERICHTE BUNSEN GESELLSCHAFT PHYSICALISCHE CHEMIE, Vol 74, 1970, pp 585-589.

48. Polanyi, J. C., Woodall, K. B., "Energy Distribution Among Reaction Products. VI. $F+H_2$, D_2", J. CHEM. PHYS., Vol 57, No 4, 1972, pp 1574-1586.

49. King, W. S., Mirels, H., "Numerical Study of a Diffusion-Type Chemical Laser", AIAA JOURN., Vol 10, No 12, 1972, pp 1647-1654.

50. Krutova, V. G. et al., "Numerical Analysis of CW Diffusion-Type Chemical Laser With Arbitrary Degree of Dissociation of Molecular Fluorine", KVANTOVAYA ELEKTRONIKA, Vol 3, No 9, 1976, pp 1919-1931.

51. Orayevskiy, A. N. et al., "Analysis of Conditions of Stimulated Emission of a CW Diffusion-Type Chemical Laser With Chain Mechanism of Excitation at Low

Degrees of Dissociation of Molecular Fluorine", KVANTOVAYA ELEKTRONIKA, Vol 3, No 1, 1976, pp 136-146.

52. Pospelov, V. A., "Flow Calculation in a CW Chemical Laser on a Mixture of Hydrogen and Fluorine", IZVESTIYA AKADEMII NAUK SSSR: MEKHANIKA ZHIDKOSTI I GAZA, No 2, 1978, pp 203-205.

53. Golovichev, V. I., Preobrazhenskiy, N. G., "Numerical Analysis of a Turbulent HF Chemical Laser of Diffusion Type in the Amplification Mode" in: "Gazovyye lazery" [Gas Lasers], edited by Associate Member of the USSR Academy of Sciences R. I. Soloukhin and Doctor of Physical and Mathematical Sciences V. P. Chebotayev, Novosibirsk, Nauka, 1977, pp 83-104.

54. Virnik, Ya. Z. et al., "Diffraction Effects in CW HF Chemical Laser With Unstable Telescopic Cavity", KVANTOVAYA ELEKTRONIKA, Vol 6, No 1, 1979, pp 236-248.

55. Biryukov, A. S., Kulagin, Yu. A., Shelepin, L. A., "Kinetics of Physical Processes in Chemical CO Laser With Supersonic Circulation", KVANTOVAYA ELEKTRONIKA Vol 5, No 7, 1978, pp 1444-1455.

56. Ortwerth, P. J., "On the Rational Design of Compressible Flow Ejectors", AIAA PAPER, No 1217, 1978, pp 1-9.

57. Driscoll, R. J., Moon, L. F., "Pressure Recovery in Chemical Lasers", AIAA JOURN., Vol 15, No 5, 1977, pp 665-673.

58. Driscoll, R. J., "Study of the Boundary Layers in Chemical Laser Nozzles", AIAA JOURN., Vol 14, 1976, pp 1571-1577.

59. Crocco, L., "One-Dimensional Treatment of Steady Gas Dynamics" in: "Fundamentals of Gas Dynamics", Vol III, Princeton, N. Y., Princeton University Press, 1958.

CHAPTER 7: CHEMICAL DETONATION LASERS

§7.1. General Information on Detonation Processes

We know that the process of detonation of solid [Ref. 1] and gaseous [Ref. 2, 3] explosives can be used for optical pumping of lasers. In this process the chemical energy of the explosive is converted directly to luminous pumping energy, and then to the energy of stimulated emission. Chemical energy conversion should be still more efficient in chemical detonation lasers with working principle based on stimulating emission directly from the zone of chemical reaction behind the detonation front [Ref. 4, 5], or from the region of free dispersal of the detonation products [Ref. 6], or from the region of discharge of the detonation products through the nozzle [Ref. 7]. In general we will apply the term *detonation laser* to a chemical laser in which detonation products serve as the active medium or as a component of this medium.

Let us give some information of a general nature on detonation.

Detonation is an explosive combustion wave for which one of the major well known properties is propagation at a constant supersonic velocity characteristic of the

given explosive and given initial parameters. If we take a coordinate system fixed on the detonation wave front, then in accordance with the one-dimensional theory of detonation the flow can be represented as shown in Fig. 7.1. The gas flows along

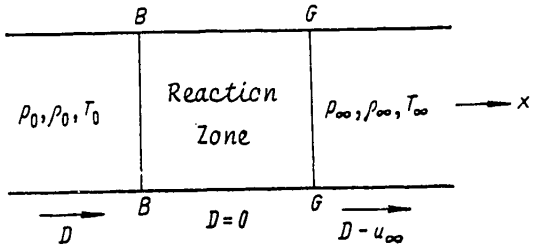

Fig. 7.1. Flow in coordinate system tied to the velocity D of the detonation front

the x-axis in the positive direction, and the wave parameters remain constant in planes perpendicular to the x-axis. Equations that describe such flow are given in Ref. 8. From these equations in coordinates of p vs. V we get a curve -- the Hugoniot adiabat -- that describes the solution for any values of the wave velocity D (Fig. 7.2):

$$V/V_0 = \frac{(p/p_0)+[(\gamma+1)/(\gamma-1)]+(2\gamma Q/c_0^2)}{[(p/p_0)(\gamma+1)/(\gamma-1)]+1}. \qquad (7.1)$$

Here $V = 1/\rho$ is specific volume; $\gamma = c_p/c_V$ is the ratio of specific heats; Q is the heat of combustion of a unit mass of the system; c_0 is the speed of sound in the initial mixture.

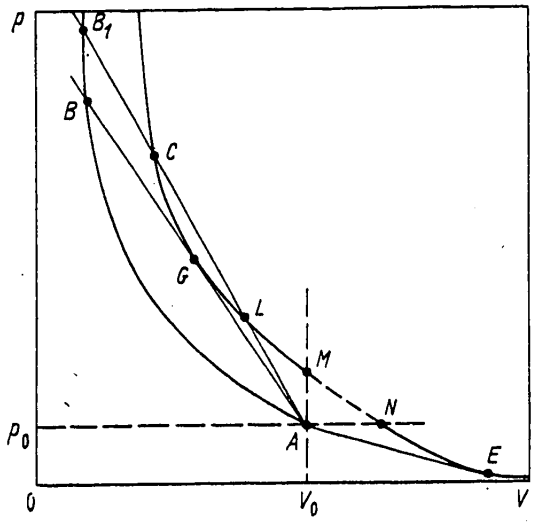

Fig. 7.2. Hugoniot adiabat

The condition of uniqueness of the detonation rate is demonstrated in Ref. 9, and has come to be called the Chapman-Jouguet rule:

$$(p - p_0)/(V_0 - V) = -(\partial p/\partial V)_S. \tag{7.2}$$

This rule implies that *normal* detonation corresponds to the minimum velocity D of all posible velocities, which is shown on the curve of p(V) (see Fig. 7.2) by the Michelson line AB tangent to the Hugionot curve CMNE at point G, known as the Jouguet point. It is typical of the process that in the state corresponding to point G, the detonation rate is equal to the sum of the flow velocity and the rate of propagation of the disturbance in the blast products, i. e.

$$D = u + c. \tag{7.3}$$

In addition to the mode of normal detonation corresponding to line AB tangent to the adiabatic curve of the detonation products, there are two other detonation modes described by curve CM: *overdriven* (CG) and *underdriven* (GM) detonations. For the former mode $u + c > D$, and for the latter $u + c < D$.

According to the *classical one-dimensional theory of detonation* [Ref. 10, 11], after the initial mixture has been compressed by the shock wave, its state corresponds to point B (see Fig. 7.2) in the case of normal detonation, and to point B_2 in the mode of overdriven detonation. Thereafter in the course of the chemical reaction the state of the medium shifts along Michelson curve BG or B_1C. States described by points G or C respectively correspond to completion of the chemical reaction. Thus the pressure should increase at points B or B_1.

The detonation wave theory that assumes the presence of a smooth wave front is based on solution of one-dimensional equations of gas dynamics and chemical kinetics.

There is a departure from this one-dimensional model in what is called *spin* detonation [Ref. 12]: the phenomenon of helical motion near the wall of a tube on the part of a single focus of a chemical combustion reaction, this focus being formed upon splitting of the wave front [Ref. 13]. Spin detonation always occurs at the limits of propagation of the detonation wave [Ref. 14].

The limits of propagation of the detonation are critical initial conditions with respect to pressure p_0 or density ρ, explosive charge diameter d, and also with respect to the concentration of components and the composition of the initial mixture, such that a change in these parameters either toward a reduction in pressure or diameter, or toward an initial mixture that is richer or leaner in the fuel component, makes it impossible for the detonation process to propagate.

According to the classical concept, the detonation wave should have a flat, smooth front far from the limits of propagation. However, the results of high-resolution photography and the wake method under these conditions have shown [Ref. 15, 16] an *inhomogeneous high-frequency structure* of real detonation waves with periodic inhomogeneities in the uneven leading edge of the wave.

Spin detonation close to its limit of propagation corresponds to the wake print of Fig. 7.3a [not included in the translation] with a thickened helical wake of

only one combustion focus moving with a trajectory at an angle χ to the generatrix of the detonation channel. With increasing distance from the limits of propagation there is a stepwise restructuring of the process: instead of a single combustion focus in the detonation front, there are 2n (n = 1, 2, 3...) combustion foci moving in contrary motion over the front with spacing Δx, undergoing collisions and reflections. A time photoscan gives the frequency of pulsations of the process:

$$\nu = D/\Delta x. \tag{7.4}$$

It is convenient to characterize such a periodic process by the *detonation mode*

$$\Omega = \nu/\nu_0 \ (\Omega \approx n), \tag{7.5}$$

where ν_0 is the minimum frequency of pulsations in the near-limit region of existence of the detonation wave with $\Omega \approx n - 1$. The spacing of the pulsations decreases with an increase in the initial pressure p_0 of the mixture or in its reactivity, e. g. by changing the chemical composition (Fig. 7.4) [Ref. 15-19]. Here the results of extrapolation of data of Ref. 20 correspond to $\Delta x \approx 5 \cdot 10^{-3}$ and $2 \cdot 10^{-3}$ mm, and $\nu \approx 7 \cdot 10^8$ and $11 \cdot 10^8$ Hz.

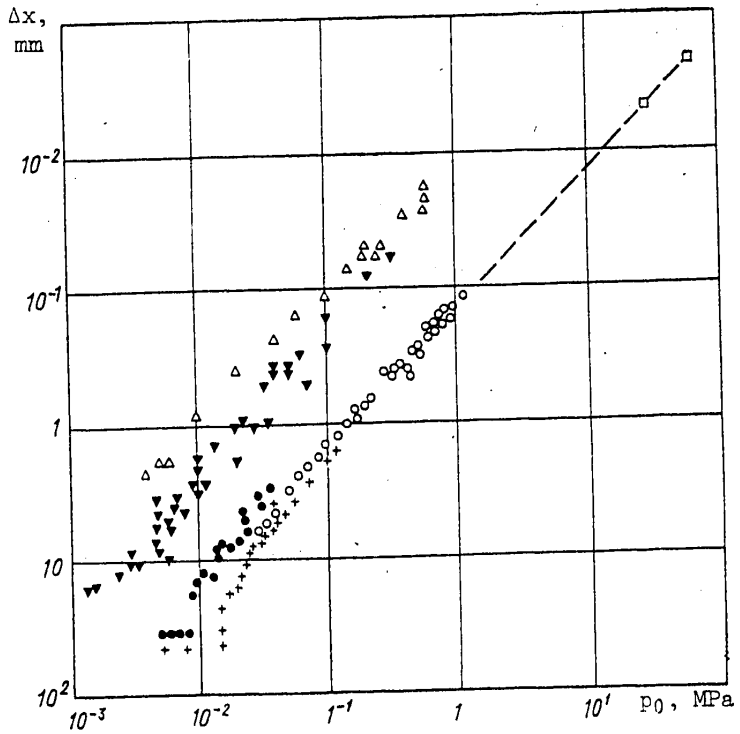

Fig. 7.4. Scale of pulsations Δx as a function of initial pressure p_0 of explosive mixtures $2H_2/O_2$ (○ [18], + [15, 16] ● [19]); $2C_2H_2/O_2$ (▼ [17-19]); C_2H_2/O_2 (△ [18]); $2H_2/O_2$ (□--extrapolation of data of Ref. 20)

Pulsations also occur in spherical detonation waves [Ref. 20], which is further evidence of the general nature of the pulsating mechanism as a property of detonation waves.

One of the peculiarities of detonation is the phenomenon of *discreteness* of the pulsation spacing Δx, frequency ν and other parameters that characterize the structure of the detonation wave as functions of initial pressure p_0.

Analysis of sequences of Δx for successive n in Ref. 22 gave an expression for the discrete spectrum of Δx in the form

$$\pi d/\Delta x = 1/n + \zeta_* (1 + 1/n)(n - 1), \; n = 1, 2, 3, \qquad (7.6)$$

Here $\zeta_* = \tan(\chi)_{\min}$, i. e. the tangent of the smallest angle χ reached far from the detonation limits.

Each of the intersecting lines on the wake prints of Fig. 7.3b, c [not included in the translation] in Ref. 15, 16 is interpreted as a trajectory of a so-called *kink*. The kink was examined in Ref. 23 in the form of three intersecting shock discontinuities: an *oblique* compression shock, a *head-on* shock wave normal to the generatrix of the detonation channel, and a shock wave that moves *tangentially* to the head-on shock wave. Gasdynamic calculation of such a model, which is the *Mach configuration*, leads to the necessity of existence of a fourth discontinuity as well: a *tangential discontinuity* emanating from the point of intersection of the other three, the *triple point*.

And indeed, a triple point delineates each of the wake lines of the kinks [Ref. 24]. The space structure of an actual detonation wave for the case with n = 2 recorded on the wake print of Fig. 7.3b [not included in the translation] is graphically shown in Fig. 7.5 [Ref. 24] for three successive times t_0, t_1, t_2. Concavity of the

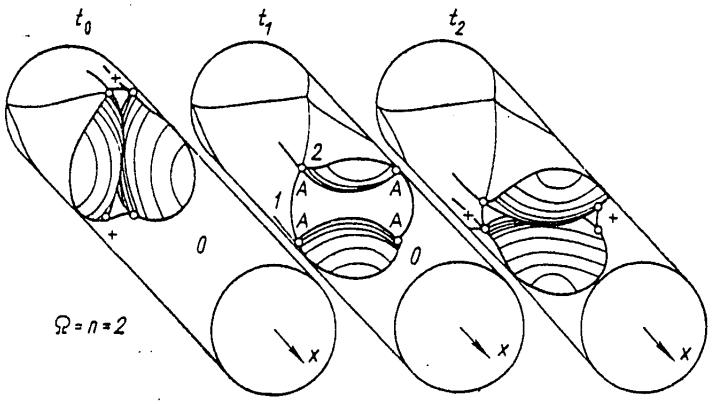

Fig. 7.5. Diagram of three-dimensional structure of detonation for $\Omega \approx n = 2$: light lines are the trajectories of triple points; heavy lines are shock discontinuities; circles indicate the triple points A; 0, 1, 2 -- states of the gas: initial, and behind oblique and head-on compression shocks respectively

wave front is replaced by convexity at collisions of triple points marked with the crosses. Pulsating behavior of the leading edge of a detonation wave has also been observed in Töpler schlieren photographs of the process of detonation in a flat

channel [Ref. 25, 17]. However, as shown in Ref. 25, the flow structure behind the leading edge for detonation at low n is still more complicated, and includes a *transverse detonation wave* suggested in Ref. 26 for spin detonation, experimentally observed in the structure of this detonation in Ref. 27-29, and studied in Ref. 30-32.

Flat Mach configurations in a detonation wave and their collision with one another were first analyzed by the method of *shock and detonation polar curves* in Ref. 24, 33 and 34. To do this, equations were derived that relate the relative pressure change ΔP in the i-th shock, $\Delta P = (p_i - p_0)/p_0 = \Delta p/p_0$, to the angle of deflection η of the flow behind the shock:

for the detonation polar curve

$$\operatorname{tg}\eta = \frac{\Delta P}{\gamma M^2 - \Delta P}\sqrt{\frac{M^2(1-q/\Delta P)}{\Delta P/(\mu^2+1)+1} - 1} \tag{7.7}$$

[M is the Mach number, $q = Q/E_0 = Q(\gamma-1)(p_0/\rho_0)^{-1}$ is the effective energy release as a fraction of the internal energy of the gas, $\mu^2 = (\gamma-1)/(\gamma+1)$];

for the shock polar curve

$$\operatorname{tg}\eta = \frac{\Delta P}{\gamma M^2 - \Delta P}\sqrt{\frac{M^2}{\Delta P/(\mu^2+1)+1} - 1}\,. \tag{7.8}$$

Solution showed that for detonation with $\Omega > 1$, collisions of Mach configurations and the resultant formation of new pulsations in the wave should be important. However, the actual process of interaction of perturbations in the detonation wave far from the limits of propagation is even more complicated than that usually considered in the plane model, and involves the influence of a *volumetric effect* on the structure of the detonation front [Ref. 35]. What is really important is that the process is three-dimensional, and that the most intense sources of disturbances that renew pulsations with Mach configurations in the wave are points of "triple" or higher multiple collisions of the Mach configurations. As a result, the pulsation multiplication factor

$$K = 1 + [(1 + N)/(n^* + N)] \tag{7.9}$$

at a sufficiently large number of initial pulsations N approaches two ($n^* = 3$ for detonation in channels of circular cross section, $n^* = 5$ for spherical detonation). The feasibility of such multiplication is implied by the reaction-kinetic data of a detonating medium [Ref. 21]. When the number of pulsations in the wave is small ($<n^*$) they may multiply by the formation of new triple points when there is an uneven change in the intensity of the discontinuities making up the Mach configuration [Ref. 36].

The question of *localization of controlling factors of the combustion zone* is an important one for an understanding of the detonation mechanism. Ref. 37 suggests a mechanism of chemical reaction under conditions of adiabatic explosion where the induction zone is a compression shock in which a few collisions between atoms or

molecules lead to chemical conversion of a small part of the explosive, and this brings about conditions for the concluding stages of the reaction. Hence we can assume that during detonation there is a thin layer (a shock-wave film) in which combustion foci are imbedded. That such a reaction zone structure is present in the detonation wave is demonstrated by methods of correlation analysis, experimental investigation of disturbances of the fine structure of spin detonation and comparison of the resultant data with calculated dimensions of the zone of vibrational relaxations of molecules [Ref. 38, 39]. The controlling factors of the combustion zone during detonation are localized in the narrow forward layer of the detonation wave with thickness of the order of the size of the zone of vibrational relaxations of the mixture; consequently, the scale of detonation pulsations may also reach values of this same order of magnitude.

§7.2. "Optical" Properties of Detonation Waves, and the Phase Nature of Their Propagation

In accordance with Fig. 7.5, the detonation wave front can be treated as consisting of elementary fronts that oscillate about some average position propagating at constant velocity. The interactions between neighboring elementary fronts are sources of new fronts. If the initial explosive is isotropic, the propagation of such a wave front should conform to laws of geometric and physical optics.

On this basis, the Fermat analytical principle and the Huygens-Fresnel principle can be applied to the process of propagation of detonation waves in an inorganic medium [Ref. 40].

The first of these states that propagation of a wavefront f in an isotropic medium from point $P_1(x_1,y_1)$ to point $P_2(x_2,y_2)$ corresponds to the extremum value of the integral

$$T=\int_{P_1}^{P_2}\frac{ds}{D(x,y)}, \tag{7.10}$$

where T is the time required for passage of the section of wave front from P_1 to P_2 and s is the length of arc of the trajectory of a point of the wave front.

The integral curve is determined from the differential equation of Euler for the extremum

$$\frac{d}{dx}\frac{y'}{D(x,y)\sqrt{1+(y')^2}}+\frac{\sqrt{1+(y')^2}}{D^2(x,y)}\frac{\partial D(x,y)}{\partial y}=0. \tag{7.11}$$

The constants of general solution y (x, C_1, C_2) are determined from the conditions

$$\left.\begin{aligned}y_1&=y(x_1,C_1,C_2),\\y_2&=y(x_2,C_1,C_2).\end{aligned}\right\} \tag{7.12}$$

In many cases the Fermat principle reduces to simple algebraic expressions for conditions of minimum time of propagation of the wave fronts, as shown for example

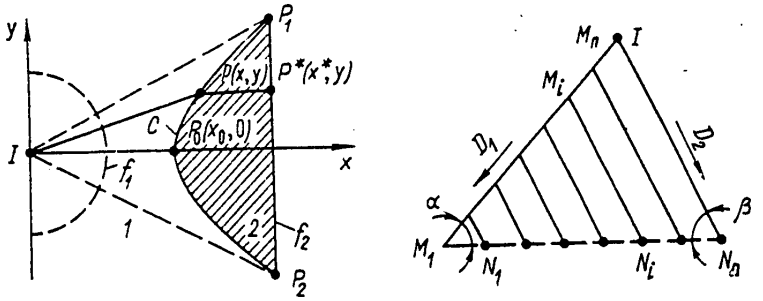

Fig. 7.6. Examples of application of the Fermat principle to the detonation process (detonation collimators): a--with two continuous explosive media 1 and 2 ($D_1/D_2>1$); b--with separate explosive channels

in Fig. 7.6a, b. In the two-dimensional case, for simultaneous emergence of all points of the detonation front f_1 emanating from a single initiation point I at straight line P_1P_2 (see Fig. 7.6a) when a compound charge is used with two media 1 and 2 having different detonation rates D_1 and D_2, the shape of the boundary between media 1 and 2 is calculated from the equations:

$$T = \sqrt{x^2+y^2}/D_1+(x^*-x)/D_2; \tag{7.13}$$

$$T_{\min} = x_0/D_1 + (x^* - x_0)/D_2. \tag{7.14}$$

When $D_1/D_2>1$, the boundary C between the media is a hyperbola. Such a generator of a straight wave front (collimator) may be important for chemical detonation lasers as a device for simultaneous input of gaseous detonation products into the optical cavity. The detonation wave generator shown in Fig. 7.6b can serve the same purpose.

Here the line M_1M_n is a channel filled with a detonating medium having detonation rate D_1, and the lines M_iN_i ($i=1, 2,\ldots, n$) are channels with a medium detonating at rate D_2. The condition of simultaneous arrival of the detonation fronts in all channels M_iN_i at the level of straight line M_1N_n is

$$T=\frac{IM_i}{D_1}+\frac{M_iN_i}{D_2} \text{ or } T=\frac{IM_1}{D_1}\Big|_{M_iN_i=0}=\frac{IN_n}{D_2}\Big|_{IM_i=0}, \tag{7.15}$$

whence

$$D_1 = D_2 \sin\beta/\sin\alpha. \tag{7.16}$$

If $\alpha=\beta$, then $D_1=D_2$ and $IM_1=IN_n$. An example of realization of such a scheme is linear detonation generators filled with gaseous explosive and made in the form of detonation channels of the same length [Ref. 3]. A device based on an analogous principle focuses the detonation wave by using hollow cylindrical shaping lenses made in the form of a stack of cylindrical diaphragms that are roughened in the central part and smooth on the edges.

A number of wave generator designs based on the Fermat principle are shown in Fig. 7.7a-r [Ref. 40]. Shown are: a, b, i, o -- designs with focusing of detonation

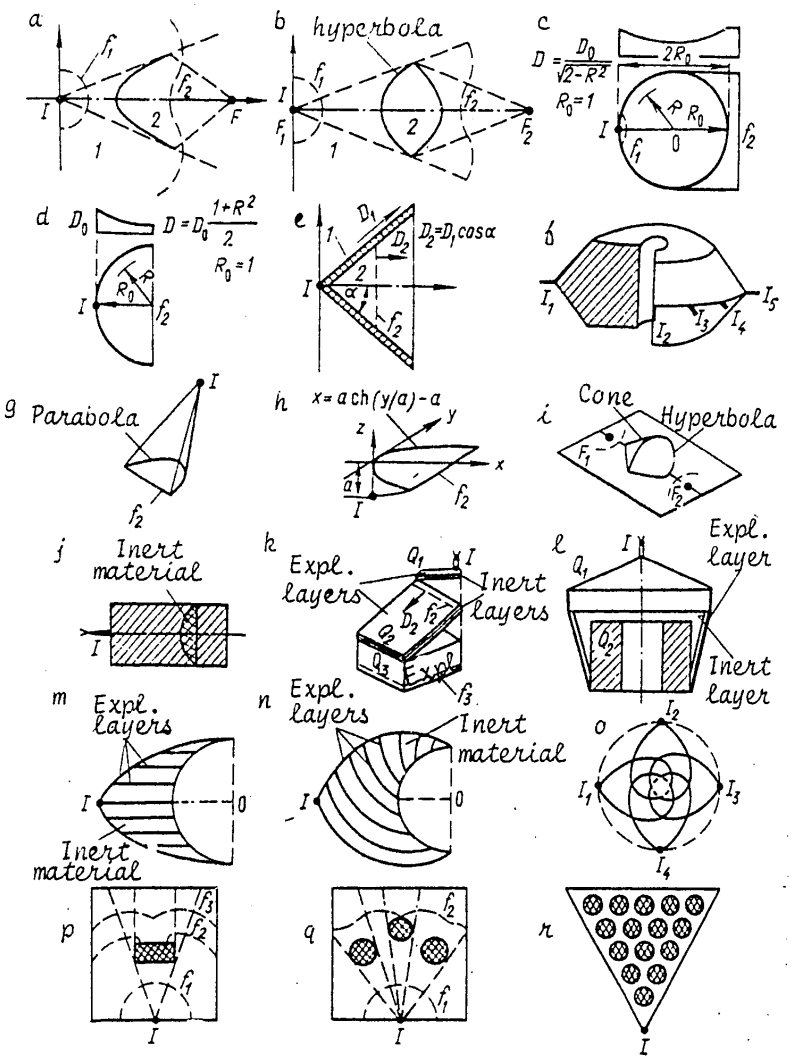

Fig. 7.7. Diagrams of detonation wave generators

fronts at a point; c, d, e, g, h, r -- linear detonation front; f, l -- focusing of detonation on the axis of the system; j, k -- generation of a planar detonation front; m, n -- generation of a curvilinear detonation front; p, q -- diffraction of detonation fronts. Designs p, q and r are based on the diffraction properties of detonation waves occasioned by the physical rather than the geometric optics of the system.

Within the framework of physical optics of detonation, the Huygens-Fresnel principle enables construction of the detonation wave front for some instant if the wave front is known at a preceding time. Such a construction is based on the fact that each point of the medium reached by the wave front is treated as a new source of oscillations.

The regions of collisions of kinks -- triple Mach configurations -- act as such new sources of pulsations in a detonation wave. The sources of new pulsations in the detonation front are responsible for the *phase nature* of propagation. After each collision of kinks, a new pulsation arises with parameters that depend only on the initial conditions. This can explain the effect of detonation wave diffraction that takes place for example when detonation waves flow around corners, or the effect of refraction on interfaces [Ref. 41]. The pattern of phase propagation of a detonation front is shown schematically in Fig. 7.8, where the numbers 1-8 denote positions of pulsation fronts corresponding to times from t_1 to t_8. The heavy lines depict regions of maximum energy release that renew pulsations in the wave.

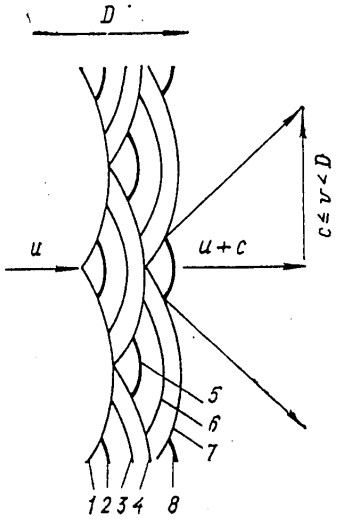

Fig. 7.8. Diagram of phase propagation of a detonation wave. For tangential velocity of development of pulsation $c \leqslant v < D$ ($v = D$ -- spin detonation, $n = 1$)

Phase propagation of such a structure at velocity D, as can be seen from Fig. 7.3b, c [not included with the translation] forms patterns similar to those observed in hydrodynamics during flow of shallow water (motion in a field of gravity of an incompressible liquid with a free surface and with depth of a layer of this liquid that is small compared with the characteristic dimensions of the flow). It is known (see for example Ref. 42) that wave processes on shallow water are described by the Kortweg – de Vries equation

$$\psi_t + D\psi_x + b\psi_{xxx} + \psi\psi_x = 0 \qquad (7.17)$$

(D is wave velocity, $b = Dl^2$, l is the scale factor). Special cases of this equation for propagation of small and finite perturbations in a medium with a chemical reaction were considered in Ref. 43.

Long-wave perturbations for the case of acoustic detonation in reacting media have been analyzed to derive an equation that describes the structure of a finite perturbation propagating in one direction in a reacting medium. The general system of equations of a reacting gas presented in §1.7 is reduced in Ref. 43 to a single equation from which the Kortweg - de Vries - Burgers equation is derived for waves on the surface of a liquid with positive viscosity in limiting cases $\tau_{ch}/T < 1$ (τ_{ch} is the time of the chemical reaction, T is the characteristic period of the initial disturbance). In this connection, condition $\tau_{ch} \sim 1$ corresponds to medium frequencies, while $\tau_{ch} > 1$ corresponds to the high-frequency approximation. The analysis implies that when a long-wave perturbation propagates through a medium with an exothermic reaction, it increases in amplitude and decreases in duration, i. e. signal amplification takes place.

The frequency response of wave bursts in each of the possible detonation modes for given initial conditions of the explosive medium can be derived by the energy method and the formalism of elementary quantum mechanics [Ref. 42] in which the state of the medium is described by a normalized function $\psi(x,t)$ that satisfies an equation of Schrödinger type as a special case of (7.17). Such a set of possible

normal frequencies of the detonation process can be obtained in the following way [Ref. 44]. Energy release Q(T) is accounted for by the equation of the second law of thermodynamics:

$$Tds = dT - (\gamma - 1)Td\rho/\rho = (1/c_V)Q(T)dt. \tag{7.18}$$

Here $s = S/c_V R$ is the dimensionless specific entropy.

To simplify the problem, we will assume that Q is a linear function of T, i. e. $Q(T) = (\partial Q/\partial T)T$, where $\partial Q/\partial T = \text{const}$. Then from equation (7.18)

$$T = T_a \exp(\omega t), \tag{7.19}$$

where $\omega = ds/dt = \frac{1}{c_V}\frac{\partial Q}{\partial T} = \frac{1}{\tau}$; τ is the ignition induction period; $T_a = T_0(\rho/\rho_0)^{\gamma-1}$ is flash point.

Each wave burst in the detonation wave is described on the average by the transported mass m, momentum $\vec{p} = m\vec{u}$ and energy E in phase space $\vec{r}$, t. By analogy with quantum mechanical formalism [Ref. 42] we write

$$ih_D \frac{\partial \psi}{\partial t} = -\frac{h_D^2}{2m}\nabla^2\psi + \left(\frac{\gamma T_a e^{\omega t}}{\gamma - 1} - \int Tds\right)\psi. \tag{7.20}$$

Here h_D is a constant that depends on the thermodynamic properties of the medium, $\psi(\vec{r},t)$ is the wave function that characterizes the wave burst in the detonation front.

To determine the constant h_D, we use one of the solutions of equation (7.20) in the form of a plane wave

$$\psi(\mathbf{r}, t) \sim \exp[-(i/h_D)(Et - \mathbf{pr}) - is_0(t)], \tag{7.21}$$

where s_0 is the initial phase of the wave.

The law of conservation of energy in such a wave is

$$E = mu^2/2 + [T_a/(\gamma - 1)]\exp \omega t. \tag{7.22}$$

We determine constant h_D by substituting (7.21) in equation (7.20). We get

$$E + h_D ds_0/dt = mu^2/2 + [T_a/(\gamma - 1)]\exp(\omega t) + T_a. \tag{7.23}$$

From expressions (7.22) and (7.23) we get

$$ds_0/dt = T_a/h_D = \omega \text{ or } h_D = T_a/\omega. \tag{7.24}$$

In a physical sense, the initial phase of the wave s_0 coincides here with the idea of specific entropy, and therefore when a new wave burst is formed by a discontinuity, not only the phase changes, but the entropy as well.

Now let us verify whether equation (7.20) satisfies the principal laws of conservation of mass and momentum. The expressions for these laws can be obtained from

expression (7.20) by averaging. For instance the law of conservation of mass

$$\frac{\partial |\psi|^2}{\partial t} = -\operatorname{div} \mathbf{j} \tag{7.25}$$

is written as $\frac{\partial}{\partial t}\int |\psi|^2 d\mathbf{u} = -\operatorname{div}\int \mathbf{j} d\mathbf{u}$, where $|\psi|^2 \sim \rho/\rho_0$, and $\vec{j} = \frac{ih_D}{2m}(\psi \nabla \psi^* - \psi^* \nabla \psi)$ is the probability flux density. Integration with respect to physical volume $\vec{r}$, t gives the averaged law of conservation of mass. The law of conservation of momentum is written as

$$\frac{\partial I_i}{\partial t} = -\frac{\partial}{\partial x_j}\hat{\Pi}_{ij}. \tag{7.26}$$

Here the momentum probability flux density tensor is

$$\hat{\Pi}_{ij} = \frac{h_D^2}{4m}[(\nabla_i \psi \nabla_j \psi^* + \nabla_i \psi^* \nabla_j \psi) - (\psi \nabla_i \nabla_j \psi^* + \psi^* \nabla_i \nabla_j \psi)] + \delta_{ij}(p_0/\rho_0)\gamma \exp(\omega t)/(\gamma - 1). \tag{7.27}$$

Analogously upon integration of (7.26) with the use of (7.21) we get an expression for the law of conservation of momentum.

Let us analyze the structure of the detonation front on the basis of equation (7.20). To do this, we consider the two-dimensional problem with longitudinal transport of wave energy in the direction of the x-axis, and along the y-axis in the transverse direction. We will look for periodic solutions with respect to y, and derivatives with respect to x, t in the form

$$\psi = \psi(x, t) \exp(iky), \tag{7.28}$$

where $k = 2\pi/\Delta y$ is the wave number, Δy is the transverse scale of the pulsations in the detonation front. From (7.20) we get

$$ih_D \frac{\partial \psi}{\partial t} = -\frac{h_D^2}{2m}\frac{\partial^2 \psi}{\partial x^2} + \left[T_a\left(\frac{e^{\omega t} + \gamma - 1}{\gamma - 1}\right) + \frac{k^2 h_D^2}{2m}\right]\psi. \tag{7.29}$$

Let us look for self-similar solutions of (7.29) for steady-state motion by a procedure analogous to that used in the theory of steady-state shock waves [Ref. 45]:

$$\psi(x, t) = \psi(x - Dt).$$

Making the self-similar substitution $\frac{\partial}{\partial x} \to -\frac{1}{D}\frac{\partial}{\partial t}$, we get

$$\frac{\partial^2 \psi}{\partial t^2} + \frac{2imD^2}{h_D}\frac{\partial \psi}{\partial t} - \frac{2mD^2}{h_D^2}\left[T_a \frac{\exp(\omega t) + \gamma - 1}{\gamma - 1} + \frac{k^2 h_D^2}{2m}\right]\psi = 0 \tag{7.30}$$

To solve this equation for eigenvalues, we use the conditions $|\psi|^2_{t=0} = 1$, $|\psi|^2_{t\to\infty} = 0$.

After the substitution

$$\psi(x, t) = \Phi(x, t) \exp(-imD^2 t/h_D) \tag{7.31}$$

(7.30) is transformed to

$$\Phi''_{tt}-\Phi\left(\frac{2mD^2}{h_D^2}\right)\left[\frac{T_a(e^{\omega t}+\gamma-1)}{\gamma-1}-\frac{1}{2}mD^2+\frac{k^2h_D^2}{2m}\right]=0. \qquad (7.32)$$

We solve this equation at $\Phi_{t=0}=1$, $\Phi_{t\to\infty}=0$. The solution can be represented as a cylindrical function of the imaginary argument $K_\nu(z)$, and then

$$\psi(x,t)=\exp\left[-\frac{imD^2}{h_D}\left(t-\frac{x}{D}\right)\right]CK_\nu\left\{a\exp\left[\frac{\omega}{2}\left(t-\frac{x}{D}\right)\right]\right\}, \qquad (7.33)$$

where $a=\frac{2D}{\omega h_D}\left(\frac{2mT_a}{\gamma-1}\right)^{1/2}$, and C is found from the normalization condition

$$\int_{-\infty}^{+\infty}|\psi|^2dv=1.$$

From the solution we get a dispersion relation for the pulsating process

$$\Omega=\frac{2D}{\omega}\left(\frac{2mT_a}{h_D^2}+k^2-m^2\frac{D^2}{h_D^2}\right)^{1/2}. \qquad (7.34)$$

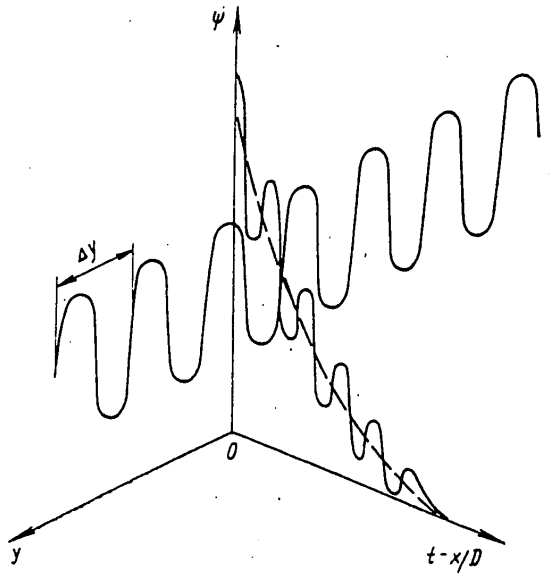

Fig. 7.9. Model of wave burst of the detonation process

Fig. 7.9 shows the resultant model of the wave burst in the form of the function ψ in coordinates y vs. t - x/D at a fixed value of Ω. Estimation of the time scale of the pulsation with respect to x in the detonation wave gives

$$\Delta t \simeq \frac{2}{\omega} \ln \left[\frac{8mD^2}{(\gamma-1)T_a} \right]^{-1/2}. \tag{7.35}$$

Using expression (7.33) for the wave function ψ and taking the representation of energy in accordance with formula (7.22) in operator form, we get after averaging

$$\bar{E} = \rho_0 T_a + \rho_0 D^2 \left[1 - \frac{\Omega^2 T_a^2}{4\rho_0^2 D^4} \right]. \tag{7.36}$$

This implies for example that for $\Omega > \bar{\varepsilon} - 1$ the Mach number of the detonation wave is

$$M = \left[\frac{\Omega}{2\gamma} + \frac{\bar{\varepsilon}-1}{2\gamma} \right]^{1/2} (\rho/\rho_0)^{\frac{\gamma-1}{2}}, \tag{7.37}$$

where $\bar{\varepsilon} = Q\bar{\mu}/RT_a^{(0)}$; $Q = \bar{E}/\rho_0$.

If the spectrum of detonation frequencies is represented in accordance with (7.5) as $\nu = \Omega\nu_0$, where ν_0 is the minimum frequency of pulsations in the near-limit region of existence of the detonation, and the specific energy release of the chemical reaction of ignition, the flash point and the average molar mass of the mixture are taken as Q, $T_a^{(0)}$ and $\bar{\mu}$ respectively, then relation (7.37) qualitatively follows the spectrum of the experimentally observed relation between the longitudinal mode and the Mach number M. This can be seen for example from a comparison on Fig. 7.10 of the experimental discrete detonation frequency spectrum (shown by the vertical lines and the broken curve; the cross shows the value calculated from the data of Ref. 18) with the results calculated by relation (7.37) (short lines and dot-and-dash curve) for a stoichiometric oxygen-hydrogen mixture.

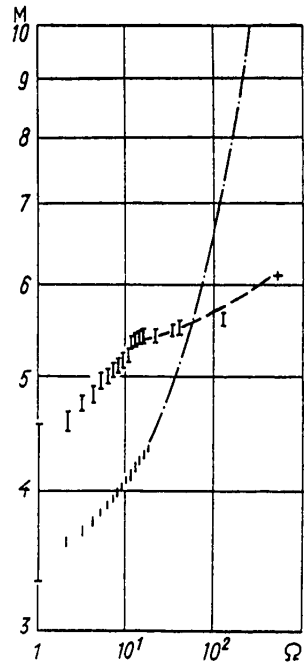

Fig. 7.10. Comparison of experimental and theoretical discrete detonation spectra

Although the comparison of theory and experiment on Fig. 7.10 shows only the qualitative correspondence between the directions of changes in parameters, nevertheless the theoretical concept that has been developed can serve as an illustration of the phase process of detonation wave propagation based on the "physical optics" of detonation waves. A condition of applicability of such consideration, of course, must be the fact that the frequency of the process $\nu = \Omega\nu_0$ must be less than the natural frequency of vibrations of the molecules.

The fundamental harmonics of detonation pulsations were also found in Ref. 46 by examining

periodic instability as a theoretical basis of the internal property of detonation -- pulsation wave structure.

A detailed mechanism of phase propagation of detonation is proposed in Ref. 47. It is based on equality of the average tangential velocities of collision D_2 and reflection D_3 of triple points A treated as *ignition points* (*ignition lines*) in the relaxation layer (film).

Actually, conditions of stable existence of detonation should be

$$D_3/D_2 = 1, \tag{7.38}$$

$$M_2 = D_2/c_1 \gtrsim 1, \tag{7.39}$$

where the latter condition means that the tangential velocity of point A is close to the speed of sound in the initial shock-compressed gas in state 1.

Suppose that shock waves collide, and Chapman-Jouguet waves are reflected. When condition (7.38) is satisfied, the conservation equations yield

$$M_2^2 = \frac{\gamma_1+1}{2\gamma_1}\,\frac{2\gamma_3(3-\gamma_1)+\gamma_1(4-\gamma_1)-3}{\{[\gamma_3(\gamma_1-1)+2\gamma_1(\gamma_1-2)]^2-4\gamma_1(\gamma_1-3)[2\gamma_3(\gamma_1-3)+} \rightarrow$$

$$\rightarrow \frac{}{+\gamma_1(\gamma_1-4)+3]\}^{1/2}-\gamma_3(\gamma_1-5)+\gamma_1^2-3} + \frac{\gamma_1-1}{2\gamma_1}. \tag{7.40}$$

In Ref. 38, 47, the motion of ignition point A during detonation is treated in a coordinate system fixed to this point as supersonic flight of a pointed wedge in a gas mixture with an exothermal reaction in the wedge. Let us represent the flow in the near vicinity of the point A as shown in Fig. 7.11. Since the collisions of ignition points (lines) are symmetric relative to the directed average velocity D, the absolutely rigid wall x-x can be taken as the axis of symmetry of the process. We will take AB as the incident wave front of oblique Mach reflection, AN as the Mach disk of this reflection, the dot-and-dash line indicating the direction of "flight" of ignition point A with dispersal of the products of isothermic reaction to both sides of this line at angles $\phi_1 \approx \phi_2$, and AK indicating the limit of dispersal in the form of a compression shock that changes into a Mach wave. In order for an oblique Mach reflection to form again after collision with x-x, the condition

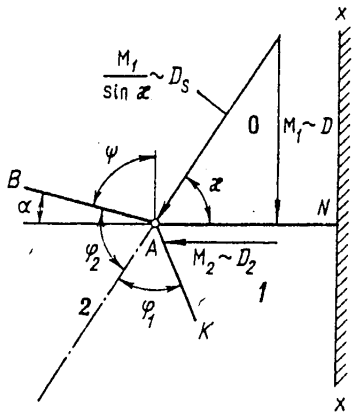

Fig. 7.11. Diagram of flow in the vicinity of an ignition point in the detailed structure of a detonation wave

$$\psi \geqslant \operatorname{arcctg}\sqrt{\frac{\gamma_2+1}{2}\frac{\rho_0}{\rho_2}\left(1-\frac{\rho_0}{\rho_2}\right)}. \tag{7.41}$$

must be satisfied.

Taking the equal sign, and assuming that the transition 0-2 is strong enough that $\rho_0/\rho_2 \approx (\gamma_2-1)/(\gamma_2+1)$, we get from (7.41)

$$\psi = \operatorname{arcctg}\sqrt{(\gamma_2-1)/(\gamma_2+1)}. \tag{7.42}$$

For angles ϕ_1 and ϕ_2 we have

$$\varphi_1 \approx \varphi_2 = \alpha + \varkappa = \frac{\pi}{2} - \psi + \varkappa \approx \varphi, \tag{7.43}$$

where

$$\varkappa = \operatorname{arctg}(D/D_2) = \operatorname{arctg}(M_1 c_0/M_2 c_1); \tag{7.44}$$

$$c_0/c_1 = \{(\gamma_1 + 1)^2 (\gamma_0 - 1)/2\gamma_1 (\gamma_1 - 1)[2 + (\gamma_0 - 1)M_1^2]\}^{1/2}. \tag{7.45}$$

From (7.44 and (7.45) with consideration of (7.43) we get

$$\varphi = \operatorname{arctg}\left\{\left(\frac{\gamma_1+1}{m} + \mu_2\right) \Big/ \left[1 - \frac{(\gamma_1+1)\mu_2}{m}\right]\right\}, \tag{7.46}$$

where

$$m = M_2\{2\gamma_1 (\gamma_1 - 1)[1 + 2/M_1^2 (\gamma_0 - 1)]\}^{1/2};$$
$$\mu_2 = [(\gamma_2 - 1)/(\gamma_2 + 1)]^{1/2}.$$

For the pressure in region 2 we have [Ref. 48]

$$p_2 = \frac{2}{n_2+1} \rho_0 D_3^2 \sin^2 \varphi, \tag{7.47}$$

which with consideration of the fact that $D_S = D/\sin\kappa$ (see Fig. 7.11) becomes

$$n_2 = \gamma_2 \frac{1 + (\gamma_2 - 1) q/2\gamma_2}{1 + (\gamma_2 - 1) q/2} \quad \left(q = \frac{2Q}{p_2/\rho_2}\right). \tag{7.48}$$

Here, in accordance with Ref. 48,

$$\frac{p_2}{p_0} = \frac{2\gamma_0 M_1^2}{n_2+1} \frac{\sin^2 \varphi}{\sin^2 \varkappa}. \tag{7.49}$$

In the given calculations, p_1/p_0 and ρ_1/ρ_0 are related to M_1 by the respective formulas

$$\frac{p_1}{p_0} = \frac{\gamma_0 M_1^2 + 1}{\gamma_1 + 1} + \left[\left(\frac{\gamma_0 M_1^2 + 1}{\gamma_1 + 1}\right)^2 + \frac{2\gamma_0 M_1^2 (\gamma_0 - \gamma_1)}{(\gamma_1+1)(\gamma_0-1)} - \frac{2\gamma_0 M_1^2 - (\gamma_1 - 1)}{\gamma_1 + 1}\right]^{1/2}; \tag{7.50}$$

$$\rho_1/\rho_0 = \left\{1 + \frac{\gamma_1+1}{\gamma_1-1}\left[\left(\frac{2\gamma_0 M_1^2}{\gamma_0+1}\right) - \frac{\gamma_0 - 1}{\gamma_0+1}\right]\right\}\left[\frac{4\gamma_0}{\gamma_0^2 - 1} + \frac{2\gamma_0 M_1^2}{\gamma_0+1}\right]^{-1}. \tag{7.51}$$

There are analogous formulas for p_2/p_1 and ρ_2/ρ_1.

From (7.40), (7.44), (7.45) for a stoichiometric hydrogen-oxygen mixture at $\gamma_0 = 7/5$, $\gamma_1 = 8/6$, $\gamma_2 = 9/7$ we get calculated values of $\kappa = 55\text{-}56^\circ$ close to the experimental results at Mach numbers $M_1 = 5\text{-}6$ typical of pulsating detonation.

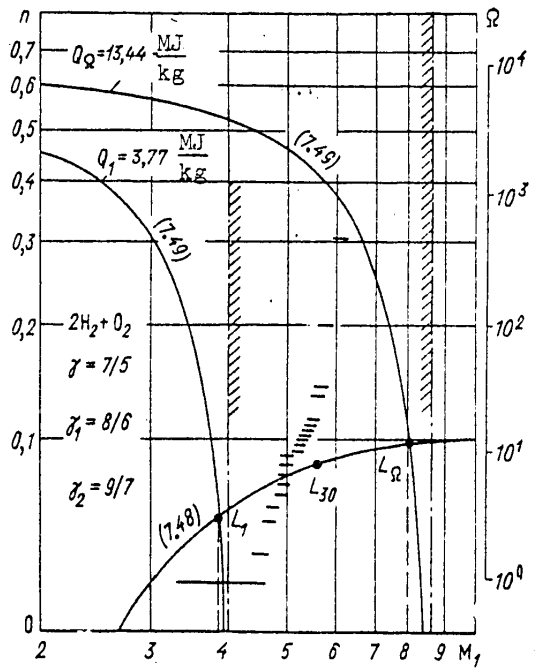

Fig. 7.12. Graphic solution of equations (7.48), (7.49) for $Q_1 = 3.77$ and $Q_\Omega = 13.44$ MJ/kg, and comparison with the limits of the experimental spectrum of detonation frequencies

The Mach number M_1 of the detonation wave in this same mixture can be conveniently determined from the graphic solution of equations (7.48) and (7.49) on Fig. 7.12, which also shows for comparison the experimental spectrum of detonation frequencies in coordinates M_1, $\Omega = \nu/\nu_0$. For pulsating detonation the region of this spectrum on the graph is bounded by the shaded dot-and-dash line. Solutions L_1 and L_Ω of equations (7.48) and (7.49) for $Q_1 = 3.77$ and $Q_\Omega = 13.44$ MJ/kg respectively show little difference from the indicated region of the experimental spectrum of detonation frequencies. Here Q_1 is the energy release for near-limit pulsating detonation with fundamental mode $\Omega = 1$, Q_Ω is the maximum theoretically possible energy release accompanying a chemical reaction in a detonation wave. The point L_{30} corresponds to detonation of a mixture of $2H_2 + O_2$ under normal initial conditions with natural frequency characterized by the mode $\Omega = 30$ and $\nu = 1.5$ MHz.

In the fan of rarefaction waves that is formed in region 2 as the reaction products disperse from ignition point A, the incoming flux may be deflected to the point where compression takes place in region 1 (see Fig. 7.11), and self-regulation is effected by this kind of "feedback". It is by this that the detonation wave

"knows" in what tangential geometry it is propagating: in channels of circular or perhaps rectangular cross section, and at the same time does not "know" the geometry of the space in the direction normal to its flow, for example whether the ends of the channel are closed or open.

§7.3. Overdriven Detonation

Of interest in application to chemical lasers of detonation type is an examination of conditions of overdriven detonation, since it is in just such modes that the effect of direct stimulation of coherent emission has so far been realized [Ref. 4]. Corresponding to modes of overdriven detonation are states on the Hugoniot adiabat lying above the Chapman-Jouguet point, e. g. on curve CG (see Fig. 7.2). Such modes can be realized by preventing the formation of a rarefaction wave behind the detonation wave front, e. g. by using a piston or some other method to compress the reaction products [Ref. 10]. Overdriven detonation is realized for example by a change in the channel geometry tangential to the wave in a narrow tube as detonation passes to it from a wide tube, by setting up an electric discharge current layer in the explosive mixture to act as an impermeable piston that pushes the shock wave [Ref. 49].

Overdriven detonation can also be realized by "driving" the detonation wave out of a high-pressure section into a section with a low-pressure explosive medium that is separated from the high-pressure section by a breakable diaphragm.

Unless they are maintained, overdriven waves have a damped velocity, and in essence should not be considered detonation waves, for which one of the major properties is steady-state propagation under fixed initial conditions.

However, there is another feature of detonation that must be taken into account -- the periodic structure identified by the wake method [Ref. 15]. The presence of such a structure in a reactive medium is evidence of energy release immediately in the wave front, and in particular during overdriven detonation.

From the way that pulsation spacing Δx changes on wake prints for known initial conditions p_0, d_{tube}, one can judge whether overdriven detonation occurs, and can select structures with a smooth front that are of interest for chemical lasers. Fig. 7.13 shows diagrams of such wake prints for some methods of exciting overdriven detonation, and graphs of the change in pulsation spacing Δx as the detonation waves from overdriving are reaching the steady Chapman-Jouguet state on length L_{CG} from the cross section in the detonation channel that corresponds to overdriving at point C of the Hugoniot adiabat until the steady state of detonation is reached, corresponding to point G (see Fig. 7.2). The overdriven detonation mode with velocity D_C was realized both by stimulated excitation (broken curves on Fig. 7.13) and by the natural onset of detonation from the unsteady combination of an accelerated flame G preceded by a shock wave S (solid curves) propagating at velocity D_y.

We can see from these diagrams that chemical detonation lasers can utilize processes shown in diagrams I, III and V on sections corresponding to overdrive compressions beyond the limit values, i. e. downstream from cross section C to points where high-frequency detonation pulsations arise. Use can also be made of the overdriven processes with smooth fronts found in Ref. 52.

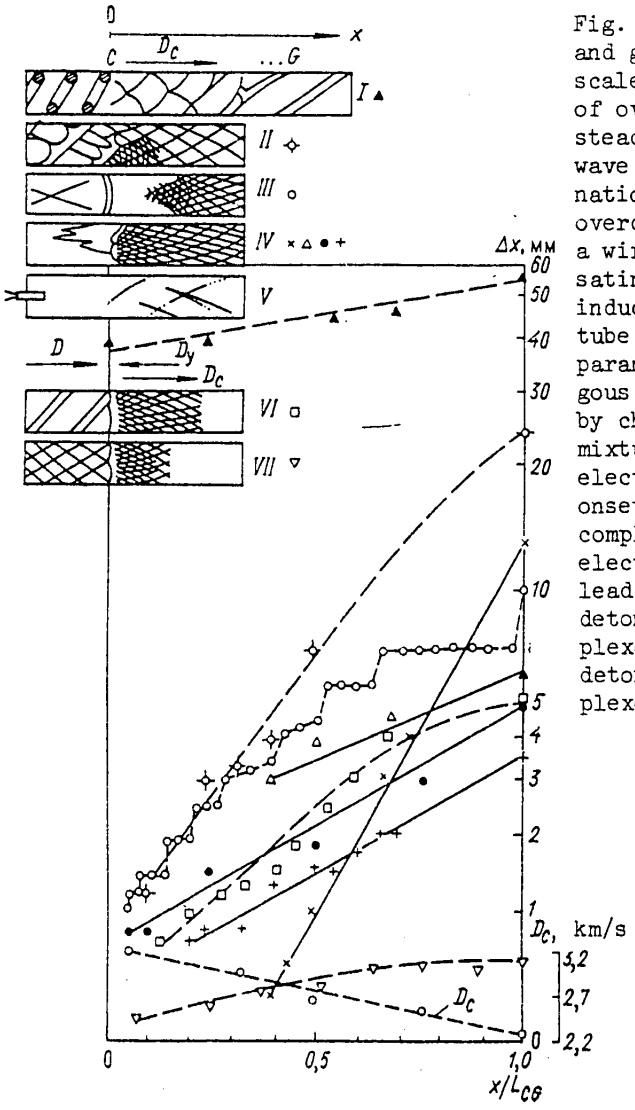

Fig. 7.13. Diagrams of wake prints and graphs of the change in pulsation scale Δx on the length of transition of overdriven detonations to the steady state, L_{CG}: I--spin detonation wave transition of a pulsating detonation artificially produced under overdriving conditions in a tube with a wire helix [Ref. 24, 50]; II--pulsating detonation transition of an induced spin detonation produced in a tube with a helix at fixed initial parameters of the mixture (an analogous result was obtained in Ref. 36 by changing the initial density of the mixture); III--strong initiation by an electric discharge [Ref. 51]; IV--onset of detonation from unsteady G-S complex; V--strong initiation by an electrodetonator or a suspension of lead azide; VI--collision of spin detonation with unsteady G-S complexes; VII--collision of pulsating detonation with unsteady G-S complexes

Mixture	Experiment	p , kPa	d_{tube}, mm	L_{CG}, mm
$CH_4/2O_2$	×	40	20	90
$2H_2/O_2$	▲	13,3	16	400
	⊹	17,3	18	50
	○	26,6	18	800
	△	40	20	30
	◕	53,3	20	40
	+	66,6	20	50
	□	9,3	16	30
	▽	40	16	8

The process by which detonation arises under conditions of overdriving is identical to the process of stimulated emission in lasers and masers, and is characterized by shock wave amplification and coherent energy release (for example, IV on Fig. 7.13) -- called the "swaser" effect in Ref. 53.

§7.4. Mechanisms of Population Inversion in Chemical Detonation Lasers

Pumping the active substance by the energy of the chemical bond. To increase the coefficient of utilization of pumping energy, it is suggested in Ref. 4 that explosion energy be converted directly by dissociation, including by photolysis, impact dissociation or some other chemical reaction through the process of premixing the working substance of the laser with the initial explosive. Such a method of producing a medium with negative absorption factor is based on the fact that any explosive in the initial state can be treated as a medium with population inversion for which the state of the combustion products is a stable state. Inversion upon detonation of an explosive can be realized by a variety of reactions in the detonating explosive medium. Let us consider some of these reactions.

a. *Two-component mixture*: explosive + working (emitting) substance.

For this case, energy conversion is realized as follows. The explosive XY dissociates:

$$XY \rightarrow \sum_{j=1}^{m} (XY_j + \Delta E_j + h\nu_j), \tag{7.52}$$

where the XY_j are products of dissociation of the initial substance; ΔE_j is the kinetic energy of the reaction products; $h\nu_j$ is the energy of a quantum emitted upon dissociation of the intial substance XY into components XY_j; m is the number of terminal products.

Upon explosion, the energy of the products of dissociation is expended on decomposition and emission of the introduced working substance AB:

$$AB + \Delta E_j \rightarrow AB^*; \tag{7.53}$$
$$AB + h\nu_j \rightarrow AB^*. \tag{7.54}$$

AB* in turn may emit a quantum as a result of reactions

$$AB^* \rightarrow A + B^* \rightarrow A + (B + h\nu); \tag{7.55}$$
$$AB^* \rightarrow A + B + h\nu + \Delta E. \tag{7.56}$$

Reaction (7.55) corresponds to emission of a product of dissociation (B*) of the excited AB* molecule, and reaction (&.56) corresponds to conversion of the working substance from the excited to the dispersed state.

Instead of the diatomic working molecule AB, the working substance may contain a monatomic substance A that in the excited state forms a metastable molecule with a dispersed lower state. The reaction scheme for this case is as follows:

$$\left.\begin{matrix} A + \Delta E_j \\ A + h\nu_j \end{matrix}\right\} A^*; \tag{7.57}$$

$$A + A^* \rightarrow A_2^*; \tag{7.58}$$
$$A_2^* \rightarrow A + A + \Delta E + h\nu. \tag{7.59}$$

From an energy standpoint it is more advantageous to use substances with low dissociation potentials such as metal salts in reactions (7.35)-(7.56). On the other hand, reactions (7.57), (7.58) can utilize noble gases or metals such as Zn, Cd and Hg that are capable of forming dispersed molecules as the substance A.

b. *Pure explosive.* The most interesting method of energy conversion is that in which the initial substance XV, one of the fission fragments XY_j and intermediate dissociation fragment XY^j are excited or deactivated according to reactions (7.53)-(7.56) or (7.57)-(7.59).

Let us examine each reaction individually. The initial substance XY dissociates into

$$XY \rightarrow \sum_{j=1}^{m} (XY_j + \Delta E_j). \tag{7.60}$$

Upon collision of the initial substance with fission fragment XY_j, a molecule XY of this substance is excited:

$$XY + \Delta E_j \rightarrow XY^* \tag{7.61}$$

and emits a quantum of light with transition of the molecule to the dispersed state:

$$XY^* \rightarrow XY^1 + XY^2 + h\nu + \Delta E_1 + \Delta E_2. \tag{7.62}$$

As the dispersing fragments interact with each other, they are converted to the terminal products of the dissociation reaction of the initial substance XY, i. e.

$$XY^1 + XY^2 \rightarrow \sum_{j=1}^{m} (XY_j + \Delta E_j). \tag{7.63}$$

The dissociation reaction products XY_j in turn enter into reaction with the initial substance XY, and the chain reaction continues until the initial reserves of substance XY are completely exhausted, the greater part of the energy stored in the substance being converted to emission energy in reaction (7.61). The terminal products of such a reaction have a low temperature since the kinetic energy of the reaction products XY_j is converted to luminous radiation in reaction (7.61).

Another mechanism of transformation of the energy of the chemical bond to luminous radiation is dissociation of the initial explosive XY in accordance with scheme (7.60). One of the fission fragments, for example XY_i that has sufficiently low dissociation energy emits a photon by reaction scheme (7.53)-(7.56), i. e.

$$XY_i + \Delta E_j \rightarrow XY_i^* \rightarrow X_i + Y_i^*; \tag{7.64}$$
$$Y_i^* \rightarrow Y_i + h\nu_i; \tag{7.65}$$
$$X_i + Y_i \rightarrow XY_i. \tag{7.66}$$

Thus the kinetic energy of fission fragments is transformed to luminous emission, and the final chemical makeup of the mixture remains unaltered.

Also of some interest may be the following reaction mechanism that leads to conversion of the energy of the chemical bond to luminous radiation, and that is: the initial explosive is divided into several intermediate fission fragments (taken as two in our case for the sake of simplicity):

$$XY \rightarrow XY^{(1)} + XY^{(2)}. \tag{7.67}$$

The fragments dissociate further into the terminal products of the decomposition reaction

$$XY^{(1)} \rightarrow \sum_{j=1}^{k} (XY_j + \Delta E_j); \tag{7.68}$$

$$XY^{(2)} \rightarrow \sum_{j=k+1}^{m} (XY_j + \Delta E_j). \tag{7.69}$$

The unstable intermediate dissociation products (complexes) may emit a light quantum with the following reaction schemes in the medium:

one of the complexes $XY^{(j)}$ is formed in the electron-excited state, and its deactivation takes place upon radiative transition of the complex to the dispersed state:

$$XY^{(l)*} \rightarrow \sum_{j=1}^{k} (XY_j + \Delta E_j) + h\nu \tag{7.70}$$

or as a result of spontaneous emission with transition to the ground state

$$XY^{(l)*} \rightarrow XY^{(l)} + h\nu \tag{7.71}$$

with subsequent dissociation in accord with reaction scheme (7.68), (7.69);

the intermediate complex is formed during collisions with the terminal reaction product

$$XY^{(l)} + \Delta E_j \rightarrow XY^{(l)*} \tag{7.72}$$

and emits a quantum upon transition to the dispersed state

$$XY^{(l)*} \rightarrow \sum_{j=1}^{k} (XY_j + \Delta E_j) + h\nu \tag{7.73}$$

or with transition to the ground state

$$XY^{(l)*} \rightarrow XY^{(l)} + h\nu \tag{7.74}$$

with further dissociation

$$XY^{(l)} \rightarrow \sum_{j=1}^{k} (XY_j + \Delta E_j). \tag{7.75}$$

These cases do not cover all possible reactions that convert the energy of the chemical bond to radiation. The given reactions are typical in that they are nonequilibrium, and that population inversion with stimulation of coherent radiation may take place in the medium in which they occur.

Feasibility of lasing on the CO molecule behind an overdriven detonation front [Ref. 54]. The detonation process, as we pointed out in §7.1, is characterized by constant average parameters that are high inside the limits of detonation propagation. This makes it difficult to vary temperature or density of the reaction products for example when using mixtures in which the ratios of components are outside the concentration limits of detonation. So far no methods have been found for chemical laser utilization of the high-frequency processes in detonation wave structure described in §7.1. Accounting for them is quite complicated, and so far it can only be assumed that the nonlinearity of the detonation structure, the local inhomogeneities of temperature and density fields, and alternation of zones of unreacted mixture and combustion products must reduce the maximum possible gain of emission. These constraints can be removed by using a mode of overdriven detonation from plane shock wave S and trailing combustion zone G. In this case, the induction time of chemical reactions may be more than five times as long as the period for reaching the thermodynamically equilibrium state of the gas behind the shock wave. It was shown by calculation in Ref. 54 that under such conditions it is possible to make CO chemical detonation lasers based on a $CS_2 + O_2$ mixture.

First the parameters behind the shock wave front are calculated without consideration of chemical transformations. The Runge-Kutta method is used with a computer to calculate the concentrations of all components from the equations of chemical kinetics. Each vibrational level of the CO(v) molecule from zero-energy to the seventeenth was taken as an individual component. The thermodynamic quantities p, ρ, T and wave velocity were taken as constant at energy release Q less than some predetermined value Δq. After calculating the new values of the thermodynamic quantities and velocity corresponding to the calculated concentrations, the rate constants of the chemical reactions were found at the new temperature values. The method of iterations was used to account for the temperature dependence of specific heats.

The principal reactions among more than 40 elementary reactions known from data in the literature for the given mixture were selected from consideration of their role in the first 75 μs from the instant when the shock wave acts on the mixture. Reactions were not considered if their elimination during this period caused no more than 0.1% deviations in the concentrations of components. The given time interval completely covers the time of existence of inversion under the conditions assumed for the given problem with respect to: a) composition of the mixture $CS_2/O_2/Ar$ = 1/2.5/40, 1/1/30, 2.5/1/10; b) temperature range T = 1400-3400 K; c) pressure p ~ 0.1 MPa; d) chemical kinetics in the given initial time interval of 75 μs determined by 16 selected principal equations of reactions with the following rate constants of these reactions (k, $cm^3 \cdot mole^{-1} \cdot s^{-1}$; E, $kJ \cdot mole^{-1}$; R, $kJ \cdot mole^{-1} \cdot K^{-1}$):

1. $CS_2 + CS_2 \rightleftarrows CS + S + CS_2$, $k_1 = 0{,}166 \cdot 10^{15} \times \exp(-183/RT)$; [55]
2. $CS_2 + Ar \rightleftarrows CS + S + Ar$, $k_2 = 0{,}364 \cdot 10^{16} \times \exp(-336/RT)$; [55]
3. $CS_2 + O \rightleftarrows CS + SO$, $k_3 = 0{,}12 \cdot 10^{14} \times \exp(-4{,}4/RT)$; [56]

$$
\begin{array}{ll}
4.\ CS_2+O\rightleftarrows OCS+S, & k_4=0{,}1\cdot10^{15}\times \\
& \times\exp(-33{,}6/RT);\ [58] \\
5.\ CS_2+S\rightleftarrows CS+S_2, & k_5=0{,}1\cdot10^{15}\times \\
& \times\exp(-16{,}7/RT);\ [58] \\
6.\ O_2+SO\rightleftarrows SO_2+O, & k_6=0{,}35\cdot10^{12}\times \\
& \times\exp(-27{,}2/RT);\ [57] \\
7.\ O_2+S\rightleftarrows SO+O, & k_7=0{,}1\cdot10^{14}\times \\
& \times\exp(-23{,}4/RT);\ [57] \\
8.\ O+OCS\rightleftarrows CO+SO, & k_8=0{,}19\cdot10^{14}\times \\
& \times\exp(-18{,}9/RT);\ [58] \\
9.\ O+S_2\rightleftarrows SO+S, & k_9=0{,}4\cdot10^{13}\ \text{при}\ T= \\
& =1100\ \text{K};\ [57] \\
10.\ O+OCS\rightleftarrows CO_2+S, & k_{10}=0{,}16\cdot10^{13}\ \text{при}\ T= \\
& =1270\ \text{K};\ [58] \\
11.\ CS+O_2\rightleftarrows OCS+O, & k_{11}=0{,}1\cdot10^{14}\times \\
& \times\exp(-50{,}3/RT);\ [58] \\
12.\ S+OCS\rightleftarrows CO+S_2, & k_{12}=0{,}19\cdot10^{14}\times \\
& \times\exp(-18{,}9/RT);\ [58] \\
13.\ SO+SO\rightleftarrows SO_2+S, & k_{13}=0{,}45\cdot10^{12}\times \\
& \times\exp(-15{,}9/RT);\ [57] \\
14.\ OCS+Ar\rightleftarrows CO+S+Ar, & k_{14}=0{,}398\cdot10^{20}T^{-1{,}37}\times \\
& \times\exp(-299/RT);\ [55] \\
15.\ O_2+CS\rightleftarrows CO^*(v)+SO, & k_{15}=0{,}55\cdot10^{11}\times \\
& \times\exp(-8{,}36/RT);\ [58] \\
16.\ O+CS\rightleftarrows CO^*(v)+S, & k_{16}=0{,}24\cdot10^{15}\times \\
& \times\exp(-8{,}36/RT).\ [58]
\end{array}
\qquad (7.76)
$$

Equations (1)-(16) characterize a complex chain reaction for which curves are shown on Fig. 7.14 obtained in Ref. 54 for the way that the concentration of reagents c_i and temperature T depend on the time t of motion of the gas volume relative to the leading shock front of overdriven detonation. The calculations were done for a mixture of $CS_2/O_2/Ar = 1/2.5/40$ at an initial gas pressure of 2 kPa and shock wave velocity of 1500 m/s. It can be seen that the temperature in the reaction zone changes insignificantly. The broken curves show the change in concentrations of O_2, CS_2, CS and CO; in calculating these concentrations, the rate constants for dissociation of CS_2 (k_1, k_2) were assumed to be zero beginning at 6 μs. After this instant the reaction may be maintained by chain branching processes, but chain initiation processes considerably accelerate combustion. With weaker dilutions, or in the undiluted working mixture the temperature may rise during reactions. For example Fig. 7.15 shows the calculation of the chemical kinetics of reaction in a mixture of $CS_2/O_2 = 1/9$ at initial pressure of the mixture of 2 kPa and shock wave velocity of 1700 m/s. Here the temperature changes from 1510 to 2800 K during the course of the reaction.

Reactions (15) and (16) determine the populations of vibrational levels of CO molecules [Ref. 59] in the same way as processes of V-V exchange with molecules of CO(v), O_2, OCS, CS_2 and V-T exchange with molecules of CO, O, Ar. Molecules of O_2, $OCS(v_3)$ and $CS_2(v_3)$ may make a transition from the ground state to the first

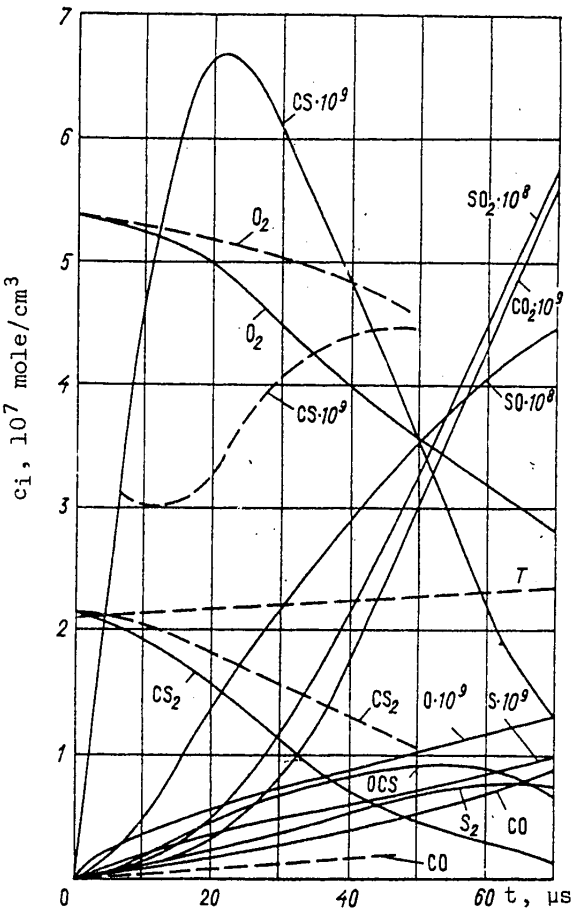

Fig. 7.14. Calculation of the change in concentration of reagents c_i and temperature T as a function of the time t in the overdriven detonation wave

excited vibrational level upon collisions with CO(v). This calculation did not consider transfer of excitation from O_2, OCS(001) and CS_2(001) to CO.

Numerical computer solution of the system of equations for chemical, relaxation and gasdynamic processes gave the time dependences of the population of vibrational levels of CO molecules behind the leading shock front of the overdriven detonation wave. The results of calculation of this dependence for complete inversion of the vibrational levels of CO are shown on Fig. 7.16. The rate constants of relaxation as a function of vibrational number v were calculated by using formulas from Ref. 60, and the emission gain in the center of the line for individual V-R transitions of $\mathcal{P}$- and $\mathcal{R}$-branches was calculated at times corresponding to the maximum complete inversion between each pair of vibrational levels. Maxwell-Boltzmann population of rotational levels was assumed at a temperature equal to the translational temperature, the half-width of the line was taken as corresponding to impact broadening, and the linewidth was assumed to be independent of quantum numbers or the kind of molecules responsible for broadening. The resultant maximum values of gain α_{max}

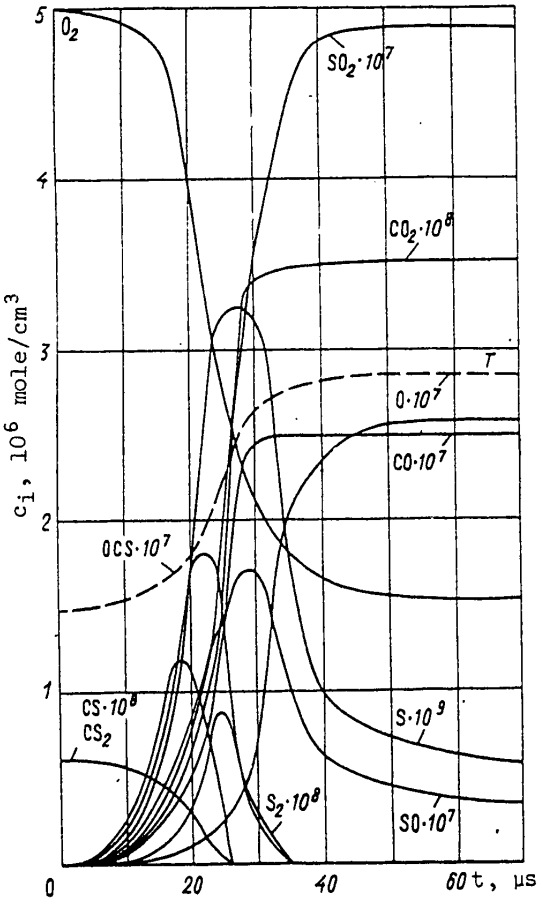

Fig. 7.15. Results of calculation of the chemical kinetics of a reaction behind the leading shock front of an overdriven detonation

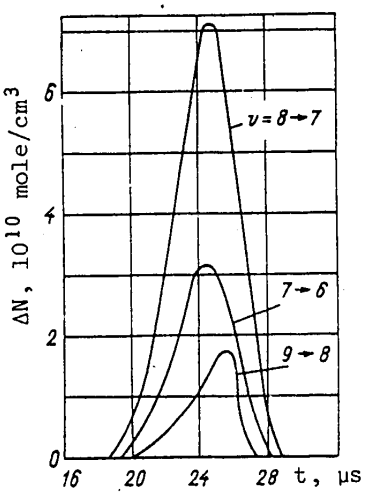

Fig. 7.16. Calculated time dependences of vibrational levels of the CO molecule behind the leading shock front of an overdriven detonation

on a given vibrational level v for a mixture of $CS_2/O_2 = 1/9$ at T = 2495 K are shown in Table 7.1. This same table gives the populations of vibrational levels n_v, n_v/n_{v-1}, and the corresponding rotational quantum number J and wave number $\omega^{v,J}_{v-1,J+1}$ of the transition on which α_{max} is reached for the $\mathcal{P}$- and $\mathcal{R}$-branches.

Analysis of the calculated data shows that during the first 1.5 μs the first inversion wave passes through all vibrational levels from 1 to 13. As we can see from Table 7.1, this wave is characterized by low populations of vibrational levels of the CO molecules and low gains ($10^{-7}-10^{-5}$ cm^{-1}). The second inversion wave is due to the intense process of chemical reactions, and under the given conditions propagates to only three vibrational levels (7, 8, 9). This wave is characterized by high values of the maximum gain ($10^{-3}-10^{-2}$ cm^{-1}) and long durations of inversion. The calculated maximum gains α_{max}, the duration of inversion τ_i, the dimensions of the inversion zone Δx_i that correspond to this duration, velocities D, temperature in the inversion zone and the transition vibrational and rotational quantum numbers corresponding to α_{max} are given in Table 7.2 for p_0 = 2 kPa.

TABLE 7.1

Results of calculation of kinetics of populations and gain [Ref. 54]

Time from start of reaction, μs	υ	n_υ, $см^{-3}$	$\frac{n_\upsilon}{n_{\upsilon-1}}$	$J_{\mathcal{P}}$	$\omega_{\upsilon-1, J_{\mathcal{P}}+1}^{\upsilon, J_{\mathcal{P}}}$, $см^{-1}$	$\alpha_{\mathcal{P}_{max}}$, $см^{-1}$	$J_{\mathcal{R}}$	$\omega_{\upsilon-1, J_{\mathcal{R}}-1}^{\upsilon, J_{\mathcal{R}}}$, $см^{-1}$	$\alpha_{\mathcal{R}_{max}}$, $см^{-1}$
0,04	13	$0,42 \cdot 10^{-7}$	1,004	32	1699,31	$1,7 \cdot 10^{-7}$	—	—	—
0,08	12	$0,19 \cdot 10^{-6}$	1,044	28	1741,71	$1,2 \cdot 10^{-6}$	8	1882,08	$1,4 \cdot 10^{-7}$
0,11	12	$0,37 \cdot 10^{-6}$	1,062	27	1770,91	$2,5 \cdot 10^{-6}$	12	1920,64	$5,4 \cdot 10^{-7}$
0,15	10	$0,73 \cdot 10^{-6}$	1,075	26	1800,22	$4,9 \cdot 10^{-6}$	14	1953,02	$1,4 \cdot 10^{-6}$
0,22	9	$0,17 \cdot 10^{-5}$	1,092	25	1829,64	$1,2 \cdot 10^{-5}$	15	1982,47	$4,2 \cdot 10^{-6}$
0,31	8	$0,36 \cdot 10^{-5}$	1,109	25	1854,74	$2,5 \cdot 10^{-5}$	17	2015,01	$1,1 \cdot 10^{-5}$
0,38	7	$0,54 \cdot 10^{-5}$	1,127	24	1884,36	$3,7 \cdot 10^{-5}$	17	2041,68	$1,8 \cdot 10^{-5}$
0,43	6	$0,67 \cdot 10^{-5}$	1,147	24	1909,63	$4,4 \cdot 10^{-5}$	18	2071,44	$2,3 \cdot 10^{-5}$
0,48	5	$0,81 \cdot 10^{-5}$	1,169	23	1939,47	$4,9 \cdot 10^{-5}$	19	2101,30	$2,8 \cdot 10^{-5}$
0,57	4	$0,17 \cdot 10^{-4}$	1,176	23	1964,92	$6,1 \cdot 10^{-5}$	19	2128,25	$3,6 \cdot 10^{-5}$
0,67	3	$0,18 \cdot 10^{-4}$	1,203	23	1990,43	$7,5 \cdot 10^{-5}$	19	2165,26	$4,8 \cdot 10^{-5}$
0,81	2	$0,30 \cdot 10^{-4}$	1,258	22	2020,58	$1,0 \cdot 10^{-4}$	20	2185,43	$7,2 \cdot 10^{-5}$
5,49	7	$0,22 \cdot 10^{-3}$	1,220	23	1888,80	$2,2 \cdot 10^{-3}$	20	2050,51	$1,5 \cdot 10^{-3}$
5,74	8	$0,31 \cdot 10^{-3}$	1,417	22	1867,93	$5,0 \cdot 10^{-3}$	21	2026,57	$4,1 \cdot 10^{-3}$
6,14	9	$0,32 \cdot 10^{-3}$	1,087	26	1825,21	$2,1 \cdot 10^{-2}$	15	1982,47	$7,2 \cdot 10^{-3}$

TABLE 7.2

Calculated characteristics of inversion zone for various detonation modes [Ref. 54]

Mode	Mixture Cs_2/O_2	D, m/s	T, K	$\upsilon \to \upsilon-1$	$J \to J-1$	α_{max}, $см^{-1}$	τ_i, μs	$\Delta\nu_i$, см
1	0,05/0,95	1700	1700	8—7	20—21	$6,1 \cdot 10^{-3}$	3,7	0,9
2	0,10/0,90	1700	1800	8—7	19—21	$9,2 \cdot 10^{-3}$	4,2	1,0
3	0,20/0,80	2000	2495	8—7	22—23	$3,8 \cdot 10^{-3}$	6,9	1,7
4	0,10/0,90	—	2495	8—7	22—23	$5,0 \cdot 10^{-3}$	3,5	—

The following conclusions are drawn in Ref. 54 from the results of such a numerical analysis of the possibilities for achieving stimulated emission on the CO molecule behind an overdriven detonation wave front in a mixture of $CS_2 + O_2$:

A change in pressure causes an inversely proportional change in all characteristic times of chemical and relaxation processes, including τ_i;

the maximum gain does not change as long as the impact approximation remains valid in calculation of the linewidth;

the inversion duration increases as the composition approaches stoichiometric proportions; increasing the temperature from 1800 to 2495 K for the same composition (modes 2 and 4) reduces both gain and inversion duration;

calculations done for an idealized one-dimensional model yield relatively high values of the gain.

Processes of population inversion in the case of adiabatic cooling of the detonation products. The chemical energy of detonation of the initial fuel mixture may also serve simply as a source of thermal energy for heating the mixture of products that are formed with added gases before they are cooled in the process of subsequent adiabatic expansion. Detonation lasers that utilize such processes are quite similar to shock-wave and chemical-gasdynamic lasers (described in chapter 6) and to gasdynamic shock-tube lasers [Ref. 61]. However, what distinguishes them is that in detonation lasers thermal pumping is realized in conditions of more intense heat release in the detonation wave than that accompanying ordinary combustion, and the components required for forming the active medium, as well as the proportions of concentrations of these components necessary for stimulated emission are produced immediately during the chemical reaction in the detonation wave. Otherwise, the process of population inversion in such lasers is analogous to the method of obtaining negative temperatures by cooling the medium that was first outlined in Ref. 62, and then in Ref. 63 and 64. In accordance with this method, a three-level system is considered that has different relaxation times between subsystems -- the levels 1, 2, 3 situated in sequence one above the other. If the relaxation time between subsystems is considerably greater than the relaxation time within each subsystem, and if radiative transitions between them are possible, then with a sufficiently rapid change in thermodynamic state, equilibrium will be established fairly rapidly within each subsystem, but there will be no equilibrium between them. Then a state is possible with negative temperature with respect to transitions from the energy levels of one subsystem to those of another.

Based on such a method of getting inverse population by an abrupt change in temperature of the medium, it was demonstrated in Ref. 65 that a state of inverse population can exist for some time with respect to vibrational levels in the case of adiabatic expansion of mixtures containing molecules that have appreciably different vibrational relaxation times and that are capable of exchanging energy of vibrational excitation. This kind of exchange is effective if the energies of the vibrational levels are close to one another, or the energy deficit is

$$|\Delta E| \ll kT. \tag{7.77}$$

Mixtures of N_2/CO_2 and N_2/NO_2 were considered in Ref. 65 as media that satisfy the resonant condition (7.77) of exchange of vibrational excitation. In these

mixtures the process takes place without chemical transformations, and hence is characteristic only for purely gasdynamic lasers. However, in chemical detonation lasers with adiabatic expansion the mixtures N_2/CO_2 and N_2/NO_2 may be either added gases, or may be part of the components formed during reaction of detonation products, and therefore it is of interest here to outline the analysis of Ref. 65.

The probability of energy transfer in the mixture of N_2/CO_2 during a single collission of a molecule at room temperature is $\beta \sim 10^{-5}$ [Ref. 66]. The exchange process is considered in the assumption of a surplus concentration of molecules that are carriers of vibrational excitation as compared with the concentration of working molecules with levels that involve inversion, $n_{N_2^*} \gg n_{CO_2}$, i. e. concentration $n_{N_2^*}$ is taken as constant in time. On the other hand the time change of the number

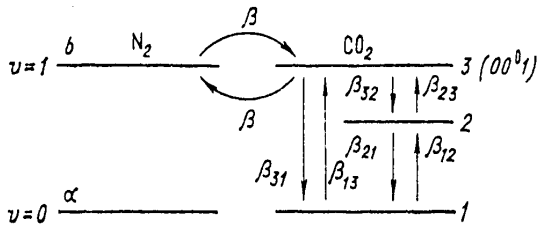

Fig. 7.17. Time change in number of CO_2 molecules on three vibrational levels

of molecules of the working gas CO_2 on three vibrational levels (Fig. 7.17) of which level 00^01 may exchange molecules of N_2^* with level $v = 1$, can be written as

$$\left.\begin{aligned} dn_3/dt &= -P_{ab}'n_3 + P_{ba}n_1 - P_{31}n_3 + P_{13}n - P_{32}n_3 + P_{23}n_2; \\ dn_2/dt &= P_{32}n_3 + P_{12}n_1 - P_{23}n_2 - P_{21}n_2. \end{aligned}\right\} \qquad (7.78)$$

Here $n_1 + n_2 + n_3 = n$ is the concentration of working molecules; P_{ba}, P_{ab} are respectively the probabilities of forward and reverse transfer of excitation between the working molecule CO_2 and the carrier molecule N_2^*; P_{31}, P_{13}, P_{32} and so on are the probabilities of thermal relaxation of a working molecule between the corresponding vibrational levels.

Let the rate of adiabatic expansion of the gas mixture be such that its cooling time from initial temperature T_1 to final temperature T_2 is much less than the inherent vibrational relaxation time of the carrier gas. After completion of expansion of the gas mixture, steady-state distribution of the working molecules is established with respect to vibrational levels. Hence by setting the right-hand members of equations (7.78) equal to zero and denoting the probabilities of relaxations during one collision by β_{21}, β_{32}, β_{31}, we can determine the population inversion between levels 3 and 2:

$$\frac{n_3 - n_2}{n_1} = \frac{\beta(\beta_{31} - \beta_{32})}{\beta_{21}(\beta + \beta_{32} + \beta_{31})} \exp\left(-\frac{E_b - E_a}{kT_1}\right). \qquad (7.79)$$

In the derivation of (7.79), thermal perturbation of the molecule was disregarded, i. e. no consideration was taken of probabilities P_{13}, P_{23}, P_{12}, but account was

taken of deactivating collisions and condition (7.77) for temperature T_2. Expression (7.79) implies that there is no inversion when $\beta_{32} > \beta_{21}$, and inversion is maximum when $\beta_{21} \gg \beta_{32}$ and under the condition where the probability of transfer of vibrational excitation β is much greater than the probability of deactivation of level 3 of the working molecule. In this case inversion is equal to the relative concentration of excited molecules of the carrier gas with initial temperature T_2.

Ref. 65 gives a specific computational example of population inversion by using a supersonic nozzle with continuous mode of adiabatic expansion of the working mixture. For example under conditions of inverse population between levels (00^01) and (10^00) of the CO_2 molecule at $T_1 = 1000$ and $T_2 = 300$ K, it is found that $(n_3 - n_2)/n_1 \sim$ ~ 1-3.5%.

Following Ref. 62-65, a number of papers were published dealing with the process of rapid expansion of a preheated mixture of molecular gases as they are discharged through nozzles or slits, thus bringing about conditions of inverse population of vibrational states of molecules [Ref. 67-74].

Such an effect can also be produced in a strongly exothermic reaction duri ig detonation with free dispersal of the reaction products [Ref. 6] without using gasdynamic devices like nozzles and slits.

As was already pointed out above, in this case the composition of the detonation products should correspond to a relaxation scheme analogous to that used in gasdynamic lasers of the type described in Ref. 67, 75 and 76. Many gaseous and condensed explosive media have such a composition of detonation products [Ref. 77, 78]. The rate of dispersal of detonation products heated to 2000-5000 K depending on the type of explosive is comparable to or greater than the flow velocity in gasdynamic lasers -- 10^5-10^6 cm/s. The process for an acetylene-air mixture is described by the exothermic chemical reaction [Ref. 79]

$$0.081C_2H_2 + 0.202(O_2 + 3.76N_2) = 0.162CO_2 + 0.081H_2O + 0.757N_2 + 108.9 \text{ kJ/mole}. \quad (7.80)$$

This process is analyzed in Ref. 6. Thus it is known from Ref. 79 that at a pressure of more than 0.05 MPa in an initial mixture with volumetric concentration of 8-14% C_2H_2 detonation is excited from a spark in tubes of diameter $d \geqslant 18$ mm. The detonation rate in this case is $1.8 \cdot 10^3$ m/s. For the conditions of reaction (7.80) the temperature of the reaction products is 2000-2400 K. It is assumed that the walls of the detonation tube are rapidly destroyed by pressure in the detonation wave. This destruction is accompanied by adiabatic expansion and cooling of the reaction products, the calculated rate of expansion being about $0.9 \cdot 10^5$ cm/s. Dispersal into vacuum will change the parameters of state of the reaction products with formation of population inversion of states *2* (00^01) and *1* (10^00) of the CO_2 molecule.

In this case, relaxation of the excited CO_2 molecules corresponds to the kinetic equation

$$\frac{dn_\alpha}{dt} = P_{N^*-C} N^* n_0 \delta_{2\alpha} - [n_\alpha/\tau_\alpha(t)], \quad (7.81)$$

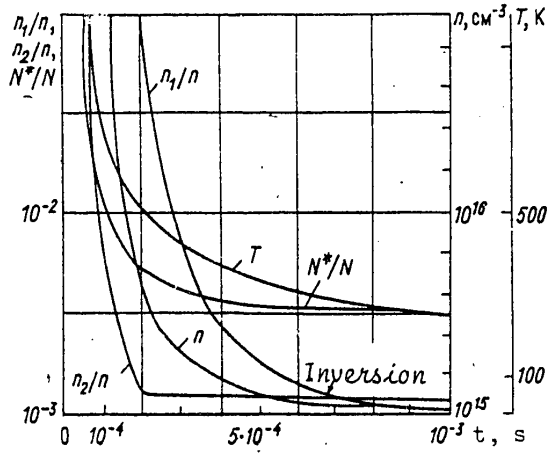

Fig. 7.18. Time dependences of gas temperature and molecule concentration in the case of cylindrical dispersal of the detonation products of an acetylene-air mixture: T--temperature of detonation products; n--concentration of CO_2 molecules; n_1/n, n_2/n and N*/N--relative populations of excited states of molecules of CO_2 and nitrogen respectively

where $\alpha = 1.2$; $\delta_{2\alpha}$ is the Kronecker delta; N*, n_0, n_α are the concentration of excited molecules of N_2, CO_2 in the ground and α-states; P_{N^*-C} is the probability of transfer of excitation from N_2 to CO_2; $\tau_\alpha(t)$ is the time of collisional relaxation.

The time dependence of gas temperature and molecule concentration have been calculated for cylindrical dispersal geometry [Ref. 6] (Fig. 7.18).

With consideration of data on the temperature dependence of the probability of collisional relaxation of CO_2 molecules [Ref. 80], the time $\tau_\alpha(t)$ has also been determined. The initial conditions here are selected from the following considerations. At a temperature below 1000 K the relaxation of excited molecules of CO_2 depends on collisions with molecules of H_2O and is most probable for the lower level. Due to the relatively large concentration of water in the reaction products the relaxation times are short and at pressures of the initial mixture higher than 0.1 MPa relaxation occurs faster than cooling of the gas. And at pressures of the initial medium below 0.05 MPa, as already stated, the process of detonation excitation is hampered in an acetylene-air mixture. Therefore the selected conditions corresponded to the following: pressure 0.05-0.1 MPa, tube diameter $d \approx 2$ cm.

Integration of kinetic equation (7.81) yields the time dependence of the population of excited states. In this connection we can disregard the transfer of energy from N_2 to CO_2 and approximate $\tau_\alpha(t)$ by power functions. It is found that relaxation of level *1* takes place more rapidly than depopulation of the level due to cooling of the gas, i. e. its population is determined by the Boltzmann factor. On the other hand, beginning with a certain instant the relaxation of level *2* takes place more slowly, and the vibrational temperature is separated from the temperature of random motion in the gas. It can be seen from the results of calculation on Fig. 7.18 that separation of the vibrational temperature of level *2* takes place at $t = 200$ μs, and population inversion arises 650 μs after the beginning of dispersal. The time

dependence of the population density of the excited level of the nitrogen atom N* is determined mainly by relaxation upon collision with CO_2 molecules. It is pointed out in Ref. 6 that accounting for the energy transfer from nitrogen to CO_2 should lead to an increase in inversion and to a reduction in time before onset of inversion, and moreover that inversion should occur at higher pressures in the initial mixture. Increased inversion is also possible when an explosive medium is used with a lower relative concentration of water in the products of explosion.

§7.5. Experimental Stimulation of Emission in Chemical Detonation Lasers

Lasing in an overdriven detonation wave. Realization of the possibility of lasing in detonation just as in a thermal explosion is so far a complex problem. The pertinent experimental results include the use of overdriven detonation for direct stimulation of emission and normal Chapman-Jouguet detonation and explosion for thermal pumping of an active medium.

Induced emission was first obtained directly from a detonation wave in a mixture of $F_2O/H_2/Ar = 1/1/20$ [Ref. 5, 81]. Before this, emission of vibrationally excited HF had been produced in the course of a chain reaction initiated by flash photolysis [Ref. 82]:

$$\left.\begin{aligned} &F + H_2 = HF + H \quad (-134\ \text{kJ/mole});\\ &OF + H_2 = HOF + H;\\ &H + F_2O = HF + OF;\\ &H + HOF = HF + OH;\\ &H + OF = FH + O \text{ or } OH + F. \end{aligned}\right\} \qquad (7.82)$$

In carrying out reaction (7.82) in a detonation wave, the process was initiated at a wave propagation rate exceeding the Chapman-Jouguet velocity, i. e. in the overdriven detonation mode. Despite heavy dilution of the mixture with argon and relatively low initial pressure (about 0.66 kPa) the wave velocity was 1.8-2 km/s with temperature on the wave front above 2000 K. In the opinion of the authors of Ref. 5, 81, under these conditions the reaction zone is apparently quite narrow, and therefore diffraction losses in the optical cavity are high, i. e. the working conditions of such a chemical laser with respect to temperature and pressure are near critical.

In Ref. 5, 81, a detonation tube was used of the type shown in Fig. 7.19a, 16.7 cm in diameter with a special nearly confocal resonator mounted flush with the walls of the tube. The output of coherent emission from the cavity was recorded by an InSb photoelectric detector using a narrow-band filter for spectral resolution. A typical record of the emission is shown in Fig. 7.19b as a two-beam oscillogram. Here the upper curve is the radiation of gas heated by the detonation wave as observed through a CaF_2 window installed upstream relative to the resonator. The lower curve is a recording of emission from the optical cavity by the InSb photoelectric detector with aperture of 1.5 mm. Comparison of these curves shows that the amplitude of the curve characterizing the coherent radiation is 10^5 times as great. This is convincing proof of reliable observation of the effect of stimulated coherent emission.

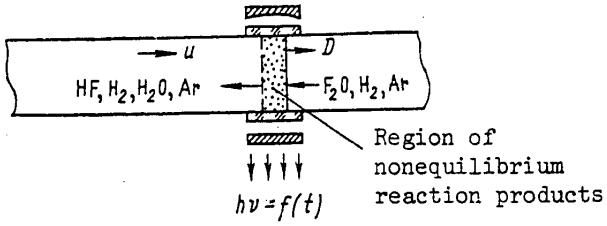

a

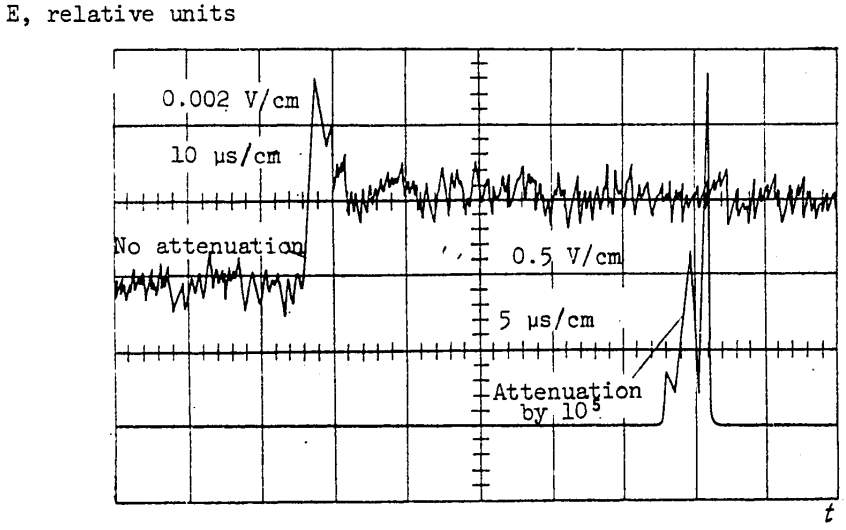

b

Fig. 7.19. Diagram of chemical detonation laser (a) and record of its output (b)

A brief report is given in Ref. 83 on theoretical analysis of processes in the chemical detonation laser described above in the form of a numerical calculation for the most realistic chemical model of the reaction. In this calculation some chemical reactions were ruled out, and the complexity of accounting for processes in the resonator was eliminated by considering the process of nonequilibrium radiation only for "zero" amplification, i. e. for the process characterized by the upper curve in Fig. 7.19. It is pointed out that the calculation utilized the results of experiments with mixtures of $F_2O/H_2/Ar$ in corresponding concentration limits from 1/1/10 to 1/1/200 with heating in the wave from 2200 to 3500 K. It is found from the calculations that during the chemical reaction the concentrations of HOF, F_2O and OF decrease rapidly to an insignificant level, so that reactions involving these components can be disregarded. Thus there remains only the first of reactions (7.83) that yields excited HF. Besides, it turned out that for the given reaction deactivation is controlled by processes of V-V transfer of energy, while V-T processes are unimportant.

Using detonation and explosion for production and thermal pumping of active laser media. Selection of the initial composition of the mixture for detonation lasers that work on the principle of adiabatic expansion of the detonation products through

a nozzle involves the relaxation scheme described in §7.4. This results in a variety of reagents that can be used, and a number of design peculiarities of the chemical detonation lasers that operate on these reagents.

We describe herewith the designs and working principles of the most typical of these lasers.

One of the first experimental lasers in which detonation was used to produce a high-temperature gas mixture at the inlet to a slit nozzle was a detonation laser based on the exothermic explosive reaction of dissociation of a hydrazoic acid molecule in a mixture of carbon dioxide and xenon [Ref. 7]. The mechanism of this reaction is determined mainly by the following processes [Ref. 84]:

$$\left.\begin{aligned} &HN_3^* \rightarrow NH + N_2 \quad (-41{,}9\ \text{kJ/mole});\\ &NH + HN_3 \rightarrow H_2 + N_2 + N_2^*\ (+635\ \text{kJ/mole});\\ &N_2^* + \varkappa HN_3 \rightarrow \varkappa HN_3^* + N_2;\\ &N_2^* + M \rightarrow N_2 + M^*;\\ &M + HN_3^* \rightarrow HN_3 + M^*. \end{aligned}\right\} \qquad (7.83)$$

When carbon dioxide is used as the diluent M, the excited nitrogen transfers its energy to the CO_2 molecule due to quasi-resonance between the vibrational levels of nitrogen and the vibrational mode (00^01) of carbon dioxide. The process of obtaining population inversion during such a chemical reaction was analyzed in detail in Ref. 85, and was investigated in Ref. 86.

A diagram [Ref. 7] of the experimental hydrazoic acid detonation laser is shown in Fig. 7.20.

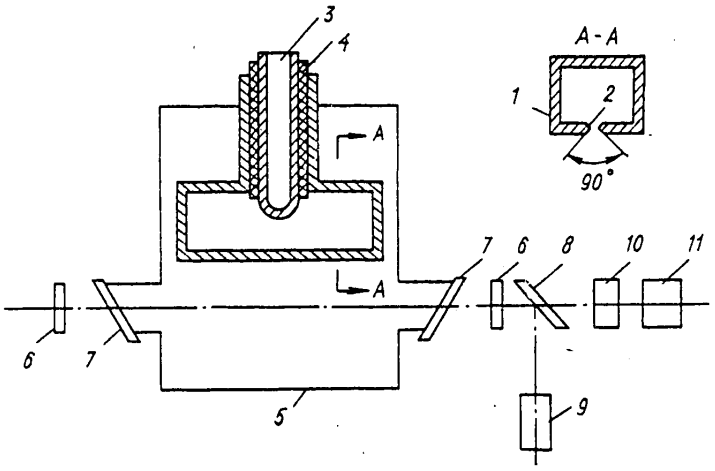

Fig. 7.20. Detonation laser based on hydrazoic acid: 1--0.3-liter high-pressure chamber; 2--200 x 0.4 mm slit; 3--metal rod with cavity; 4--heat insulation; 5--ballast tank with volume of 0.012 cu. m; 6--gold-coated mirrors 25 mm in diameter, one of which has an output aperture 2.5 mm in diameter; 7--Brewster windows of NaCl; 8--plane-parallel germanium plate; 9--calorimeter; 10--photocell; 11--oscilloscope

The gaseous mixture is admitted to tank 5 and then frozen out on hollow metal rod 3 with cavity 4 filled with liquid nitrogen. Detonation was initiated by an electric spark. The pressure and temperature in the high-pressure chamber after dispersal of the detonation products were about 1-2 MPa and 2000-3000 K depending on the amount and composition of the gas mixture. The time of discharge of the detonation products and diluents through the slit was evaluated as the ratio of the volume of the high-pressure chamber to the product of the slit area multiplied by the speed of sound in the critical cross section, and was about a millisecond. The distance from the slit to the axis of the cavity was adjusted in the experiment. The optimum distance was about 3 cm. The duration of the stimulated pulse at the optimum composition of the mixture was close to the time of discharge of the gas through the slit.

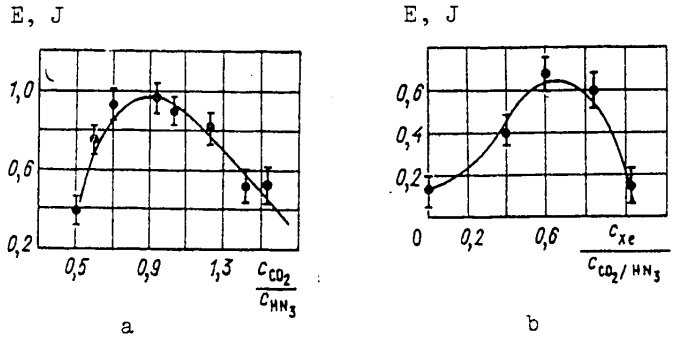

Fig. Fig. 7.21. Energy characteristics of HN_3 laser with a change in the content of CO_2 (a) and Xe (b) in the mixture

Shown in Fig. 7.21 are experimental curves for the output energy as a function of: a--the content of CO_2 in the HN_3/CO_2 mixture for a predetermined content of HN_3 (0.5 g); b--the content of Xe in the mixture $HN_3/CO_2/Xe$ for the same amount of HN_3 and CO_2 (0.33 g). The maximum energy (about 1 J) was attained at a relative content of components corresponding to initial temperatures of detonation products of about 2500 K, which is much greater than the temperatures given as optimum by Ref. 69 for mixtures of $N_2/CO_2/He$. In Ref. 7 the cause of this was discovered in the difference of gasdynamic parameters of the experimental facilities, and in the way that temperature of the mixture depends on change in composition.

Thermodynamic calculation and analysis of the detonation products showed that nearly all the hydrogen (about 90%) was oxidized to water, reducing part of the carbon dioxide to carbon monoxide. In this process, the water content in the mixture reached 15-20%. The addition of chlorine to the mixture in an amount close to the stoichiometric value for reaction with hydrogen led to a sharp (approximately triple) increase in the radiated energy. There was a concomitant reduction of water content in the products to 2-4%.

The H_2O molecules deactivate symmetric and deformation vibrational modes of the CO_2 molecule, and therefore small amounts of water in the detonation products improve the emission characteristics of the active medium. However, most explosive lasers use hydrocarbon fuels that yield so much water in the reaction products that it leads to deactivation of both the antisymmetric mode of CO_2 and the vibrationally excited N_2 molecules, i. e. to losses of vibrational energy. To reduce such losses,

additives that interact with hydrogen are introduced that form compounds for which losses of vibrational energy from the antisymmetric mode of CO_2 and the vibrational mode of N_2 are lower than for water molecules.

Research results given in Ref. 87 deal with the question of the influence that chlorine additives have on gain of a laser working on products of explosion of a hydrocarbon fuel, and specifically methane-oxygen mixtures. This paper points out that under the conditions of Ref. 7 the explanation of a nearly triple increase in lasing power as due to a reduction of water content when chlorine is added is not completely unambiguous. Actually, when hydrogen was bound by chlorine there was an increase in CO_2 content as compared with preceding experiments. It is also possible that the conditions (fairly high water vapor content) were close to the lasing threshold, and here even a slight increase in gain due to an increase in CO_2 content could significantly increase the lasing power.

In Ref. 87, in order to study the influence of additives, an explosive laser was used that consisted of an explosive chamber (volume 500 cc), a wedge-shaped nozzle (height of the critical cross section 1 mm, half-angle of the vertex 15°) and a receiver. Width of the gas stream was 400 mm. At a degree of expansion equal to 18, the wedge-shaped profile of the nozzle was changed to a plane-parallel section. The gain (absorption) of the medium was measured by a CO_2 electric-discharge laser at a distance of 80 mm from the critical cross section of the nozzle. The mixture was made up of methane, oxygen and nitrogen in partial pressures of: CH_4--30.6, O_2--61.3 and N_2--288 kPa. Chlorine additives were introduced in amounts of 25, 50, 75 and 100% of the stoichiometric content of chlorine with respect to hydrogen, and a comparison was made between the resultant gains and the gains without chlorine added. The results of thermodynamic calculation of the composition of the products of explosion as a function of the content of chlorine additive are shown in Fig. 7.22. The experimental dependence of the maximum gain on the chlorine content in

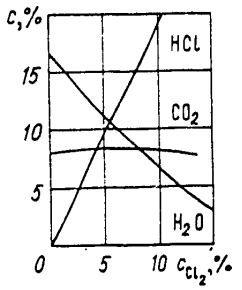

Fig. 7.22. Thermodynamic calculation of concentrations of CO_2, H_2O and HCl in the products of explosion of mixtures of $CH_4/O_2/N_2/Cl_2$ as a function of chlorine content in the initial mixture

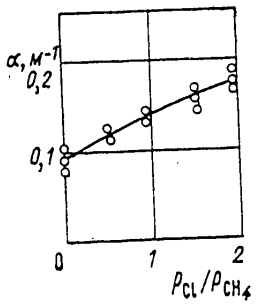

Fig. 7.23. Maximum gain in the products of explosion of a mixture of $CH_4/O_2/N_2/Cl_2$ as a function of the ratio of chlorine and methane pressures (p_{CH_4} = 30 kPa)

the initial mixture is shown in Fig. 7.23. The pressure in the prechamber in front of the nozzle that corresponds to maximum gain increases with an increase in the chlorine content in the initial mixture, and changes from 0.15 MPa in mixtures without chlorine added, to 0.25 MPa with the stoichiometric amount of Cl_2 with respect to hydrogen. At equal pressures in the prechamber the gain increases

monotonically with increasing content of Cl_2 in the initial mixture up to the stoichiometric level with respect to hydrogen. It is concluded from the research of Ref. 87 that adding chlorine to the hydrocarbon fuel reduces losses of vibrational energy from the upper energy level of stimulated emission in a laser that operates on the products of explosion of these fuels, and consequently improves the energy characteristics of these lasers.

Also operating on hydrocarbon fuel is a detonation laser proposed in Ref. 88. Experiments on achieving lasing in products of gas detonation were done on the following explosive chemical reactions:

$$\left.\begin{aligned} &1)\ C_2H_2+2{,}5\,O_2+\varkappa N_2\rightarrow 2\,CO_2+H_2O+\varkappa N_2+Q_\varkappa;\\ &2)\ CO+N_2O+\varphi\,He\rightarrow CO_2+N_2+\varphi\,He+Q_\varphi, \end{aligned}\right\} \qquad (7.84)$$

where $Q_{\kappa,\phi}$ is energy release, κ and ϕ are the fractions of nitrogen and helium dopants respectively. The properties of the initial gas mixtures are summarized in Table 7.3.

TABLE 7.3

Characteristics of explosive mixtures [Ref. 88]

Mixture composition by partial pressure	Q, J/g	Detonation rate D, m/s
$C_2H_2/O_2/N_2$ 16,7/41,6/41,7	5650	2150
12,6/31,4/56,5	4030	1920∓20
$CO/N_2O/He/H_2$ 35/35/28/2	6340	2240∓20

The relative concentrations of initial components were selected in accordance with contradictory requirements on the composition of the final mixtures and on the detonation properties of the initial mixtures. In reaction (2) of equations (7.84) the catalyst was traces of hydrogen. The experiments were done on a detonation laser diagrammed in Fig. 7.24.

The explosive gas mixture at atmospheric pressure in tube 2 was ignited by a spark, an igniter or an electric ignition wire 15. The resultant self-accelerating combustion becomes detonation moving in the direction shown by the arrows on the diagram. The double input of the detonation wave to explosion chamber 1 is to ensure more simultaneous rupture of mylar film 14 cemented to slit 3, 40 cm in length. The gas mixture of predetermined composition heated behind the detonation wave front flows through the slit into vacuum space 6 after the film breaks and is cooled upon rapid expansion. Inversion of the population of V-R levels 00^01 and 10^00 of the CO_2 molecules takes place in the gas stream. The jet of active medium shown by the broken line on Fig. 7.24 disperses through a transverse optical cavity 1.5 m long formed by two copper or gold-coated mirrors -- one flat (11) and the other spherical (4) with radius of curvature of 5 m. The distance between the slit and the axis of the cavity is 4 cm. Emission is coupled out to GeAu photoresistor 9 through an annular or circular opening in flat mirror 11. Wavelengths shorter than 8 μm are cut off by InSb filter 12 in front of photoresistor 9.

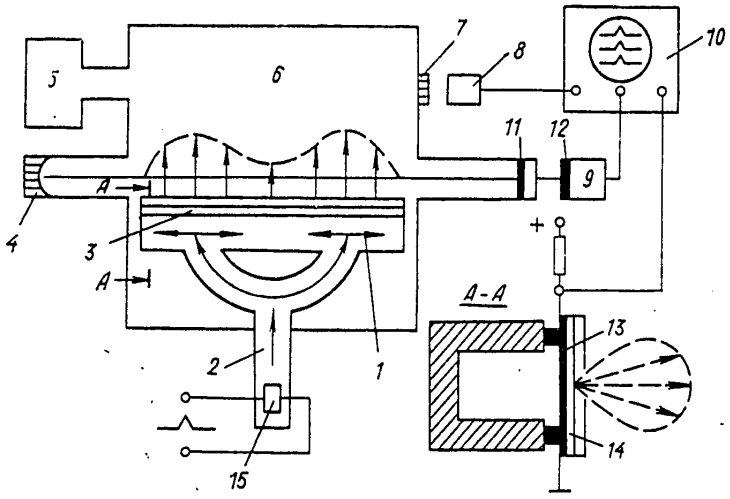

Fig. 7.24. Diagram of detonation laser with breakable film diaphragm: 1--explosion chamber; 2--tube with explosive gas mixture; 3--slit; 4--opaque mirror; 5--vacuum pump; 6--vacuum chamber; 7--NaCl window; 8, 9--Ge-Au photocells; 10--oscilloscope; 11--output mirror; 12--InSb filter; 13--contact sensor; 14--mylar film; 15--ignition

Lasing was realized on all three mixtures shown in the table as the detonation products were discharged through a slit 1 mm wide. For the CO/N_2O/He mixture, lasing was also observed as the detonation products were discharged through a slit up to 4 mm in width.

It is pointed out in Ref. 88 that each lasing pulse has its own more detailed structure, apparently due to the complex gasdynamic process of unsteady discharge of the detonation products.

From the given laser designs using detonation for production and thermal pumping of act ve media, it can be seen that one of the peculiarities that to a great extent determines the overall design of a detonation laser is handling the problem of a *method of containment* of the initial substance in the reaction space, and cutting off this space from the evacuated optical cavity until the beginning of discharge of the products of detonation or explosion.

In Ref. 7 this problem was solved by phase transformation of the working substance to the initial condensed state. In Ref. 88 the job was handled by separating the explosion chamber from the evacuated space by a diaphragm in the form of a mylar film that was ruptured by the detonation wave.

Peculiarities of this kind are chiefly what determine the designs of other detonation lasers as well. For example Ref. 89, 90 investigated the operation of a laser (Fig. 7.25) in which the stop of gas-tight high-pressure valve 4 is released by solenoid tripper 3 at the end of the period of the explosive process in a mixture of $CO/O_2/H_2/N_2$ initiated by spark plug 1 inside chamber 2. This ensures rapid expansion of the products of explosion in two-dimensional slit nozzle 5, population inversion, and lasing in the region of optical cavity 6 with subsequent exhaust of these products into vacuum chamber 7.

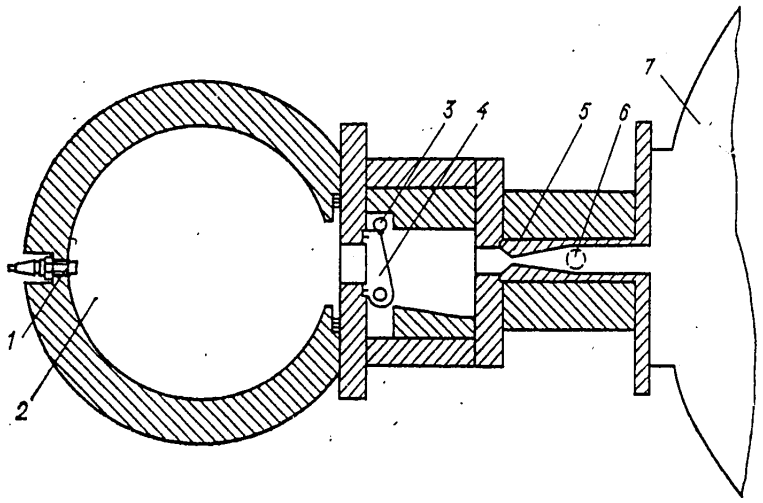

Fig. 7.25. Diagram of detonation laser with electric-release valve: 1--ignition; 2--explosion chamber; 3--solenoid release; 4--valve; 5--nozzle; 6--cavity; 7--vacuum chamber

The most typical conditions in such experiments were: composition of products of explosion $CO_2/N_2/H_2O = 15/83.5/1.5$; stagnation temperature and pressure 1500 K and 1 MPa respectively. Temperature and pressure in the cavity region 300 K and about 13 kPa respectively, Mach number $M = 4.5$. Periodicity of operation about 3 minutes.

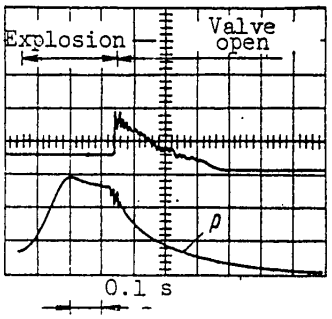

Fig. 7.26. Change of gas pressure and power of stimulated emission in a detonation laser

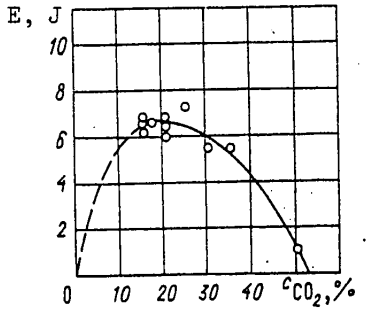

Fig. 7.27. Energy output as a function of CO_2 concentration

The changes of pressure in explosion chamber 2 and variation of stimulated emission in cavity 6 are illustrated by the synchronous oscilloscope record on Fig. 7.26. It can be seen that from the instant the valve opens, lasing begins (upper curve), whereas the pressure p in the explosion chamber falls comparatively slowly (lower curve) as the explosion products are discharged and cooled.

Of some interest are measurements made in Ref. 89 of the way that energy output depends on CO_2 concentration (Fig. 7.27). In experiments using the three types of nozzle sets shown in Fig. 7.28 -- wedge-shaped (a), profiled (b) and a block of

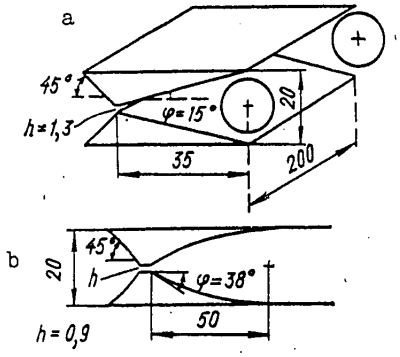

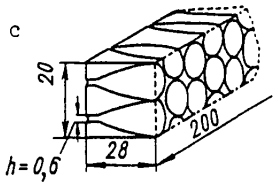

Fig. 7.28. Types of nozzle sets: a--wedge-shaped; b--profiled; c--block of axisymmetric nozzles

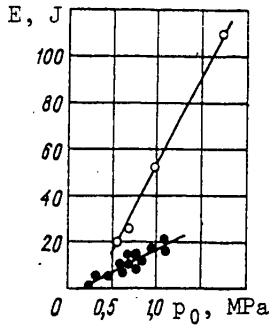

Fig. 7.29. Comparison of the energy output of a laser with different types of nozzles: o--profiled; •--wedge-shaped

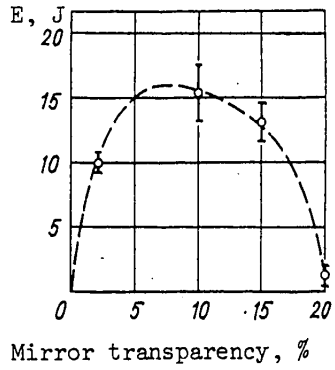

Fig. 7.30. Output energy as a function of transparency of the mirror of the optical cavity

axisymmetric nozzles (c), it was found that the energy output for the profiled nozzle is approximately 2.5 times the value for the wedge-shaped nozzle (Fig. 7.29). On this graph the blackened circles correspond to lasing processes with gas expansion in a wedge-shaped nozzle, while the unblackened circles correspond to lasing with gas expansion in the profiled nozzle. The stagnation temperature was equal to 1400 K. This difference in output energies is partly due to a reduction in the relaxation rates of molecules with more intense expansion of the flow in the profiled nozzle.

The output energy is a function of the transparency of the mirror in the optical cavity. An experimental curve for this function in the case of a profiled nozzle set is shown in Fig. 7.30 for stagnation pressure and temperature of 0.54 MPa and 1100 K respectively. The gain determined from these data was approximately 0.7 m^{-1}, whereas this parameter was about 0.4 m^{-1} for the wedge-shaped nozzle set, although the stagnation temperature is considerably higher -- 1400 K. This indicates that better conditions for freeze-out of the upper energy level of population exist for profiled nozzles. The maximum energy obtained in the described detonation laser was 110 J for a profiled nozzle. This is 0.06% of the thermal energy contained in

the initial gas. Experiments with the block of axisymmetric nozzles show that shock waves and turbulent wakes in the flow from the boundaries of the nozzles cause heating of the gas and optical inhomogeneity of the medium in the cavity.

High energy losses in a laser of the described design can be attributed to the following causes:

1. Following the end of the laser pulse about 50% of the gas remains in the explosion chamber. This is due to pressure elevation in the vacuum space -- an effect that can be reduced by using a diffuser.

2. Heat is lost to the walls as the gas expands.

3. Losses to relaxation in the nozzle.

4. The small dimensions of the cavity in the direction of flow (about 1 cm) prevent complete utilization of the energy contained in the N_2 due to slow energy transfer from $N_2(v)$ to $CO_2(00v)$, and the lower energy level cannot completely transfer its energy to the vibrational mode because of the rapid transit of gas through the cavity. Estimates show that these factors account for a loss of about 50% of the energy entering the optical cavity.

5. Flow losses in the cavity due to nonoptimality.

It is suggested in Ref. 90 that by minimizing these losses or some of them an overall efficiency of about 0.5% can be achieved, and this value can be increased still further by increasing the stagnation temperature.

In contrast to the described laser design, the problem of containment of the initial substance in the reaction zone and cutting off this space from the evacuated volume of the optical cavity is handled by using an electromagnetic valve of periodic action in Ref. 91, enabling operation of the device in periodically repeated cycles (twice a minute). A schematic diagram of such a laser with explosive pumping is shown in Fig. 7.31.

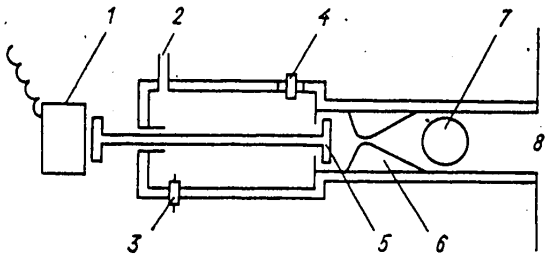

Fig. 7.31. Detonation laser with periodically acting electromagnetic valve: 1--electromagnet; 2--input of mixture; 3--spark plug; 4--pressure sensor; 5--valve; 6--nozzle; 7--optical cavity; 8--reservoir for removal of the used gas mixture

After the explosion chamber has been filled with the gas mixture to the necessary pressure, electromagnet 1 is disengaged and ignition takes place. When the maximum temperature has been attained and the burning gas has reached the maximum pressure,

valve 5 is opened and the gas rushes through nozzle 6. The pressure in front of the nozzle is recorded by sensor 4, and the temperature in this zone is calculated from the pressure increase in the chamber. Direct measurements of the temperature in this zone have shown good agreement between the results of measurements and calculated values.

After exit through the electromagnetic valve, the products of explosion expand in the nozzle, and then are removed to reservoir 8 in analogy with the design described above. Optical cavity 7, with active length of 20 cm, is placed across the gas stream at the nozzle outlet. Both mirrors of the cavity are 76 mm from the gas stream to prevent contamination during operation of the laser.

For a nozzle with $h = 1.5$ mm, ratio of cross sectional areas $S/S^* = 15$, and half-angle of the vertex $\phi = 15°$, the gas flow leaves the nozzle with $M \approx 4$, and at $h = 0.75$ mm, $S/S^* = 30$ and $\phi = 15°$, we have $M \approx 5$.

It has been established that the beginning of amplification coincides with the instant of opening of the valve in a system that uses an explosive mixture of CO/H_2 and a mixture of $CO_2/N_2/H_2O = 1.5/8.3/0.2$. For an area ratio $S/S^* = 15$, the pressure in the explosion chamber increased from 0.2 to 0.5 MPa within the first 0.15 s after initiating the explosion, and after the valve was opened fell to zero within the next 0.15 s and again slowly rose to the initial value of 0.2 MPa. At the instant of opening of the valve, optical amplification increased and there was a simultaneous increase in the power of the stimulated output radiation to 60 W with a pulse duration of this emission of 0.8 s.

After the pressure in the combustion chamber had fallen to zero, a rapid increase in optical absorption was observed in the active medium. Moreover it can be noted that the process of amplification of the active medium and generation of stimulated emission were accompanied by fluctuations in the gain of the active medium and the power of the output radiation, which were due to a change in conditions during expansion of the gas through the nozzle, and apparently to certain gasdynamic instabilities inherent in the given design.

It would be a good idea in the described lasers to consider the feasibility of using ordinary hydrocarbons as the fuel. However, the large amounts of water vapor that are liberated upon combustion of such fuel may to a considerable extent inhibit processes of stimulated emission since the cross section of processes of relaxation of antisymmetric modes of the CO_2 molecules under the action of H_2O molecules is large [Ref. 80]. To determine the influence of water vapor on the characteristics of the described lasers, a study was done in Ref. 91 on several types of CO/H_2 mixtures that yield different amounts of water vapor upon ignition. Fig. 7.32 gives the results of these studies in the form of curves for the gain as a function of the percent content of water vapor.

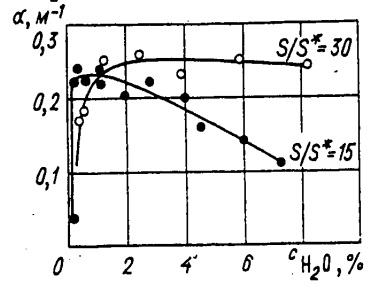

Fig. 7.32. Gain α as a function of water vapor content c_{H_2O} in the active medium

It can be seen that for a nozzle with $h = 1.5$ mm ($S/S^* = 15$) the gain reaches the maximum value at a water vapor content of ~1%, and falls to about one-half at a water vapor content of ~8%. With more rapid expansion of the gas, i. e. for $h = 0.75$ mm ($S/S^* = 30$) amplification decreases

with increasing water vapor content in the active mixture much more slowly than in the first case. The laser design with h = 0.75 mm was less sensitive to water vapor content, and therefore several types of hydrocarbon fuels were used in this design to check the extent to which the additional combustion products that are inevitably present in such fuel affect the characteristics of the system. The use of three types of such fuels -- acetylene, propane and natural gas -- was characterized by generation of an intense pulse of stimulated emission regardless of whether there was an excess or insufficiency of oxygen in this case. For example when natural gas was used as the fuel, and the active medium was $CO_2/N_2/H_2O$ = 0.66/8.0/1.34, the power of the output radiation reached 60 W with duration of the pulses of this radiation of the order of 0.03 s. On the other hand when the fuel was acetylene and the active medium was $CO_2/N_2/H_2O$ = 1.2/8.2/0.6, the power of the output radiation was 70-75 W at a pulse duration of about 0.08 s. If propane was used as the fuel, and the active medium was a mixture of $CO_2/N_2/H_2O$ = 0.85/8.0/1.15, the output radiation had a pronounced series of very short beams with power of some of them being greater than 100 W.

Further research in the area of developing the described lasers is possible in the direction of increasing the working pressure and temperature. At high temperatures there is a strong increase in the percentage of energy associated with vibrational states of the molecules, and this should mean a considerable increase in the power and energy of the stimulated coherent radiation. The use of large pressures is necessary in turn for getting higher temperatures and higher gas flow rates. Then the increased energy of coherent emission will be released in shorter periods of time, and consequently there will be a considerable increase in the peak power of the output radiation.

REFERENCES

1. B. B. Dunne, "Shock Wave Optically Pumped Laser," U. S. Patent 3451008, 1969.

2. "Problems of Electrophysics of Combustion," No 36, Moscow, "Nauchnyye issledovaniya energeticheskogo instituta imeni G. M. Krzhizhanovskogo" [Scientific Research of the Power Engineering Institute imeni G. M. Krzhizhanovskiy], 1975; REFERATIVNYY ZHURNAL: MEKHANIKA, No 11, 1976, p 101.

3. V. K. Ablekov, Yu. N. Denisov, F. N. Lyubchenko et al., "A Laser," USSR Patent 589841, 2 Nov 76, Patent Bulletin No 4, 1979, p 251.

4. V. K. Ablekov, "A Method of Producing a Medium with Negative Absorption Factor," USSR Patent No 475964, 27 Nov 64, Patent Bulletin No 4, 1979, p 251.

5. R. W. F. Gross, R. R. Giedt, T. A. Jacobs, "Stimulated Emission Behind Overdriven Detonation Waves in F_2O-H_2 Mixtures," J. CHEM. PHYS., Vol 51, No 3, 1969, p 1250.

6. V. M. Marchenko, A. M. Prokhorov, "On the Feasibility of Producing an Inverse Medium for Lasers by Explosion," PIS'MA V ZHURNAL EKSPERIMENTAL'NOY I TEORETICHESKOY FIZIKI, Vol 14, No 2, 1971, pp 116-120.

7. M. S. Dzhidzhoyev, V. V. Korolev, V. N. Markov et al., "The Gasdynamic Detonation Laser," PIS'MA V ZHURNAL EKSPERIMENTAL'NOY I TEORETICHESKOY FIZIKI, Vol 13, 1971, pp 73-76.

8. F. A. Williams, "Theory of Combustion," translation from English by S. S. Novikova and Yu. S. Ryazantseva, Moscow, Nauka, 1971, 615 pages.

9. D. L. Chapman, "On the Rate of Explosion in Gases," PHIL. MAG. J. SCI., 1899, Vol 47, series 5, No 284, pp 90-104.

10. Ya. B. Zel'dovich, "On the Theory of Propagation of Detonation in Gaseous Systems," ZHURNAL EKSPERIMENTAL'NOY I TEORETICHESKOY FIZIKI, Vol 10, No 5, 1940, pp 542-568; "On Distribution of Pressure and Velocity in Detonation Explosion Products, in Particular in the Case of Spherical Propagation of a Detonation Wave," ZHURNAL EKSPERIMENTAL'NOY I TEORETICHESKOY FIZIKI, Vol 12, No 9, 1942, pp 389-406; "Teoriya goreniya i detonatsiya gazov" [Theory of Combustion and Detonation of Gases," Moscow-Leningrad, USSR Academy of Sciences, 1944, 72 pages.

11. J. Neuman, "Theory of Detonation Waves," Office of Scientific Research and Development Report No 549, 1942; W. Döring, "Über den Detonationsvorgang in Gasen," ANN. PHYSIK, Vol 43, 1943, pp 421-436.

12. C. Campbell, D. W. Woodhead, "The Ignition of Gases by an Explosion Wave. I. Carbon Monoxide and Hydrogen Mixtures," J. CHEM. SOC., Vol 129, 1926, pp 3010-3012; "Striated Photographic Records of Explosion Waves," J. CHEM. SOC., Vol 130, pp 1572-1578.

13. Yu. N. Denisov, B. V. Voytsekhovskiy et al., "The Phenomenon of Wave Splitting (Fine Structure) of Spin Detonation," Certificate of Discovery No 134, Priority 12 Feb 57, 24 Feb 58, BYULLETEN' IZOBRETENIY I OTKRYTIY, No 48, 1973, pp 4, 5.

14. M. A. Rivin, A. S. Sokolik, "Explosive Limits of Gas Mixtures, 3. Limits in Mixtures of Carbon Monoxide and Methane," ZHURNAL FIZICHESKOY KHIMII, Vol 8, 1936, pp 767-773; Ya. K. Troshin, K. I. Shchelkin, "On Spin at the Limits of Gas Detonation," IZVESTIYA AKADEMII NAUK SSSR: OTDELENIYE TEKHNICHESKIKH NAUK, No 8, 1957, pp 142-143.

15. Yu. N. Denisov et al., "The Phenomenon of Instability of a Detonation Wave in Gases," Certificate of Discovery, No 111, Priority 5 Nov 57, BYULLETEN' IZOBRETENIY I OTKRYTIY, No 24, 1972, pp 4, 5; Yu. N. Denisov, Ya. K. Troshin, "Pulsating and Spin Detonation of Gas Mixtures in Tubes," DOKLADY AKADEMII NAUK SSSR, Vol 125, No 1, 1959, pp 110-113.

16. Yu. N. Denisov, Ya. K. Troshin, "Structure of Gas Detonation in Tubes," ZHURNAL TEKHNICHESKOY FIZIKI, Vol 30, No 4, 1960, pp 450-459.

17. B. V. Voytsekhovskiy, V. V. Mitrofanov, M. Ye. Topchiyan, "Struktura Detonatsii v gazakh" [Structure of Detonation in Gases], Novosibirsk, Izdatel'stvo SO AN SSSR [Siberian Department, USSR Academy of Sciences], 1963, p 168.

18. V. I. Manzhaley, V. V. Mitrofanov, V. A. Subbotin, "Measurement of Inhomogeneities of a Detonation Front in Gas Mixtures at Elevated Pressures," FIZIKA GORENIYA I VZRYVA, No 1, 1974, pp 102-110.

19. R. A. Strehlow, C. D. Engel, "Transverse Waves in Detonations: II. Structure and Spacing in H_2-O_2, C_2H_2-O_2, C_2H_4-O_2 and CH_4-O_2 Systems," AIAA JOURN., Vol 7, No 3, 1969, pp 492-496.

20. A. Schmidt, "Über den Nachweis der Gültigkeit der hydrodynamisch-thermodynamischen Theorie der Detonation für feste und flüssige Sprengstoffe," Z. PHYS. CHEM., Vol A189, 1941, pp 88-94.

21. B. F. Volin et al., "On the Kinetic-Reaction Nature of Inhomogeneities in a Shock Front, and Their Role in the Process of Propagation of a Gas Detonation," ZHURNAL PRIKLADNOY MEKHANIKI I TEKHNICHESKOY FIZIKI, No 2, 1960, pp 78-89.

22. Yu. N. Denisov, Ya. K. Troshin, "Concerning the Discrete Nature of Change in Structure of a Gas Detonation," ZHURNAL PRIKLADNOY MEKHANIKI I TEKHNICHESKOY FIZIKI, No 2, 1967, pp 90-92.

23. K. I. Shchelkin, "Bystroye goreniye i spinovaya detonatsiya gazov" [Rapid Combustion and Spin Detonation of Gases], Moscow, Voyenizdat, 1949, 195 pages.

24. Yu. N. Denisov, Ya. K. Troshin, "Mechanism of Detonation Burning," ZHURNAL PRIKLADNOY MEKHANIKI I TEKHNICHESKOY FIZIKI, No 1, 1960, pp 21-34.

25. V. V. Mitrofanov, "Structure of a Detonation Wave in a Flat Channel," ZHURNAL PRIKLADNOY MEKHANIKI I TEKHNICHESKOY FIZIKI, No 4, 1962, pp 100-105.

26. A. N. Voinov, "On the Mechanism of Arisal of Detonation Spin," DOKLADY AKADEMII NAUK SSSR, Vol 73, No 1, 1950, pp 125-128.

27. B. V. Voytsekhovskiy, "On Spin Detonation," DOKLADY AKADEMII NAUK SSSR, Vol 11,, 1957, pp 717-720.

28. B. V. Voytsekhovskiy, "Investigation of the Structure of a Spin Detonation Front" in: "Trudy MFTI" [Transactions of Moscow Physicotechnical Institute], Moscow, Oborongiz, 1958, pp 81-91.

29. B. V. Voytsekhovskiy, "Optical Studies of a Spin Detonation Wave Front," IZVESTIYA SIBIRSKOGO OTDELENIYA AKADEMII NAUK SSSR, No 4, 1958, pp 74-80.

30. B. V. Voytsekhovskiy, V. V. Mitrofanov, M. Ye. Topchiyan, "On Flow Structure in a Spin Detonation Wave," ZHURNAL PRIKLADNOY MEKHANIKI I TEKHNICHESKOY FIZIKI, No 3, 1962, pp 27-30.

31. M. Ye. Topchiyan, "Experimental Studies of Spin Detonation by Pressure Sensors," ZHURNAL PRIKLADNOY MEKHANIKI I TEKHNICHESKOY FIZIKI, No 4, 1962, pp 94-99.

32. V. V. Mitrofanov, V. A. Subbotin, M. Ye. Topchiyan, "On Pressure Measurement in a Transverse Spin Wave," ZHURNAL PRIKLADNOY MEKHANIKI I TEKHNICHESKOY FIZIKI, No 3, 1963, pp 45-48.

33. Yu. N. Denisov, Ya. K. Troshin, "Thermogasdynamic Model of Pulsating Detonation" in: "Tret'ye Vsesoyuznoye soveshchaniye po teorii goreniya" [Third All-Union Conference on Combustion Theory], Vol 1, Moscow, Izdatel'stvo Akademii Nauk SSSR, 1960, pp 200-207.

34. Yu. N. Denisov, Ya. K. Troshin, "On the Mechanism of Detonative Combustion" in: "Eighth Symp. on Combustion," Baltimore, 1962, pp 600-610.

35. Yu. N. Denisov, "Influence of the Volume Effect on the Structure of the Detonation Front," DOKLADY AKADEMII NAUK SSSR, Vol 187, No 2, 1969, pp 358-361.

36. V. Ye. Gordeyev, "The Reason for Multiplication of Kinks of a Detonation Front," DOKLADY AKADEMII NAUK SSSR, Vol 226, No 2, 1976, pp 288-291.

37. A. V. Dremin, "Current Problems of Studying Detonation in Condensed Media," in: "Nauchnyye trudy Instituta mekhaniki Moskovskogo universiteta" [Scientific Papers of the Institute of Mechanics, Moscow University], No 21, Moscow, Moscow State University, 1973, pp 150-157.

38. Yu. N. Denisov, "High-Frequency Processes in the Core of a Spin Detonation," FIZIKA GORENIYA I VZRYVA, No 3, 1974, pp 386-392.

39. Yu. N. Denisov, I. I. Podtiynkov, "Components of the High-Frequency Process in Detonation Waves" in: "Chetvertyy Vsesoyuznyy simpozium po goreniyu i vzryvu. Annotatsiya dokladov" [Fourth All-Union Symposium on Combustion and Explosion. Abstracts of the Papers], Chernogolovka, Institute of Chemical Physics, Academy of Sciences of the USSR, 1974, p 45; in: "Goreniye i vzryv" [Combustion and Explosion], Moscow, Nauka, 1977, pp 454-460.

40. M. Busco, "Optical Properties of Detonation Waves (Optics of Explosives)" in: "Proc. Fifth Symp. (Int.) on Detonation, 1970, Pasadena, Calif.," Arlington, pp 513-522; W. B. Benedick, "Detonation Wave Shaping" in: "Behav. and Util. Explos. Eng. Des. and Biomech. Princip. Appl. Clin. Med. Proc. 12th Annu. Symp., Albuquerque, New Mexico, 1972," Albuquerque, N. M., pp 47-56.

41. T. V. Bazhenova, L. V. Gvozdeva, Yu. S. Lobastov et al., "Udarnyye volny v real'nykh gazakh" [Shock Waves in Real Gases], Moscow, Nauka, 1968, 198 pages.

42. I. A. Kunin, "Teoriya uprugikh sred s mikrostrukturoy" [Theory of Elastic Media with Microstructure], Moscow, Nauka, 1975, 416 pages.

43. A. A. Borisov, "Long-Wave Perturbations in Reacting Media" in: "Issledovaniya po gidrodinamike i teploobmenu" edited by S. S. Kutateladze, Novosibirsk, Izdatel'stvo SO AN SSSR, 1976, pp 94-95.

44. V. I. Aref'yev, Yu. N. Denisov, "On the Phase Theory of Propagation of Detonation Waves in Plasma-Like Media" in: "Elektromagnitnyye protsessy v neodnorodnykh sredakh" [Electromagnetic Processes in Inhomogeneous Media], Vladivostok, Izdatel'stvo DVNTs [Far Eastern Science Center], 1977, p 48.

45. Ya. B. Zel'dovich, Yu. P. Rayzer, "Fizika udarnykh voln i vysokotemperaturnykh gidrodinamicheskikh yavleniy" [Physics of Shock Waves and High-Temperature Hydrodynamic Phenomena], Moscow Fizmatgiz, 1963, 632 pages.

46. S. K. Aslanov, "On Periodic Instability as a Theoretical Basis of Pulsation Structure of Detonation," DOKLADY AKADEMII NAUK UKRAINSKOY SSR, SER. A, No 4, 1977, pp 318-321.

47. Yu. N. Denisov, "Investigation of Detailed Detonation Mechanism" in: "Dvenadtsataya Vsesoyuznaya konferentsiya po voprosam ispareniya, goreniya i gazovoy dinamiki dispersnykh sistem. Tezisy dokladov" [Twelfth All-Union Conference on

Problems of Vaporization, Combustion and Gas Dynamics of Dispersed Systems. Abstracts of the Papers], Odessa, 1976, p 41; "Detailed Mechanism of Detonation," DOKLADY AKADEMII NAUK SSSR, Vol 251, No 3, 1980, pp 628-632.

48. F. A. Baum, S. A. Kaplan, K. P. Stanyukovich, "Vvedeniye v kosmicheskuyu gazodinamiku" [Introduction to Space Gasdynamics], Moscow, Fizmatgiz, 1958, 424 pages.

49. Y. H. Lee, R. Knystautas, C. M. Guirao, "Critical Power Density for Direct Initiation of Unconfined Gaseous Detonation" in: "15th Symp. (Intern.) Combust., Tokyo, 1974," Pittsburgh, Pasadena, 1974, pp 53-66.

50. Yu. N. Denisov, P. I. Kopeyka, S. K. Aslanov, "Arisal of Spin Detonation" in: "Fizika aerodispersnykh sistem" [Physics of Aerodispersed Systems], No 11, Kiev, Vysha shkola, 1974, pp 66-71.

51. V. Ye. Gordeyev, "Maximum Overdriven Detonation Rate and Stability of Discontinuities in a Detonation Spin," DOKLADY AKADEMII NAUK SSSR, Vol 226, No 3, 1976, pp 619-622.

52. V. I. Manzheley, V. A. Subbotin, "Experimental Investigation of Stability of an Overdriven Detonation in a Gas," FIZIKA GORENIYA I VZRYVA, Vol 12, No 6, pp 935-942.

53. J. H. S. Lee, "Recent Advances in Gaseous Detonation," AIAA Paper, 1979, No 0287.

54. V. M. Akulintsev, A. S. Bashkin, N. N. Gorshunov et al., "Concerning the Feasibility of Lasing on the CO Molecule Behind an Overdriven Detonation Wave Front in a $Cs_2 + O_2$ Mixture," FIZIKA GORENIYA I VZRYVA, Vol 12, No 5, 1976, pp 739-744.

55. V. N. Kondrat'yev, "Konstanty skorostey gazofaznykh reaktsiy. Spravochnik" [Rate Constants of Gas-Phase Reactions. A Reference], Moscow, Nauka, 1971, 351 pages.

56. R. D. Stuart, P. H. Dawson, G. H. Kimbell "CS_2/O_2 Chemical Lasers: Chemical and Performance Characteristics," J. APPL. PHYS., Vol 43, No 3, 1972, pp 1022-1032.

57. K. H. von Homann, G. Krome, H. G. Wagner, "Schwefelkohlenstoff-Oxydation, I. Geschwindigkeit von Elementarreaktionen," BERICHTE DER BUNSEN-GESELLSCHAFT FÜR PHYSIKALISCHE CHEMIE, Vol 78, 1968, pp 998-1004; II. "Zur Oxydation von Carbonylsulfid," Ibid., Vol 73, No 10, 1969, p 967; III. "Die Isotherme-oxydation von Schwefelkohlenstoff," Ibid., Vol 74, No 7, pp 654-659.

58. D. W. Howgate, T. A. Barr, Jr., "Dynamics of the CS_2-O_2 Flame," J. CHEM. PHYS., Vol 59, No 6, 1973, pp 2815-2829.

59. G. Hancock, C. Morley, W. M. Smith, "Vibrational Excitation of CO in the Reaction: $O + CS \rightarrow CO + S$," CHEM. PHYS. LETT., Vol 12, No 1, 1971, pp 193-196.

60. B. F. Gordiyets, A. I. Osipov et al., "Vibrational Relaxation in Gases, and the Molecular Laser," USPEKHI FIZICHESKIKH NAUK, Vol 108, No 4, 1972, pp 655-699.

61. J. D. Anderson, M. T. Madden, "Population Inversions Behind Normal Shock Waves," AIAA JOURN., Vol 9, No 8, 1971, pp 1630-1632.

62. N. G. Basov, A. N. Orayevskiy, "Getting Negative Temperatures by the Method of Heating and Cooling a System," ZHURNAL EKSPERIMENTAL'NOY I TEORETICHESKOY FIZIKI, Vol 44, No 5, 1963, pp 1742-1745.

63. I. R. Hurle, A. Hertzberg, "On the Possible Production of Population Inversions by Gas Dynamic Techniques," Minutes of the 1963 Annual Meeting of the Division of Fluid Dynamics, Cambridge Massachusetts, 25-27 Nov 1963, BULL. AMER. PHYS. SOC., Vol 9, No 5, 1964, pp 582-595.

64. I. R. Hurle, A. Hertzberg, "Electronic Population Inversion by Fluid-Mechanical Techniques," PHYS. FLUIDS, Vol 8, No 9, 1965, pp 1601-1607.

65. V. K. Konyukhov, A. M. Prokhorov, "Inverse Population with Adiabatic Expansion of a Gas Mixture," PIS'MA V ZHURNAL EKSPERIMENTAL'NOY I TEORETICHESKOY FIZIKI, Vol 3, No 11, 1966, pp 436-439.

66. J. E. Morgan, H. I. Schiff, "The Study of Vibrationally Excited N_2 Molecules with the Aid of an Isothermal Calorimeter," CANAD. JOURN. CHEMISTRY, Vol 41, No 4, 1963, pp 903-912.

67. V. K. Konyukhov, I. V. Matrosov, A. M. Prokhorov et al., "A Gasdynamic cw Laser Based on a Mixture of Carbon Dioxide, Nitrogen and Water," PIS'MA V ZHURNAL EKSPERIMENTAL'NOY I TEORETICHESKOY FIZIKI, Vol 12, No 10, 1970, pp 461-464.

68. N. G. Basov, A. N. Orayevskiy, V. A. Shcheglov, "Thermal Methods of Laser Excitation," ZHURNAL TEKHNICHESKOY FIZIKI, Vol 37, No 2, 1967, pp 339-348.

69. D. M. Kuehn, D. J. Monson, "Experiments with a CO_2 Gas-Dynamic Laser," APPL. PHYS. LETT., Vol 16, No 1, 1970, pp 48-51.

70. A. P. Dronov et al., "A Gas-Dynamic CO_2 Laser with Discharge of a Mixture Heated in a Shock Tube Through a Slit," PIS'MA V ZHURNAL EKSPERIMENTAL'NOY I TEORETICHESKOY FIZIKI, Vol 11, No 11, 1970, pp 516-519.

71. B. R. Bronfin, L. R. Boedecker, J. P. Cheyer, "Thermal Laser Excitation by Mixing in a Highly Convective Flow," APPL. PHYS. LETT., Vol 16, No 5, 1970, pp 214-216.

72. A. S. Biryukov, B. F. Gordiyets, L. A. Shelepin, "Nestatsionarnyye sposoby sozdaniya inversnoy zaselennosti kolebatel'nykh urovney molekuly CO_2" [Unsteady Methods of Setting up Population Inversion of Vibrational Levels of the CO_2 Molecule], Preprint No 41, Physics Institute imeni Lebedev, 1969, p 51.

73. A. S. Biryukov, L. A. Shelepin, "A Chemical-Mechanical Molecular Laser," ZHURNAL TEKHNICHESKOY FIZIKI Vol 40, No 12, 1970, pp 2575-2577.

74. N. G. Basov et al., "Population Inversion of Molecules in a Supersonic Binary Gas Flow in a Laval Nozzle," ZHURNAL TEKHNICHESKOY FIZIKI, Vol 38, No 12, 1968, pp 2031-2041.

75. "Avco Describes Gas-Dynamic System That Attains 60-Kilowatt Pulses," LASER FOCUS, Vol 6, No 7, 1970, pp 16-18.

76. E. Gerry, "The Gas-Dynamic Laser," LASER FOCUS, Vol 6, No 12, 1970, pp 27-31.

77. F. A. Baum, K. P. Stanyukovich, B. I. Shekhter, "Fizika vzryva" [Physics of Explosion], Moscow, Fizmatgiz, 1959, p 800.

78. K. K. Andreyev, A. F. Belyayev, "Teoriya vzryvchatykh veshchestv" [Theory of Explosives], Moscow, Oborngiz, 1960, 595 pages.

79. B. A. Ivanov, "Fizika vzryva atsetilena" [Physics of Explosion of Acetylene], Moscow, Khimiya, 1969.

80. R. I. Taylor, S. Bitterman, "Survey of Vibrational Relaxation Data for Processes Important in the CO_2-N_2 Laser System," REV. MOD. PHYS., Vol 41, 1969, pp 26-47.

81. R. W. F. Gross, R. R. Giedt, T. A. Jacobs, "Stimulated Emission Behind Overdriven Detonation Waves in F_2O-H_2 Mixtures," IEEE J. QUANT. ELECTRON., Vol QE-6, 1970, p 168.

82. R. W. F. Gross, N. Cohen, T. A. Jacobs, "Chemical Laser Produced by Flash Photolysis of F_2O-H_2 Mixtures," J. CHEM. PHYS., Vol 48, No 8, 1968, pp 3821-3822.

83. N. Cohen, R. Wilkins, T. A. Jacobs, "Theoretical Calculations of Detonation Initiated Chemical Lasers," IEEE J. QUANT. ELECTRON., Vol QE-6, 1970, pp 168-169.

84. V. G. Voronkov, A. G. Rozenberg, "Explosive Properties of Mixtures of Gaseous Hydrazoic Acid With Inorganic Diluents," DOKLADY AKADEMII NAUK SSSR, Vol 177, No 4, 1967, pp 835-838.

85. M. S. Dzhidzhoyev, M. I. Pimenov, V. G. Platonenko, et al., "On Producing Population Inversion in Polyatomic Molecules Through the Energy of a Chemical Reaction", ZHURNAL EKSPERIMENTAL'NOY I TEORETICHESKOY FIZIKI, Vol 57, No 2, 1969, pp 411-420.

86. N. G. Basov, V. V. Gromov, Ye. L. Koshelev et al., "Induced Radiation in Explosion of HN_3 and CO_2," PIS'MA V ZHURNAL EKSPERIMENTAL'NOY I TEORETICHESKOY FIZIKI, Vol 10, No 1, 1969, pp 5-8.

87. N. Ya. Vasilik, V. M. Shmelev, A. D. Margolin, "Influence of Chlorine on the Gain of a CO_2 Gasdynamic Laser Based on Products of Combustion of Methane Mixtures," KVANTOVAYA ELEKTRONIKA, Vol 3, No 10, 1976, pp 2171-2175.

88. Yu. A. Bokhon, I. I. Davletchin, V. M. Marchenko et al., "Observation of Stimulated Emission in a Gas-Dynamic Laser Based on Products of Gas Detonation," KRATKIYE SOOBSHCHENIYA PO FIZIKE, No 11, 1972, pp 52-56.

89. S. Jatsiv, E. Greenfield, F. Dothan-Deutsch et al., "Pulsed CO_2 Gas-Dynamic Laser," APPL. PHYS. LETT., Vol 19, No 3, 1971, pp 65-68.

90. S. Jatsiv et al., "Experiments with a Pulsed CO_2 Gas-Dynamic Laser," IEEE J. QUANT. ELECTRON., Vol QE-8, No 2, 1972, pp 161-163.

91. J. Tulip, H. Seguin, "Explosion-Pumped Gas-Dynamic CO_2 Laser," APPL. PHYS. LETT., Vol 19, No 8, 1971, pp 263-265.

6610
CSO: 1862/212

- END -